

Manuel Gregoritz

Click Hydrogels for Controlled Local Antibody Delivery

Click Hydrogels for Controlled Local Antibody Delivery

**Dissertation
zur Erlangung des Doktorgrades der
Naturwissenschaften
(Dr. rer. nat.)
der Fakultät für Chemie und Pharmazie
der Universität Regensburg**



vorgelegt von
Manuel Gregoritzka
aus Finsing

September 2017

Diese Arbeit entstand in der Zeit von November 2013 bis September 2017 am Lehrstuhl für Pharmazeutische Technologie der Universität Regensburg.

Die Arbeit wurde von Herrn Prof. Dr. Achim Göpferich angeleitet.

Promotionsgesuch eingereicht am: 15.09.2017

Datum der mündlichen Prüfung: 17.11.2017

| | |
|--------------------------|---|
| Prüfungsausschuss | Prof. Dr. Joachim Wegener (Vorsitzender) |
| | Prof. Dr. Achim Göpferich (Erstgutachter) |
| | Prof. Dr. Rainer Müller (Zweitgutachter) |
| | Prof. Dr. Sigurd Elz (Drittprüfer) |

Meiner Familie

Contents

| | |
|---|-----------|
| Click hydrogels for controlled local antibody delivery | 1 |
| 1 The Diels–Alder reaction: A powerful tool for the design of drug delivery systems and biomaterials | 3 |
| 1.1 Introduction | 5 |
| 1.2 Diels–Alder chemistry | 6 |
| 1.3 Advantages of the Diels–Alder reaction | 8 |
| 1.4 Pharmaceutical and biomedical applications of the Diels–Alder reaction | 9 |
| 1.4.1 Synthesis of copolymers | 10 |
| 1.4.2 Synthesis of branched polymers and dendrimers | 14 |
| 1.4.3 Surface functionalization | 16 |
| 1.4.4 Bioconjugation | 19 |
| 1.4.5 Nanotechnology | 22 |
| 1.4.6 Hydrogels | 24 |
| 1.5 Pitfalls and challenges of the Diels–Alder reaction | 30 |
| 1.6 Summary and perspectives | 33 |
| 2 Goals of the thesis | 35 |
| 3 Design of hydrogels for delayed antibody release utilizing hydrophobic association and Diels–Alder chemistry in tandem | 39 |
| 3.1 Introduction | 41 |
| 3.2 Materials and methods | 42 |
| 3.2.1 Materials | 42 |
| 3.2.2 ¹ H-NMR spectroscopy | 43 |
| 3.2.3 Synthesis of Boc-12-aminododecanoic acid | 43 |
| 3.2.4 Synthesis of unmodified macromonomers | 43 |
| 3.2.5 Synthesis of hydrophobically modified macromonomers | 44 |
| 3.2.6 Determination of the critical micelle concentration | 46 |
| 3.2.7 Viscosity measurements | 46 |
| 3.2.8 Hydrogel preparation and characterization | 46 |
| 3.2.9 Young’s modulus of compression | 47 |
| 3.2.10 Swelling, degradation and antibody release | 47 |
| 3.2.11 Hydrolytic stability of maleimides | 48 |
| 3.2.12 Statistical analysis | 48 |

| | | |
|----------|---|-----------|
| 3.3 | Results and discussion | 48 |
| 3.3.1 | Association of macromonomers in aqueous solution | 48 |
| 3.3.2 | Viscosity of macromonomer solutions | 51 |
| 3.3.3 | Acceleration of gel formation by hydrophobic association | 53 |
| 3.3.4 | Network mesh size and mechanical properties | 55 |
| 3.3.5 | Swelling, degradation and antibody release | 57 |
| 3.4 | Conclusion | 62 |
| 4 | Controlled antibody release from degradable thermoresponsive hydrogels cross-linked by Diels–Alder chemistry | 63 |
| 4.1 | Introduction | 65 |
| 4.2 | Materials and methods | 67 |
| 4.2.1 | Materials | 67 |
| 4.2.2 | ¹ H-NMR spectroscopy | 67 |
| 4.2.3 | Synthesis of four-armed macromonomers | 67 |
| 4.2.4 | Synthesis of eight-armed macromonomers | 68 |
| 4.2.5 | Gel formation and rheological properties | 68 |
| 4.2.6 | Swelling and degradation | 69 |
| 4.2.7 | Hydrolytic stability of maleimides | 69 |
| 4.2.8 | Cytotoxicity | 69 |
| 4.2.9 | Antibody release and analytics | 70 |
| 4.2.10 | Statistical analysis | 70 |
| 4.3 | Results and discussion | 71 |
| 4.3.1 | Hypothesis and proof of concept | 71 |
| 4.3.2 | Gel formation and mechanical properties | 72 |
| 4.3.3 | Hydrogel swelling and degradation | 74 |
| 4.3.4 | Cytotoxicity | 78 |
| 4.3.5 | Controlled antibody release | 79 |
| 4.4 | Conclusion | 83 |
| 5 | Fabrication of antibody-loaded microgels using microfluidics and thiol-ene photoclick chemistry | 85 |
| 5.1 | Introduction | 87 |
| 5.2 | Materials and methods | 88 |
| 5.2.1 | Materials | 88 |
| 5.2.2 | Synthesis of macromonomers | 89 |
| 5.2.3 | Hydrogel preparation, swelling and network mesh size | 91 |
| 5.2.4 | Rheology | 91 |
| 5.2.5 | Microgel fabrication | 92 |
| 5.2.6 | <i>In vitro</i> release | 93 |
| 5.2.7 | Simulation of stress conditions | 93 |
| 5.2.8 | Cytotoxicity | 94 |
| 5.2.9 | Statistical analysis | 94 |

| | | |
|----------|---|------------|
| 5.3 | Results and discussion | 95 |
| 5.3.1 | Gelation and material properties | 95 |
| 5.3.2 | Microfluidics, stress conditions and toxicity | 99 |
| 5.3.3 | Network mesh size and release studies | 103 |
| 5.4 | Conclusion | 106 |
| 6 | Polyanions effectively prevent protein conjugation and activity loss during hydrogel cross-linking | 107 |
| 6.1 | Introduction | 109 |
| 6.2 | Materials and methods | 111 |
| 6.2.1 | Materials | 111 |
| 6.2.2 | Functionalization of polymers | 112 |
| 6.2.3 | Incubation of lysozyme | 112 |
| 6.2.4 | Degree of lysozyme PEGylation | 112 |
| 6.2.5 | Lysozyme activity assay | 113 |
| 6.2.6 | Turbidity measurement | 113 |
| 6.2.7 | Release experiments | 113 |
| 6.2.8 | Size-exclusion chromatography | 114 |
| 6.2.9 | Circular dichroism spectrometry | 114 |
| 6.2.10 | Statistical analysis | 114 |
| 6.3 | Results and discussion | 115 |
| 6.3.1 | Influence of polyanions on lysozyme PEGylation and activity | 115 |
| 6.3.2 | Factors influencing the “shielding” effect of polyanions . . . | 119 |
| 6.3.3 | Investigation of alternative cross-linking mechanisms | 125 |
| 6.3.4 | Impact of polyanions on protein release from hydrogels . . . | 127 |
| 6.4 | Conclusion | 130 |
| 7 | Summary and Conclusion | 133 |
| 7.1 | Summary | 134 |
| 7.2 | Conclusion | 137 |
| | Appendix | 183 |
| | Supplementary Spectroscopic Information | 185 |
| | Acronyms | 191 |
| | Symbols | 195 |
| | Curriculum Vitae | 197 |
| | Publications | 199 |
| | Acknowledgements | 201 |

| | |
|-------------------------------------|------------|
| Statement in Lieu of an Oath | 203 |
|-------------------------------------|------------|

Click hydrogels for controlled local antibody delivery

The important thing is not to stop questioning. Curiosity has its own reason for existing.

(Albert Einstein)

Chapter 1

Introduction

The Diels–Alder reaction: A powerful tool for the design of drug delivery systems and biomaterials

Published in *European Journal of Pharmaceutics and Biopharmaceutics*

The content of this chapter was published as: *Eur. J. Pharm. Biopharm.*, 97, part B: 438–453, 2015. doi: 10.1016/j.ejpb.2015.06.007

Abstract

Click reactions have the potential to greatly facilitate the development of drug delivery systems and biomaterials. These reactions proceed under mild conditions, give high yields, and form only inoffensive by-products. The Diels–Alder cycloaddition is one of the click reactions that do not require any metal catalyst; it is one of the most useful reactions in synthetic organic chemistry and material design. Herein, possible applications of the Diels–Alder reaction in pharmaceuticals and biomedical engineering are highlighted. Particular focus is placed on the synthesis of polymers and dendrimers for drug delivery, the preparation of functionalized surfaces, bioconjugation techniques, and applications of the Diels–Alder reaction in nanotechnology. Moreover, applications of the reaction for the preparation of hydrogels for drug delivery and tissue engineering are reviewed. A general introduction to the Diels–Alder reaction is presented, along with a discussion of potential pitfalls and challenges. At the end of the chapter, a set of tools is provided that may facilitate the application of the Diels–Alder reaction to solve important pharmaceutical or biomedical problems.

1.1 Introduction

The formation of new chemical bonds between molecules is one of the key challenges in the development of drug delivery systems and biomaterials. For example, the synthesis of polymer-drug conjugates, the assembly of nanomaterials, the attachment of targeting moieties onto delivery systems, or the preparation of hydrogels require fast, efficient, and selective coupling reactions. These reactions are typically performed in aqueous solution; moreover, mild reaction conditions are preferred to preserve the activity of biopharmaceuticals such as proteins, nucleic acids, or living cells. Click chemistry has the potential to greatly facilitate the development of drug delivery systems and biomaterials [1–5]. The term “click chemistry” was first introduced by Sharpless and coworkers in 2001 to define a group of “spring-loaded” reactions that proceed under mild conditions, give high chemical yields, and generate only inoffensive by-products [6, 7]. Furthermore, click reactions are stereospecific and modular, i.e., the reactions are applicable to various materials and environments. During the last decade and a half, click chemistry has opened up new possibilities in polymer chemistry, materials science, nanotechnology, and drug discovery [8–12]. In the biomedical field, click chemistry has become a powerful tool for the synthesis of polymers and dendrimers for drug delivery, the functionalization of surfaces, and for the preparation and functionalization of nanoscale drug delivery systems. Moreover, click chemistry has emerged as an efficient cross-linking method for the preparation of hydrogels [1–5]. Several chemical reactions have been identified that meet the criteria of click chemistry [6, 7]. One of the most popular click reactions is the copper(I)-catalyzed azide-alkyne Huisgen cycloaddition (CuAAC). The reaction reaches almost quantitative conversion in both aqueous and organic media and offers “an unprecedented level of selectivity” [13, 14]; it is often referred to as “the cream of the crop” of click chemistry [6, 7]. However, the potential toxicity of the copper(I) catalyst is a major concern in the design of drug delivery systems and biomaterials; furthermore, the presence of copper(I) can be detrimental to biomolecules such as lipids, nucleic acids, polysaccharides, or proteins [2–4]. Consequently, there has been considerable interest in identifying alternative, metal-free click reactions. While the azide-alkyne Huisgen cycloaddition can also be achieved in the absence of metal catalysts, the extremely low reaction rate at room temperature limits its practical usefulness. To increase the rate of the coupling reaction, Bertozzi and coworkers developed a copper-free, strain-promoted azide-alkyne cycloaddition (SPAAC) [15]. Compared

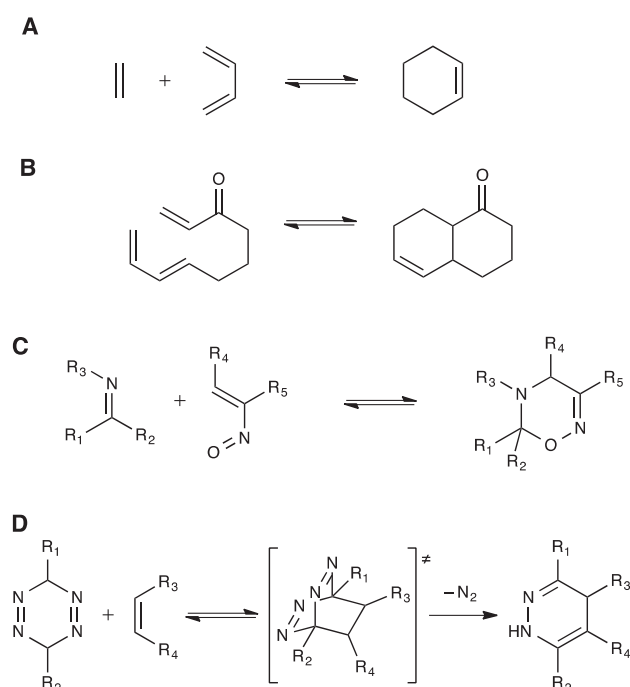
to terminal alkynes, the reactivity of cyclooctyne derivatives toward azides is greatly enhanced [16], in particular when difluorinated cyclooctynes are used [17]. However, these cyclooctyne derivatives are difficult to synthesize, which may limit the widespread use of SPAAC. The Diels–Alder (DA) cycloaddition is another click reaction that does not require any metal catalyst [18–21]. Although being accelerated by Lewis acids [22–25], the DA reaction remains efficient in the absence of catalysts, even though the reaction rate can then be slow at room temperature. The reaction was first described by Otto Diels and his student, Kurt Alder, in 1928 [26, 27]. In appreciation of their discovery, Diels and Alder were awarded the Nobel prize in chemistry in 1950. The DA reaction is stereoselective, atom economical, and highly efficient; it is one of the most powerful methods to synthesize unsaturated six-membered rings [28]. For example, the DA reaction was utilized in the total synthesis of steroids by Woodward et al. [29], or in the first total synthesis of morphine by Gates and Tschudi [30, 31]. The DA cycloaddition is undoubtedly one of the most useful reactions in synthetic organic chemistry and its importance for biomedical applications, such as the development of drug delivery systems or biomaterials, is steadily increasing.

In this chapter possible applications of the DA reaction in pharmaceuticals and biomedical engineering will be highlighted. Particular focus will be placed on the synthesis of polymers and dendrimers for drug delivery, the preparation of functionalized surfaces, bioconjugation techniques, and applications of the DA reaction in nanotechnology. Moreover, applications of the reaction for the preparation of hydrogels for drug delivery and tissue engineering will be reviewed. The chapter is complemented by a general introduction to the DA reaction, along with a discussion of potential pitfalls and challenges. A major goal of this chapter is to provide a set of tools that may facilitate pharmaceutical or biomedical applications of the DA reaction.

1.2 Diels–Alder chemistry

The DA reaction is a $[4 + 2]$ cycloaddition of a conjugated diene and a substituted alkene (also termed dienophile) during which six π -electrons rearrange to form a cyclic, six-membered product (Scheme 1.1A). If both the diene and the dienophile are part of the same molecule, the DA reaction is usually referred to as intramolecular DA cycloaddition (Scheme 1.1B). Moreover, DA reactions are known in which at least one heteroatom is involved; these are collectively called

hetero-DA reactions (Scheme 1.1C). Since the discovery of the DA reaction, the precise reaction mechanism has been subject of controversial discussion. It has been debated whether the DA reaction occurs by a two-step mechanism involving a diradical, or by a one-step mechanism. Today, the “prevailing opinion” is that the DA cycloaddition is a concerted, synchronous reaction involving a cyclic transition state [32–36]. The mechanism of the DA reaction is frequently explained by using ethylene and 1,3-butadiene as reaction partners. However, this particular reaction should be understood as a theoretical example as it proceeds exceptionally slowly.



Scheme 1.1: Normal electron-demand Diels–Alder (DA) reaction (A), intramolecular DA reaction (B), hetero-DA reaction (C), and inverse electron-demand DA reaction (D).

The reason for the slow reaction kinetics is the unfavorable electron distribution within the reaction partners. The cycloaddition proceeds dramatically faster if electron-poor dienophiles are reacted with electron-rich dienes (normal electron-demand DA reaction). Therefore, typical DA reactants are substituted accordingly: reactive dienophiles are substituted with electron withdrawing groups, such as carbonyls, ketones, carboxyls, nitriles or halogens, whereas “good” dienes are substituted with electron donating groups, such as alkyl chains. In accordance with Sharpless’ demands for click reactions, a major advantage of the DA cycloaddition

is its predictable stereochemistry. The configuration of the substituents in both the diene and the dienophile is preserved in the cycloaddition adduct (“cis-principle”) [37]. If cyclic dienes or dienophiles are involved, a bridged product is formed that can be either endo- or exo-oriented. In most cases, the endo-product is favored due to secondary orbital interactions (“endo-rule”). However, the ratio of endo to exo isomers can vary depending on whether the reaction is kinetically or thermodynamically controlled [37, 38]. At this point it should be noted that the DA reaction and its counterpart, the retro-Diels–Alder (rDA) reaction, are reversible under certain conditions. Increasing the temperature favors the rDA reaction and shifts the equilibrium position, which offers exciting possibilities in polymer chemistry and material design [39–42]. In addition to the normal electron-demand DA reaction, which typically involves electron-rich dienes and electron-poor dienophiles, an alternative reaction, in which the electron distribution between the two reactants is reversed, has been described. During this reaction, which is termed inverse electron-demand DA (IEDDA) reaction, a six-membered ring is formed between an electron-poor diene and an electron-rich dienophile (Scheme 1.1D) [34, 43].

1.3 Advantages of the Diels–Alder reaction

The DA reaction plays an essential role in synthetic organic chemistry [28], and its importance for pharmaceutical or biomedical applications is steadily increasing. Suitable diene-dienophile pairs (e.g., furan and maleimide) are readily available, and the molecules of interest can be easily functionalized with the reactive moieties. For example, to introduce furan moieties, carboxylic acids can be reacted with furfuryl alcohol or furfurylamine. In the same manner, amines can be reacted with 3-furoic acid or 3-(2-furyl)propionic acid. Alcohols can be directly reacted with 2-furoyl chloride, or converted to amines for further derivatization. To introduce maleimide moieties, amines can be reacted with N-methoxycarbonylmaleimide or 3-(maleimido)propionic acid. Furthermore, the DA reaction has a number of favorable characteristics that make its application particularly appealing. In the case of medicinal products and devices, purity and safety of the employed materials are important prerequisites. Consequently, it is advantageous that the DA reaction readily proceeds in water; expensive and potentially toxic solvents are not required. Interestingly, the reaction is greatly accelerated in water due to both enhanced hydrogen bonding to the activated complex and enforced hydrophobic interactions

between the reactants [44–47]. But most importantly, the DA reaction can go to completion at room temperature, even though the reaction kinetics is slow under these mild conditions [48–50]. For example, when peptides equipped with hexadienyl and maleimide groups were exposed to each other at 25 °C in water, the cycloaddition proceeded smoothly with a conversion of 92% after 47 h [48]. For that reason, the DA reaction is a useful bioconjugation reaction with many potential applications, e.g., in the preparation of polymer-drug conjugates or in the development of targeted nanoparticles. However, it should be noted that both the equilibrium conversion and the reaction rate depend on the substitution pattern of the involved diene-dienophile pair [51]. Moreover, in many cases, purification of the product is hardly necessary, as no catalyst or initiator is required and no by-product is formed. This is particularly important if macromolecules, such as polymers, dendrimers, proteins or nucleic acids, are involved in the reaction. Due to these favorable characteristics (i.e., reaction in water, reaction at room temperature without the use of catalysts, absence of by-products, etc.), the DA reaction is also an effective cross-linking method to prepare *in situ* forming materials, such as hydrogels for drug delivery and tissue engineering. In contrast to the above-mentioned features, the reversibility of the reaction, which has already been discussed in the previous section, can be considered both advantageous and disadvantageous. For example, the DA cycloaddition/cycloreversion reaction can be used to protect or deprotect functional groups; furthermore, the DA/rDA equilibrium can be exploited in the preparation of degradable or self-healing materials, or in the design of controlled drug delivery systems. On the other hand, the reversibility of the DA reaction may prove problematic if stable adducts should be formed, e.g., in bioconjugation reactions. Interestingly, the reversibility of the DA reaction can be controlled by selecting the proper diene-dienophile pair, or by changing the solvent system [51, 52].

1.4 Pharmaceutical and biomedical applications of the Diels–Alder reaction

The following section provides examples of pharmaceutical and biomedical applications of the DA reaction. The section is divided into six subsections that highlight applications of the DA reaction in the synthesis of copolymers, the synthesis of branched polymers and dendrimers, the functionalization of surfaces, the synthesis

of bioconjugates, the assembly or disassembly of nanomaterials, and in the preparation of hydrogels for drug delivery and tissue engineering. The advantages and disadvantages of the DA reaction are briefly discussed throughout the text; a more detailed discussion of potential pitfalls and challenges can be found at the end of the chapter.

1.4.1 Synthesis of copolymers

Copolymers are polymers that are composed of two or more different monomers (e.g., monomers A and B). Depending on how the monomers are organized along the backbone, different types of copolymers can be distinguished. In statistical copolymers, the sequence of monomer units follows statistical rules (e.g., A-A-B-A-B-A-B-B-B-A), whereas block copolymers comprise two or more homopolymer subunits (e.g., A-A-A-A-A-B-B-B-B-B). Graft copolymers are a special type of branched polymer in which the side chains are constitutionally different from the main chain; the individual chains can be distinct homopolymers or copolymers. Since the individual segments of block copolymers or graft copolymers can have different physicochemical properties, such as hydrophobicity or crystallinity, copolymers have many potential applications in drug formulation, biomaterial design and nanotechnology. For example, copolymers consisting of hydrophobic and hydrophilic segments are able to self-assemble in water to form micellar structures, which have numerous applications in drug delivery [53–56] and gene therapy [57, 58]; they are also used to prepare nanomaterials [59–61], surface coatings [62–64] or hydrogels [65–67]. Block copolymers can be synthesized by living polymerization, such as atom transfer free radical polymerization (ATRP), reversible addition fragmentation chain transfer (RAFT), ring-opening metathesis polymerization (ROMP), and living anionic or cationic polymerizations. Another strategy to prepare block copolymers is the stepwise coupling of homopolymer precursors made of different monomers. To avoid tedious purification procedures, the coupling reaction should be both efficient and chemoselective, i.e., the coupling reaction must not interfere with other functional groups present in the same molecule. The DA reaction meets these criteria and offers the possibility to create thermoreversible bonds, which is a key difference to other click reactions.

Among all possible reaction partners, the DA reaction of furan and maleimide has received particular attention [19, 21]. The rDA reaction of the furan-maleimide adduct occurs at relatively low temperature (i.e., around 100 °C), which opens the

way to many interesting applications, such as self-healing or recyclable materials. In the following section, those approaches with potential pharmaceutical or biomedical applications will be highlighted. For example, Inoue et al. [68] described the synthesis and characterization of recyclable shape-memory polymers. For this purpose, star-shaped poly(lactic acid) (PLA) macromonomers were functionalized with furyl groups and cross-linked with bismaleimides via DA reaction. In a similar manner, recyclable shape-memory polymers were prepared by melt-blending star-shaped poly(ϵ -caprolactone)s end-functionalized with furan and maleimide moieties [69, 70]. In a further approach for the synthesis of biodegradable shape-memory elastomers, Ninh and Bettinger [71] coupled hyperbranched furan-modified poly(glycerol-*co*-sebacate) precursors with bifunctional maleimide cross-linking agents (Fig. 1.1). These kinds of biodegradable shape-memory polymers may be useful in the biomedical field [72, 73]. For example, stents used in endovascular aneurysm repair must be designed to allow administration by minimally invasive techniques. Implants made of shape-memory polymers have a compact shape at room temperature; they can be inserted through keyhole incisions and unfold to their functional shape inside the body.

In addition to the reversible coupling of polymers, the DA reaction of furan and maleimide can be used to protect the maleimide group during polymerization. For example, Onbulak et al. [74] prepared biodegradable poly(carbonate)s with pendant, furan-protected maleimide groups. Deprotection via rDA reaction yielded maleimide groups that could react with thiol-containing molecules in a Michael-type addition reaction. This thermal deprotection is interesting, especially for biodegradable polymers, because acid or basic catalysts, which are prone to degrade the polymer in the presence of water, are not required. The only requirement is that the polymer has to be thermally stable at the temperature at which the rDA reaction takes place. Another interesting application of the DA reaction is the preparation of organic-inorganic hybrid materials. The synthesis of these polymer hybrids was accomplished by reacting a styrene copolymer bearing pendant furan moieties with a maleimide-containing silane coupling agent in the presence of tetraethoxysilane [75]. Such hybrid materials, which combine the advantages of both organic and inorganic materials, could be used as biomaterials in certain applications requiring high mechanical strength. For example, the stiffness and compressive strength of polymeric biomaterials are often insufficient to be used as scaffolds for bone tissue engineering. Organic-inorganic nanocomposites usually

show improved mechanical characteristics compared to their individual components and are, therefore, regarded as promising alternative to polymeric scaffolds [76].

Besides the furan-maleimide pair, the DA reaction between anthracene and maleimide has been used for the preparation of block copolymers [77], graft copolymers [78], and star-shaped copolymers [79]. Since the rDA reaction of the anthracene-maleimide adduct occurs at temperatures above 200 °C, the cycloaddition of anthracene and maleimide yields stable conjugates [19]. For example, poly(methyl methacrylate)-*b*-polystyrene (PMMA-*b*-PS), poly(ethylene glycol)-*b*-polystyrene (PEG-*b*-PS), and PMMA-*b*-PEG copolymers were obtained in almost quantitative yields, demonstrating the high efficiency of the coupling reaction [77]. Biodegradable Y-shaped block copolymers were synthesized in a similar way using hydrophobic poly(ϵ -caprolactone) and hydrophilic PEG; the polymers formed micelles in aqueous media, which could be used as a carrier for the anti-cancer drug vinorelbine [80]. Similarly, poly(ethylene terephthalate) copolymers containing 2,6-anthracenedicarboxylate units were cross-linked by DA reaction with bismaleimides [81]. Furthermore, the combination of DA reaction and CuAAC allowed the one-pot synthesis of triblock copolymers consisting of polystyrene, PMMA, and PEG or poly(ϵ -caprolactone) [82]. Besides these examples, the hetero-DA reaction [83, 84] and the IEDDA reaction [85–88] have been successfully applied to the synthesis of copolymers. While the DA cycloaddition between anthracene and maleimide requires temperatures in excess of 110 °C and long reaction times (48–120 h) [77], Inglis et al. [83] demonstrated that the hetero-DA cycloaddition between cyclopentadienyl-terminated PEG and polymers bearing pyridinyl dithioester groups can be completed within 10 min. The efficiency of this reaction is comparable to other click reactions, such as CuAAC or thiol-ene reactions, which typically require reaction times ranging from 5 min to 3 h to achieve completion [89–92].

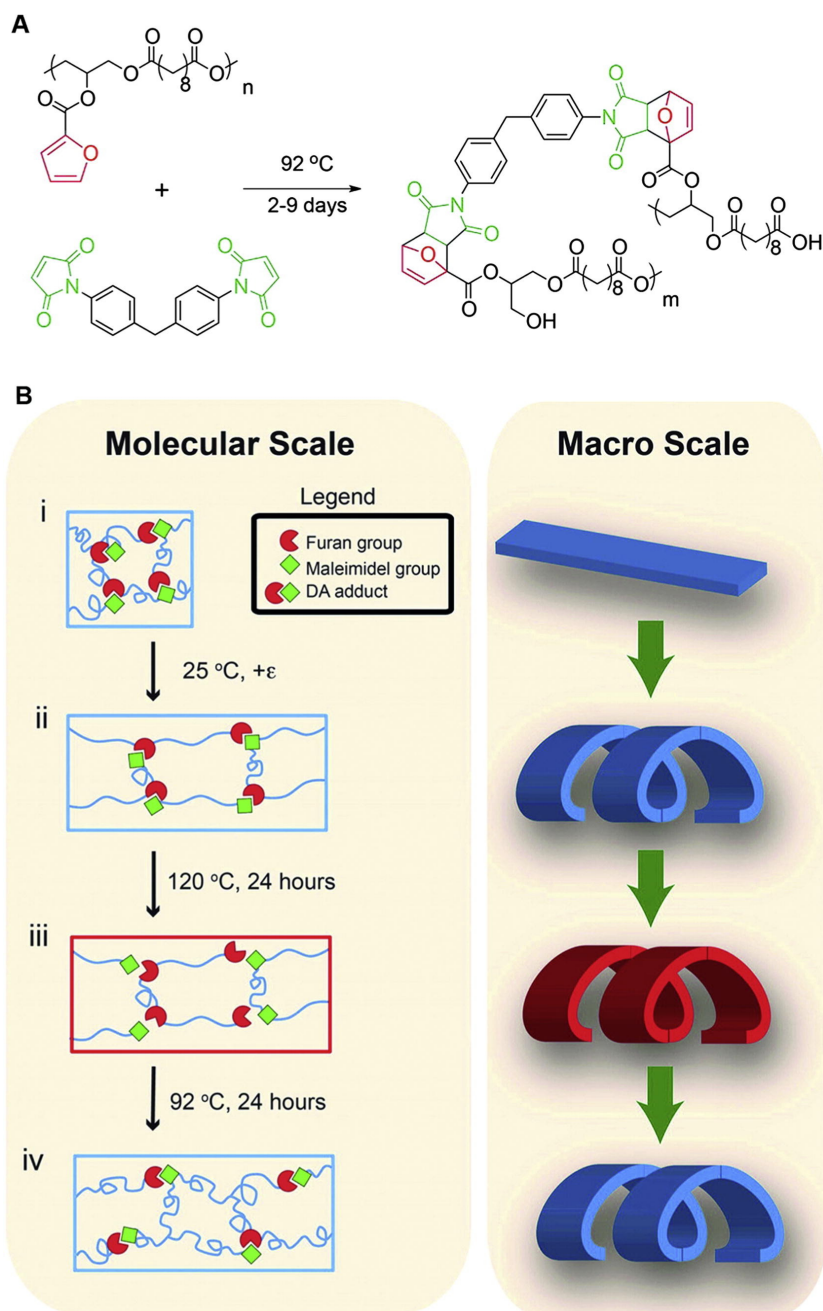


Figure 1.1: Cross-linking of hyperbranched furan-modified poly(glycerol-*co*-sebacate) precursors with 1,10-(methylenedi-4,1-phenylene) bismaleimide (A). Fabrication of elastomers via DA/rDA reaction. The process reprograms the polymer network into a complex permanent geometry (B). The material can be fixed into a temporary planar geometry below the glass transition temperature; when heated above the glass transition temperature, the material returns to its permanent helical shape. Adapted with permission from Ref. [71].

1.4.2 Synthesis of branched polymers and dendrimers

Dendrimers are highly branched molecules; the name is derived from the Greek word *dendron*, which translates into “tree”. Unlike star-shaped polymers, dendrimers are monodisperse; they are typically symmetric, spherical compounds with nanoscale dimensions. The large number of functional groups on their surface enables the conjugation of targeting ligands, dye molecules or pharmaceutically active compounds. Due to these favorable properties, dendrimers have strong potential as diagnostic agents, drug carriers or vehicles for gene delivery [93–95]. Monodisperse dendrimers can be synthesized by divergent or convergent methods. Divergent methods start from a multifunctional core, which is extended outward by repeated branching reactions. Each reaction step must be driven to completion to avoid imperfections and impurities, which are extremely difficult to separate. Alternatively, dendrimers can be built starting from the periphery; in these convergent methods, small molecules are assembled to larger dendrons and eventually attached to a central core. The removal of impurities is less problematic; however, the resulting dendrimers are usually not as large as those synthesized by divergent methods. The molecular weight of dendrimers is increasing with the number of branching cycles that are performed during synthesis. As a consequence thereof, the number of functional groups on the surface is increasing with each successive generation.

The DA reaction has been successfully applied to the synthesis of dendrimers; the synthetic strategies are quite similar to those used in the preparation of block copolymers. In most approaches, the coupling between furan and maleimide was utilized to assemble symmetrical, thermally responsive dendrimers. For instance, benzyl aryl ether based dendrons with furan moieties at their focal point were cross-linked with a bismaleimide linker [96, 97]. Since the DA reaction does not require metal catalysts, the formed dendrimers are free of metal impurities, which is an advantage if their biological use is intended. Furthermore, approaches combining the CuAAC and the furan-maleimide DA reaction have been described [98, 99]. These approaches yield thermally reversible dendrimers that disassemble at 90–120 °C via rDA reaction and reassemble at 50 °C. A similar strategy has been used to prepare dendrimers carrying multiple drug molecules, which are released under physiological conditions by rDA reaction [100]. A dendrimer core was synthesized via a sequence of CuAAC reactions; lipoic acid was then conjugated to the periphery using DA chemistry (Fig. 1.2). Lipoic acid, which was used as a

model drug, is an important cofactor and antioxidant; the synthesized dendrimers could protect microglial cells from oxidative stress. However, it should be noted that the combination with CuAAC eliminates the advantage of the DA cycloaddition of being a metal-free click reaction. In a different approach, furan-functionalized poly(aryl ether) dendrons were reacted with maleimide-functionalized polyester dendrons to obtain segment block dendrimers [101]. In contrast to other approaches, in which the DA reaction was utilized to assemble symmetrical dendrimers, this is an example for the synthesis of unsymmetrical dendrimers. Moreover, the DA reaction was exploited in the synthesis of carbosilane dendrimers [102, 103] and spherical polyphenylene dendrimers [104].

As already discussed in the previous section, the DA reaction between furan and maleimide can be used to protect the maleimide group during incompatible reaction steps, such as radical polymerizations or Michael-type additions. For example, polyester dendrons containing furan-protected maleimide groups at their focal point were synthesized. *In situ* thermal deprotection exposed the maleimide groups; these were then reacted with an anthracene-appended polystyrene to afford dendronized polymers [105]. The same group described the synthesis of diblock and triblock dendron-polymer conjugates containing biodegradable polyester blocks and PEG [106]. It might be possible to cast such dendronized polymers as hydrophilic films; the multiple hydroxyl groups on these films could be converted to more reactive groups and functionalized with molecules of interest. In a different approach, multiarm star polymers were synthesized by ATRP using an initiator containing a furan-protected maleimide group. Thermal deprotection provided a thiol-reactive maleimide group; the polymer core was then successfully functionalized with glutathione [107]. The combination of DA chemistry and Michael-type addition reaction is, therefore, a promising strategy to decorate dendrimers with peptides or proteins.

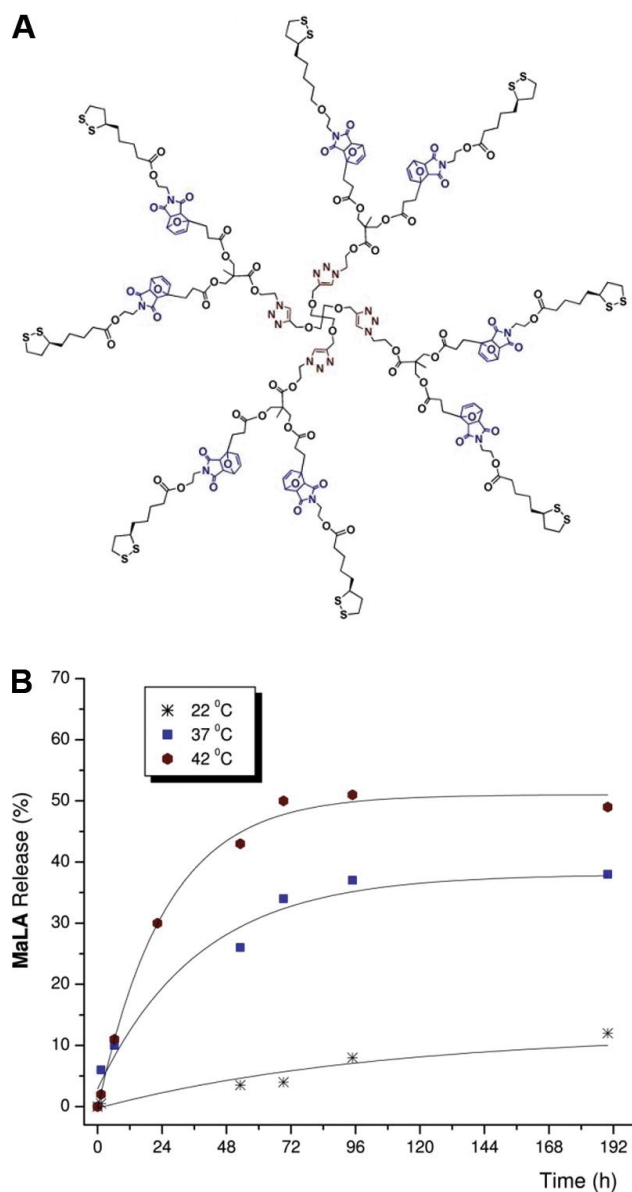


Figure 1.2: Lipoic acid (MaLA) is conjugated to the periphery of thermosensitive dendrimers via DA reaction (A). The rDA-mediated release of MaLA is temperature-dependent, as evaluated by ^1H -NMR spectroscopy (B). Adapted from Ref. [100] with permission of The Royal Society of Chemistry.

1.4.3 Surface functionalization

The fabrication of surfaces that interact with cells in a specific way is an enormous challenge in the development of biomaterials. For example, hydrophobic surfaces are frequently coated with hydrophilic polymers, such as PEG or poly(vinyl alcohol),

to create “stealth” materials, which effectively prevent the non-specific adsorption of plasma proteins and cells. On the other hand, synthetic materials that do not inherently interact with cells, such as hydrophilic polymer matrices, can be modified with proteins of the extracellular matrix (ECM), such as collagen, fibronectin, laminin or vitronectin, to provide “cues” that regulate cell attachment, proliferation and differentiation [108, 109]. Alternatively, biomaterials can be functionalized with short peptides such as Arg–Gly–Asp (RGD), Tyr–Ile–Gly–Ser–Arg (YIGSR) or Ile–Lys–Val–Ala–Val (IKVAV). The RGD sequence is derived from the integrin-binding site of fibronectin; surfaces modified with this tripeptide were shown to promote cell adhesion and spreading [110, 111]. The combination of both design principles (i.e., immobilization of PEG and functionalization with cell-binding peptides) enables the fabrication of biomimetic materials that interact with specific cell types in a certain way. The DA reaction is without doubt a useful tool for surface functionalization. The modification process basically comprises two major steps: first, either a diene or a dienophile is chemically bound to the surface; in a second step, a biomolecule is added that has been modified with the appropriate counterpart. Since the DA reaction proceeds in water without metal catalysts, the process can be carried out under physiological conditions and in the presence of cells.

For example, the DA cycloaddition has been successfully used for the immobilization of streptavidin–diene conjugates on maleimide-functionalized glass surfaces [48, 112]. Sun et al. [113] described a similar method for the chemoselective immobilization of biomolecules through DA chemistry. To this end, heterobifunctional PEG linkers containing cyclopentadiene in the α -position and a biomolecule in the ω -position were synthesized. The linkers were then coupled to maleimide-functionalized glass slides; in this way, biotin, lactose and protein A could be immobilized on solid substrates. The same group demonstrated the applicability of sequential DA reaction and CuAAC for the immobilization of biomolecules [114]. PEG linkers carrying cyclopentadiene and alkyne groups were immobilized on maleimide-functionalized glass slides via DA reaction; the alkyne groups on the surface enabled the conjugation of azide-containing biomolecules via CuAAC. Similar strategies could be applied to immobilize ECM proteins or antibodies on solid substrates; however, it should be kept in mind that the presence of copper(I) can induce severe damage to biomolecules [2–4]. Another way of functionalizing surfaces with cell adhesion peptides is the DA reaction between benzoquinone and cyclopentadiene. In this example, cyclopentadiene-tagged RGD peptides were

immobilized on a benzoquinone-functionalized substrate [115]. Interestingly, benzoquinone could be electrically reduced to hydroquinone; these hydroquinone groups were unable to react with cyclopentadiene-tagged RGD peptides, which allowed the generation of patterned surfaces.

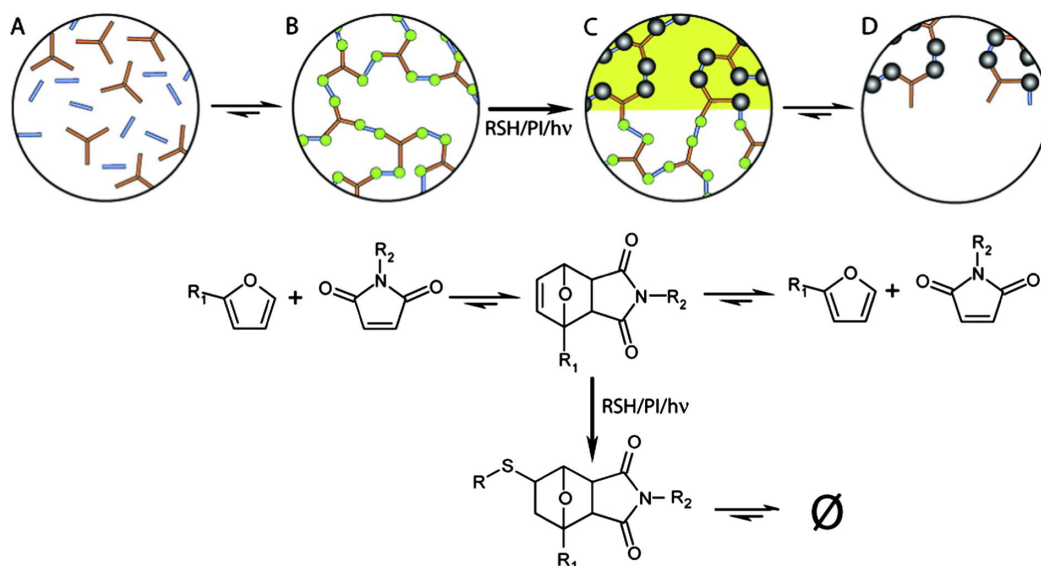


Figure 1.3: Generation of complex 3D structures by photolithography. Multifunctional furan and maleimide monomers (A) form a cross-linked polymer network (B) by DA reaction. In the irradiated areas (C), oxy-norbornene groups are converted to irreversible cross-links by radical reaction with thiol-containing molecules. Heating induces the rDA reaction and removes the material from the non-irradiated areas (D). Adapted with permission from Ref. [116].

Photolithography is another method for surface modification; thereby, patterned surfaces and complex 3D structures can be created with high precision. For this purpose, multifunctional furan and maleimide monomers were first cross-linked by DA reaction to form oxy-norbornene groups [116]. Irradiation and radical reaction with thiol-containing molecules converted these oxy-norbornene groups to irreversible cross-links. Heating the sample caused the material in the non-irradiated areas to depolymerize by rDA reaction, while leaving the irradiated regions unaffected (Fig. 1.3). In conjunction with thiol-functionalized molecules, such as cysteine-containing peptides, this process would enable the fabrication of patterned surfaces or complex 3D structures with defined chemical functionalization. A related method involved the modification of silicon oxide surfaces with photoreactive 3-(hydroxymethyl)naphthalene-2-ol moieties [117]. Irradiation with UV light generated reactive moieties, which rapidly underwent DA reaction with

suitable dienophiles. In this way, various molecules, such as fluorescent dyes or vinyl ether-biotin conjugates, could be selectively immobilized in the light-exposed areas.

1.4.4 Bioconjugation

As described in the previous section, the DA reaction can be utilized to immobilize biomolecules on solid substrates. Similar strategies can be applied to the functionalization of nanoparticles with DNA [118] or antibodies [119–123]. For example, Shi and Shoichet [119] synthesized furan-functionalized, amphiphilic block copolymers. Using a membrane dialysis method, these polymers self-assembled into nanoparticles with a hydrophobic inner core and a hydrophilic outer shell carrying furyl groups. Anti-HER2 antibodies (trastuzumab) were modified with maleimide functional groups in their Fc region and covalently bound to the nanoparticles via DA coupling (Fig. 1.4) [120]. These anti-HER2 immuno-nanoparticles specifically bound with HER2-overexpressing SKBR-3 breast cancer cells, demonstrating their capacity for targeted drug delivery. As a further proof of concept, the chemotherapeutic doxorubicin was bound to anti-HER2 immuno-nanoparticles via DA coupling [121]. While free doxorubicin showed similar cytotoxicity against both SKBR-3 cells and healthy HMEC-1 cells, doxorubicin-conjugated immuno-nanoparticles were significantly more cytotoxic against SKBR-3 cells. A similar strategy was used for the targeted delivery of small interfering RNAs and antisense oligonucleotides [123]. A potential disadvantage of this bioconjugation method is the electrophilicity of maleimide, which can result in side reactions with nucleophilic groups (e.g., sulfhydryl or amino groups) of other molecules (e.g., polymers, peptides or proteins), cells or tissues.

Furthermore, the DA/rDA reaction of furan and maleimide can facilitate the synthesis of maleimide-terminated polymers, which react with cysteine residues of proteins in a Michael-type addition reaction. For example, heterotelechelic polymers with a biotin group at one end and a furan-protected maleimide group at the other end were synthesized by RAFT polymerization [124]. After thermal deprotection, the polymer was conjugated to model proteins and anchored to streptavidin-functionalized surfaces. A similar approach was pursued by Mantovani et al. [125]; they used an initiator containing a furan-protected maleimide for the synthesis of hydrophilic polymers via ATRP. After the polymerization step, the maleimide group was reintroduced by rDA reaction; these maleimide-terminated polymers

were successfully employed in conjugation reactions with reduced glutathione and bovine serum albumin. Besides the preparation of protein-polymer conjugates, the hetero-DA reaction has been successfully used for the covalent modification of the interior surface of viral capsids [126]. Moreover, the DA reaction has been used for the preparation of peptide-oligonucleotide conjugates and synthetic neoglycoproteins; for this purpose, the reaction partners were equipped with a suitable diene-dienophile pair [127, 128].

Besides the normal electron-demand DA reaction, the IEDDA reaction is a valuable tool for bioconjugation. Both reactions share common characteristics; for example, they proceed in water at room temperature and do not require any catalyst. However, the IEDDA reaction has the additional advantage of being bioorthogonal, i.e., the reaction is inert to the myriad of functionalities found in proteins or cells. This opens up further possibilities for bioconjugation. In this context, especially the cycloaddition of s-tetrazine and trans-cyclooctene derivatives has proven to be useful. The reaction proceeds in high yield in organic solvents, water, cell media, or cell lysate [129, 130]. It has been utilized for site-specific fluorescence labeling of proteins on the cell surface and inside living mammalian cells [131]. Another important application of the IEDDA reaction is tumor pretargeting. In this approach, an antibody-conjugated trans-cyclooctene was injected into tumor bearing BALB/C mice [132]. After binding of the antibody to the tumor tissue, a tetrazine-functionalized clearing agent was injected. This clearing agent was bound to the circulating antibody via IEDDA coupling and enabled its rapid removal from blood. Afterward, a radiolabeled tetrazine was injected and coupled to the tumor-bound antibody via IEDDA reaction. This approach could boost the tumor radiation dose compared to non-pretargeted radioimmunotherapy. Using a similar principle, Zeglis et al. [133] developed a pretargeted PET imaging technology. A human A33 antibody was modified with trans-cyclooctene and injected into mice bearing SW1222 xenografts; afterward, the mice were injected with a radiolabeled tetrazine for PET imaging.

Using the IEDDA ligation, a temozolomide (TMZ) BioShuttle has been developed for the treatment of prostate cancer and brain tumors [134, 135]. In brief, a cell penetrating peptide (CPP) was linked via a redox-sensitive disulfide bridge to a nuclear localization sequence (NLS) carrying a cyclooctatetraene as the dienophile. In a second step, a TMZ-tetrazine conjugate was linked to the peptide via IEDDA ligation. The CPP module can facilitate cellular uptake of the cargo, while the NLS module mediates its transport into the nucleus. Compared to TMZ

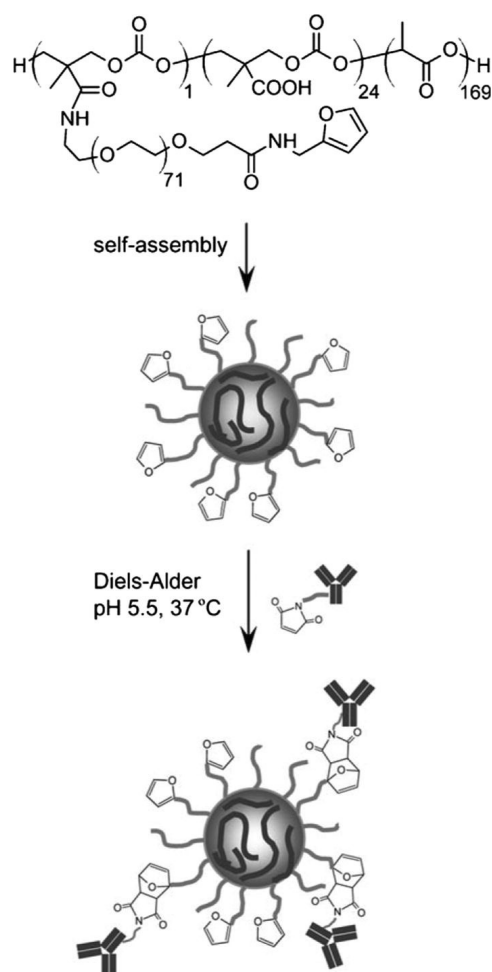


Figure 1.4: Functionalization of nanoparticles with antibodies. Furan-functionalized, amphiphilic block copolymers self-assemble into nanoparticles with a hydrophobic core and a hydrophilic outer shell carrying furyl groups. Maleimide-labeled anti-HER2 antibodies are covalently bound to the nanoparticles via DA coupling. Reprinted with permission from Ref. [120].

alone, the TMZ-BioShuttle was more cytotoxic against prostate cancer and human glioblastoma cell lines. Moreover, the IEDDA reaction has been employed to enable the instantaneous release of drug substances. To this end, Versteegen et al. [136] developed a novel bioorthogonal elimination reaction. First, a (*E*)-cyclooct-2-en-1-yl doxorubicin carbamate was prepared; IEDDA reaction with tetrazine and subsequent cleavage of the carbamate released the drug from the conjugate in a second step. Using this strategy, it would be possible to prepare antibody-drug-conjugates; the drug would be released from the tumor-bound antibody through

reaction with subsequently administered tetrazine. At this point it should be mentioned that other ligation reactions, such as the tandem [3 + 2] cycloaddition-retro-DA reaction, are promising bioconjugation methods as well. In this reaction, trifluoromethyl-substituted oxanorbornadiene derivatives react with various azides to form stable 1,2,3-triazole-linked products [137, 138].

1.4.5 Nanotechnology

Nanomaterials, such as dendrimers, polymeric micelles, polyplexes, nanoparticles, nanocapsules or liposomes, afford new opportunities in drug development and drug delivery. For example, many nanomaterials improve the solubility of hydrophobic drugs, prolong the circulating half-life, and reduce potential immunogenicity. Furthermore, nanomaterials can provide sustained or triggered release of drugs, and thus reduce the administration frequency. Nanoscale drug delivery systems often accumulate in specific tissues (e.g., tumors) through the enhanced permeability and retention effect (passive drug targeting). In addition, the presence of targeting ligands, such as antibodies or aptamers, can enhance the retention and cellular uptake of nanomaterials (active drug targeting). Both principles can enhance the therapeutic efficacy of drugs and reduce undesired side effects. Besides drug development and drug delivery, nanotechnology is also benefitting the development of diagnostics and biomaterials. In the field of tissue engineering, nanotechnology can enable the fabrication of scaffolds that closely resemble the native ECM [139].

The DA/rDA reaction has been successfully used for the assembly or disassembly of nanostructures. For example, Bapat et al. [140] synthesized block copolymers of maleic anhydride and styrene; subsequent ring opening of the anhydride groups with furfurylamine resulted in pendant furyl groups. These block copolymers were allowed to pre-assemble into polymeric micelles. The addition of a bismaleimide gave thermoreversible, core-crosslinked micelles; heating caused the micelles to dissociate back to the individual polymers. In an approach to control the dispersion and migration of nanomaterials, Costanzo et al. [141, 142] coated gold nanoparticles with thiol-terminated PS-*b*-PEG copolymers, where the PS and PEG blocks were joined via thermoreversible DA linkages. These PEG-functionalized nanoparticles were dispersed in a PS-*b*-PMMA copolymer matrix. Since PEG and PMMA are miscible, the nanoparticles were preferentially located within the PMMA domains of the matrix. Thermal treatment caused the PS-*b*-PEG copolymers to dissociate and exposed the PS ligands on the surface of the nanoparticles. Since PS and

PMMA are immiscible, migration of the nanoparticles to the PS domains of the matrix could be observed. Moreover, the rDA reaction has been exploited to fabricate reactive nanostructures via thermal nanoimprint lithography [143]. To this end, a polymer film with furan-masked maleimide groups was spin-coated onto a silicon substrate. Nanoimprinting was performed with a patterned silicon mold at 175 °C and a pressure of 400 psi; thereby, the mold pattern was transferred into the polymer. The high temperature simultaneously triggered the rDA reaction to yield a maleimide-patterned surface. These surfaces could be post-functionalized with iron oxide nanoparticles or RGD peptides. The reactive patterns may provide versatile scaffolds, e.g., for cellular patterning.

The rDA reaction can also be exploited to control drug release from nanoparticulate carriers. Bakhtiari et al. [144] developed an interesting approach for the release of molecules based on the photothermal effect of gold nanoparticles. A fluorescein dye was anchored on the surface of silica-gold core-shell nanoparticles via a thermoreversible DA linker. The fluorescence emission was efficiently quenched by the gold layer of the nanoparticles. When the system was illuminated at the surface plasmon resonance (SPR) wavelength of gold nanoparticles (typically 400 - 1100 nm), the absorbed light energy was converted into heat. This induced the rDA reaction; the dye was released from the nanoparticles, as indicated by the increasing fluorescence intensity (Fig. 1.5). The developed technology provides both temporal and spatial control of release and would, therefore, be useful for drug delivery and other biomedical applications. In a similar approach, gold nanorods were modified with PEG chains through DA cycloadducts [145]. Gold nanorods have an SPR band in the near-infrared (NIR) region, where light has its maximum tissue penetration depth. When the modified gold nanorods were irradiated with NIR light, the rDA reaction was induced by the photothermal effect and the PEG chains were released from the gold nanorods. This technology would enable the preparation of controlled release systems that respond to external stimuli.

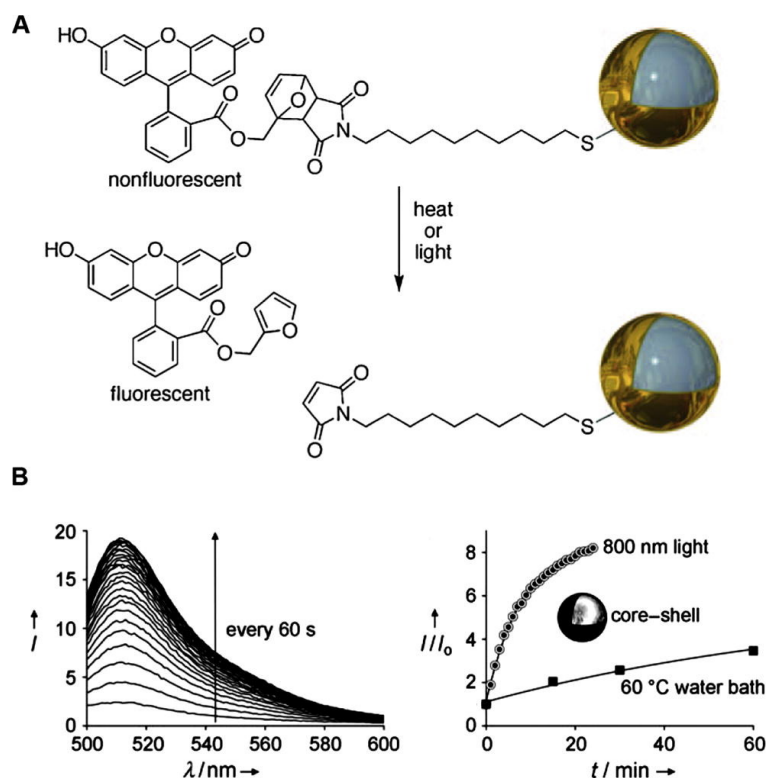


Figure 1.5: A fluorescein dye is anchored on the surface of silica-gold core-shell nanoparticles via a thermoreversible DA linker (A). The fluorescence intensity increases when aqueous dispersions of nanoparticles are heated or irradiated with NIR light (B). The technology enables the development of drug delivery systems that respond to external stimuli. Adapted with permission from Ref. [144].

1.4.6 Hydrogels

Hydrogels are polymer networks that are expanded throughout their whole volume by water; they can be fabricated from a wide range of natural (e.g., alginate, dextran or hyaluronic acid) and synthetic polymers (e.g., PEG or polymers based on acrylate monomers). Depending on how the polymer networks are formed, hydrogels can be classified into physical and chemical gels. In physical hydrogels, the networks are formed by reversible aggregation of polymer chains (e.g., hydrophobic interactions or ionic bonding), whereas chemical hydrogels contain covalently cross-linked networks [109, 146]. Covalently cross-linked hydrogels are versatile materials with many favorable properties (e.g., high water content, biocompatibility, mechanical flexibility, etc.). It is therefore not surprising that many pharmaceutical and biomedical applications of hydrogels have been proposed and investigated.

Hydrogels for drug delivery

The use of hydrogels as release systems for biopharmaceuticals, such as therapeutic proteins, seems highly attractive: many hydrogels can be administered by injection, they protect incorporated proteins against degradation, and they provide sustained or triggered drug release [146]. Drug loading and cross-linking are often performed simultaneously; the release rate can be adjusted by controlling the cross-linking density and, hence, the mechanical properties and permeability of the hydrogel. This requires efficient cross-linking reactions that do not adversely affect the stability of incorporated proteins. The DA reaction meets these criteria: the reaction proceeds in water at room temperature; furthermore, no purification step is required to remove potentially toxic catalysts or initiators. The DA reaction is, therefore, a suitable cross-linking method to prepare hydrogels.

For example, a self-healing dextran-based hydrogel was formed by cross-linking of a fulvene-modified dextran with a dichloromaleic acid-modified PEG [147]. Although the DA reaction between fulvene and dichloromaleic acid proved to be straightforward, the furan-maleimide pair is predominantly used for hydrogel formation. In most approaches, linear polymer chains with pendant furan moieties were cross-linked with bismaleimides. For example, hydrogels were prepared from N-vinyl-2-pyrrolidone, poly(N-isopropylacrylamine) or poly(furfuryl amine maleic acid monoamide-*co*-N-isopropyl-acrylamide) [148–150]. In this context, it has been shown that the gelation time, cross-linking density and swelling capacity depend on both the furan intake and the maleimide concentration. In contrast to that, the depolymerization temperature was only marginally influenced by the furan and maleimide concentrations [151]. At this point it should be mentioned that molecules bearing two furan moieties can act as cross-linking agent as well. For example, amphiphilic gels were prepared by DA reaction of acetylene dicarboxylate-containing PEG with furan-functionalized oligomers [152]. Alternatively, hydrogels can be formed by multiple DA reactions between two linear polymer chains with pendant furan and maleimide groups, respectively [153, 154]. For example, furan- and maleimide-functionalized HA derivatives formed biodegradable hydrogels in aqueous environment at 37 °C. Two model proteins, insulin and lysozyme, were successfully encapsulated and released over 21 days. However, possible side reactions between maleimide-functionalized HA and encapsulated proteins were not investigated in this study. Furthermore, the hydrogels preserved the viability of human adipose-

derived stem cells [154]. Therefore, these polysaccharide hydrogels may serve as a platform for both drug delivery and tissue engineering.

Despite the reversibility of the DA/rDA reaction, most hydrogels cross-linked by DA reaction do not readily degrade at 37 °C. It has been shown that the equilibrium conversion of the furan-maleimide pair varies from 74% at 85 °C to 24% at 155 °C; at sufficiently high temperature, significant depolymerization occurs via rDA reaction [49]. In order to cause degradation, multiple rDA reactions must occur simultaneously at significant rate, which is unlikely in densely cross-linked networks at 37 °C. However, Kirchhof et al. [155, 156] recently reported the preparation of PEG-based hydrogels that degraded under physiological conditions via rDA reaction. Star-shaped PEG was end-functionalized with furan and maleimide groups, respectively; hydrogels were formed by step-growth polymerization of the obtained macromonomers. Interestingly, the cross-linked gels degraded at pH 7.4 and 37 °C by rDA reaction and subsequent ring-opening hydrolysis of the generated maleimide groups (Fig. 1.6). Removal of the maleimide groups from the DA/rDA equilibrium by hydrolysis caused the DA adducts to revert to the starting materials. In this way, the rate of the rDA reaction was increased according to Le Châtelier's principle without the need for elevated temperatures. The gel properties (e.g., gel time, complex shear modulus and degradation time) were found to depend on the concentration, branching factor and molecular weight of the macromonomers. The determined values of the average network mesh size indicated that the prepared hydrogels could provide controlled release of therapeutic antibodies.

In the above-mentioned examples, the polymer networks were formed by DA reaction of suitable diene-dienophile pairs. However, it is also possible to combine two different gelation mechanisms (e.g., thermal gelation and covalent cross-linking). For example, Hsu et al. [157] synthesized furan-terminated poly(ethylene glycol)-*b*-poly(L-lactide) and poly(ethylene glycol)-*b*-poly(D-lactide) copolymers. Micellar solutions of the two polymers showed a temperature-dependent sol-gel phase transition at concentrations above 25%; the addition of a bismaleimide cross-linker could reinforce the gel structure, as indicated by the increased storage modulus. The combination of two different gelation mechanisms is an effective strategy to overcome the long gelation time of hydrogels cross-linked by DA reaction. This is particularly important when drug-loaded hydrogels are formed *in situ* (e.g., after subcutaneous or intravitreal injection) and rapid diffusion of the active ingredient from the injection site must be avoided. Besides serving as cross-linking reaction, the DA reaction between furan and maleimide can be used to

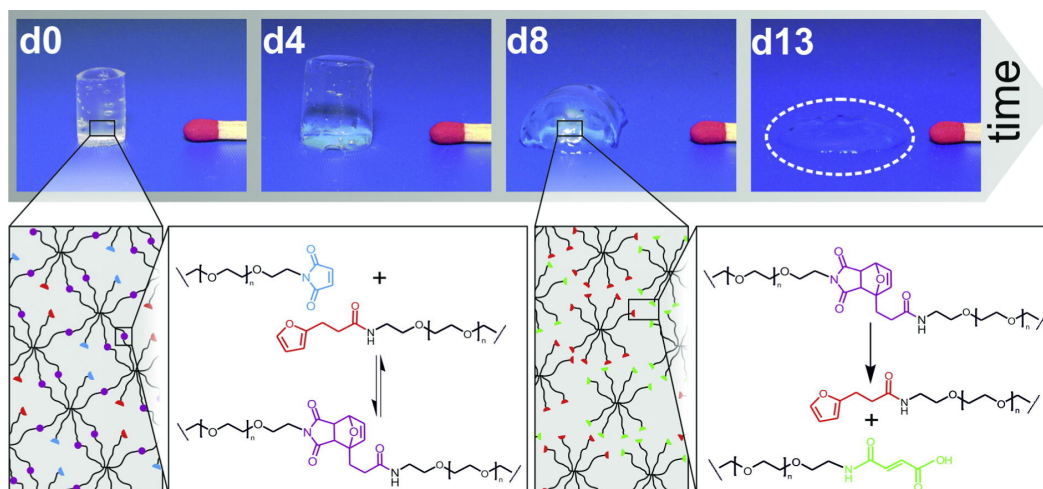


Figure 1.6: Preparation of degradable DA hydrogels. Eight-armed PEG is functionalized with furan and maleimide groups, respectively; hydrogels are formed by DA reaction of the obtained macromonomers. The cross-linked gels degrade under physiological conditions by rDA reaction and subsequent ring-opening hydrolysis of the generated maleimide groups. Reprinted from Ref. [156] with permission from The Royal Society of Chemistry.

protect the maleimide group during cross-linking. For example, hydrogels could be synthesized by radical polymerization of PEG monomethyl ether methacrylate and a furan-protected maleimide monomer [158]. Thermal deprotection by rDA reaction afforded maleimide-containing hydrogels. In a second step, these gels could be functionalized with a thiol-containing fluorescent dye or a thiol-containing biotin derivative via thiol-ene addition.

Hydrogels for tissue engineering

In the field of tissue engineering, hydrogels can be used as space filling agents, as vehicles for the delivery of bioactive molecules, or as scaffolds for cell delivery. Hydrogels designed to encapsulate cells must meet specific requirements. For example, the gelation process and the cross-linked material must be compatible with cells and the surrounding tissue, the hydrogel must allow the diffusion of nutrients and metabolites, and the scaffold must have sufficient mechanical integrity to withstand the occurring mechanical loads [109]. Furthermore, the hydrogel must present chemical and physical stimuli to direct the formation of a desired tissue [159]. Since the DA cycloaddition proceeds under physiological conditions without any catalyst or initiator, the reaction is suitable for the preparation of

cell-laden hydrogels. In general, two strategies involving the DA reaction can be distinguished: first, the DA reaction can be used as a cross-linking method; second, the DA/rDA equilibrium can be exploited for the conjugation and/or release of bioactive molecules that regulate cell growth, spreading or differentiation. Therefore, most hydrogels are hybrid materials consisting of both synthetic and natural compounds.

For example, furan-modified hyaluronic acid (HA) derivatives were cross-linked with maleimide-functionalized PEG [160]. The mechanical and degradation properties of the resulting hydrogels could be tuned by varying the furan to maleimide molar ratio. Since neither additional cross-linking agents nor catalysts were required, HA-PEG hydrogels showed a high level of cell survival, suggesting that these hydrogels would be suitable for applications in tissue engineering. Furthermore, epidermal growth factor gradients could be generated by photopatterning [161]. These chemical gradients are important in guiding cell migration, development and growth. In a related approach, an injectable HA-PEG hydrogel was prepared by integrating two cross-linking processes [162]. HA was modified with tyramine and furylamine functional groups; the hydrogel was formed by enzymatic cross-linking between the tyramine groups, followed by a second cross-linking step between furan groups and maleimide-functionalized PEG. As already discussed in the previous section, the combination of two different cross-linking methods ensures the fast gelation of *in situ* forming hydrogels. Encapsulated ATDC-5 cells showed high viability and proliferation, indicating the great potential of HA-PEG hydrogels in cartilage tissue engineering. To refine the system, interpenetrating networks were synthesized from HA, gelatin and chondroitin sulfate. Cross-linking by DA chemistry gave biodegradable hydrogels that are expected to mimic the natural ECM of cartilage [163].

To enhance cell adhesion and better mimic the ECM, Silva et al. [164] synthesized a novel peptide-modified gellan gum hydrogel. To this end, a maleimide-containing GRGDS peptide was linked to furan-modified gellan gum via DA chemistry. These GRGDS-modified hydrogels have been shown to promote adhesion and proliferation of neural stem/progenitor cells (NSPCs). Co-culture with olfactory ensheathing glia could further improve survival and outgrowth of NSPCs. Therefore, the developed system may be beneficial in regenerative medicine, e.g., to promote repair after spinal cord injury. Besides the normal electron-demand DA reaction, the tetrazine-norbornene IEDDA reaction has been used for the formation of cell-laden hydrogels [165]. A multifunctional PEG-tetrazine macromonomer was

reacted with an enzymatically degradable dinorbornene peptide; a norbornene-containing RGDS peptide was added to promote cell adhesion. Encapsulated human mesenchymal stem cells (hMSCs) showed high viability after 72 h, demonstrating the cytocompatibility of the cross-linking reaction.

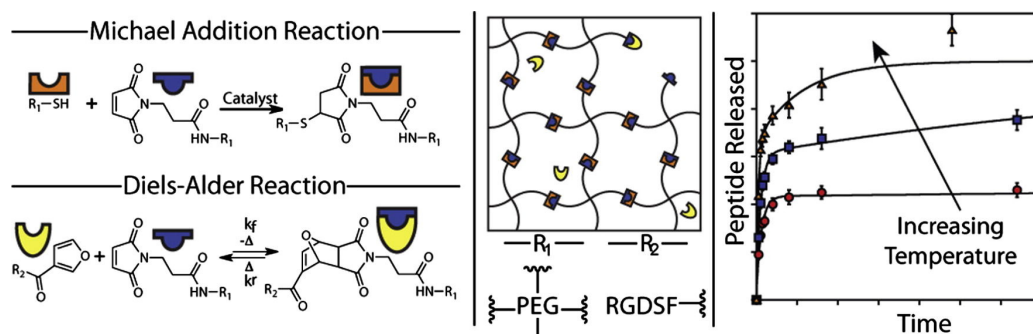


Figure 1.7: rDA-mediated release of RGDS peptides from PEG hydrogels. Furan-labeled RGDS peptides are covalently linked to tetrafunctional PEG-maleimide macromonomers via DA reaction. Hydrogels are formed by Michael addition reaction between PEG-maleimide and tetrafunctional PEG-thiol macromonomers. The release of furan-labeled RGDS is mediated by rDA reaction; increasing the temperature results in higher release rates. Reprinted with permission from Ref. [166].

As already mentioned before, the DA/rDA equilibrium can be exploited to control and sustain the release of drugs from hydrogels. As a proof of concept, furan-labeled RGDS peptides were covalently linked to multifunctional PEG-maleimide macromonomers via DA reaction; a Michael-type addition reaction between the remaining maleimide groups and multifunctional PEG-thiol macromonomers was then performed to create a covalently cross-linked hydrogel [166]. *In vitro* release experiments at three distinct temperatures demonstrated rDA-mediated release of the furan-labeled RGDS peptide from the hydrogel (Fig. 1.7). To demonstrate the practical utility of this approach, a furan-containing dexamethasone peptide was covalently linked to a PEG hydrogel via DA reaction as described above [167]. In a 2D culture model, rDA-mediated release of dexamethasone stimulated hMSCs to undergo osteogenic differentiation. More distinct differences were observed in 3D culture, when a dexamethasone releasing hydrogel was encapsulated within an hMSC-laden hydrogel, as indicated by increased alkaline phosphatase activity and mineral deposition.

1.5 Pitfalls and challenges of the Diels–Alder reaction

As outlined in the previous section, the DA reaction has been successfully applied to various problems in drug delivery and biomaterial design. However, to exploit the full potential of the DA reaction, it is necessary to talk about possible pitfalls and challenges as well. Although the DA reaction is extremely efficient, the comparatively slow reaction rate at room temperature may be a potential drawback. While the reaction rate may be less of an issue in applications such as the synthesis of polymers or dendrimers, it is certainly critical in the preparation of *in situ* forming hydrogels. Such hydrogels must completely encapsulate the drug after injection and rapidly form a drug depot at the application site, e.g., under the skin or inside the eye. Cross-linking via DA reaction can result in dose dumping; this may cause adverse effects or drug-induced toxicity. In theory, the gel time could be decreased by increasing the temperature [49] or pressure [168]; furthermore, Lewis acids, such as AlCl_3 , $\text{Cu}(\text{NO}_3)_2$ or $\text{Ni}(\text{NO}_3)_2$, can dramatically accelerate the DA reaction [22–25]. However, these reaction conditions are not compatible with biological systems or proteins. Instead, the gel time can be decreased by combining two separate cross-linking processes. For example, fast-gelling thermoresponsive hydrogels were obtained by stereocomplex formation of enantiomeric PLA and concomitant DA reaction [157]. Similarly, the integration of enzymatic cross-linking and DA chemistry proved to be successful in the preparation of injectable hydrogels [162]. Furthermore, it has been reported that the addition of β -cyclodextrin catalyzes the DA reaction of some dienes and dienophiles [44, 169]. Therefore, β -cyclodextrin might serve as innocuous alternative to Lewis acids and accelerate the formation of hydrogels.

Besides the reaction rate, the reversibility of the normal electron-demand DA reaction represents another potential pitfall that needs to be considered. Although the reversibility of the reaction opens up many possibilities, such as the fabrication of degradable materials or the development of controlled release systems, the formation of stable adducts may be required in applications such as the synthesis of non-degradable polymers or dendrimers. Similarly, the functionalization of surfaces or nanoparticles with biomolecules often requires the formation of stable conjugates. While the furan-maleimide pair undergoes rDA reaction at around 100 °C, the cycloreversion of the anthracene-maleimide adduct occurs at temperatures above 200 °C [19]. It is therefore possible to prepare stable conjugates by using anthracene

as diene and maleimide as dienophile. Furthermore, the reversibility of the reaction can be controlled by changing the substitution pattern of the involved DA pair, or by changing the solvent system [51, 52]. To circumvent the above-mentioned drawbacks, the IEDDA reaction has been proposed as an alternative ligation method [129, 130]. The primary adduct of the IEDDA reaction stabilizes by eliminating nitrogen so that the reverse reaction is excluded (Scheme 1.1D). Furthermore, systems can be designed in such a way that the DA reaction can be “locked” and “unlocked” using light [170]. In the first step, a photoresponsive dithienylfuran was reacted with N-ethylmaleimide. Irradiation with UV light led to ring closure of the DA product; this ring-closed photoisomer lacked the cyclohexene ring necessary for the rDA reaction to proceed. However, irradiation with visible light regenerated the ring-open photoisomer and the ability to undergo rDA reaction. This concept could be used, e.g., to control drug release. It would be possible to bind drug molecules to a polymeric carrier and turn “off” the rDA reaction by UV irradiation. This would effectively prevent premature drug release, e.g., during storage. Irradiation with visible light would then “unlock” the DA reaction and enable drug release. In the context of bioconjugation, the necessity to insert reactive moieties, such as maleimide or trans-cyclooctene groups, into the biomolecule represents another disadvantage of the DA reaction [120, 127, 131, 133]. The relevant groups can be incorporated by reacting the biomolecule, e.g., with N-succinimidyl 4-maleimidobutyrate or (E)-cyclooct-4-en-1-yl succinimidyl carbonate; however, these labeling reactions are not site-specific and the product needs to be purified by dialysis, ultrafiltration or size-exclusion chromatography. The site-specific incorporation of norbornene, trans-cyclooctene or furan moieties into proteins can be realized using the pyrrolysyl-tRNA synthetase/tRNA_{CUA} pair from *Methanosarcina* species [171–174]. These genetically encoded groups enable the selective modification of proteins via DA or IEDDA chemistry. In approaches where the DA/rDA equilibrium is exploited to control the release of drugs, it should be furthermore considered that incorporated furan or maleimide moieties remain attached to the molecule after release. These remaining “tags” may affect the stability, bioactivity, receptor affinity or immunogenicity of peptides and proteins [175–181].

However, the most serious drawback is that the normal electron-demand DA reaction is not inert to nucleophiles of proteins or cells. For example, maleimide is a strong electrophile; it can undergo Michael-type addition with cysteine, lysine, arginine, histidine and tryptophan residues of proteins [182]. This side reaction can

on the one hand inhibit the DA cycloaddition; on the other hand, it can result in the formation of unwanted side products, e.g., during the synthesis of bioconjugates (Fig. 1.8A). When the DA reaction is used to prepare hydrogels, the Michael-type addition of nucleophilic amino acid residues to maleimide groups can affect both the availability and biological activity of entrapped biomolecules [182–184]. To prevent this side reaction, the bioconjugation or cross-linking reaction should be carried out in acidic buffer (e.g., MES buffer pH 4.5–5.5). Amino groups are protonated at this pH; this lowers the nucleophilicity of basic amino acid residues and inhibits their Michael-type addition to maleimide [182]. Another advantage is the increased stability of maleimide at acidic pH. As a result, bioconjugation or cross-linking processes become more efficient, as less maleimide groups are consumed by ring-opening hydrolysis [156]. However, it should be noted that lowering the pH may induce protein denaturation and aggregation [185, 186]. To develop a nucleophile-tolerant DA ligation reaction, Tang et al. [187] calculated the Gibb’s free energies of activation (ΔG^\ddagger) of DA and Michael-type addition reactions. They found that the Michael-type addition of methanethiol to N-methylmaleimide has a much lower energy barrier ($\Delta G^\ddagger = +3.4 \text{ kcal mol}^{-1}$) than the DA reaction of 1,3-butadiene and N-methylmaleimide ($\Delta G^\ddagger = +20.9 \text{ kcal mol}^{-1}$). Compared with this, the energy barrier for the thiol addition to 1,2-bis(hydroxymethyl)-3-carboxycyclopropene is much higher ($\Delta G^\ddagger = +26.2 \text{ kcal mol}^{-1}$); however, the energy barrier for the DA reaction ($\Delta G^\ddagger = +24.2 \text{ kcal mol}^{-1}$) is still relatively low due to the ring strain of cyclopropene. Therefore, 1,2-bis(hydroxymethyl)-3-carboxycyclopropene may act as a nucleophile-tolerant dienophile in DA ligation reactions (Fig. 1.8B). As a last point, I would like to remind the reader that the IEDDA reaction is, unlike the normal electron-demand DA reaction, a bioorthogonal ligation reaction that tolerates a broad range of biological functionality [129, 130].

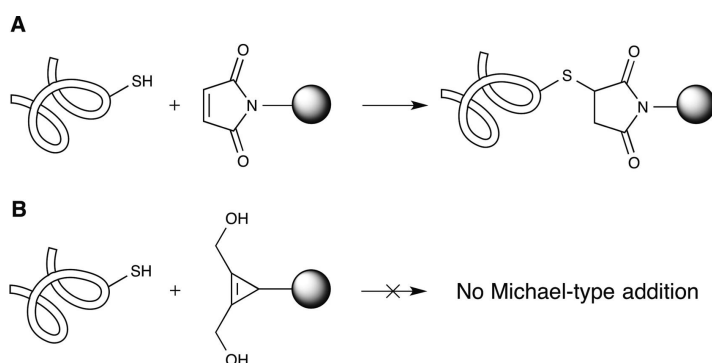


Figure 1.8: Michael-type addition reaction of the thiol group to maleimide (A). 1,2-Bis(hydroxymethyl)cyclopropene derivatives may act as nucleophile-tolerant dienophiles in DA ligation reactions (B).

1.6 Summary and perspectives

Although the DA reaction has certain limitations, it is without doubt one of the most useful reactions for the development of drug delivery systems and biomaterials. Fig. 1.9 illustrates possible applications of the DA reaction in pharmaceuticals and biomedical engineering. For reasons of clarity, the furan-maleimide pair is exemplarily used in the illustration; in practice, other diene-dienophile pairs, such as anthracene and maleimide, can be employed as well. The DA cycloaddition is an efficient and selective coupling reaction that can be employed for the synthesis of copolymers and dendrimers (Fig. 1.9A). In this context, the cycloaddition of furan and maleimide can protect the maleimide functionality during incompatible reaction steps, e.g., during radical polymerizations (Fig. 1.9B). In the biomedical field, the DA reaction (and in particular the IEDDA reaction) can be applied to bioconjugation. For example, the DA cycloaddition can be employed for the functionalization of drug delivery systems with targeting ligands such as peptides, antibodies or aptamers (Fig. 1.9C). In the context of drug delivery systems, the DA/rDA equilibrium can also be exploited to control and sustain the release of active ingredients from nanoparticulate carriers or hydrogels (Fig. 1.9D). Similar strategies can be applied to the functionalization of surfaces with biomolecules, such as cell adhesion peptides or ECM proteins (Fig. 1.9E). And last but not least, the DA reaction can be used as a cross-linking method for hydrogel preparation (Fig. 1.9F). These kinds of hydrogels may serve as controlled release systems for biopharmaceuticals or as three-dimensional scaffolds for cell transplantation. At

the end, I hope that the herein provided set of tools may facilitate the application of the DA reaction to solve important pharmaceutical or biomedical problems.

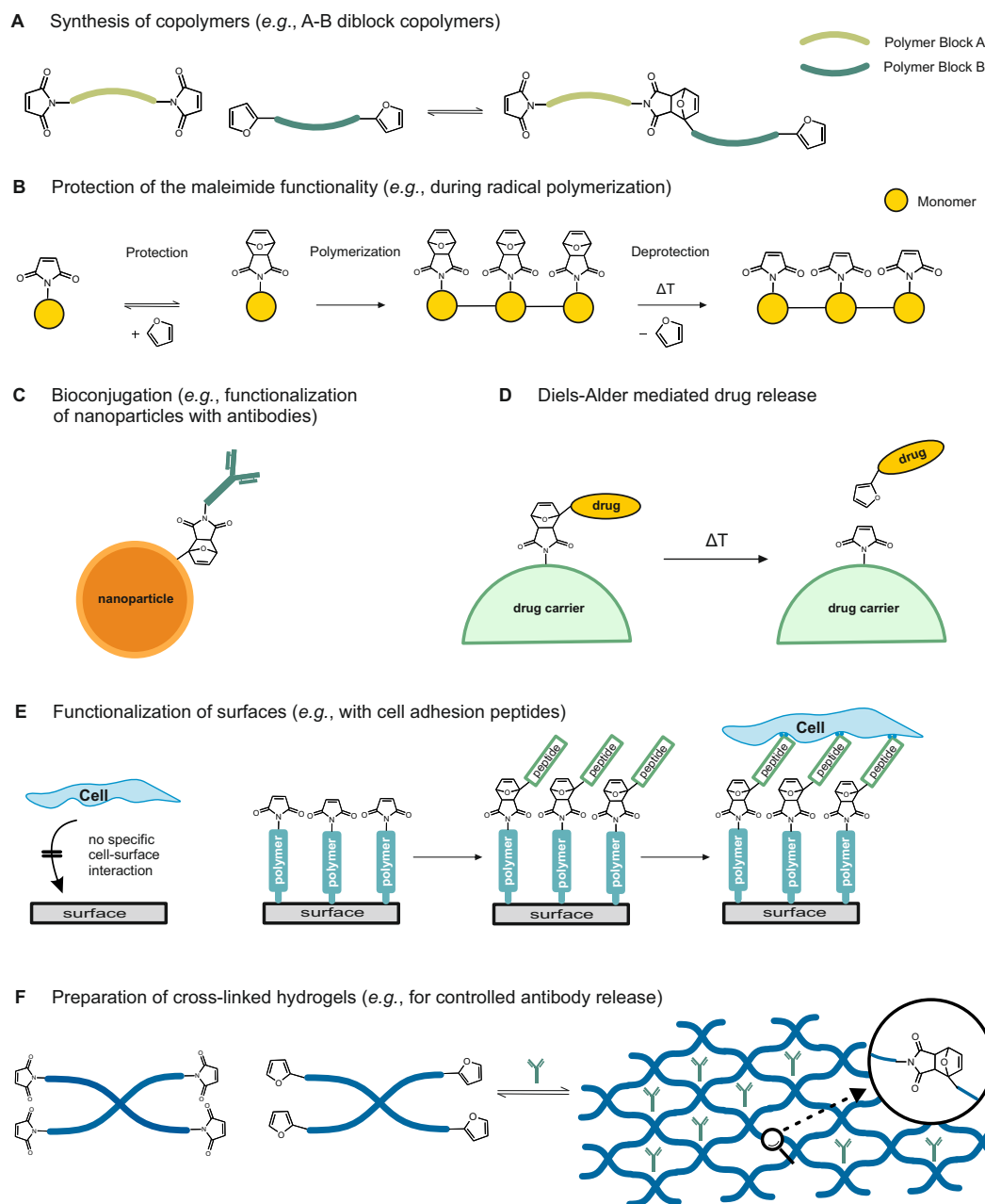


Figure 1.9: Possible applications of the DA reaction in pharmaceuticals and biomedical engineering.

Chapter 2

Goals of the thesis

Since the approval of the first monoclonal antibody Muromonab-CD3 by the US Food and Drug Administration in 1986, antibodies have revolutionized the treatment of cancer, autoimmune disorders, and other severe diseases [188, 189]. However, despite their high specificity, systemic administration of antibodies can be associated with adverse effects, such as immune reactions, autoimmune conditions, platelet disorders, and infections [190]. Therefore, localized antibody therapy can be superior to systemic administration when diseases are confined to a specific area or tissue. In local therapy, antibodies are directly administered to the site of disease. During this treatment, comparably low antibody doses can be utilized to achieve therapeutic goals while avoiding systemic effects and reducing therapy costs [191].

Local antibody delivery has already been demonstrated to be beneficial for a variety of diseases. Prominent examples include intra- or peritumoral injections [192–194], intraarticular injections for the treatment of arthritic joint diseases [195], and intrathecal injections to alleviate disorders of the central nervous system [196]. A particularly interesting example is intravitreal antibody administration for the treatment of vitreoretinal diseases, such as neovascular age-related macular degeneration (AMD) or proliferative diabetic retinopathy (PDR) [197, 198]. During the treatment, VEGF-neutralizing antibodies or antibody fragments are injected directly into the vitreous humor to mitigate retinal and choroidal neovascularization [199]. As the ocular half-life of commonly used antibodies is limited, e.g., 9.8 days for bevacizumab [200] and 7.2 days for ranibizumab [201], injections must be repeated on a regular basis to maintain therapeutic levels. However, intravitreal injections are associated with patient discomfort and may be accompanied by rare but serious complications [202]. Antibody reservoirs that enable controlled long-term release would help to reduce the dosing frequency, improve patient compliance, and reduce treatment costs. Therefore, the development of delivery systems that provide controlled local antibody release is a core aspect for improving antibody therapy in general and for the treatment of vitreoretinal diseases in particular.

Hydrogels can be considered nearly ideal carriers for antibody delivery as they can be administered using minimally invasive techniques, are biocompatible, provide a protective environment against degradation, and can be loaded with high amounts of antibody [146, 184]. There is a myriad of materials and a great variety of gelation mechanisms that can be utilized to prepare hydrogels. As introduced in **Chapter 1**, the Diels-Alder (DA) reaction, especially the one between maleimide and furan, is a highly promising click reaction for the design of hydrogels and

biomaterials. DA click hydrogels can be formed via covalent cross-linking at mild conditions without the need for a catalyst. Moreover, no toxic by-products are formed and the resulting hydrogels are degradable. Therefore, DA hydrogels can be cross-linked directly at the site of injection which makes them highly attractive for pharmaceutical applications. However, it has also been highlighted in the previous chapter that the use of DA reactions is limited by two major drawbacks. First, gel formation proceeds slowly which prevents rapid depot formation at the site of injection. Consequently, antibodies may not be reliably entrapped inside the gel matrix which could result in dose dumping and adverse effects. Second, maleimide cannot only undergo DA reactions as a dienophile but is also a strong electrophile. Therefore, Michael-type addition reactions with nucleophilic residues on proteins are a serious concern that should be prevented because these reactions could alter antibody structure, lead to activity loss, or adversely affect release. The goal of this thesis was to utilize click chemistry for the development of antibody delivery systems. A particularly important aim was to identify new ways to circumvent the drawbacks of the DA click reaction while maintaining its advantages. In this way, the full potential of DA click hydrogels as a delivery system for local antibody therapy could be utilized.

For the preparation of conventional DA hydrogels, multi-armed poly(ethylene glycol) (PEG) functionalized with maleimide or furyl groups are combined in aqueous solution and gelation is achieved via chemical cross-linking [155]. However, as mentioned above the gel formation proceeds too slowly for many applications. In a first approach to accelerate gelation, hydrophobic alkyl spacers were inserted between the PEG backbone and the functional end-groups. The goal of this approach was to induce hydrophobic association of the terminal ends and to facilitate the interaction of the functional groups. Consequently, a more efficient cross-linking process should be achieved which would be accompanied by shorter gel times, fewer network defects, improved mechanical properties, and the ability to delay antibody release (**Chapter 3**).

In an alternative approach, macromonomers were synthesized employing poloxamine instead of PEG as a polymer backbone. Poloxamine solutions are biocompatible and well-known for exhibiting temperature induced gelation. Ideally, functionalization of four-armed poloxamines with maleimide and furyl groups would lead to dual gelling hydrogels that immediately gel at body temperature and concomitantly

cross-link via the DA reaction. Such hybrid hydrogels combine the immediate physical sol-gel transition with the stability of chemically cross-linked hydrogels and, therefore, the best properties of both mechanisms. Moreover, eight-armed macromonomers were synthesized to study the effect of branching and to tailor mechanical properties and antibody release profiles (**Chapter 4**).

As introduced above, Michael-type reactions of maleimide with nucleophilic amino acid side chains are a serious concern. In order to overcome this issue, antibodies could be loaded into micro-sized gel particles to safeguard them from detrimental side-reactions. Moreover, such antibody-loaded microgels could be utilized as a delivery platform for local antibody delivery. However, the fabrication of antibody-loaded microgels with narrow size-distribution and without negatively affecting antibody stability is highly challenging. To achieve this goal, the combination of microfluidics and thiol-ene photoclick chemistry was evaluated as a protein compatible fabrication process for antibody-loaded microgels (**Chapter 5**).

Finally, it would be ideal if undesired side-reactions could be suppressed by simply adding a protective excipient before cross-linking. In this way, hydrogel properties, macromonomer structure, and cross-linking conditions could remain unchanged while protein-conjugation and activity loss is circumvented. Various pharmaceutically relevant polyanions were evaluated as protective excipients. In this approach it was hypothesized that electrostatic interactions cause reversible binding of polyanions to the protein surface and thereby act as a “shield” to protect the proteins against detrimental reactions. The effect of polyanions on protein-polymer conjugation, protein activity, and release was investigated (**Chapter 6**).

Chapter 3

Design of hydrogels for delayed antibody release utilizing hydrophobic association and Diels–Alder chemistry in tandem

Published in *Journal of Materials Chemistry B*

The content of this chapter was published as: *J. Mater. Chem. B*, 4: 3398–3408, 2016.
doi: 10.1039/c6tb00223d

Abstract

Biodegradable hydrogels were prepared from furan- and maleimide-functionalized eight-armed poly(ethylene glycol) with an average molecular mass of 40,000 Da (8armPEG40k-furan and 8armPEG40k-maleimide) using the Diels–Alder (DA) reaction as a cross-linking mechanism. Hydrophobic 6-aminohexanoic acid (C_6) and 12-aminododecanoic acid (C_{12}) spacers were introduced between the polymer backbone and the functional end-groups; the influence on the gel properties was studied. Modification with C_6 and C_{12} spacers induced hydrophobic interactions between the macromonomers leading to association and increased viscosity of the polymer solutions; both effects were influenced by the spacer length. In combination with DA cross-linking, hydrophobic derivatives of 8armPEG40k-furan and 8armPEG40k-maleimide led to hydrogels with improved properties. Upon introduction of C_{12} spacers, gelation of 8armPEG40k hydrogels occurred twice as fast. Interestingly, no effect was observed when only one of the two components had been modified. Our experiments suggest that the association of macromonomers by hydrophobic interactions facilitates chemical cross-linking via DA chemistry. This hypothesis is supported by calculations of the network mesh size and the Young’s modulus of compression, which showed an increased cross-linking density of hydrophobically modified hydrogels. As a consequence of the increased cross-linking density, the degradation stability of C_{12} -modified hydrogels increased by a factor of 4. Moreover, hydrophobic modification improved the hydrolytic resistance of maleimides; this also contributes to gel stability. The *in vitro* release of bevacizumab, which served as a model antibody, could be delayed for almost 60 days using modification with C_{12} . Similar trends were observed for C_6 -modified 8armPEG40k hydrogels; however, the effects were considerably weaker. In summary, utilizing hydrophobic association and chemical cross-linking in tandem is a promising approach to create biodegradable hydrogels for delayed antibody release.

3.1 Introduction

Since the introduction of recombinant insulin [203] more than three decades ago, the steady progress in pharmaceutical biotechnology has resulted in the launch of numerous biologics. In 2014 alone, 12 new biologics, such as recombinant proteins and monoclonal antibodies, were approved by the US Food and Drug Administration [204]. Among these, monoclonal antibodies are exceptionally promising therapeutics as they provide great specificity and affinity toward their clinical targets [205–207]. Indeed, therapeutic antibodies have significantly advanced the treatment of severe diseases, such as cancer [208], rheumatoid arthritis [209], or age-related macular degeneration [197]. However, despite their therapeutic value, antibodies have two major shortcomings that limit potential applications [210]. Firstly, antibodies are fragile molecules and, therefore, prone to aggregation [211] and degradation [212]. Secondly, most antibodies have to be administered by injection or infusion, as their oral bioavailability is generally low [213]. To improve the compliance and reduce the administration frequency, innovative drug delivery systems that provide sustained, delayed or intermittent antibody release are needed.

Among these drug delivery systems, hydrogels are particularly suitable for controlled antibody release [146]. Firstly, hydrogels can act as a drug depot that protects the incorporated protein from degradation. Secondly, the release rate can be tailored to the specific therapeutic needs; for example, hydrogels can prolong the dosing intervals by providing sustained or delayed antibody release. Hydrogels can be prepared from a wide range of natural and synthetic polymers via physical or chemical cross-linking [183, 214]. Physical cross-linking (e.g., via ionic or hydrophobic interactions) enables the preparation of *in situ* forming hydrogels that respond to external stimuli, such as ionic strength or temperature [67, 215–217]. These systems can be administered in liquid form and rapidly turn into a solid gel after injection. However, the resulting hydrogels are often considered not stable enough for sustained drug release [218–220]. Chemically cross-linked hydrogels, on the other hand, provide superior mechanical properties and stability against dissolution. However, only few chemical reactions are suitable for *in situ* cross-linking [184]; furthermore, controlling the cross-linking rate can be challenging. Gelation must be fast enough to completely encapsulate the drug after injection; on the other hand, rapidly gelling formulations can clog the needle and prevent the application of the gel. As a consequence, the combination of physical interactions

and chemical cross-linking may open up new possibilities to design rapidly forming hydrogels with improved stability.

Recently, the Diels–Alder (DA) reaction has been introduced as a promising cross-linking mechanism for the preparation of degradable, poly(ethylene glycol) (PEG) based hydrogels [155, 156, 221]. Since the DA reaction proceeds at body temperature in the absence of potentially toxic catalysts, it is in principle suitable for *in situ* cross-linking. However, the slow cross-linking rate can prove problematic and prevent the formation of a drug depot after injection [222]. In conventional DA hydrogels, star-shaped PEG is end-functionalized with furyl and maleimide groups; gelation occurs by step-growth polymerization of complementary macromonomers. In this study, hydrophobic alkyl spacers were introduced between the PEG chains of eight-armed PEG and the reactive end-groups. In this way, amphiphilic macromonomers were created. The hydrophilic PEG core ensures water solubility, while the hydrophobic end-groups are expected to stick together and facilitate cross-linking via DA reaction. In the first part of this study, the association of amphiphilic macromonomers in aqueous solution was investigated by means of fluorescence spectroscopy and viscosity measurements. In the second part, hydrogels were prepared and the impact of physical interactions on gel formation, average network mesh size, and mechanical properties was studied. In the last part, the hydrogels were characterized regarding their swelling and degradation behavior. Finally, the gels were loaded with bevacizumab and the *in vitro* release was determined.

3.2 Materials and methods

3.2.1 Materials

Anhydrous 1,4-dioxane, dichloromethane, sodium bicarbonate (NaHCO_3), sodium sulfate (Na_2SO_4), and triphenylphosphine were purchased from Acros Organics (Geel, Belgium). Boc-6-aminohexanoic acid was purchased from Bachem (Weil am Rhein, Germany). Diethyl ether was obtained from CSC Jäcklechemie (Nuremberg, Germany). Eight-armed poly(ethylene glycol) with a molecular mass of 40,000 Da (8armPEG40k-OH) was purchased from JenKem Technology (Allen, TX, USA). Cetareth-20 was obtained from Kolb Distribution Ltd (Hedingen, Switzerland). Acetyl chloride, 12-aminododecanoic acid, anhydrous dimethylformamide, anhydrous tetrahydrofuran, deuterated chloroform (CDCl_3), N,N'-dicyclohexylcarbodiimide (DCC), diisopropyl azodicarboxylate, N,N'-diisopropyl-

ethylamine, di-*tert*-butyl dicarbonate, fluorescamine, 3-(2-furyl)propanoic acid, N-hydroxysuccinimide (NHS), N-methoxycarbonylmaleimide, piperidine, and pyrene were received from Sigma-Aldrich (Taufkirchen, Germany). All other chemicals were obtained from Merck KGaA (Darmstadt, Germany). Bevacizumab (Avastin[®], 25 mg mL⁻¹, Roche Ltd, Basel, Switzerland) was kindly provided by the hospital pharmacy of the University of Regensburg (Germany). Purified water was freshly prepared using a Milli-Q water purification system (Millipore, Schwalbach, Germany).

3.2.2 ¹H-NMR spectroscopy

¹H-NMR spectra were recorded in CDCl₃ at 295 K using a Bruker Avance 300 spectrometer (Bruker BioSpin GmbH, Rheinstetten, Germany).

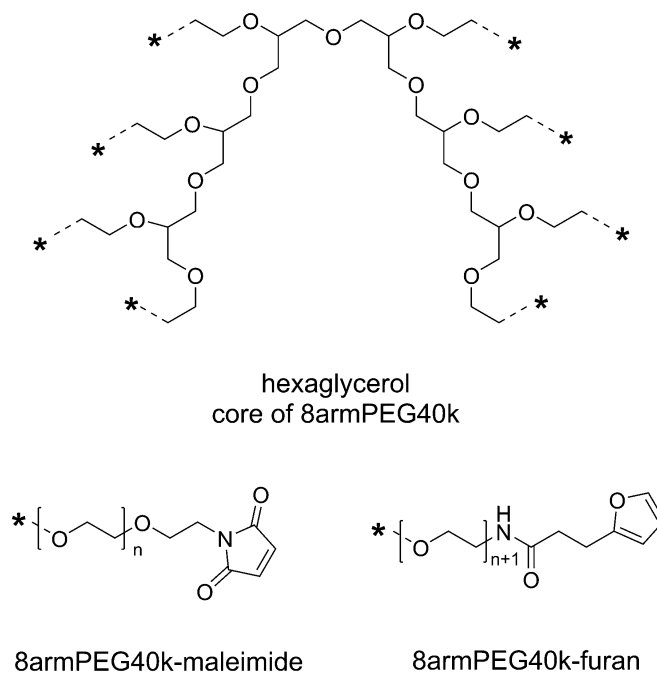
3.2.3 Synthesis of Boc-12-aminododecanoic acid

Boc-12-aminododecanoic acid was synthesized as described by Dorn et al. [223] with the following modifications. 12-Aminododecanoic acid (9.3 mmol, 2.0 g) was suspended in 30 mL of absolute methanol containing triethylamine (11.2 mmol, 1.5 mL). Di-*tert*-butyl dicarbonate (9.3 mmol, 2.0 g) was dissolved in 10 mL of absolute methanol and added to the suspension. The mixture was heated to 60 °C and refluxed under stirring for 12 hours, leading to a clear solution. The solvent was removed under reduced pressure and the residue was dissolved in ethyl acetate. The solution was extracted four times with 0.25 M HCl. The organic phase was dried over anhydrous Na₂SO₄ and filtered. The solvent was evaporated to give a white solid (94% yield). The complete Boc-protection of the primary amino groups was confirmed using a fluorescamine assay [224].

3.2.4 Synthesis of unmodified macromonomers (Scheme 3.1)

Eight-armed PEG-amine with a molecular mass of 40,000 Da (8armPEG40k-NH₂) was synthesized as previously described [225]. The resulting PEG-amine was then functionalized with furyl (8armPEG40k-furan) or maleimide groups (8armPEG40k-maleimide) as described for 8armPEG20k-NH₂ [155]. However, higher reagent concentrations were required due to the lower concentrations of amino groups. For the synthesis of 8armPEG40k-furan, 16 equivalents of 3-(2-furyl)propanoic acid, NHS, DCC, and NaHCO₃ were used; for the preparation of

8armPEG40k-maleimide, 40 equivalents of N-methoxycarbonylmaleimide were used. The degree of end-group functionalization was 75-80% for 8armPEG40k-furan and 65-70% for 8armPEG40k-maleimide, as determined by $^1\text{H-NMR}$. The degree of functionalization was reproducible and sufficient to enable cross-linking.

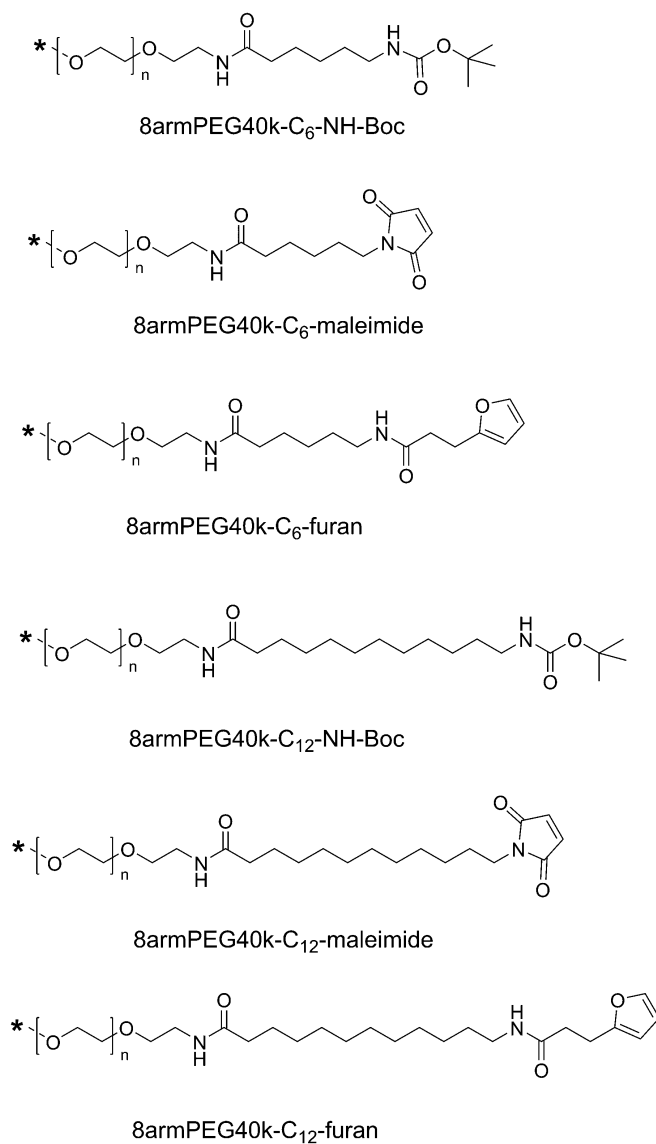


Scheme 3.1: Functional end-groups of 8armPEG40k-maleimide and 8armPEG40k-furan. Both macromonomers were synthesized from 8armPEG40k-OH (molecular mass 40,000 Da, hexaglycerol core) as previously described.

3.2.5 Synthesis of hydrophobically modified macromonomers (Scheme 3.2)

8armPEG40k-NH₂ was first reacted with Boc-6-aminohexanoic acid as previously described for 8armPEG20k-NH₂ [221]. The complete functionalization with Boc-6-aminohexanoic acid was confirmed by a fluorescamine assay. Following this procedure, the obtained 8armPEG40k-C₆-NH-Boc was deprotected (8armPEG40k-C₆-NH₂) and subsequently functionalized with furyl (8armPEG40k-C₆-furan) or maleimide groups (8armPEG40k-C₆-maleimide) as described above. 8armPEG40k-C₁₂-NH-Boc, 8armPEG40k-C₁₂-furan and 8armPEG40k-C₁₂-maleimide were synthesized in the same way using Boc-12-aminododecanoic acid instead of Boc-6-aminohexanoic acid. The degree of end-group functionalization was 65-70% for

8armPEG40k-C₆-furan and 8armPEG40k-C₁₂-furan, and 60-65% for 8armPEG40k-C₆-maleimide and 8armPEG40k-C₁₂-maleimide, as determined by ¹H-NMR. The degree of functionalization was reproducible and sufficient to enable cross-linking.



Scheme 3.2: End-groups of hydrophobically modified macromonomers. Hydrophobic 6-aminohexanoic acid (C₆) or 12-aminododecanoic acid (C₁₂) spacers were introduced between the PEG backbone and the functional end-groups.

3.2.6 Determination of the critical micelle concentration

To check for the presence of micellar structures, emission spectra of pyrene in pure water, a micellar solution of cetareth-20, and a 20% (w/V) solution of 8armPEG40k-C₁₂-NH-Boc were recorded at an excitation wavelength of 339 nm, using a Perkin Elmer LS-55 fluorescence plate reader (Perkin Elmer, Wiesbaden, Germany). The emission spectra were normalized to the peak at 383 nm (I₃); the results of five independent measurements were averaged. To determine the critical micelle concentration (CMC), aqueous solutions of 8armPEG40k-OH, 8armPEG40k-C₆-NH-Boc, and 8armPEG40k-C₁₂-NH-Boc were prepared; concentrations of 0.1%, 0.25%, 0.5%, 1.0%, 2.5%, 5.0%, 7.5%, 10%, 15%, and 20% were used. First, 30 mg of pyrene was dissolved in 750 μ L of acetone. Equivalents of this solution corresponding to 1.0 mg of pyrene were transferred to amber glass vials and the acetone was allowed to evaporate. Then, 200 μ L of the polymer solutions were added and the samples were incubated on an orbital shaker for 24 hours. Following this, 100 μ L of each sample were transferred into a 96-well plate (Greiner Bio-One, Frickenhausen, Germany) and the fluorescence intensity of pyrene was determined at an excitation wavelength of 339 nm and an emission wavelength of 390 nm. A linear regression was performed for both the non-ascending and the ascending part of the graph; the CMC was determined from the intersection of the two lines.

3.2.7 Viscosity measurements

Aqueous solutions of 8armPEG40k-OH, 8armPEG40k-C₆-NH-Boc, and 8armPEG40k-C₁₂-NH-Boc were prepared; the polymer concentrations were 2% (w/V) and 20% (w/V). Viscosity measurements were performed on a TA Instruments Discovery HR-2 rheometer (TA Instruments, Eschborn, Germany) at a constant temperature of 25 °C. The instrument was equipped with a 20 mm parallel steel plate; the sample volume was 350 μ L. The shear rate was increased from 0.1 to 10.0 s⁻¹. The TA Instruments Trios software was used to calculate the viscosity from the relation between shear rate and stress assuming Newtonian flow behavior.

3.2.8 Hydrogel preparation and characterization

For hydrogel preparation, equal molar amounts of 8armPEG40k-furan and 8armPEG40k-maleimide, 8armPEG40k-C₆-furan and 8armPEG40k-C₆-maleimide, or 8armPEG40k-C₁₂-furan and 8armPEG40k-C₁₂-maleimide were separately dissolved

in water. Gel formation was initiated by mixing complementary macromonomer solutions; the overall polymer concentrations were 5% (w/V), 10% (w/V) and 15% (w/V). Rheological characterization was performed using a TA Instruments AR 2000 rheometer (TA Instruments, Eschborn, Germany) as previously described [155]. Storage (G') and loss modulus (G'') were recorded over time; the crossover of G' and G'' was regarded as the gel point. The average mesh size (ξ) was determined as previously described [221].

3.2.9 Young's modulus of compression

To characterize the mechanical properties of hydrogels, the Young's modulus of compression (E) was determined. For this purpose, gel cylinders with a volume of 250 μL were prepared as described above. The gel samples were cross-linked for 6 hours at 37 °C. The polymer concentrations were 5% (w/V), 10% (w/V) and 15% (w/V). Diameter and height of the gel cylinders were determined using a caliper. The samples were then subjected to a compression test on an Instron 5542 materials testing machine (Norwood, MA, USA). For this purpose, the gel cylinders were placed upright on the lower steel plate of the instrument. The upper steel plate was set to compress the samples at a velocity of 1 mm min⁻¹. The compressive force (N) and the compressive strain (%) were recorded over time. The Young's modulus of compression was determined from the linear part of the curve between 10% and 50% compression using the Instron Bluehill Software (Norwood, MA, USA). Data is presented as mean \pm standard deviation, based on the results of three independent samples.

3.2.10 Swelling, degradation and antibody release

Swelling and degradation of 8armPEG40k, 8armPEG40k-C₆ and 8armPEG40k-C₁₂ hydrogels was studied in phosphate buffer, pH 7.4 at 37 °C as previously described [221]. The polymer concentrations were 5% (w/V), 10% (w/V) and 15% (w/V). For the release experiments, 8armPEG40k, 8armPEG40k-C₆ and 8armPEG40k-C₁₂ hydrogels were loaded with bevacizumab (Avastin[®]); cross-linking was carried out in 5 mM acetate buffer, pH 5.0. The polymer concentration was 10% (w/V); the bevacizumab loading was 5 mg mL⁻¹. The *in vitro* release of bevacizumab was determined in phosphate buffer, pH 7.4 at 37 °C as previously described [221].

3.2.11 Hydrolytic stability of maleimides

In order to investigate the hydrolytic stability of maleimides, 20.0 mg of 8arm-PEG40k-maleimide, 8armPEG40k-C₆-maleimide or 8armPEG40k-C₁₂-maleimide were dissolved in 2.0 mL of 50 mM phosphate buffer, pH 7.4. The polymer solutions were transferred into 10 mm quartz cuvettes. The absorbance at 299 nm was recorded for 900 min using a Kotron UVIKON[®] 941 spectrophotometer (Kotron Instruments S.p.A., Milan, Italy). The cuvette holder was equipped with a heating jacket; the temperature was set to 37 °C.

3.2.12 Statistical analysis

All results are presented as mean \pm standard deviation, based on the data obtained from at least $n = 3$ samples. Statistical significance was determined by means of one-way ANOVA, followed by Tukey's *post hoc* test using GraphPad Prism 6.0 (GraphPad Software Inc., La Jolla, CA, USA). Differences were considered statistically significant at $p < 0.05$.

3.3 Results and discussion

3.3.1 Association of macromonomers in aqueous solution

The major goal of this study was to prepare *in situ* forming hydrogels for drug delivery by combining physical interactions with DA chemistry. In order to induce hydrophobic interactions between the macromonomers, hydrophilic 8armPEG40k-NH₂ was first reacted with Boc-6-aminohexanoic acid (C₆) or Boc-12-aminododecanoic acid (C₁₂). After deprotection, the hydrophobically modified PEG was functionalized with furyl and maleimide groups, respectively. While it has already been shown in a previous publication that introducing hydrophobic C₆ spacers gives hydrogels with increased stability to degradation [221], the present study aimed at providing a deeper mechanistic understanding of the molecular processes responsible for the improved gel properties. Furthermore, another goal of this study was to investigate whether the gel properties, such as gel time and stability to degradation, depend on the spacer length. In the first experiment, the hydrophobic interactions between the synthesized macromonomers were investigated. To this end, the association of 8armPEG40k-C₆-NH-Boc or 8armPEG40k-C₁₂-NH-Boc in water was studied using pyrene as a probe molecule. The Boc-protected polymers were chosen since

they were uncharged. Furthermore, their association is solely due to hydrophobic interactions; covalent cross-linking via DA reaction cannot take place.

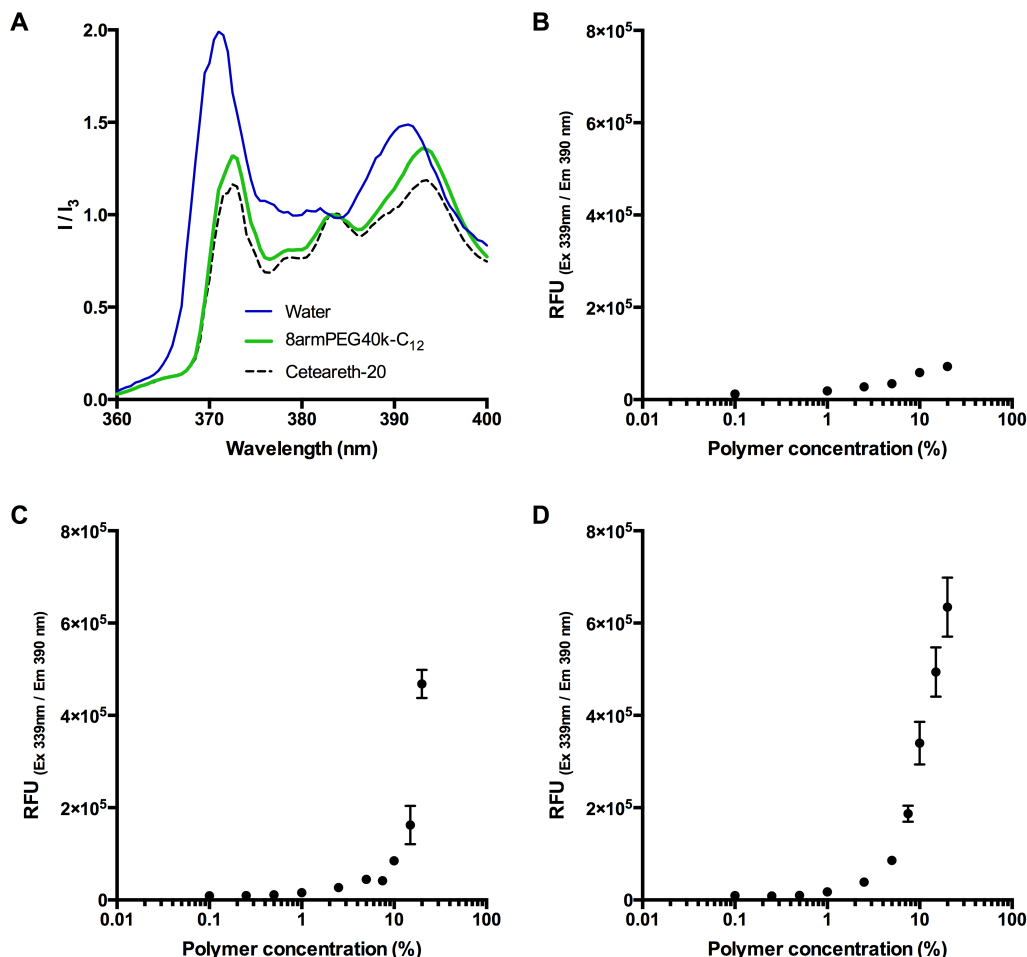


Figure 3.1: Emission spectra of pyrene in pure water (negative control), a micellar solution of ceteareth-20 (positive control), and a 20% (w/V) solution of 8armPEG40k-C₁₂-NH-Boc (A). The spectra are normalized to the fluorescence intensity at 383 nm (I_3); a decrease of the peak at 372 nm (I_1) is an indicator for micelle formation. Pyrene fluorescence in aqueous solutions of 8armPEG40k-OH (B), 8armPEG40k-C₆-NH-Boc (C) and 8armPEG40k-C₁₂-NH-Boc (D) at concentrations ranging from 0.1% (w/V) to 20% (w/V). A sharp increase in the fluorescence intensity (C and D) indicates the beginning of polymer association.

To check for the existence of polymeric micelles, the emission spectra of pyrene in pure water (negative control), a micellar solution of the detergent ceteareth-20 (positive control), and a 20% (w/V) solution of 8armPEG40k-C₁₂-NH-Boc were compared. Pyrene is commonly used to probe the formation of micelles as its

fluorescence intensity is greatly influenced by the hydrophobicity of the environment. The emission spectra were normalized to the peak at 383 nm (I_3). Fig. 3.1A shows that, in comparison to water, the relative intensity at 372 nm (I_1) strongly decreased for both cetareth-20 and 8armPEG40k- C_{12} -NH-Boc. A decrease in I_1 has been reported as an indicator for micelle formation [226–228]. In addition, the ratio between I_1 and I_3 was determined. In hydrophobic environments, the ratio is relatively low (e.g., 0.53 in hexane), whereas in hydrophilic environments, the ratio is significantly higher (e.g., 1.88 in water). In cetareth-20 and 8armPEG40k- C_{12} -NH-Boc, values of 1.12 and 1.26 have been determined. I_1/I_3 values of about 1.2 have been reported to be typical for associative polymers and surfactant micelles in aqueous solutions [229]. This suggests that pyrene is located within hydrophobic domains of cetareth-20 and 8armPEG40k- C_{12} -NH-Boc, respectively. To follow the formation of micelles, pyrene fluorescence was measured in aqueous solutions of 8armPEG40k-OH, 8armPEG40k- C_6 -NH-Boc and 8armPEG40k- C_{12} -NH-Boc at concentrations ranging from 0.1% (w/V) to 20% (w/V). As expected, in solutions of 8armPEG40k-OH, no micelle formation was detected (Fig. 3.1B). However, in solutions of 8armPEG40k- C_6 -NH-Boc and 8armPEG40k- C_{12} -NH-Boc, a sharp increase in the fluorescence intensity was detected above a certain concentration (Fig. 3.1C and D). This indicates the beginning of polymer association and the formation of micelles. The critical micelle concentrations (CMCs) were determined as 10.4% (2.3 mM) and 3.3% (0.73 mM) for 8armPEG40k- C_6 -NH-Boc and 8armPEG40k- C_{12} -NH-Boc, respectively. In comparison, for poloxamer 407, an amphiphilic poly(ethylene oxide)-*b*-poly(propylene oxide)-*b*-poly(ethylene oxide) copolymer, CMC values of 0.26–0.8% (w/V) have been determined [230]; for linear PEGs end-capped with n-hexadecyl groups, CMC values of 2–5 mM have been reported [231]. These values compare with the results reported in the present study.

Fig. 3.1 clearly shows that modification of 8armPEG40k-NH₂ with hydrophobic residues leads to hydrophobic interactions between the macromonomers. Moreover, the interactions become stronger as the length of the hydrophobic alkyl chain increases, as indicated by the lower CMC. It, therefore, seems reasonable to employ even longer alkyl spacers, such as 18-aminooctadecanoic acid, to amplify the effect. However, it should be kept in mind that increasing the spacer length can affect the water solubility of the polymer. In fact, another hydrophobically modified PEG was synthesized by reacting 8armPEG40k- C_{12} -NH₂ with further molecules of 12-aminododecanoic acid. However, the obtained macromonomer (8armPEG40k- C_{12} - C_{12} -NH₂) was almost insoluble in water (data not shown). As water solubility of

the macromonomers is a prerequisite for the formation of hydrogels, this derivative was not included in the present study.

3.3.2 Viscosity of macromonomer solutions

The presence of polymeric micelles above a certain macromonomer concentration is an interesting finding. To understand possible effects on hydrogel formation, the mechanism of polymer association should be discussed in more detail. It is well established that water-soluble polymers with hydrophobic end-modification form flower- or star-like micelles [232, 233], i.e., associates with a dense hydrophobic core surrounded by a corona of hydrophilic polymer chains [234]. In addition, amphiphilic polymers are known to increase the viscosity of aqueous solutions; they are, therefore, referred to as associative thickeners [235, 236]. This behavior can be explained by the transient network theory [237]. Water-soluble polymers with “sticky” hydrophobic end-groups associate in water to form physically stabilized networks in which the cross-links are weak enough to constantly break and re-combine. Winnik and Yekta reviewed the available literature and discussed how the formation of micelles and transient networks can explain the behavior of associative polymers in aqueous solution [238]. Based on this combined theory, the association of 8armPEG40k-C₆ and 8armPEG40k-C₁₂ macromonomers solution can be described as follows. At very low concentrations, isolated macromonomers exist that only engage in transient random interactions (Fig. 3.2A). Therefore, solutions of 8armPEG40k-C₆-NH-Boc or 8armPEG40k-C₁₂-NH-Boc should exhibit nearly the same viscosity as solutions of polymers without hydrophobic end-modification. However, with increasing concentration, interactions between individual macromonomers become more likely and the hydrophobic end-groups start to associate (Fig. 3.2B). With further increasing concentration, more and more micelles are formed. These micelles are ultimately bridged by polymer chains resulting in the formation of transient networks that consequently increase the viscosity of the solution (Fig. 3.2C). Solutions of 8armPEG40k-C₆-NH-Boc or 8armPEG40k-C₁₂-NH-Boc should, therefore, exhibit much higher viscosities than equally concentrated solutions of polymers without hydrophobic end-modification.

To test this hypothesis, aqueous solutions of 8armPEG40k-OH, 8armPEG40k-C₆-NH-Boc and 8armPEG40k-C₁₂-NH-Boc were prepared; their viscosities were measured at room temperature (Fig. 3.3). At polymer concentrations of 2% (w/V), viscosities of about 2 mPa s were determined. There were no significant differences

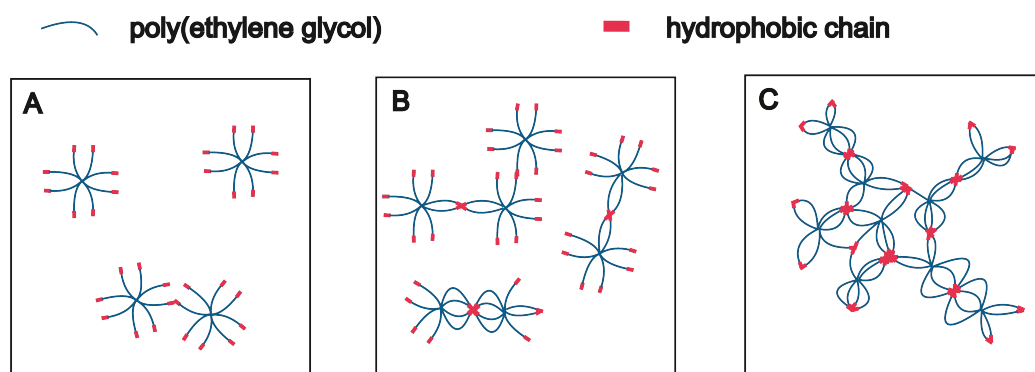


Figure 3.2: Association of hydrophobically modified eight-armed PEG in aqueous solution at increasing concentrations. Isolated macromonomers engage in random interactions at low macromonomer concentrations (A). With increasing concentration, interactions become more likely and the hydrophobic end-groups start to associate (B). Formation of bridged micelles and transient networks at high macromonomer concentrations (C).

between the polymer types, suggesting no additional physical interactions between macromonomers with hydrophobic end-groups. After increasing the polymer concentrations to 20% (w/V), i.e., above the CMC of 8armPEG40k-C₆-NH-Boc and 8armPEG40k-C₁₂-NH-Boc, the viscosities of all polymer solutions had increased accordingly. However, compared with 8armPEG40k-OH, solutions of 8armPEG40k-C₆-NH-Boc and 8armPEG40k-C₁₂-NH-Boc showed significantly higher viscosities. For example, the viscosity of a 20% (w/V) solution of 8armPEG40k-C₆-NH-Boc was 1.6-times higher than the viscosity of an equally concentrated solution of 8armPEG40k-OH. This finding clearly demonstrates the existence of additional physical interactions between 8armPEG40k-C₆ macromonomers. The effect was even more pronounced when 8armPEG40k-C₁₂-NH-Boc was used; the viscosity was 5.5-times higher than for 8armPEG40k-OH. The differences between 8armPEG40k-C₆-NH-Boc and 8armPEG40k-C₁₂-NH-Boc were expected based on the determined CMC values (10.4% vs. 3.3%). Macromonomers end-capped with long alkyl chains (e.g., 12-aminododecanoic acid) show a higher tendency for hydrophobic interaction than those end-capped with short chains (e.g., 6-aminohexanoic acid). In summary, it can be concluded that star-shaped PEG molecules end-capped with hydrophobic alkyl chains are capable of physical interactions; the association of macromonomers with hydrophobic end-groups is likely to influence hydrogel formation.

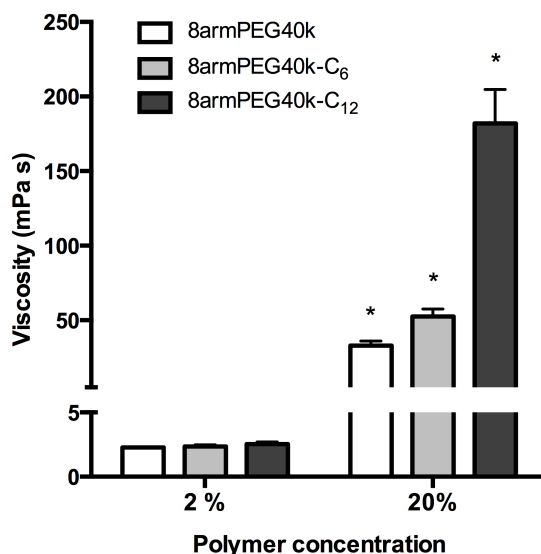


Figure 3.3: Viscosity of aqueous solutions of 8armPEG40k-OH, 8armPEG40k-C₆-NH-Boc and 8armPEG40k-C₁₂-NH-Boc at 25 °C. * indicates statistically significant differences to all other groups of the same polymer concentration.

3.3.3 Acceleration of gel formation by hydrophobic association

For the following experiments, hydrogels were prepared from macromonomers functionalized with furyl and maleimide end-groups; different alkyl spacer lengths were used. In the first experiment, the effect of macromonomer association on the gel time of DA hydrogels was studied. The DA reaction allows the preparation of covalently cross-linked, degradable hydrogels. In contrast to other cross-linking reactions, such as radical polymerization or the copper(I)-catalyzed azide-alkyne cycloaddition, the use of potentially toxic initiators or catalysts can be avoided. This is important for applications such as controlled protein release or cell encapsulation. However, a major disadvantage of the DA reaction is the comparably low cross-linking rate at ambient temperature. Consequently, it would be beneficial if gel formation were accelerated by hydrophobic interactions between macromonomers.

As shown in Fig. 3.4A, the gel times of plain 8armPEG40k-hydrogels were 166 min (5% polymer), 83 min (10% polymer) and 57 min (15% polymer). Upon modification with 12-aminododecanoic acid, the gel times decreased on average by 55%, with gel points at 78 min (5% polymer), 36 min (10% polymer) and 26 min (15% polymer) being determined. Apparently, the association of macromonomers by hydrophobic interactions promotes the cross-linking process independent from the polymer concentration. In comparison, modification with 6-aminohexanoic acid

also influenced the gel formation rate, but the effect was much weaker. This is in line with the previous results, which showed that both macromonomer association and viscosity enhancement depend on the spacer length. To elucidate the contribution of macromonomer association on gel formation, a further experiment was done (Fig. 3.4B). When both 8armPEG40k- C_{12} -furan and 8armPEG40k- C_{12} -maleimide were used, gelation proceeded twice as fast as in hydrogels made from unmodified macromonomers, i.e., 8armPEG40k-furan and 8armPEG40k-maleimide. How-

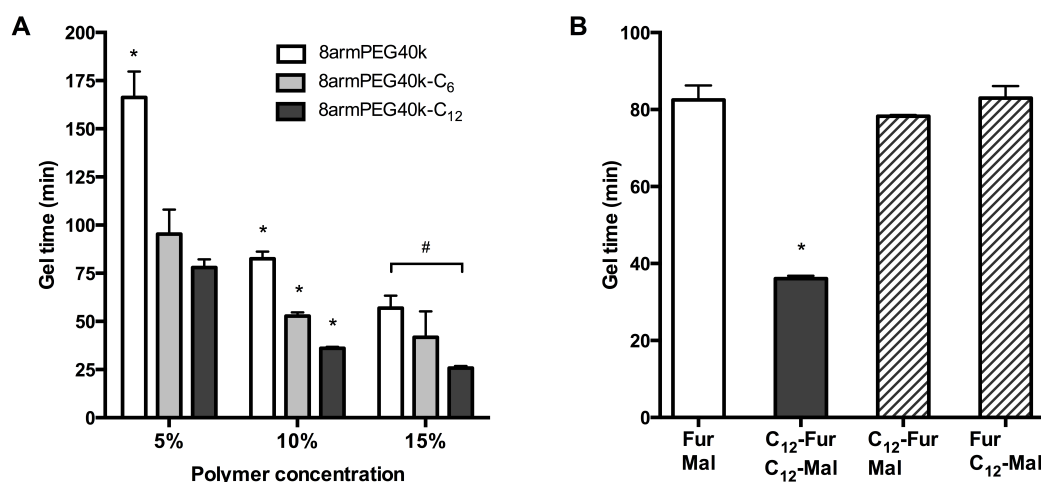


Figure 3.4: Gel time of 8armPEG40k, 8armPEG40k- C_6 and 8armPEG40k- C_{12} hydrogels at 37 °C (A). Influence of hydrophobic interactions on gel formation (B). Gel formation only proceeded twice as fast when both components (i.e., 8armPEG40k-furan or 8armPEG40k-maleimide) were modified with hydrophobic C_{12} spacers (C_{12} -Fur/ C_{12} -Mal). The polymer concentration was 10% (w/V). * indicates statistically significant differences to all other groups of the same polymer concentration; # indicates statistically significant differences between the specified groups.

ever, when 8armPEG40k- C_{12} -furan was combined with unmodified 8armPEG40k-maleimide, or *vice versa*, no significant acceleration of gelation was observed. Although association of 8armPEG40k- C_{12} -furan (or 8armPEG40k- C_{12} -maleimide) occurs at the tested concentration, this does apparently not affect cross-linking via DA reaction. This result, therefore, suggests that hydrophobic modification of both macromonomers (i.e., 8armPEG40k-furan and 8armPEG40k-maleimide) is required to accelerate gel formation. It is conceivable that the association of 8armPEG40k- C_{12} -furan and 8armPEG40k- C_{12} -maleimide into mixed micelles brings the reactive furyl and maleimide groups into close proximity. This makes the cross-linking process more efficient and accelerates gel formation.

3.3.4 Network mesh size and mechanical properties

To study the influence of hydrophobic modification on the cross-linking density of hydrogels, the average network mesh size (ξ) of 8armPEG40k, 8armPEG40k-C₆ and 8armPEG40k-C₁₂ hydrogels was determined as previously described [155]. In brief, the gel volume after cross-linking, V_{gc} , and after swelling in water, V_{gs} , was determined by weighing cylindrical gel samples in air and hexane. Afterwards, the gel samples were freeze-dried and the volume of the dry polymer, V_p , was determined. After calculating the polymer fraction of the hydrogel after cross-linking ($v_{2c} = \frac{V_p}{V_{gc}}$) and in the swollen state ($v_{2s} = \frac{V_p}{V_{gs}}$), the number of moles of elastically active chains within the network, ν_e , was calculated using a modified version of the Flory–Rehner eqn (3.1) [239–241].

$$\nu_e = -\frac{V_p}{V_1 v_{2c}} \cdot \frac{[\ln(1 - v_{2s}) + v_{2s} + \chi_{12} v_{2s}^2]}{\left[\left(\frac{v_{2s}}{v_{2c}} \right)^{\frac{1}{3}} - \frac{2}{f} \left(\frac{v_{2s}}{v_{2c}} \right) \right]} \quad (3.1)$$

The calculation requires several parameters, namely the molar volume of water ($V_1 = 18 \text{ mL mol}^{-1}$), the branching factor of the macromonomers ($f = 8$), and the polymer-water interaction parameter (χ_{12}). The parameter χ_{12} describes the average extent of interaction between a macromonomer and water; it depends on the hydrophilic lipophilic balance (HLB) of the macromonomer. For amphiphilic macromonomers that are composed of both ethylene oxide (EO) and hydrocarbon chains (HC), χ_{12} can be calculated according to [242]:

$$\chi_{12} = \omega_{EO} \chi_{W,EO} + (1 - \omega_{EO}) \chi_{W,HC} - \frac{V_W}{V_{HC}} (1 - \omega_{EO}) \omega_{EO} \chi_{HC,EO} \quad (3.2)$$

In this equation, ω_{EO} represents the weight fraction of the ethylene oxide chain; V_W and V_{HC} are the molar volumes of water and the hydrocarbon part of the macromonomer. The water-ethylene oxide interaction parameter ($\chi_{W,EO}$) was set to 0.4; the water-hydrocarbon interaction parameter ($\chi_{W,HC}$) was set to 2.0 and the term $\chi_{HC,EO} \left(\frac{V_W}{V_{HC}} \right)$ was taken as 0.4. Based on these values, the interaction parameters for 8armPEG40k-C₆ ($\chi_{12} = 0.42$) and 8armPEG40k-C₁₂ in water ($\chi_{12} = 0.45$) were calculated; for unmodified 8armPEG40k hydrogels, the PEG–water

interaction parameter ($\chi_{12} = 0.40$) was used. Together with the average bond length along the PEG backbone ($l = 0.146$ nm), the molecular mass of the PEG repeating unit ($M_r = 44$ g mol⁻¹), the total mass of PEG in the hydrogel (m_p), and the Flory characteristic ratio ($C_n = 4$), ν_e allows the calculation of ξ according to eqn (3.3) [243]:

$$\xi = v_{2s}^{-\frac{1}{3}} l \left(\frac{2m_p}{\nu_e M_r} \right)^{\frac{1}{2}} C_n^{\frac{1}{2}} \quad (3.3)$$

The data listed in Table 3.1 shows that ξ is decreasing with increasing polymer concentration. The effect was more pronounced in 8armPEG40k and 8armPEG40k-C₆ hydrogels than in 8armPEG40k-C₁₂ hydrogels. The modification of 8armPEG40k with 6-aminohexanoic acid spacers only had a minor influence on ξ . In contrast to that, modification with more hydrophobic 12-aminododecanoic acid spacers significantly decreased ξ . Apparently, the association of 8armPEG40k-C₁₂-furan and 8armPEG40k-C₁₂-maleimide results in more densely cross-linked hydrogels with less network defects.

Table 3.1: Average network mesh size (ξ) and Young's modulus of compression (E) of 8armPEG40k, 8armPEG40k-C₆ and 8armPEG40k-C₁₂ hydrogels at concentrations of 5, 10 and 15% (w/V).

| Polymer type | Concentration(%) | ξ (nm) | E(kPa) |
|----------------------------|------------------|----------------|------------------|
| 8armPEG40k | 5 | 25.9 ± 0.2 | 8.1 ± 4.1 |
| | 10 | 19.6 ± 0.1 | 33.2 ± 4.0 |
| | 15 | 17.5 ± 0.1 | 87.2 ± 19.6 |
| 8armPEG40k-C ₆ | 5 | 24.3 ± 1.0 | 25.0 ± 4.0 |
| | 10 | 20.3 ± 0.6 | 50.3 ± 5.4 |
| | 15 | 17.4 ± 1.7 | 117.5 ± 13.1 |
| 8armPEG40k-C ₁₂ | 5 | 18.2 ± 0.6 | 38.9 ± 4.6 |
| | 10 | 15.4 ± 0.1 | 79.6 ± 12.1 |
| | 15 | 14.3 ± 0.2 | 172.8 ± 28.4 |

Since cross-linking density and material stiffness are closely related, the association of 8armPEG40k-C₁₂-furan and 8armPEG40k-C₁₂-maleimide should also be reflected in the mechanical properties of the hydrogels. To confirm this relation, the Young's modulus of compression (E) was determined. It is defined as the ratio of compressive stress to compressive strain and frequently used to describe the mechanical properties of materials [161, 244]. As expected, the modification of macromonomers with hydrophobic residues had a strong effect on the mechanical properties of hydrogels. For example, the Young's modulus of 8armPEG40k-C₁₂ hydrogels (10% and 15% polymer concentration) was twice as high as that of unmodified 8armPEG40k hydrogels. The effect was even more pronounced at low polymer concentrations; the Young's modulus of 5% (w/V) 8armPEG40k-C₁₂ hydrogels was approximately five times higher than that of unmodified 8armPEG40k hydrogels (Table 3.1). As already observed in the other experiments, modification with 6-aminohexanoic acid residues resulted in much weaker effects. In summary, using hydrophobically modified macromonomers for hydrogel preparation resulted in higher cross-linking densities, as indicated by the values of ξ and E. The association of hydrophobically modified macromonomers to micelles and transient networks is thought to make the cross-linking process more efficient. As a consequence, more densely cross-linked networks are formed and the number of imperfections, such as elastically inactive chains, is reduced.

3.3.5 Swelling, degradation and antibody release

As discussed in the previous section, using hydrophobically modified macromonomers increases the cross-linking density of hydrogels. Since the cross-linking density has a strong influence on hydrogel degradation, the swelling behavior of gel cylinders in phosphate buffer pH 7.4 was monitored over time at 37 °C (Fig. 3.5). As expected, the swelling and degradation behavior of hydrogels was dependent on the polymer concentration. Furthermore, it was found that hydrophobically modified macromonomers yielded hydrogels with increased stability to degradation. For example, at a concentration of 10% (w/V), 8armPEG40k hydrogels showed a 9-fold mass increase during incubation, whereas the mass of 8armPEG40k-C₆ and 8armPEG40k-C₁₂ hydrogels increased only 6-fold and 4-fold, respectively. The gel samples were completely degraded after 20 (8armPEG40k hydrogels), 40 (8armPEG40k-C₆ hydrogels) and 60 days (8armPEG40k-C₁₂ hydrogels). In summary, upon introduction of hydrophobic residues, the swelling of hydrogels

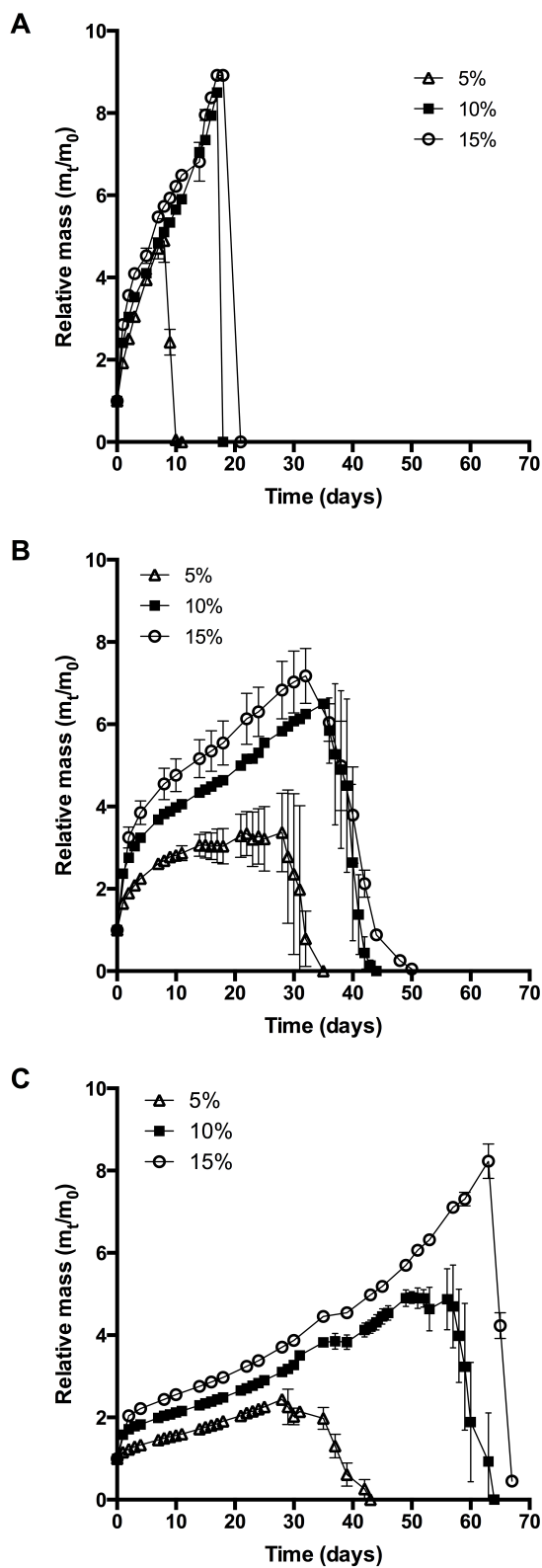


Figure 3.5: Swelling and degradation of 8armPEG40k (A), 8armPEG40k- C_6 (B), 8armPEG40k- C_{12} hydrogels (C) in phosphate buffer, pH 7.4 at 37 °C.

proceeds more slowly and the mass increase is less pronounced. In addition, hydrogels made of hydrophobically modified macromonomers showed considerably higher resistance to degradation than unmodified hydrogels.

This may be due to several reasons. On the one hand, the extent of interaction between water and polymer chains has an impact on hydrogel swelling. The interaction between water and purely hydrophilic polymers is preferred over interactions with polymers that comprise both hydrophilic and hydrophobic parts. The presence of hydrophobic domains within the hydrogel network may, therefore, limit the overall degree of swelling [245–247]. In addition, hydrogels made of hydrophobically modified macromonomers have a higher crosslinking density than 8armPEG40k hydrogels. This directly translates into reduced swelling and improved stability to degradation. Finally, the degradation rate of DA hydrogels is governed by the hydrolytic stability of the involved maleimide groups [156]. It has been shown that degradation occurs by retro-Diels–Alder (rDA) reaction and subsequent ring-opening hydrolysis of the newly generated maleimide groups. The rate of the rDA reaction is low at 37 °C; however, ring-opening hydrolysis of maleimide to unreactive maleamic acid shifts the DA/rDA equilibrium and significantly accelerates the degradation rate. To check the influence of hydrophobic modification, the hydrolytic stability of 8armPEG40k-maleimide, 8armPEG40k-C₆-maleimide and 8armPEG40k-C₁₂-maleimide was determined in phosphate buffer, pH 7.4 at 37 °C (Fig. 3.6). Assuming a pseudo-first-order reaction, rate constants (k_{obs}) and half-lives ($t_{1/2}$) were calculated by fitting the integrated form of eqn (3.4) to the experimental data.

$$-\frac{d[\text{maleimide}]}{dt} = k_{\text{obs}}[\text{maleimide}] \quad (3.4)$$

The results listed in Table 3.2 show that hydrophobic modification increases the stability of maleimide groups. The half-lives of 8armPEG40k-C₆-maleimide and 8armPEG40k-C₁₂-maleimide were 2.2 and 3.4 times longer than the half-life of unmodified 8armPEG40k-maleimide. These results are in good agreement with literature data, which also showed improved hydrolytic stability of N-alkyl substituted maleimides [248–251]. Electron-donating N-substituents, such as alkyl groups, stabilize the C–N–C bonds of maleimide; moreover, the enolization of the carbonyl group is accelerated by N-alkyl substituents. Both effects retard the nucleophilic attack by hydroxide ions [248].

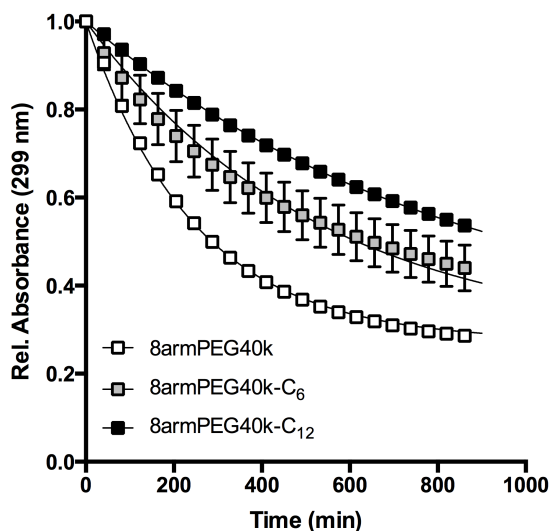


Figure 3.6: Absorbance of 8armPEG40k-maleimide, 8armPEG40k-C₆-maleimide and 8armPEG40k-C₁₂-maleimide in phosphate buffer, pH 7.4 at 37 °C. The absorbance decreased due to ring-opening hydrolysis of maleimide; hydrophobic modification resulted in improved hydrolytic resistance. Experimental data are indicated by symbols; solid lines represent the best fits of eqn (3.4).

Table 3.2: Calculated rate constants (k_{obs}) and half-lives ($t_{1/2}$) for the ring-opening reaction of 8armPEG40k-maleimide, 8armPEG40k-C₆-maleimide and 8armPEG40k-C₁₂-maleimide in phosphate buffer, pH 7.4 at 37 °C.

| Polymer type | k_{obs} (min ⁻¹) | $t_{1/2}$ (min) | R ² |
|---------------------------------------|---------------------------------------|-----------------|----------------|
| 8armPEG40k-maleimide | 4.06×10^{-3} | 170 | 0.9986 |
| 8armPEG40k-C ₆ -maleimide | 1.89×10^{-3} | 367 | 0.9853 |
| 8armPEG40k-C ₁₂ -maleimide | 1.19×10^{-3} | 585 | 0.9998 |

In the final experiment, hydrogels were loaded with bevacizumab (Avastin[®]), which served as a model antibody. The release of bevacizumab from 8armPEG40k, 8armPEG40k-C₆ and 8armPEG40k-C₁₂ hydrogels is shown in Fig. 3.7; the polymer concentration was 10% (w/V) in all groups. As it was expected from the previous studies, the release rate was strongly influenced by the length of the hydrophobic spacer. Release from unmodified 8armPEG40k hydrogels was comparatively fast; the incorporated bevacizumab was completely released after 10 days. In contrast to 8armPEG40k, release from 8armPEG40k-C₆ and 8armPEG40k-C₁₂ hydrogels was significantly delayed. Both release profiles had a hyperbolic shape; however,

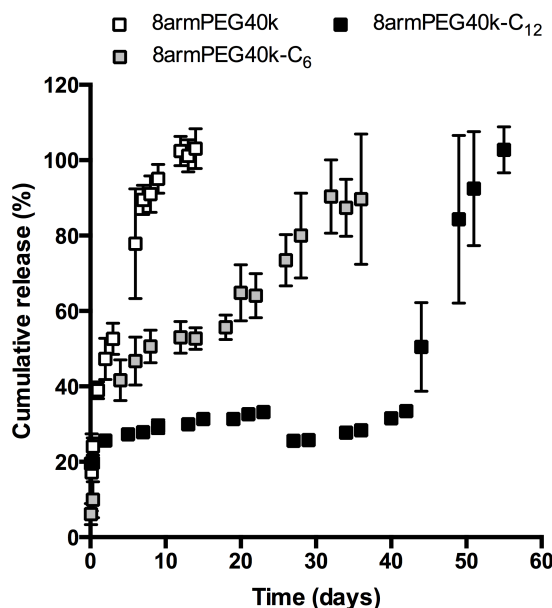


Figure 3.7: Release of bevacizumab from 8armPEG40k, 8armPEG40k-C₆ and 8armPEG40k-C₁₂ hydrogels in phosphate buffer, pH 7.4 at 37 °C. The polymer concentration was 10% (w/V) in all groups.

their time scales were different. The first phase was characterized by fast, diffusion-controlled release. This was followed by a plateau during which little or no protein release was observed. Apparently, the incorporated protein is physically trapped within the polymer network. In addition, a small fraction of the protein is immobilized during cross-linking by Michael-type addition to 8armPEG40k-C₆-maleimide and 8armPEG40k-C₁₂-maleimide. The third phase of release starts with the onset of hydrogel degradation. Once a critical mesh size had been exceeded after 20 (8armPEG40k-C₆) and 45 days (8armPEG40k-C₁₂), the entrapped bevacizumab was suddenly released; the release was completed after 30 (8armPEG40k-C₆) and 55 days (8armPEG40k-C₁₂). Although it is obvious that bevacizumab release is mainly controlled by degradation, some discrepancies appear when the swelling and release data are compared. For example, 8armPEG40k-C₁₂ hydrogels started to degrade after approximately 55 days, while the onset of antibody release was after approximately 45 days. A possible explanation for the observed time difference between the beginning of degradation and the onset of antibody release may be the fact that the incorporation of proteins into hydrogels can lead to network imperfections, which consequently affect the degradation rate. This explanation seems likely, as a correlation between the extent of network defects and the incorporation of cells

[252] or nanoparticles [253] into hydrogels has already been described. In summary, the obtained *in vitro* data suggests that 8armPEG40k-C₆ and 8armPEG40k-C₁₂ hydrogels may be suitable for controlled protein release in general, and for delayed antibody release in particular.

3.4 Conclusion

Cross-linking via DA chemistry is a promising method to prepare hydrogels for controlled release of therapeutic proteins. However, before their application in pre-clinical studies, the hydrogels still need to be optimized regarding their gel points, stability to degradation and time frames of drug release. In this study, it has been demonstrated that the combination of hydrophobic interactions and DA chemistry can contribute to improved hydrogel properties, such as faster gelation and increased stability to degradation. Modification of hydrophilic PEG with alkyl chains induces hydrophobic interactions between the macromonomers, which result in the formation of micellar structures and transient networks. The resulting inner structure of the polymer solution has been shown to facilitate crosslinking via DA chemistry. Using hydrophobically modified macromonomers, therefore, results in hydrogels with improved properties, in particular if long alkyl chains (e.g., C₁₂) are employed. For example, hydrogels prepared from 8armPEG40k-C₁₂-furan and 8armPEG40k-C₁₂-maleimide were characterized by significantly faster gelation, smaller mesh sizes, higher cross-linking densities, increased resistance to mechanical stress and improved stability to degradation. As a consequence, the *in vitro* release of incorporated proteins is considerably delayed; for example, bevacizumab was released from 8armPEG40k-C₁₂ hydrogels after almost 60 days. Interestingly, the observed effects have been demonstrated to correlate with the length of the hydrophobic moieties. Short alkyl chains (e.g., C₆) result in much weaker effects regarding gelation time, stability to degradation and time frame of drug release. Thus, hydrogel characteristics can be tailored by employing shorter or longer alkyl chains for hydrophobic modification. In summary, the combination of hydrophobic association and chemical cross-linking is a promising approach to improve the properties of hydrogels and bring them closer to clinical application.

Chapter 4

Controlled antibody release from degradable thermoresponsive hydrogels cross-linked by Diels–Alder chemistry

Published in *Biomacromolecules*

The content of this chapter was published as: *Biomacromolecules*, 18(8): 2410–2418, 2017. doi: 10.1021/acs.biomac.7b00587

Abstract

Amine-modified four- and eight-armed poloxamines were prepared and subsequently functionalized with maleimide or furyl groups. Aqueous solutions of these polymers exhibited an immediate gelation at a temperature above 37 °C. Concomitantly, Diels–Alder reactions gradually cross-linked and cured the gels. Different ratios between four- and eight-armed macromonomers were used to tune hydrogel stability and mechanical properties. In this way, hydrogel stability could be precisely controlled in the range of 14 to 329 days. Controlled release of the model antibody bevacizumab was achieved over a period of 7, 21, and 115 days. Release profiles were triphasic with a low burst; approximately 87% of the released antibody was intact and displayed functional binding. The hydrogels presented in this study are degradable, nontoxic, rapidly gelling, stable, and provide controlled antibody release. They can be tailored to match the demands of various applications and present an attractive platform for antibody delivery.

4.1 Introduction

The Diels–Alder (DA) reaction is a highly attractive reaction for the design of *in situ* cross-linking hydrogels. DA reactions of maleimide and furan are particularly promising, as they are efficient, require no catalysts, form no toxic side products, and can be carried out in water at ambient temperatures [254]. Recently, the DA reaction between maleimide and furan has been introduced as a cross-linking mechanism for the preparation of degradable poly(ethylene glycol) (PEG) based hydrogels [155]. Overall, these hydrogels have outstanding potential for antibody delivery and controlled release. However, they are associated with relatively long gel times of 14 min or more due to the slow reaction kinetics of the DA reaction. As this is regarded a major drawback for future applications as injectable depot system, attempts have been made to accelerate gel formation, for example, by utilizing hydrophobic association [254] or by introducing additional branches [221]. Although both approaches led to significant decreases in gel times, instantaneous gel formation could still not be achieved.

As an alternative approach to design DA hydrogels that gel more quickly, the DA reaction could be combined with a second gelation mechanism that provides immediate gel formation upon injection. This could be achieved by using materials that respond to external stimuli, such as temperature, pH, or ionic strength [67, 255–257]. For example, *in situ* forming hydrogels can be prepared using thermoresponsive block copolymers, for example, poly(N-isopropylacrylamide), poloxamer (Pluronic[®]), and poloxamine (Tetronic[®]) [258]. These polymers exhibit a sudden reduction in solubility above a certain temperature, leading to rapid gel formation. This respective temperature is referred to as lower critical solution temperature (LCST). Therefore, the goal of this study was to develop thermoresponsive materials that can additionally undergo DA cross-linking. In this way, immediate gelation could be achieved, while at the same time, a major drawback of exclusively physically cross-linked gels can be eliminated: low resistance against dissolution and, thus, limited stability after administration [218–220].

For example, in a recent approach by Boere et al. thermal gelation was combined with native chemical ligation to obtain degradable hydrogels with controlled mechanical properties [259]. However, until now, most attempts to combine thermal gelation and covalent cross-linking have involved Michael-type additions between acrylate and thiol groups. For example, Cellesi et al. designed materials for cell encapsulation [260–262], Cho et al. developed tissue sealants [263], and Censi et al.

prepared a controlled release system for bradykinin [264]. Although Michael-type additions between thiol and acrylate groups are suitable for dual gelation and *in situ* cross-linking, there are some disadvantages associated with the reaction that render it unsuitable for antibody delivery. For example, thiol groups on polymer chains can form dimers or alter the protein structure through thiol-disulfide exchange [182]. Furthermore, thiol-Michael additions are often conducted in a basic environment to accelerate the reaction [265]. However, high pH could be detrimental for antibody stability for example as many antibodies are formulated in acidic buffers, such as, adalimumab (pH 5.2), ranibizumab (pH 5.5), trastuzumab (pH 6.0), and bevacizumab (pH 6.2) [186].

In this study, degradable hydrogels for controlled antibody delivery were prepared based on a dual approach involving both thermal gelation and the DA reaction. After rapid gel formation at body temperature, DA reactions gradually cured and stabilized the hydrogel. In this way, *in situ* forming yet highly stable hydrogels could be obtained. To prepare four-armed macromonomers, poloxamine, a tetrafunctional thermoresponsive polymer, was end-functionalized with maleimide (4armPoloxamine-maleimide) or furyl groups (4armPoloxamine-furan). To prepare eight-armed macromonomers, branched poloxamines were first synthesized and then end-functionalized (8armPoloxamine-maleimide, 8armPoloxamine-furan). DA-Poloxamine hydrogels were prepared by dissolving the macromonomers in water using a polymer concentration of 30 wt %. Different hydrogel types were prepared using various ratios of 8armPoloxamine to 4armPoloxamine. In the first part of the study, rheological experiments were carried out to characterize gel formation and mechanical properties. In the next part, hydrogel stability was analyzed and cytotoxicity was assessed. Finally, hydrogels were loaded with the model antibody bevacizumab (Avastin[®]) to analyze the *in vitro* release. Bevacizumab was selected as intravitreal injections of this antibody are currently used to treat neovascular age-related macular degeneration and the treatment might benefit from controlled long-term release. Finally, antibody binding ability after release was confirmed to exclude a negative influence of gel formation on antibody stability.

4.2 Materials and methods

4.2.1 Materials

Boc-6-aminohexanoic acid and Fmoc-Lys(Boc)-OH were purchased from Bachem (Weil am Rhein, Germany). 3-(4,5-Dimethylthiazol-2-yl)-2,5-diphenyltetrazolium bromide (MTT) was obtained from PanReac AppliChem (Darmstadt, Germany). Poloxamine (Tetronic[®] 1107) was provided by BASF SE (Ludwigshafen am Rhein, Germany). Deuterated chloroform (CDCl₃), N,N'-dicyclohexylcarbodiimide (DCC), Eagle's minimum essential medium (EMEM), fetal calf serum (FCS), 3-(2-furyl)propanoic acid, N-hydroxysuccinimide (NHS), and N-methoxycarbonyl-maleimide were received from Sigma-Aldrich (Taufkirchen, Germany). Mouse fibroblast L-929 cells were a kind gift from the group of Prof. Armin Buschauer (University of Regensburg). Bevacizumab (Avastin[®], 25 mg mL⁻¹, Roche Ltd, Basel, Switzerland) was kindly provided by the hospital pharmacy of the University of Regensburg (Germany). All other chemicals were obtained from Merck KGaA (Darmstadt, Germany). Purified water was freshly prepared using a Milli-Q water purification system (Millipore, Schwalbach, Germany).

4.2.2 ¹H-NMR spectroscopy

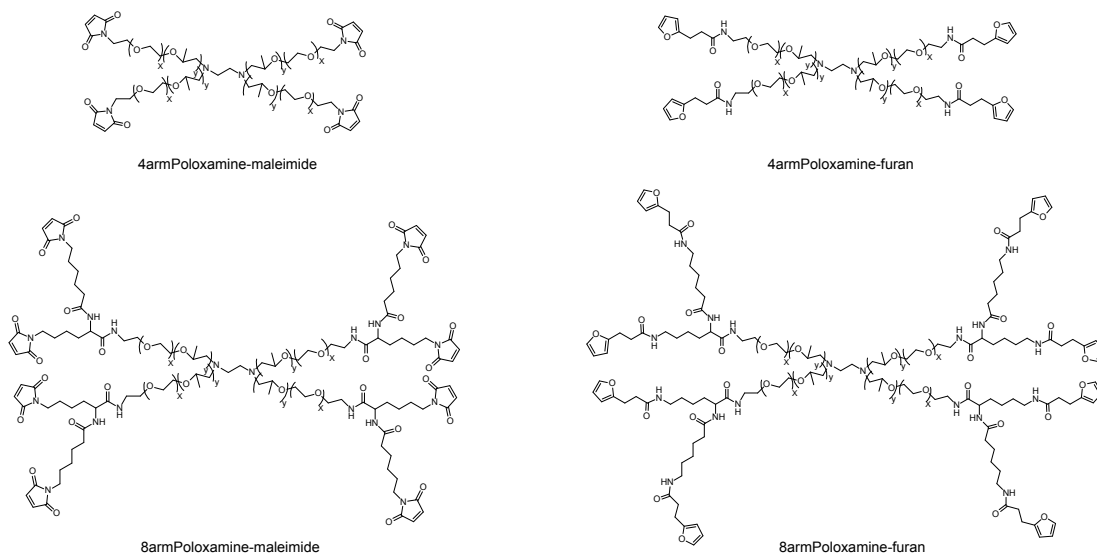
¹H-NMR spectra were recorded in CDCl₃ at 295 K using a Bruker Avance 300 spectrometer (Bruker BioSpin GmbH, Rheinstetten, Germany).

4.2.3 Synthesis of four-armed macromonomers

The terminal poloxamine hydroxyl groups were first converted to amino groups [225], and then end-functionalized with maleimide and furyl moieties (Scheme 4.1) as previously described for poly(ethylene glycol) (PEG)-based macromonomers [155, 225]. In brief, poloxamine (Tetronic[®] 1107) was converted to 4armPoloxamine-NH₂ by means of a Mitsunobu reaction, followed by hydrazinolysis. 4armPoloxamine-NH₂ was then reacted with N-methoxycarbonylmaleimide to yield 4armPoloxamine-maleimide. The reaction of 4armPoloxamine-NH₂ with 3-(2-furyl)propanoic acid, DCC, and NHS led to 4armPoloxamine-furan. The degree of end-group functionalization among the batches was 76 ± 8% for 4armPoloxamine-maleimide and 81 ± 1% for 4armPoloxamine-furan, as determined by ¹H-NMR.

4.2.4 Synthesis of eight-armed macromonomers

Eight-armed poloxamines were synthesized through branching as previously described for PEG-based macromonomers [221]. Briefly, 4armPoloxamine-NH₂ was first reacted with Fmoc-Lys(Boc)-OH, DCC, and NHS. The Fmoc-groups were removed and Boc-6-aminohexanoic acid was reacted with the free amino-group via DCC/NHS chemistry. All Boc-groups were then removed and the free amino-groups were functionalized with furyl (8armPoloxamine-furan) or maleimide moieties (8armPoloxamine-maleimide) as described above. The degree of end-group functionalization among the batches was $64 \pm 6\%$ for 8armPoloxamine-maleimide and $82 \pm 4\%$ for 8armPoloxamine-furan as determined by ¹H-NMR.



Scheme 4.1: Four- and eight-armed poloxamines were end-functionalized with maleimide or furyl groups. Macromonomers were synthesized from Tetronic[®] 1107; the x (poly(ethylene glycol), PEG) to y (poly(propylene glycol), PPG) ratio was 70:30. Branching was achieved by introducing lysine and 6-aminoheptanoic acid residues.

4.2.5 Gel formation and rheological properties

For hydrogel preparation, the respective polymers were dissolved in water using a total polymer concentration of 30 wt %. Various ratios between 8armPoloxamine and 4armPoloxamine were used to prepare hydrogels with different properties. For example, in order to prepare 1000 mg of a hydrogel composed of 20 wt % 8armPoloxamine and 10 wt % 4armPoloxamine, that is, a 20%/10% hydrogel, a total amount of 300 mg polymer was dissolved in 700 mg water. To be more precise, for

this type of hydrogel 100 mg 8armPoloxamine-maleimide, 100 mg 8armPoloxamine-furan, 50 mg 4armPoloxamine-maleimide, and 50 mg 4armPoloxamine-furan were used. Immediate gel formation could be induced by increasing the temperature to 37 °C.

Rheological characterization was performed on a TA Instruments AR 2000 rheometer (TA Instruments, Eschborn, Germany). Oscillatory shear experiments were carried out using a 40 mm parallel plate geometry with a 500 μm gap size at a constant frequency of 0.5 Hz. Polymer solutions were prepared as described above; a sample volume of 750 μL was used. Absolute values of the complex shear modulus ($|G^*|$) and phase angles (δ) were recorded as a function of time. In order to characterize the thermoresponsive behavior of the polymer solutions, heating (20 to 37 °C) and cooling (37 to 20 °C) steps were included in the procedure. Water evaporation was minimized by using a solvent trap and by pipetting silicone oil around the gap between the plates. However, in order to minimize the influence of drying on the obtained $|G^*|$ values, rheological experiments were limited to 100 min.

4.2.6 Swelling and degradation

Swelling and degradation of DA-Poloxamine hydrogels was studied in 50 mM phosphate buffer, pH 7.4 at 37 °C as previously described [221]. Different ratios between 8armPoloxamine and 4armPoloxamine were used as described above; a polymer concentration of 30 wt % was used for all hydrogels.

4.2.7 Hydrolytic stability of maleimides

The hydrolytic stability of 4armPoloxamine-maleimide and 8armPoloxamine-maleimide was investigated in phosphate buffer, pH 7.4 at 37 °C as previously described [254].

4.2.8 Cytotoxicity

In order to assess the cytotoxicity of DA-Poloxamine hydrogels a metabolic assay using the reagent 3-(4,5-dimethylthiazol-2-yl)-2,5-diphenyltetrazolium bromide (MTT) was performed according to ISO 10993-5:2009 (Biological evaluation of medical devices, part 5: Tests for *in vitro* cytotoxicity). In brief, 300 μL of 0%/30%, 15%/15%, and 30%/0% hydrogels were prepared, cast into a 24-microtiter plate and

allowed to cross-link overnight in cell culture conditions (37 °C, 5% CO₂). On the next day, extracts were prepared by adding 2.0 mL of EMEM supplemented with 10% FCS to the hydrogels, which were then incubated for 24 h. Mouse fibroblast L-929 cells were seeded in 96-microtiter plates at a density of 10,000 cells per well and allowed to adhere overnight. 100 μ L of extract was added to each well. SDS (0.1%) served as a negative control and pure medium as a positive control ($n = 12$). Cells were incubated with the test media for 24 h after which the medium was removed and 200 μ L of serum-containing medium with 1.5 mM MTT was added to each well. After 5 h of incubation the MTT solution was removed and 200 μ L PBS containing 10% SDS was added to each well. After 16 h of incubation, absorbance at 570 and 690 nm was determined for each well using a FluoStar Omega fluorescence microplate reader (BMG Labtech, Ortenberg, Germany). The difference in absorbance at 570 and 690 nm was used to calculate the viability of cells. The viability of the treated cells was normalized to the value for the positive control, that is, medium alone.

4.2.9 Antibody release and analytics

Release experiments were carried out as previously described [254]. However, in this study the bevacizumab loading was 6.25 mg mL⁻¹ and the polymer concentration used was 30 wt %. Due to the high stability of some hydrogels, release experiments were only carried out using 0%/30%, 5%/25%, and 10%/20% hydrogels. In order to investigate a potential negative influence of hydrogel preparation and cross-linking reactions on the stability of bevacizumab, the antibody was analyzed after release. Functional binding to vascular endothelial growth factor (VEGF) was investigated using a Shikari[®] Q-beva enzyme-linked immunosorbent assay (ELISA) kit (Matriks Biotek, Ankara, Turkey). The amount of binding antibody was compared to a solution containing the same concentration of fresh bevacizumab.

4.2.10 Statistical analysis

All results are presented as mean \pm standard deviation, based on the data obtained from at least $n = 3$ samples. Statistical significance was determined by means of one-way ANOVA, followed by Tukey's *post-hoc* test using GraphPad Prism 6.0 (GraphPad Software Inc., La Jolla, CA, U.S.A.). Differences were considered statistically significant at $p < 0.05$.

4.3 Results and discussion

4.3.1 Hypothesis and proof of concept

The goal of this study was to develop hydrogels that combine thermal gelation and DA chemistry in a dual gelation process. This combination has several advantages for the delivery of therapeutic antibodies. First, precursor solutions can easily be prepared by dissolving the polymer components in water or buffer together with the antibody to be encapsulated. Second, due to the slow reaction kinetics of the DA reaction, the fluidity of the polymer solution will remain unaffected at room temperature for a time span long enough to allow convenient handling and application. Third, the thermoresponsive behavior will lead to immediate gel formation at a site of injection. In that way, high amounts of antibody can be “encapsulated” *in situ*. Finally, in contrast to hydrogels that rely exclusively on thermal gelation, these hydrogels are expected to be significantly more stable concerning degradation as a result of covalent cross-linking.

In a proof of concept experiment, the rheological properties of modified 4arm-Poloxamines (“DA-Poloxamine”) were investigated and compared to unmodified commercially available Tetronic[®] 1107 (“Poloxamine”). For this purpose, 30 wt % polymer was dissolved in water and analyzed using a three-step temperature program (Fig. 4.1). Absolute values of the complex shear modulus ($|G^*|$) and phase angles were recorded over time to monitor gel formation and stiffness. At 20 °C, both Poloxamine and DA-Poloxamine were in the liquid state which was confirmed by $|G^*|$ values of 0.7 ± 0.2 Pa for Poloxamine and 0.8 ± 0.4 Pa for DA-Poloxamine. The phase angles (δ) were $90.1 \pm 0.2^\circ$ (Poloxamine) and $88.5 \pm 2.4^\circ$ (DA-Poloxamine), and the loss modulus (G'') was larger than the storage modulus (G') indicating mainly viscous behavior. Upon increasing the temperature to 37 °C ($+\Delta T$), the $|G^*|$ values for both sample types immediately increased confirming their thermoresponsive properties. Directly after heating, the $|G^*|$ values were 48.6 ± 6.9 kPa for Poloxamine and 36.2 ± 9.8 kPa for DA-Poloxamine; differences were not statistically significant ($p < 0.05$). At the same time, δ strongly decreased for both samples indicating the formation of a viscoelastic gel ($G' > G''$). During the following incubation time at 37 °C, the stiffness of Poloxamine gels remained unchanged. In contrast, $|G^*|$ values for DA-Poloxamine gels increased to 67.0 ± 13.7 kPa. The increase in stiffness was attributed to covalent cross-linking reactions that occurred while already in the gel state. It could also be observed that the increase in $|G^*|$ was mainly governed by the strongly rising G' . The contribution

of G'' was much weaker. In a third step, the temperature was lowered to 20 °C ($-\Delta T$). As expected, unmodified Poloxamine gels returned to the liquid state ($|G^*| = 0.7 \pm 0.3$ Pa, $\delta = 90.3 \pm 0.2^\circ$, $G' < G''$), whereas DA-Poloxamines remained in the gel state ($|G^*| = 15.3 \pm 3.2$ kPa, $\delta = 3.5 \pm 0.3^\circ$, $G' > G''$). Taken together, the experiment confirmed the hypothesis that DA-Poloxamines exhibit thermal gelation and DA cross-linking in a dual gelation process.

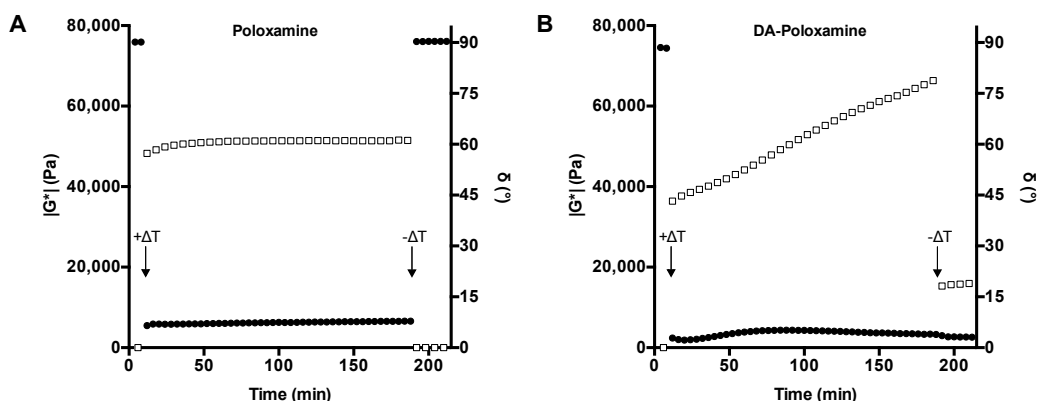


Figure 4.1: Rheological behavior of 30 wt % Poloxamine (A) and DA-Poloxamine (B) solutions in the course of a three-step temperature program. Absolute values of the complex shear modulus ($|G^*|$), represented as white squares, and phase angles (δ), represented as black circles, were recorded as a function of temperature and time at a 0.5 Hz oscillatory frequency. The initial temperature was set to 20 °C. After 10 min, the temperature was increased to 37 °C ($+\Delta T$) and kept constant for 180 min. In the third step, the temperature was again reduced to 20 °C ($-\Delta T$). Both polymer solutions displayed thermal gelation, however, only for DA-Poloxamines stiffness increased during incubation and could be retained after cooling. For the sake of clarity, error bars are not shown in the diagram.

4.3.2 Gel formation and mechanical properties

In order to utilize DA-Poloxamines for antibody delivery, hydrogels with tunable properties would be desired. To this end, both four- and eight-armed macromonomers were employed for hydrogel preparation. In this way, hydrogels with different amounts of functional groups and, therefore, cross-linking densities could be obtained. In the following section, hydrogels composed of both 4armPoloxamines and 8armPoloxamines were analyzed for their thermal gelation properties and gel stiffness. In the nomenclature used to describe the compositions, the first number denotes the amount of 8armPoloxamine in the mixture, the

second number refers to the amount of 4armPoloxamine. For example, in order to prepare 1000 mg of a 20%/10% hydrogel, 100 mg 8armPoloxamine-maleimide, 100 mg 8armPoloxamine-furan, 50 mg 4armPoloxamine-maleimide, and 50 mg 4armPoloxamine-furan were dissolved in 700 mg water. The total polymer concentration was 30 wt % for all hydrogel types. This was identified as the minimum concentration to induce immediate thermal gelation.

In the next experiment, the rheological behavior of hydrogels with different 8arm to 4arm ratios was analyzed (Fig. 4.2). $|G^*|$ was recorded at 20 °C for 10 min. Then, the temperature was increased to 37 °C and kept constant for 90 min. Initially, all compositions were liquid and did not show significant stiffness; $|G^*|$ values ranged between 0.5 and 0.8 Pa. After 10 min at 20 °C the stiffness had slightly increased due to the beginning DA cross-linking, for example to 1.0 ± 0.6 Pa for 0%/30% gels and to 1.7 ± 0.3 Pa for 20%/10% gels. Here, the slow reaction kinetic of the DA reaction is an advantage as faster covalent cross-linking could cause faster gel formation and might prevent administration, for example, by clogging the needle. For example, hydrogels that rely on the relatively fast Michael-type addition reaction already exhibit gel formation after about 100 s at room temperature and neutral pH [266].

Upon increasing the temperature to 37 °C, stable viscoelastic gels were formed immediately. $|G^*|$ values determined directly after increase in temperature are listed in Table 4.1. For all compositions, a strong increase in stiffness was observed. Interestingly, there was no significant difference between $|G^*|$ values directly after the increase in temperature ($p < 0.05$). Consequently, the strength of the thermally induced gel formation is governed by the backbone and is hardly affected by the number of functional end-groups on the macromonomer. The thermoresponsive properties were comparable for all compositions. In contrast, the increase in stiffness after 90 min at 37 °C strongly depended on the 8arm/4arm-ratio used. For 0%/30% hydrogels, a $|G^*|$ increase of only 1.4-fold could be observed. However, the $|G^*|$ increase was considerably more pronounced for hydrogels containing a higher concentration of branched macromonomers, for example, 3.6-fold for 20%/10% hydrogels. This observation can be explained by the fact that hydrogel curing is caused by covalent DA cross-linking while already in the gel state. When more functional groups are present, both the likelihood of covalent reactions and the maximum number of elastically active chains increases.

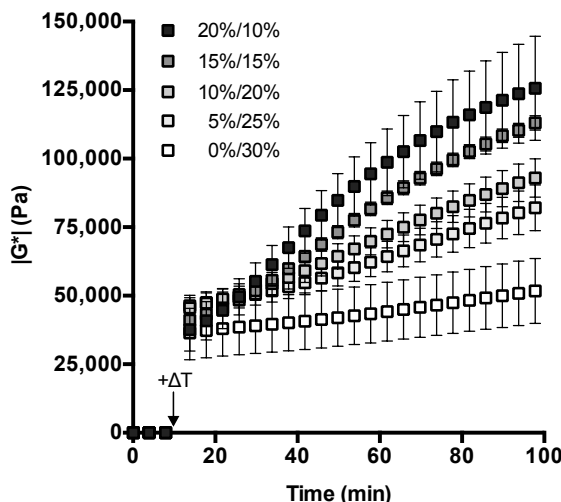


Figure 4.2: Initial thermal gelation and subsequent increase of stiffness for different 8armPoloxamine and 4armPoloxamine mixtures using an overall polymer concentration of 30 wt %. Absolute values of the complex shear modulus ($|G^*|$) were recorded over time at a 0.5 Hz oscillatory frequency. The initial temperature was set to 20 °C. After 10 min, the temperature was increased to 37 °C ($+\Delta T$) and then kept constant for 90 min. All polymer solutions were characterized by an immediate increase of stiffness at 37 °C. The further increase of stiffness was attributed to covalent cross-linking via Diels–Alder reaction and was stronger when more functional end-groups were present in the solution.

Table 4.1: Absolute values of the complex shear modulus ($|G^*|$) determined for hydrogels with different 8armPoloxamine to 4armPoloxamine ratios, measured directly after increase of temperature (0 min) and after incubation (90 min).

| Hydrogel composition | $ G^* (0 \text{ min}), \text{ kPa}$ | $ G^* (90 \text{ min}), \text{ kPa}$ |
|----------------------|-------------------------------------|--------------------------------------|
| 20%/10% | 35.6 ± 10.3 | 126.7 ± 19.0 |
| 15%/15% | 40.6 ± 1.3 | 114.0 ± 2.6 |
| 10%/20% | 45.2 ± 3.7 | 94.0 ± 7.2 |
| 5%/25% | 46.1 ± 3.9 | 83.0 ± 8.5 |
| 0%/30% | 36.2 ± 9.8 | 52.1 ± 11.9 |

4.3.3 Hydrogel swelling and degradation

In the previous experiments, it was demonstrated that DA-Poloxamines can be prepared using different amounts of four- and eight-armed macromonomers. For all compositions, immediate gel formation at body temperature was observed.

Hydrogel stiffness could be increased using a higher amount of 8armPoloxamine. Due to their rapid gelation and controllability, DA-Poloxamine hydrogels present an attractive candidate as a “smart” material for drug delivery. However, in order to utilize these hydrogels for controlled antibody delivery, sufficient stability must be demonstrated. To this end, the swelling and degradation behavior of DA-Poloxamine gel cylinders was analyzed in phosphate buffer, pH 7.4 at 37 °C (Fig. 4.3A). Similar to hydrogel stiffness, the stability and swelling properties of

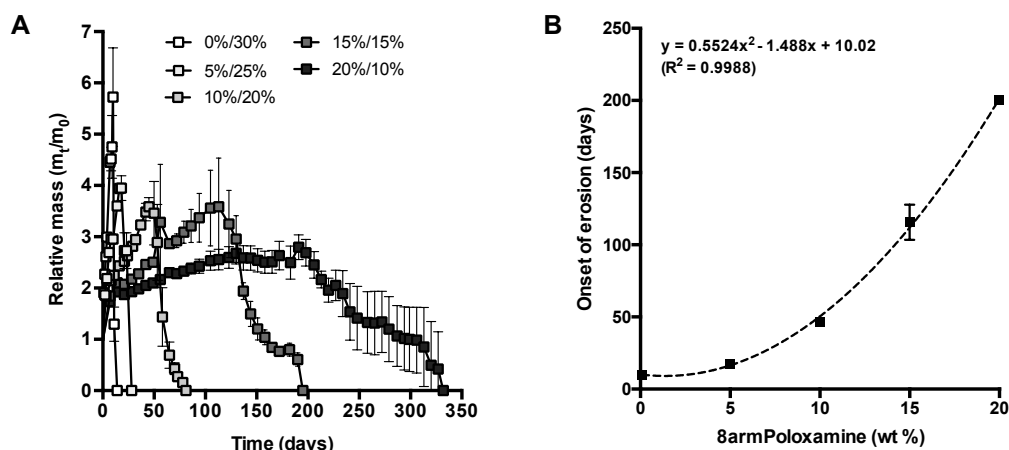
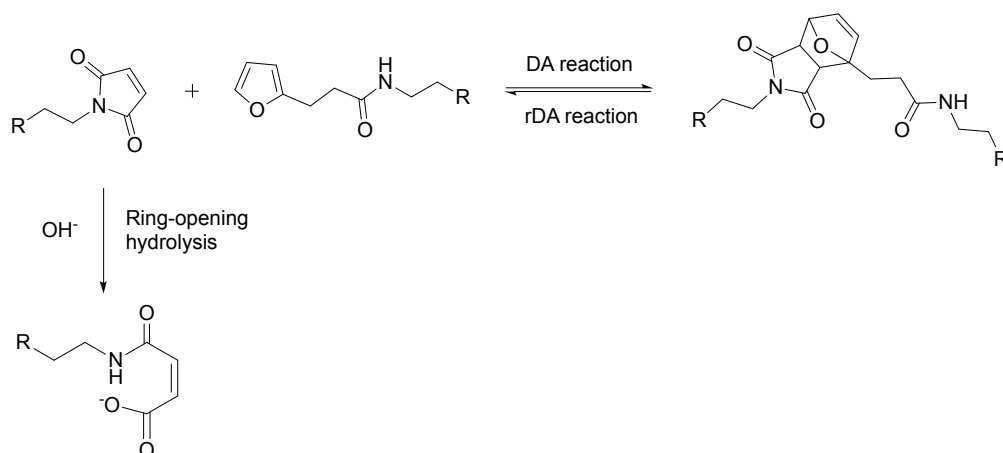


Figure 4.3: Swelling and degradation of DA-Poloxamine hydrogels with different compositions in phosphate buffer, pH 7.4 at 37 °C (A). A higher number of functional end-groups correlated with an increase in stability and a lower degree of swelling. The onset of hydrogel erosion, that is, beginning decrease of relative hydrogel mass, could be correlated with the concentration of 8armPoloxamine using a second-order polynomial (B).

DA-Poloxamine hydrogel can be controlled by choosing the right composition. For example, hydrogels prepared based on four-armed macromonomers alone (0%/30%) completely dissolved after approximately 14 days. The maximum relative mass increase was 5.7 ± 1.0 . In comparison, hydrogels containing the highest amount of branched macromonomers (20%/10%) completely dissolved after 329 days and reached a relative mass of only 2.9 ± 0.3 .

In order to select the right composition for a certain application it would be highly desirable to be able to predict hydrogel stability. Therefore, the relationship between onset of hydrogel erosion and 8armPoloxamine content was investigated (Fig. 4.3B). The onset of erosion was defined as the time-point where the relative hydrogel mass started to decrease. Interestingly, the relation between 8armPoloxamine content and onset erosion can be described using a second-order polynomial ($R^2 = 0.9988$).

This correlation can be used to predict the stability of a specific composition or to tailor hydrogel stability for a given application. In order to understand why the relationship between 8armPoloxamine concentration and stability is not a linear but a quadratic one, it must be taken into account that there are two factors influencing DA-Poloxamine hydrogel stability. On the one hand, hydrogels



Scheme 4.2: Diels–Alder (DA) reactions of maleimide and furyl functionalized poloxamines (R) lead to covalent hydrogel cross-linking. Hydrogel degradation is mediated by retro-Diels–Alder (rDA) reactions followed by the ring-opening hydrolysis of maleimide.

containing a higher amount of branched macromonomers possess a higher number of functional end-groups and can, therefore, build up more elastically active chains. Hydrogels with a higher cross-linking density exhibit a higher resistance to swelling and more cross-links have to be broken until hydrogels degrade. On the other hand, it has already been described by Kirchhof et al. that maleimide hydrolysis plays a pivotal role for DA-hydrogel stability (Scheme 4.2) [156]. As degradation occurs by retro-Diels–Alder (rDA) reaction and subsequent ring-opening hydrolysis of maleimide moieties, a higher hydrolytic resistance is accompanied by an increase in hydrogel stability. In the course of synthesizing branched poloxamines, lysine and 6-aminohexanoic acid residues were introduced between the polymer backbone and the maleimide moieties. According to literature, N-alkylation generally increases the hydrolytic stability of maleimides [248–251]. This can be explained by the fact that electron donating N-substituents stabilize the C–N–C bond of maleimide and that enolization of the carbonyl group can be accelerated by N-alkylation [248]. Consequently, nucleophilic attacks by hydroxide ions that lead to maleimide hydrolysis are hampered. This is in line with the experimental results obtained for

4armPoloxamine-maleimide and 8armPoloxamine-maleimide (Fig. 4.4). Maleimide hydrolysis was monitored for both macromonomers in phosphate buffer, pH 7.4 at 37 °C. Assuming a pseudo-first order reaction, half-lives ($t_{1/2}$) and rate constants (k_{obs}) were calculated by fitting the integrated form of eqn (4.1) to the experimental data.

$$-\frac{d[maleimide]}{dt} = k_{obs}[maleimide] \quad (4.1)$$

The results are listed in Table 4.2. On average, the half-life of 8armPoloxamine-maleimide was 2.8-fold higher than for 4armPoloxamine-maleimide. Interestingly, the half-life of 8armPoloxamine-maleimide ($t_{1/2} = 874$ min) was also considerably higher than for PEG-based macromonomers, which were branched using the same chemistry ($t_{1/2} = 412$ min) [221], or macromonomers bearing an even longer C₁₂ N-alkyl spacer ($t_{1/2} = 585$ min) [254]. Similarly, 4armPoloxamine-maleimide ($t_{1/2} = 315$ min) displayed a much longer half-life than PEG-based maleimides, for example, 8armPEG20k-maleimide ($t_{1/2} = 177$ min) [221]. These observations can be explained by the more hydrophobic PEG-PPG polymer backbone used in this study. Taken together, the combined effects of retarded hydrolysis and increased cross-linking density contribute to the massive stability increase observed for hydrogels containing 8armPoloxamine.

Table 4.2: Calculated rate constants (k_{obs}) and half-lives ($t_{1/2}$) for the ring-opening reaction of 4armPoloxamine-maleimide and 8armPoloxamine-maleimide in phosphate buffer, pH 7.4 at 37 °C.

| Macromonomer | $k_{obs}(\text{min}^{-1})$ | $t_{1/2}(\text{min})$ | R^2 |
|--------------------------|----------------------------|-----------------------|--------|
| 4armPoloxamine-maleimide | 2.20×10^{-3} | 315 | 0.9972 |
| 8armPoloxamine-maleimide | 0.79×10^{-3} | 874 | 0.9972 |

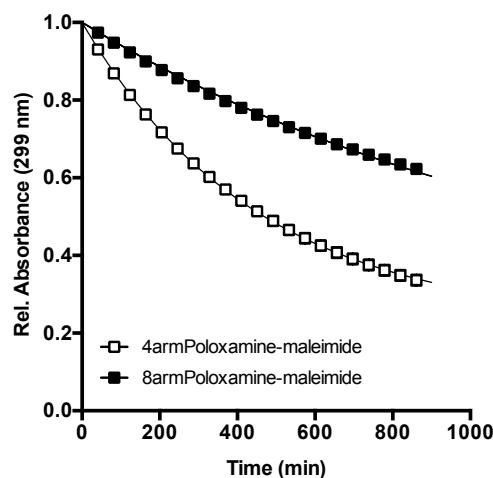


Figure 4.4: Absorbance of 4armPoloxamine-maleimide and 8armPoloxamine-maleimide in phosphate buffer, pH 7.4 at 37 °C. The absorbance decreased due to ring-opening hydrolysis of maleimide. Experimental data are indicated by box symbols; solid lines represent the best fits of eqn (4.1).

4.3.4 Cytotoxicity

Before application of DA-Poloxamine hydrogels in preclinical studies, toxicological safety should be demonstrated. PEG–PPG block copolymers like poloxamer (Pluronic[®]) and poloxamine (Tetronic[®]) are generally regarded as safe and are approved by regulatory authorities such as the U.S. Food and Drug Administration [267–269].

However, as the poloxamines were chemically modified in this study their toxicological potential should be reassessed. In particular, leaching of side-products and reactants that could not be removed during purification might have toxic potential. In order to assess the cytotoxicity of DA-Poloxamine hydrogels, an MTT assay was performed. The test was carried out using mouse fibroblast L-929 cells according to ISO 10993-5:2009. Extracts were prepared by incubating FCS containing medium with 0%/30%, 15%/15%, or 30%/0% hydrogels for 24 h at 37 °C (Fig. 4.5). Cell viability after exposure to the extracts was referenced to pure medium (positive control); medium containing 0.1% (w/V) SDS served as a negative control. The relative cell viabilities were $93.9 \pm 5.4\%$ (0%/30%), $96.6 \pm 5.7\%$ (15%/15%), and $100.7 \pm 5.8\%$ (30%/0%). Therefore, incubation with extracts from DA-Poloxamine hydrogels did not exhibit a strong negative effect on cell viability. However, hydrogels composed of 4armPoloxamine alone displayed a significantly higher cytotoxicity

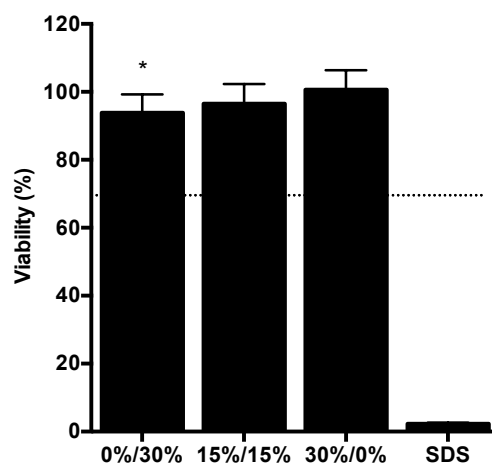


Figure 4.5: L-929 cell viability after exposure to extracts from 0%/30%, 15%/15%, and 30%/0% DA-Poloxamine hydrogels was determined using an MTT assay. Cell culture medium containing 0.1% (w/V) SDS served as a negative control. A cell viability of < 70% (dotted line) was considered cytotoxic. * indicates statistically significant differences to all other groups.

than hydrogels containing 8armPoloxamine ($p < 0.05$). This can be explained based on two effects: When macromonomers were not properly bound to the network or covalent cross-links were broken, polymer could be eluted. As eight-armed macromonomers bear more functional end-groups, they are bound more strongly to the network. Therefore, the likelihood for an elution of 4armPoloxamine during extraction is higher. This is reflected by a higher cellular toxicity. One potential source for the cytotoxicity of the extracted polymer is its surface-active properties that might interfere with the integrity of cell membranes. A second source for cytotoxic effects could be the extraction of acidic Poloxamine-maleamic acid which could alter the pH of the cell culture medium. In summary, DA-Poloxamines displayed a very low cellular toxicity. However, in future *in vivo* investigations are necessary to confirm these results and to ensure biocompatibility.

4.3.5 Controlled antibody release

In the final experiment, antibody release from DA-Poloxamine hydrogels was studied. To this end, three hydrogel compositions were loaded with the model antibody bevacizumab (Avastin[®]), and the *in vitro* release was analyzed in phosphate buffer, pH 7.4 at 37 °C (Fig. 4.6). As expected from swelling and degradation experiments, the release rate was strongly influenced by hydrogel composition. The least stable

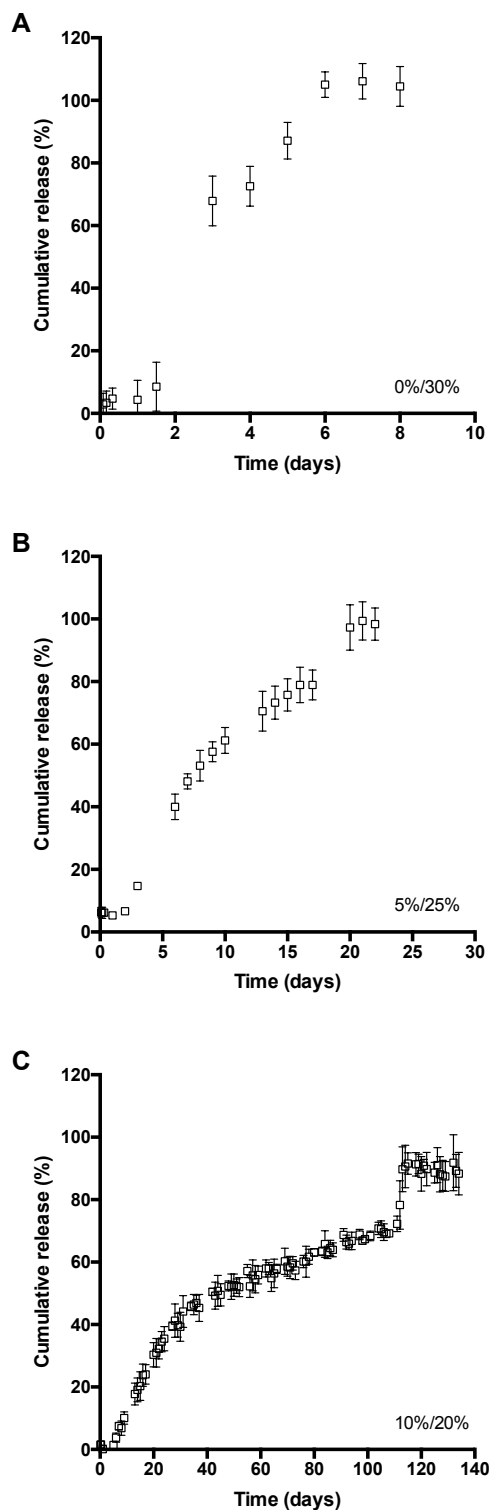


Figure 4.6: Release of bevacizumab from 0%/30%, 5%/25%, and 10%/20% DA-Poloxamine hydrogels in phosphate buffer, pH 7.4 at 37 °C.

hydrogel (0%/30%) released the antibody after 7 days. When higher ratios of branched macromonomer was used for gel preparation, antibody release could be significantly delayed. Bevacizumab was released over the course of 21 days for 5%/25% hydrogels and 115 days for 10%/20% hydrogels. In all three cases, more than 90% of the antibody that had been loaded could be recovered after release. Interestingly, the release profiles for the three hydrogel types all had a comparable shape but on different time-scales. Initially, a notably low burst release of about 2 - 6% was observed. After a short lag phase, a rapid antibody release could be observed. The fast release can be explained by an increase of meshwork size resulting from hydrogel swelling. Consequently, antibodies were able to freely diffuse out of the network. The cumulative antibody release in the first phase was $67.9 \pm 8.0\%$ (0%/30%), $53.2 \pm 4.9\%$ (5%/25%), and $30.3 \pm 3.9\%$ (10%/20%). The amount of antibody released in this phase was higher for hydrogels with a lower number of covalent cross-links. In the next phase, antibody release was considerably slower. During this plateau phase, the majority of antibody was trapped within the polymer network. During this phase, single cross-links were broken over time due to rDA reaction and maleimide hydrolysis. Consequently, antibody release was strongly delayed. In case of the most stable gel, this plateau phase spanned over 93 days. In the third phase, a rapid antibody release was observed. The constant breaking of cross-links led to a gradual increase of average meshwork size until a critical meshwork size had been exceeded. At this point, the previously entrapped antibody was rapidly released.

A triphasic release profile could be beneficial for various applications. One example could be in the treatment of ocular neovascularizations, in which anti-VEGF antibodies are directly administered into the vitreous body. As the ocular half-life of antibodies is 7-10 days [270] sustained release systems could be used to provide sufficient antibody concentrations over weeks. However, as VEGF is a key player in maintaining cone photoreceptors and the choroidal vasculature, a constant blockage of VEGF signaling might lead to additional side effects. The intermittent release profile provided by DA-Poloxamine hydrogels might be an attractive alternative as VEGF-dependent structures can recover from the action of VEGF-neutralizing antibodies during the plateau phase [271, 272]. Another potential application for DA-Poloxamine hydrogels could be in the administration of vaccines. The intermittent release profile could be used to deliver antigens in a pulsed manner following a single administration [273–275]. Moreover, DA-Poloxamine hydrogels could most likely also be used for the controlled release of

other biopharmaceuticals, for example, immunoglobulin G with a size comparable to bevacizumab.

Finally, as hydrogel preparation and cross-linking are known to potentially impair protein stability the binding ability of released bevacizumab was analyzed. To this end, bevacizumab was incorporated into 0%/30% and 5%/25% hydrogels. The hydrogels were then allowed to fully degrade for 7 and 30 days, respectively. Samples were taken and bevacizumab binding to VEGF was analyzed using ELISA. Fresh bevacizumab in the same concentration as the sample solution was used as a reference. As the focus was put on the influence of preparation and cross-linking, the antibody binding was not analyzed for 10%/20% hydrogels. The long degradation time of more than 100 days would have influenced the results through unspecific effects, such as oxidation, deamidation, aggregation, and adsorption to the vial surface [276–278]. For both hydrogel types, most of the released bevacizumab retained its binding properties (Table 4.3). The proportion of binding antibody was $87.0 \pm 5.6\%$ for 0%/30% hydrogels and $87.1 \pm 1.7\%$ for 5%/25% hydrogels. Consequently, preparation, thermal gelation, and cross-linking had only a minimal influence on antibody binding. Interestingly, when bevacizumab was incubated in phosphate buffer pH 7.4 for 30 days at 37 °C, the amount of binding bevacizumab was only $82.5 \pm 2.7\%$. When compared to bevacizumab released from 5%/25% hydrogels over 30 days, the amount of intact antibody was significantly lower ($p < 0.05$). Consequently, it can be concluded that DA-Poloxamine hydrogels exhibit a protective effect against antibody degradation *in vitro*.

Table 4.3: Analytical investigation of bevacizumab released from DA-Poloxamine hydrogels. Bevacizumab binding to VEGF was quantified using ELISA; results were compared to a solution containing the same concentration of fresh bevacizumab.

| Hydrogel composition | Time-scale (days) | Binding antibody (%) |
|----------------------|-------------------|----------------------|
| 0%/30% | 7 | 87.0 ± 5.6 |
| 5%/25% | 30 | 87.1 ± 1.7 |

To summarize, it could be demonstrated that DA-Poloxamine hydrogels are an outstanding material for the controlled release of therapeutic antibodies. Time-scales of release can be influenced by hydrogel composition. The general release profile was independent from hydrogel composition and is characterized by three phases and a low burst release. In all cases, $> 90\%$ of the loaded bevacizumab was

released and about 87% of the released antibody showed a binding comparable to fresh bevacizumab.

4.4 Conclusion

In this study, poloxamines were branched and end-functionalized with maleimide or furyl groups to yield four- and eight-armed macromonomers. At room temperature, aqueous solutions of these polymers were viscous fluids. Upon increasing the temperature to 37 °C, viscoelastic gels were immediately formed while subsequent DA reactions covalently cross-linked the gel. In this way, the many advantages of the DA reaction for hydrogel design could be utilized while avoiding the drawback of slow gelation. In addition, the hydrogels presented in this work are degradable and nontoxic. Their mechanical properties can be precisely tailored to match the demands of various applications using appropriate compositions. Moreover, hydrogel stability could be adjusted between 14 days and 329 days; the onset of hydrogel erosion could be predicted using a second-order polynomial. Controlled *in vitro* release of the model antibody bevacizumab was achieved over periods of 7, 30, and 115 days. In all cases, more than 90% of the loaded bevacizumab was released and 87% exhibited binding capabilities comparable to fresh bevacizumab.

Chapter 5

Fabrication of antibody-loaded microgels using microfluidics and thiol-ene photoclick chemistry

Submitted for publication

The content of this chapter was submitted for publication.

Abstract

Reducing burst effects, providing controlled release, and safeguarding biologics against degradation are a few of several highly attractive applications for microgels in the field of controlled release. However, the incorporation of proteins into microgels without impairing stability is highly challenging. In this proof of concept study, the combination of microfluidics and thiol-ene photoclick chemistry was evaluated for the fabrication of antibody-loaded microgels with narrow size distribution. Norbornene-modified eight-armed poly(ethylene glycol) with an average molecular mass of 10,000 Da, 20,000 Da, or 40,000 Da were prepared as macromonomers for microgel formation. For functionalization, either hydrolytically cleavable ester or stable amide bonds were used. A microfluidic system was employed to generate precursor solution droplets containing macromonomers, the cross-linker dithiothreitol, and the initiator Eosin-Y. Irradiation with visible light was used to trigger thiol-ene reactions which covalently cross-linked the droplets. For all bond-types, molecular masses, and concentrations gelation was very rapid (< 20 s) and a plateau for the complex shear modulus was reached after only 5 min. The generated microgels had a rod-like shape and did not show considerable cellular toxicity. Stress conditions during the fabrication process were simulated and it could be shown that fabrication did not impair the activity of the model proteins lysozyme and bevacizumab. It was confirmed that the average hydrogel network mesh size was similar or smaller than the hydrodynamic diameter of bevacizumab which is a crucial factor for restricting diffusion and delaying release. Finally, microgels were loaded with bevacizumab and a sustained release over a period of 28 and 46 days could be achieved *in vitro*.

5.1 Introduction

Microgels have several properties that make them highly attractive for drug delivery applications, e.g., their size, swelling and mechanical properties are tunable, they can be loaded with cargo, are considered biocompatible, and their surface can be modified [279–281]. One way to utilize this potential is to load microgels with biologics and employ them as a delivery system for controlled local release. Moreover, many frequently used cross-linking reactions for bulk hydrogels can negatively impact the stability of the incorporated proteins, e.g., the Diels–Alder reaction, Michael-type additions or radical polymerizations [182, 282]. In this context, microgels could serve as a protective carrier system that can safeguard proteins during bulk hydrogel preparation. Furthermore, antibody-loaded microgels with a small network mesh size could be used to reduce burst effects from bulk hydrogels by restricting uncontrolled antibody diffusion [283] or providing pulsed antibody release as demonstrated for vaccines [273]. However, the incorporation of proteins into microgels without negatively affecting conformational and colloidal stability is highly challenging. Therefore, in this proof of concept study a protein-compatible method for protein loading of microgels was developed to provide a platform technology for drug delivery applications.

In order to achieve this goal, several prerequisites had to be met. On the one hand, a narrow size distribution was desired, as particle size and surface area are factors that most likely influence release properties [284]. On the other, the method used for droplet generation must not generate excessive stress. For these reasons, microfluidics was selected for droplet generation. Next, the generated droplets had to be cross-linked to yield stable microgels. For this purpose, a fast, efficient, and protein compatible cross-linking reaction was required. This reaction mechanism should also require a trigger for initiation in order to avoid premature gelation and to preserve fluidity of the precursor solution. In order to meet all these requirements, the thiol-ene photoclick reaction was selected as a cross-linking reaction. In recent years, this reaction has received growing attention, e.g., for protein immobilization [285, 286], tissue engineering [287–291], preparation of microcapsules [292], microspheres [293, 294], microgels [295], and hydrogels [296–298]. As with other click reactions, thiol-ene chemistry proceeds at mild conditions, is highly specific, efficient, and does not form toxic side-products [299]. Most notably, the reaction is considered to be compatible with proteins. For example, McCall et al. [300] have shown that thiol-ene photoclick reactions can be

carried out in presence of proteins without negatively affecting their bioactivity. In addition, there are several studies in which the reaction has been successfully employed for the incorporation of proteins and cells into hydrogels, e.g., bovine serum albumin and carbonic anhydrase [301], valvular interstitial cells [302], human mesenchymal stem cells [287, 288], and pancreatic β -cells [303]. Another advantage for biomedical applications is that they can be initiated using the biocompatible radical starter Eosin-Y [304, 305] in combination with visible light [295]. Briefly, the reaction mechanism can be explained as a cyclic process [299]: In the first step, irradiation excites a photoinitiator that causes the formation of a thiyl radical. In the next step, the thiyl radical propagates across the ene's carbon-carbon double bond generating a carbon radical. Finally, chain-transfer from the carbon radical to a new thiol group regenerates the thiyl radical and the process repeats.

The goal of this study was to evaluate the combination of microfluidics and thiol-ene chemistry for the fabrication of antibody-loaded microgels. For this purpose, eight-armed PEGs were end-functionalized with norbornene moieties using either ester or amide bonds to yield degradable and stable macromonomers. Under irradiation and in presence of a suitable initiator, norbornene groups can undergo reactions with thiol groups. In the first part of the study, rheological experiments were used to study light-induced gel formation and mechanical properties. Thereby, gelation times and stiffness could be determined. In the next part, droplets were generated using a microfluidic device and then irradiated to yield covalently cross-linked microgels. Microgel size distribution was analyzed and cellular toxicity was evaluated. Moreover, stress conditions during the fabrication process were simulated and their influence on the activity of three model proteins was investigated. In the final part, the average hydrogel network mesh sizes were determined and suitable microgel types were selected for antibody loading. Finally, the model antibody bevacizumab (Avastin[®]) was incorporated into microgels and the *in vitro* release was studied.

5.2 Materials and methods

5.2.1 Materials

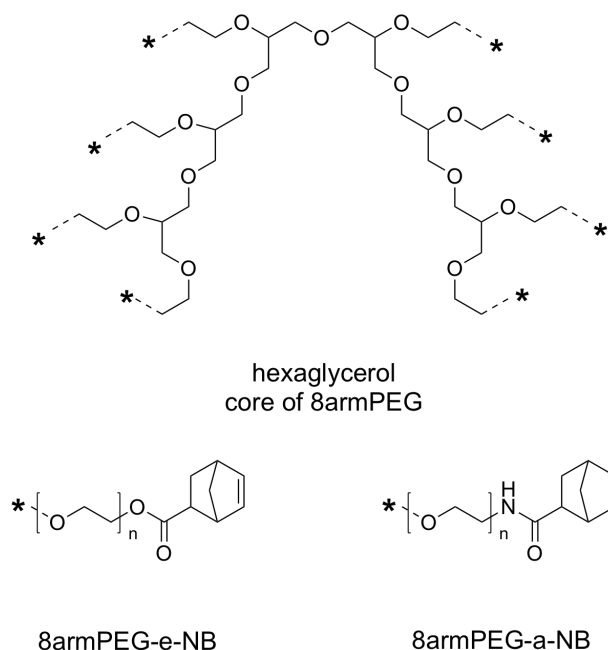
Dichloromethane (DCM) and 4-dimethylaminopyridine (DMAP) were purchased from Acros Organics (Geel, Belgium). Diethyl ether was obtained from CSC Jäcklechemie (Nuremberg, Germany). 3-(4,5-dimethylthiazol-2-yl)-2,5-diphenyltetra-

zolium bromide (MTT) was obtained from PanReac AppliChem (Darmstadt, Germany). Eight-armed poly(ethylene glycol) with molecular masses of 10,000 g mol⁻¹, 20,000 g mol⁻¹, and 40,000 g mol⁻¹ were purchased from JenKem Technology (Allen, TX, USA). Deuterated chloroform (CDCl₃), N,N'-dicyclohexylcarbodiimide (DCC), dithiothreitol (DTT), N,N-diisopropylethylamine (DIPEA), Eagle's minimum essential medium (EMEM), Eosin-Y, fetal calf serum (FCS), L-lactate dehydrogenase (from rabbit muscle), lysozyme (from chicken egg white), methoxy poly(ethylene glycol) with a molecular mass of 5000 g mol⁻¹, micrococcus lysodeikticus, exo-5-norbornenecarboxylic acid, pyruvate and silicone oil were received from Sigma-Aldrich (Taufkirchen, Germany). Poly(tetrafluoroethylene) (PTFE) tubing (1/16" × 0.50 mm inner diameter) was bought from Vici AG International (Schenkon, Switzerland). Female luer fitting systems (1/16") and a poly(etheretherketone) (PEEK) MicroTee (1/16") were received from Cole-Parmer GmbH (Wertheim, Germany). 2 mL and 10 mL B. Braun Injekt[®] luer-lock syringes were purchased from Carl Roth GmbH & Co KG (Karlsruhe, Germany). All other chemicals were obtained from Merck KGaA (Darmstadt, Germany). Bevacizumab (Avastin[®], 25 mg mL⁻¹, Roche Ltd, Basel, Switzerland) was kindly provided by the hospital pharmacy of the University of Regensburg (Germany). Mouse fibroblast L-929 cells were a kind gift from the group of Prof. Armin Buschauer (University of Regensburg). Purified water was freshly prepared using a Milli-Q water purification system (Millipore, Schwalbach, Germany).

5.2.2 Synthesis of macromonomers

In order to prepare suitable macromonomers, eight-armed PEG molecules with a molecular mass of 10,000 Da (8armPEG10k), 20,000 Da (8armPEG20k), and 40,000 Da (8armPEG40k) and methoxy PEG with a molecular mass of 5000 Da (mPEG5k) were end-functionalized with norbornene moieties (Scheme 5.1). Hydrolytically cleavable and non-cleavable end-groups were introduced using either amide or ester bonds.

For the synthesis of macromonomers with hydrolytically cleavable functionalities, 8armPEGs were end-functionalized with exo-5-norbornenecarboxylic acid by esterification using a slightly modified version of the synthesis described in literature [287, 296]. In brief, exo-5-norbornenecarboxylic acid (5-fold excess of PEG hydroxyl groups) and DCC (2.5-fold excess of OH-groups) were dissolved in anhydrous DCM and stirred for 30 min at 0 °C. After removing the precipitate,



Scheme 5.1: Eight-armed PEG was end-functionalized with norbornene (NB) moieties. Ester (8armPEG-e-NB) or amide (8armPEG-a-NB) bonds were used to yield macromonomers with hydrolytically cleavable or non-cleavable functionalities. PEG with molecular masses of 10,000 Da, 20,000 Da, and 40,000 Da were used.

the solution was combined with a PEG solution containing pyridine (5-fold excess of OH-groups) and DMAP (0.5-fold of OH-groups). After overnight stirring in an ice-bath the solution was washed with a 5% sodium bicarbonate solution two times and with brine once. The product was then precipitated in cold diethyl ether. The degree of end-group functionalization was 71 - 85% as determined by $^1\text{H-NMR}$.

For the synthesis of hydrolytically stable macromonomers, PEG hydroxyl groups were first converted to amino groups (8armPEG-NH₂) by means of a Mitsunobu reaction followed by hydrazinolysis [225] and then reacted with exo-5-norbornenecarboxylic acid using DCC chemistry. In brief, exo-5-norbornenecarboxylic acid (4-fold excess of PEG amino groups) and DCC (2-fold excess of NH₂-groups) were dissolved in anhydrous DCM and stirred for 30 min at 0 °C. After filtration, the solution was combined with a solution of PEG in DCM, neutralized with DIPEA (2-fold excess of NH₂-groups), stirred for at least 1.5 hours at room temperature and was then precipitated in cold ethyl ether. The degree of end-group functionalization was 73 - 83% as determined by $^1\text{H-NMR}$.

5.2.3 Hydrogel preparation, swelling and network mesh size

Precursor solutions for the formation of hydrogel cylinders were prepared by dissolving appropriate amounts of the respective macromonomer in purified water. DTT (0.5-fold of NB-groups) and Eosin-Y (0.1 mM) were added. 375 μ L of the precursor solution were cast into cylindrical molds and gels were formed by irradiation with Luxeon[®] Rebel LXML PM01 0100 green light emitting diodes (LEDs, $\lambda = 520 - 550$ nm) for at least 15 min. Hydrogel swelling and degradation was analyzed as previously described [221]. The average network mesh size (ξ) of 8armPEG10k-e-NB, 8armPEG20k-e-NB, and 8armPEG40k-e-NB hydrogels with concentrations of 5%, 10%, and 15% (w/V) was determined as previously described [221, 254].

5.2.4 Rheology

Precursor solutions were prepared as described above. 750 μ L of the precursor solution were used for the measurements; the polymer concentrations were 5%, 10% and 15 % (w/V). Oscillatory shear experiments were conducted on a TA Instruments AR 2000 rheometer (TA Instruments, Eschborn, Germany) at a temperature of 25 °C and a constant frequency of 0.5 Hz. The instrument was equipped with a 40 mm parallel steel plate and a flat transparent glass plate underneath (Fig. 5.1). H6-RGB-9 LEDs with a wavelength maximum at 515 - 520 nm (Roithner Lasertechnik GmbH, Vienna, Austria) were installed below the transparent plate to allow irradiation of the sample during the measurement. First, LEDs were switched off to analyze the rheological properties of the precursor solutions and to demonstrate that no gel formation occurred without light. After one minute, LEDs were switched on to investigate light-induced gel formation. The absolute value of the complex shear modulus ($|G^*|$) was recorded over time.

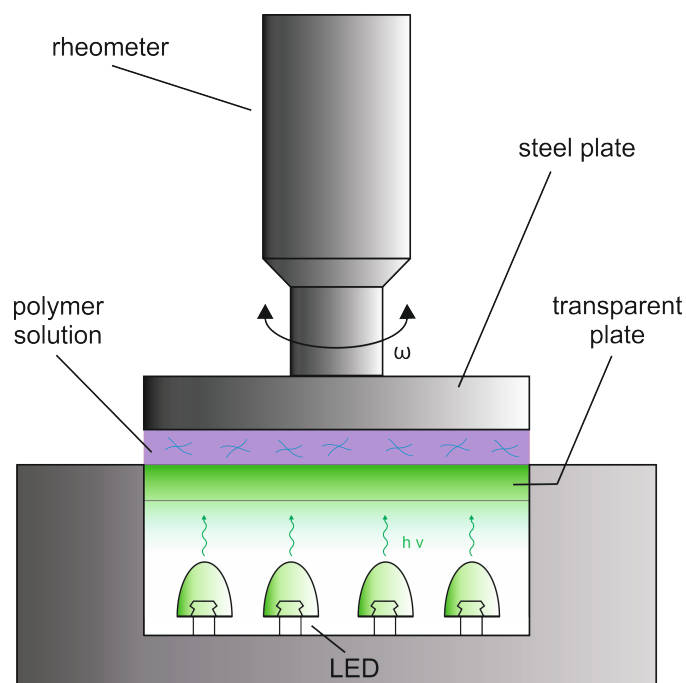


Figure 5.1: A rheometer was modified with a transparent lower plate to allow irradiation during oscillatory shear measurements. In this way, gel formation in response to green light could be followed in real-time.

5.2.5 Microgel fabrication

A suitable amount of the respective macromonomer and DTT (0.5-fold of NB-groups) were dissolved in phosphate buffered saline (PBS); 0.1 mM Eosin-Y was added. This precursor solution was transferred to a 2.0 mL syringe and another 10.0 mL syringe was filled with silicone oil with a dynamic viscosity (η) of 5 mPa s. Both syringes were connected to PTFE tubes using a Luer lock system and then mounted on a KDS 220 infusion pump (Cole Parmer, Vernon Hills, IL, USA). The pump was adjusted to yield a constant flow of 20 $\mu\text{L}/\text{min}$. Droplets were generated using a T junction and cross-linking was induced by 5 min of irradiation at a wavelength of 520 - 550nm. Microgels were collected in a glass vial filled with 1.0 mL of PBS and the silicone oil was removed. In order to study microgel size, the length and width of 100 microgel particles were determined using a Leica DM IRB optical microscope (Leica Microsystems GmbH, Wetzlar, Germany) connected to a DS-5M digital camera (Nikon GmbH, Düsseldorf, Germany) in combination with EclipseNet software (Nikon GmbH, Düsseldorf, Germany). In order to study

the influence of flow ratio on microgel size, a 2 mL syringe was used to yield the silicone oil flow instead of a 10 mL syringe.

5.2.6 In vitro release

For the release studies, 8armPEG10k-e-NB, 8armPEG20k-e-NB, and 8armPEG40k-e-NB microgels were loaded with 5 mg/mL bevacizumab. A polymer concentration of 5% (w/V) was used. Microgels were transferred to glass vials containing 4.0 mL PBS and incubated in a shaking water bath at 37 °C. 300 μ L release media were drawn at defined time-points and replaced with fresh media; samples were stored at 2 - 8 °C until further analysis. The amount of released bevacizumab was determined by fluorescence spectroscopy ($\lambda_{ex.}$ = 280 nm and $\lambda_{em.}$ = 335 nm) on a PerkinElmer LS 55 Fluorescence spectrometer (Perkin Elmer, Wiesbaden, Germany). For the release curves, the amount of bevacizumab was standardized to the concentration at the final plateau.

5.2.7 Simulation of stress conditions

Stress conditions that occurred during microgel fabrication were simulated and their influence on protein stability was investigated. Sample solutions containing 10% mPEG5k-e-NB, DTT (0.5-fold of NB-groups), 0.1 mM Eosin-Y and either 1 mg mL⁻¹ lysozyme, 1 mg mL⁻¹ L-lactate dehydrogenase (LDH), or 5 mg mL⁻¹ bevacizumab were prepared. Linear mPEG5k-e-NB was used to simulate thiol-ene reactions while avoiding actual hydrogel formation. To study the influence of the cross-linking reaction on protein stability the sample solutions were irradiated (λ = 520 - 550 nm) for 5 min. In addition, the microgel fabrication process was carried out as described above without irradiation to study the effect of microfluidics alone. Moreover, the combined effects of microfluidics and cross-linking on protein stability were studied. After stress simulation, protein activity was analyzed and compared to a non-treated sample solution which served as a positive control. Lysozyme activity was analyzed using a micrococcus lysodeikticus assay as suggested by Shugar [306]. LDH activity was determined by measuring the decrease of pyruvate absorbance over time as described by Bergmeyer and Bernt [307]. Functional binding of bevacizumab (Avastin[®]) was investigated using a Shikari[®] Q-beva enzyme-linked immunosorbent assay (ELISA) kit (Matriks Biotek, Ankara, Turkey).

5.2.8 Cytotoxicity

To study the cytotoxicity of thiol-ene microgels an MTT assay was carried out according to ISO 10993-5:2009 (Biological evaluation of medical devices, part 5: Tests for *in vitro* cytotoxicity). Over the course of the experiment, the toxicity of the microgels was evaluated both directly, by adding particles to wells containing cells, and indirectly, by preparing extracts.

Briefly, 8armPEG10k-e-NB, 8armPEG20k-e-NB and 8armPEG40k-e-NB microgels with a polymer concentration of 10% (w/V) were fabricated; a total volume of 600 μ L was prepared for each gel type. Extract media were prepared by incubating one half of the microgels with 1.0 mL of EMEM supplemented with 10% FCS for 24 hours at 37 °C. The other half of the microgel samples was stored at 2 - 8 °C overnight to be directly added to cell culture. Mouse fibroblast L-929 cells were seeded in 96-microtiter plates at a density of 10,000 cells per well and allowed to adhere overnight. 100 μ L of extract was added per well. Alternatively, 100 μ L microgel suspension were added directly to the wells. 0.1% SDS served as a negative control and pure medium as a positive control ($n = 10$). Cells were incubated with the test media for 24 hours. For the extract samples, the medium was removed and 200 μ L of serum-containing medium with 1.5 mM MTT was added to each well. For the microgel samples, media was not removed and 100 μ L of serum-containing medium with 3.0 mM MTT was added. After 4 hours of incubation, the MTT solution was removed and 200 μ L PBS containing 10% SDS was added to each well. After 16 hours, absorbance at 570 nm and 690 nm was determined for each well using a FluoStar Omega fluorescence microplate reader (BMG Labtech, Ortenberg, Germany). The difference in absorbance at 570 nm and 690 nm was used to calculate the viability of cells. The viability of the treated cells was normalized to the value for the positive control, i.e., medium alone.

5.2.9 Statistical analysis

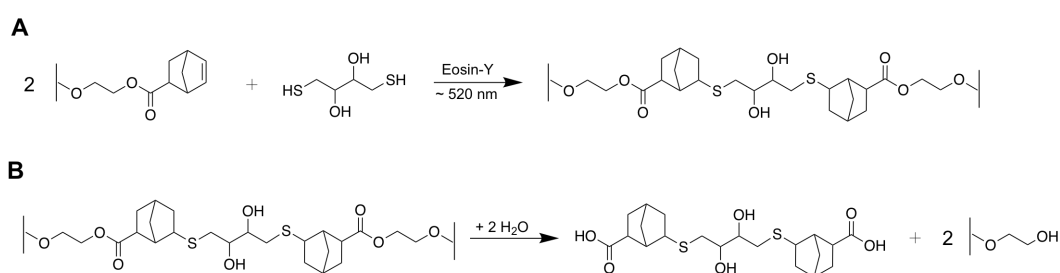
All results are presented as mean \pm standard deviation based on data obtained from at least $n = 3$ samples. Statistical significance was determined by means of one-way ANOVA, followed by Tukey's *post-hoc* test using GraphPad Prism 6.0 (GraphPad Software Inc., La Jolla, CA, USA). Differences were considered statistically significant at $p < 0.05$.

5.3 Results and discussion

5.3.1 Gelation and material properties

The goal of this study was to fabricate protein-loaded microgels with a narrow size distribution for drug delivery applications. The first prerequisite for this process was to select a method for droplet generation that leads to uniform droplets and is compatible with fragile antibodies. To this end, droplets containing antibodies and reactive macromonomers were generated using microfluidics. Then, chemical reactions were triggered to cross-link the droplets and incorporate the antibody inside the generated microgels. For cross-linking, the radical-based reaction between norbornene and thiol groups was selected. This photoclick reaction is rapid, highly specific, proceeds at mild conditions, and does not form toxic side-products. Additionally, in contrast to many other reactions that involve free radicals [308, 309], polymerizations based on thiol-ene reactions are efficient step-growth processes that are accompanied by relatively short radical lifetimes [310].

In order to yield suitable macromonomers, eight-armed PEG was end-functionalized with norbornene groups; DTT was used as a cross-linker and Eosin-Y as an initiator (Scheme 5.2A). Norbornene (NB) moieties were selected as they undergo rapid and nearly ideal thiol-ene reactions with a minimum degree of homopolymerization and chain-growth [299, 311]. Consequently, hydrogels with few network defects can be obtained while minimizing stress on the proteins to be incorporated. Modification with NB groups was carried out employing either amide (8armPEG-a-NB) or ester (8armPEG-e-NB) bonds. The use of



Scheme 5.2: Light induced cross-linking of PEG-e-NB with dithiothreitol (DTT) via thiol-ene reaction (A). Ester hydrolysis which is fundamental for hydrogel degradation (B).

amide bonds should lead to non-degradable hydrogels while ester bonds should lead to hydrolytically degradable ones (Scheme 5.2B). As a proof of concept,

degradability of the prepared hydrogels was investigated in a swelling study at 37 °C in phosphate buffer pH 7.4 (Fig. 5.2). Gel cylinders were prepared using a polymer concentration of 10% (w/V) and mass increase due to swelling was monitored over time. As expected, 8armPEG40k-a-NB did not show considerable swelling and did not degrade over a period of at least 150 days. In contrast, the swelling of 8armPEG40k-e-NB hydrogels led to a 5-fold mass increase within 50 days and the hydrogels were fully degraded after about 60 days. The shape of the swelling curves was comparable to the ones reported in the literature [296].

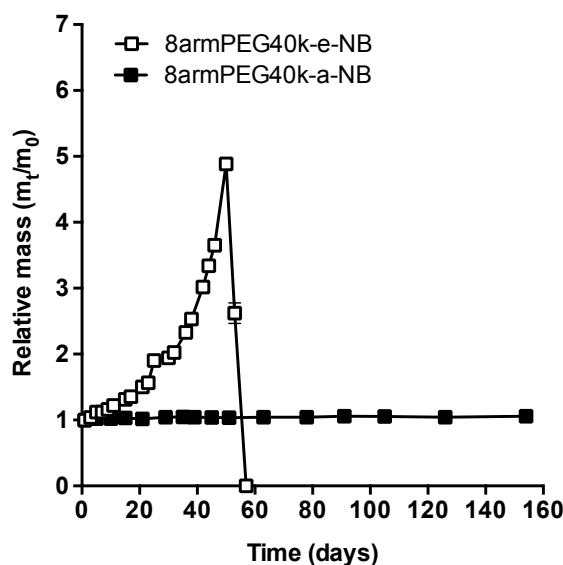


Figure 5.2: Swelling and degradation of 10% (w/V) 8armPEG40k-e-NB and 8armPEG40k-a-NB hydrogels in phosphate buffer, pH 7.4 at 37 °C.

Prior to application in combination with microfluidics, gel times and mechanical properties had to be analyzed. In this way, the general suitability of the synthesized macromonomers and the cross-linking reaction was assessed. For this purpose, oscillatory shear experiments were performed to determine the gel point and the absolute value of the complex shear modulus ($|G^*|$) as a function of irradiation and time. In order to study light-induced gel formation, an experimental setup was used to record these parameters in real-time. Precursor solutions containing macromonomers, DTT and Eosin-Y were prepared and irradiation with green light was initiated one minute into the measurement (Fig. 5.3).

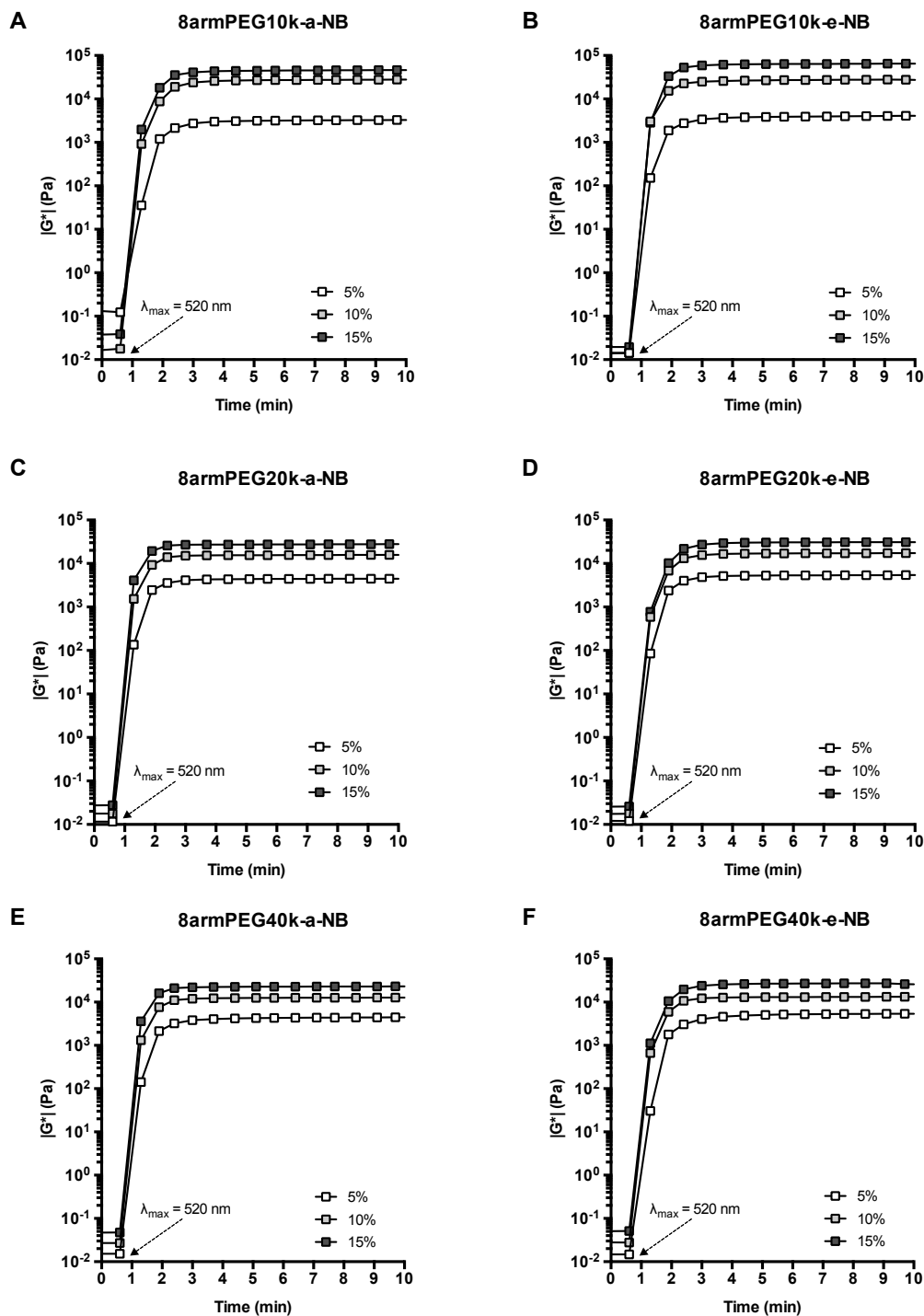


Figure 5.3: Gelation of hydrogels with amide or ester bonds, a molecular mass of 10,000 Da, 20,000 Da, or 40,000 Da, and a concentration of 5%, 10% or 15% (w/V) were studied at 37 °C. Without light (0 - 1 min) no gel formation occurred. Irradiation with green light (1 - 10 min) triggered rapid gelation. After about 5 min, a plateau in $|G^*|$ was reached and cross-linking was considered completed.

Macromonomers with different molecular masses (10,000 Da, 20,000 Da, 40,000 Da) and bonds (ester, amide) at various polymer concentrations (5, 10, 15% (w/V)) were used. Overall, all precursor solutions displayed a very similar gelation behavior. During the first minute without irradiation, no gel formation was observed. At this point, $|G^*|$ values were < 0.1 Pa and viscous properties were dominant (storage modulus (G') $<$ loss modulus (G'')). This finding was important for a later application in microfluidics as maintaining fluidity is a prerequisite for droplet formation. Upon irradiation, $|G^*|$ values increased rapidly and elastic properties became dominant ($G' > G''$). Rapid gelation (< 20 s) could be observed for all sample types at all polymer concentrations investigated. It was concluded that thiol-ene reactions proceed fast enough to cross-link droplets during microfluidics.

Besides rapid gelation, it would be favorable if cross-linking were completed rapidly in order to avoid unnecessarily long irradiation times and to reduce the process duration. Indeed, a plateau phase for $|G^*|$ could be observed in all cases (Fig. 5.3A-F). After 5 min of irradiation, the further increase of $|G^*|$ was only marginal and the gelation process was considered complete. The $|G^*|$ values determined after 5 min of irradiation are listed in Table 5.1. As expected, hydrogel stiffness increased with polymer concentration and decreased with macromonomer molecular mass. Additionally, it could be verified that the bond type has no considerable influence on hydrogel stiffness in most cases. $|G^*|$ values were not significantly different ($p < 0.05$) except for 8armPEG10k-a-NB and 8armPEG10k-e-NB hydrogels at a concentration of 15%.

In summary, all synthesized macromonomers were considered suitable for microgel fabrication. All gel types displayed rapid gel formation with an early plateau and did not gel without exposure to light. The desired stiffness could be tailored by varying molecular mass and concentration. However, as degradability is often considered a prerequisite for biomedical applications, all further experiments were carried out using hydrolytically degradable hydrogels.

Table 5.1: Absolute plateau values of the complex shear modulus ($|G^*|$) for the different hydrogel types after 5 min of irradiation as determined using rheology.

| Polymer type | Concentration (%) | $ G^* $ (kPa) |
|-----------------|-------------------|----------------|
| 8armPEG10k-a-NB | 5 | 3.2 ± 0.8 |
| | 10 | 27.2 ± 1.0 |
| | 15 | 45.1 ± 5.8 |
| 8armPEG10k-e-NB | 5 | 3.9 ± 0.4 |
| | 10 | 27.2 ± 4.9 |
| | 15 | 63.8 ± 9.3 |
| 8armPEG20k-a-NB | 5 | 4.4 ± 0.3 |
| | 10 | 15.6 ± 0.6 |
| | 15 | 27.4 ± 1.6 |
| 8armPEG20k-e-NB | 5 | 5.3 ± 0.5 |
| | 10 | 17.1 ± 1.9 |
| | 15 | 30.6 ± 0.8 |
| 8armPEG40k-a-NB | 5 | 4.3 ± 0.6 |
| | 10 | 12.6 ± 1.2 |
| | 15 | 22.8 ± 2.7 |
| 8armPEG40k-e-NB | 5 | 5.2 ± 0.8 |
| | 10 | 13.1 ± 2.0 |
| | 15 | 26.9 ± 0.7 |

5.3.2 Microfluidics, stress conditions and toxicity

As a next step, thiol-ene reactions were utilized for droplet cross-linking. To generate droplets, a microfluidic system which allowed for subsequent irradiation was used (Fig. 5.4).

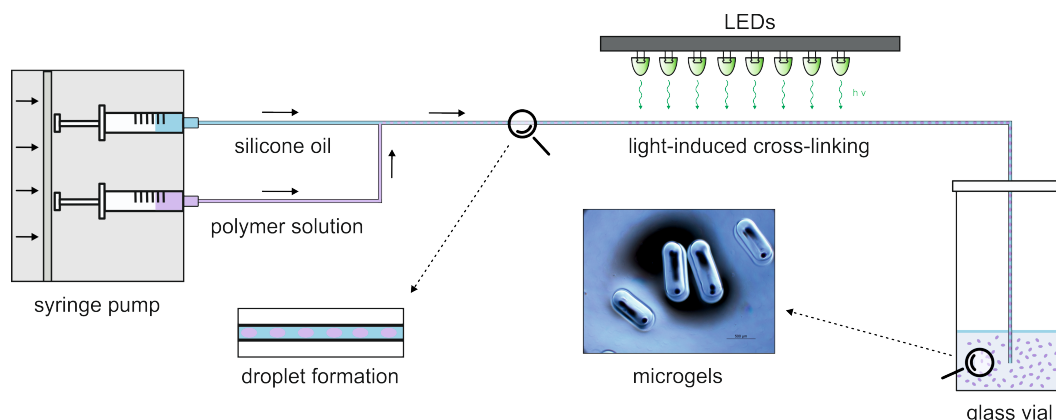


Figure 5.4: Precursor solution droplets were generated using a microfluidic system. Irradiation with visible light induced thiol-ene reactions which yielded covalently cross-linked microgels.

A syringe pump provided a continuous flow of silicone oil and aqueous polymer solution in two 500 μm diameter tubes. The polymer solution contained the selected macromonomer, DTT, and Eosin-Y. As silicone oil and aqueous solutions are immiscible, droplets could be formed by connecting the tubes and converging the fluids. For this purpose, the T-junction, which was first utilized by Thorsen et al. [312] was selected from the various ways described in literature [313]. After droplet formation, 5 min of irradiation with green light, i.e., the time required for complete gelation as determined by rheology, were used to cross-link the droplets while moving through the tube. Interestingly, the prepared microgels had a rod-like shape. This is explained by the large droplet volume which was squeezed into the tube before the droplet breaks off. Besides surface tension, viscosity and capillary forces [314], the droplet volume in the present system mainly depends on the ratio between the flow rate of silicone oil and polymer phase [315, 316]. Therefore, changes in this ratio can be used as a tool to control microgel length. For example, when two 2 mL syringes were used, the average microgel length was $2150 \pm 108 \mu\text{m}$ and the average microgel width was $385 \pm 13 \mu\text{m}$. When the flow ratio was changed by employing a 10 mL syringe for silicone oil in combination with a 2 mL syringe for the polymer solution, the microgel length decreased to $1395 \pm 48 \mu\text{m}$. In both cases the size distribution was very narrow with relative standard deviations of 3.5 - 5.0% for microgel length and 3.5 - 4.9% for microgel width. As microgel width mainly depends on the tube diameter, this parameter was not significantly influenced by changes in flow ratio ($377 \pm 18 \mu\text{m}$). In conclusion, the developed process can be used to generate microgels with a narrow size distribution while

microgel length and width can be adjusted by changing the flow rates and the tube diameter. Droplet size and shape result from a complex interplay of various parameters. Therefore, it should be noted that an in-depth investigation of all influence factors would be beyond the scope of the present study.

Besides narrow size distribution, another important argument for the selection of microfluidics was protein compatibility. During the microfluidic process a protein-compatible cross-linking reaction was used in combination with visible light. Nevertheless, it had to be demonstrated that the herein used process could be employed for microgel fabrication while preserving protein activity. Therefore, in the next experiment stress conditions that arise during the process were simulated. To this end, the process was carried out as described above, however, in this experiment monofunctional mPEG5k-e-NB was employed to simulate cross-linking while avoiding actual microgel formation. Moreover, one of the model proteins lysozyme, L-lactate dehydrogenase (LDH), and bevacizumab was added to the polymer solution. Furthermore, the influence of cross-linking alone, i.e., irradiation for 5 minutes, and microfluidics alone, i.e., droplet generation without irradiation, were evaluated. Protein activity was determined directly after the experiment and related to a non-treated control solution (Table 5.2).

Table 5.2: Residual activity of lysozyme and LDH, and residual binding ability of bevacizumab to VEGF after exposure to stress factors arising during microgel fabrication.

| | Microfluidics | Irradiation | Combined Process |
|-------------------------|-------------------|------------------|------------------|
| Bevacizumab | $103.4 \pm 1.5\%$ | $95.9 \pm 1.8\%$ | $96.3 \pm 1.6\%$ |
| Lysozyme | $91.1 \pm 0.3\%$ | $95.1 \pm 0.5\%$ | $93.1 \pm 0.4\%$ |
| L-lactate dehydrogenase | $78.8 \pm 0.5\%$ | $64.0 \pm 0.7\%$ | $24.7 \pm 1.7\%$ |

It was found that the amount of binding bevacizumab decreased only marginally to $95.9 \pm 1.8\%$ after irradiation and to $96.3 \pm 1.6\%$ after the combined process. For microfluidics alone, no decrease was observed; the value $> 100\%$ was attributed to measurement variations. Similarly, for lysozyme only a slight decrease of activity to $91.1 \pm 0.3\%$ (microfluidics), $95.1 \pm 0.5\%$ (irradiation), and $93.1 \pm 0.4\%$ (combined process) was determined. In contrast, for LDH a significant decrease of activity was detected. The amount of active LDH decreased to $78.8 \pm 0.5\%$ after treatment with microfluidic stress and to $64.0 \pm 0.7\%$ after irradiation. After the combined process, a LDH activity of only $24.7 \pm 1.7\%$ remained. In summary, the developed

microfluidic process can be considered suitable for the incorporation of proteins. Bevacizumab binding and lysozyme activity were hardly influenced by either of the stress factors. However, it should be noted that the stability of very sensitive proteins like LDH can be impaired by both microfluidics and cross-linking. In case of microfluidics, shear forces and, even more importantly, interfacial phenomena are reported to exhibit the greatest effect on protein stability [317]. Moreover, although silicone oil is frequently used as a coating material for the primary packaging of protein pharmaceuticals, it has been reported to induce protein aggregation [318]. In case of cross-linking, radical formation is still the greatest factor influencing protein stability despite the short radical lifetimes. In combination, all stress factors may amplify their effects and lead to significant activity loss. Therefore, protein stability should always be evaluated carefully when microfluidics and thiol-ene reactions are combined for protein loading.

In order to utilize the prepared microgels in the pharmaceutical and medical field, their toxicological safety has to be demonstrated. For example, reactants and unbound macromonomers which could be leached out of the gels might have toxic potential. Therefore, in order to assess the cytotoxicity of the microgels, an MTT assay was performed. In all cases, the average cell viability did not decrease below 70% which is regarded the critical threshold according to ISO (Fig. 5.5).

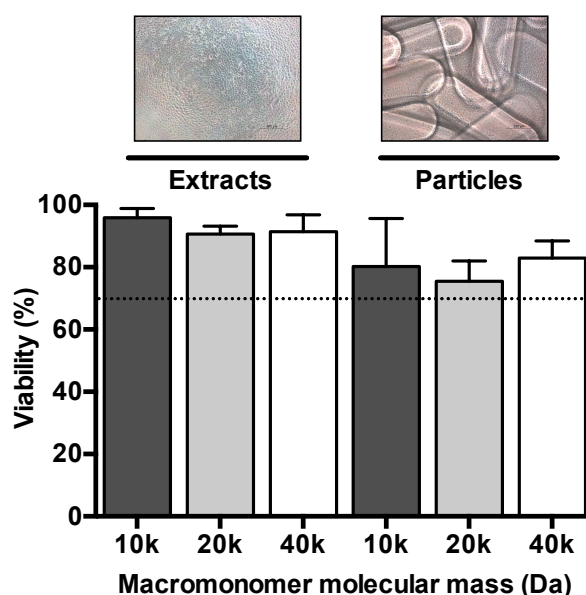


Figure 5.5: L-929 cell viability after direct contact with microgels or exposure to extracts was determined using an MTT assay. A cell viability of < 70% (dotted line) was considered cytotoxic.

However, it was observed that viabilities were lower when particles were added directly to the cells. It is very likely that this was the result of cell abrasion during handling caused by the direct contact of the particles with the cell layer. In summary, neither the microgels themselves nor potentially leached out reactants displayed considerable cellular toxicity. However, with regard to therapeutic applications the *in vivo* biocompatibility needs to be assessed.

5.3.3 Network mesh size and release studies

In the previous sections, it was demonstrated that microfluidics in combination with subsequent thiol-ene reactions can be employed to generate microgels with a narrow size distribution. Moreover, it was shown that the developed process is compatible with bevacizumab and that the generated microgels are non-toxic. In the final part of the study it was investigated whether bevacizumab can be incorporated and retained inside the microgels. In order to select an appropriate gel type for the release study, the average meshwork size (ξ) was determined first. ξ is an important parameter for release studies as it has to be smaller than the average diameter of the incorporated protein to restrict Fickian diffusion. ξ was determined as previously described [221, 254]. Briefly, the polymer fraction of the hydrogel after cross-linking and in the swollen state were determined and the polymer-water interaction parameters (χ_{12}) were calculated as suggested by Kronberg [242]. χ_{12} was taken as 0.49 for 8armPEG10k-e-NB, 0.44 for 8armPEG20k-e-NB, and 0.42 for 8armPEG40k-e-NB. These values were then used to calculate the number of elastically active chains (ν_e) using a modified version of the Flory-Rehner equation [239–241]. With ν_e , it was then possible to determine ξ as suggested by Canal and Peppas [243]:

$$\xi = v_{2s}^{-\frac{1}{3}} l \left(\frac{2m_p}{\nu_e M_r} \right)^{\frac{1}{2}} C_n^{\frac{1}{2}} \quad (5.1)$$

In eqn (5.1), M_r represents the molecular mass of the PEG repeating unit (44 g mol⁻¹), l is the average bond length along the PEG backbone (0.146 nm), m_p is the total mass of PEG in the hydrogel, and C_n is the Flory characteristic ratio (4). ξ values were determined for 8armPEG10k-e-NB, 8armPEG20k-e-NB, and 8armPEG40k-e-NB hydrogels with a polymer concentration of 5%, 10%, and 15% (w/V). The data listed in Table 5.3 shows that ξ values decrease with

decreasing molecular mass and increasing polymer concentration. This data is in good agreement with theoretical considerations which predict a decrease of ξ with increasing number of functional groups and, consequently, cross-links. As discussed above, ξ should ideally be smaller than the hydrodynamic diameter of the antibody (d_H) to enable long-term release by restricting diffusion. According to literature, the hydrodynamic radius of bevacizumab is approximately 6.5 nm ($d_H = 13$ nm) [319]. As all determined ξ values are below or only slightly higher, all hydrogel types could theoretically be used to retard the release of bevacizumab. However, when assessing ξ , it should be kept in mind that the calculated values only represent the mean and conclusions on the width of the distribution cannot be drawn.

Table 5.3: Average network mesh size (ξ) of 8armPEG10k-NB, 8armPEG20k-NB and 8armPEG40k-NB at polymer concentrations of 5, 10 and 15% (w/V).

| Polymer type | Concentration (%) | ξ (nm) |
|-----------------|-------------------|----------------|
| 8armPEG10k-e-NB | 5 | 10.0 ± 0.7 |
| | 10 | 5.1 ± 0.1 |
| | 15 | 4.5 ± 0.2 |
| 8armPEG20k-e-NB | 5 | 9.5 ± 0.4 |
| | 10 | 8.4 ± 0.3 |
| | 15 | 6.8 ± 0.3 |
| 8armPEG40k-e-NB | 5 | 13.9 ± 0.6 |
| | 10 | 12.0 ± 0.2 |
| | 15 | 10.5 ± 0.1 |

In the final experiment, microgels were loaded with bevacizumab and the *in vitro* release was studied (Fig. 5.6). To this end, microgels were prepared using 8armPEG10k-e-NB, 8armPEG20k-e-NB, and 8armPEG40k-e-NB using a polymer concentration of 5% (w/V). In all cases, after the initial burst a sustained and almost linear release profile was determined. As expected, the most rapid release was observed for 8armPEG40k-e-NB microgels. Here, bevacizumab was released over a period of only 28 days. In contrast, both 8armPEG10k-e-NB and 8armPEG20k-e-NB microgels provided sustained release over about 46 days. Interestingly, despite

the difference in macromonomer molecular mass, the release behavior of these microgel types was very similar. This is in line with their ξ values of 10.0 ± 0.7 nm and 9.5 ± 0.4 nm which are also not significantly different ($p < 0.05$). In general, the release behavior from thiol-ene microgels can be explained as follows. First, bevacizumab loosely bound to the gel surface or located in areas with a less dense network is released during an initial burst phase. As expected, at $30.5 \pm 6.9\%$ the highest burst release was observed for 8armPEG40k-e-NB microgels as it has the highest average mesh size. However, the majority of bevacizumab is prevented from diffusing out of the microgel network as $\xi < d_H$. During the following time, ester bonds are subjected to hydrolytic degradation following a pH dependent pseudo-first-order reaction kinetic [296]. As a result of the constant breaking of cross-links, average network mesh size gradually increases and bevacizumab is released when $\xi > d_H$.

In summary, bevacizumab could be successfully incorporated into different microgels and an almost linear release profile was achieved over 28 and 46 days *in vitro*. In order to tailor release kinetics, polymer concentration and molecular mass can be varied to influence microgel mesh sizes and, ultimately, the time-scales for antibody release.

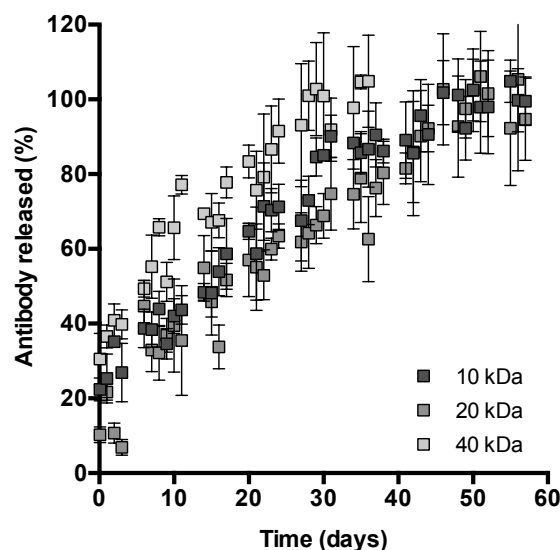


Figure 5.6: Release of bevacizumab from 8armPEG10k-e-NB, 8armPEG20k-e-NB and 8armPEG40k-e-NB microgels in PBS at 37 °C. A polymer concentration of 5% (w/V) was used.

5.4 Conclusion

Microfluidics and thiol-ene photoclick chemistry present a powerful combination for the fabrication of antibody-loaded microgels. Hydrogel particles could be prepared with a narrow size distribution and microgel length could be adjusted by employing different flow ratios between silicone oil and polymer solution. Microgel stability, stiffness, and network mesh size could be tailored by varying macromonomer concentration and molecular mass. Microgels were non-cytotoxic *in vitro* and the microgel fabrication process was demonstrated to generally be protein compatible. Finally, microgels were successfully employed to sustain the release of bevacizumab over a period of 28 and 46 days *in vitro*. The herein presented microgels could be used to provide sustained intravitreal release of bevacizumab during the treatment of neovascular age-related macular degeneration. Moreover, incorporation of antibodies into microgels could be used as a tool to protect proteins against detrimental cross-linking reactions. However, to prove that the technology is suitable for these applications further studies are necessary.

Chapter 6

Polyanions effectively prevent protein conjugation and activity loss during hydrogel cross-linking

Published in *Journal of Controlled Release*

The content of this chapter was published as: *J. Control. Release*, 238: 92–102, 2016.
doi: 10.1016/j.jconrel. 2016.07.030

Abstract

In situ encapsulation is a frequently used method to prepare hydrogels loaded with high quantities of therapeutic proteins. However, many cross-linking reactions, such as Michael-type addition or Diels–Alder (DA) reaction are not tolerant toward nucleophiles; therefore, side-reactions with proteins can occur during cross-linking. This may lead to undesired protein conjugation, activity loss and incomplete protein release. In this study, a number of polyanions, namely alginate, dextran sulfate, hyaluronic acid, heparin, and poly(acrylic acid), were screened for their capability to protect proteins during covalent cross-linking. To this end, lysozyme was incubated with furyl- and maleimide-substituted methoxy poly(ethylene glycol); different pH values were tested. The degree of PEGylation and the residual activity of lysozyme were investigated. Without polyanions, 61.1% of the total lysozyme amount was PEGylated at pH 7.4; the residual activity was 20.3% of the initial activity. With the most effective polyanion (dextran sulfate), PEGylation could be completely suppressed; the residual activity was 98.4%. The protective effect of polyanions was attributed to electrostatic interactions with proteins; the “shielding” could be reversed by adding high salt concentrations. Furthermore, the protective effect was dependent on the concentration and molecular mass of the polyanion, but almost independent of the protein concentration. As a proof of concept, hydrogels were loaded with lysozyme and bevacizumab during cross-linking via DA reaction. Without polyanions, a large fraction of the protein was covalently bound to the polymer network resulting in degradation-controlled release; the residual activity of lysozyme was 50.0%. With polyanions, the protein molecules were mobile and their release was diffusion-controlled. The residual activity of lysozyme was 88.9%; the released bevacizumab was structurally intact. Polyanions can, therefore, be used as protective additive to prevent chemical protein modification during hydrogel cross-linking.

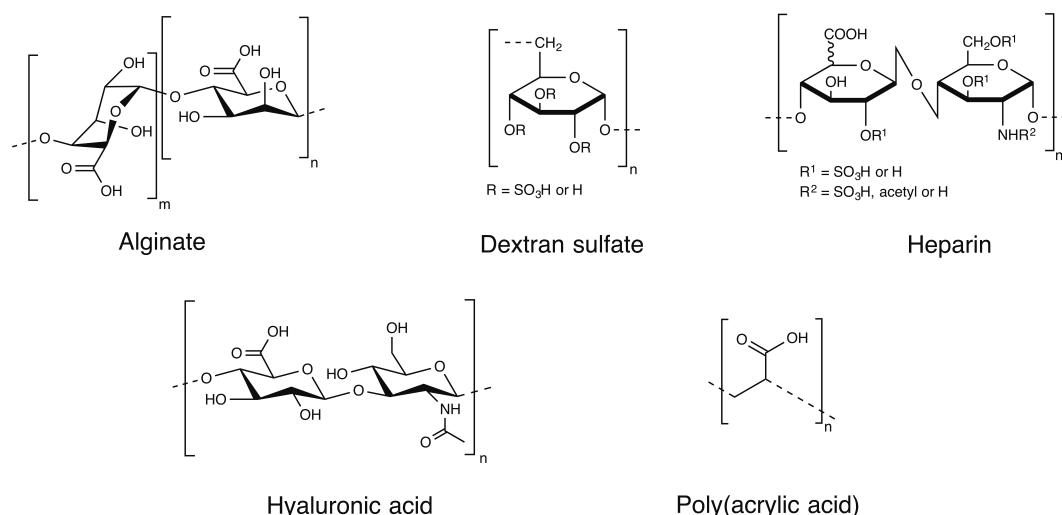
6.1 Introduction

Hydrogels are frequently used as carrier systems for the delivery of therapeutic proteins [146, 183]. In general, protein loading can be achieved by incubating pre-formed hydrogels in concentrated protein solutions (post-fabrication partitioning), or by cross-linking the hydrogel-forming polymers together with the protein (*in situ* encapsulation) [184]. While post-fabrication partitioning is beneficial for protein stability, the method provides less control over the amount of protein loading. Therefore, *in situ* encapsulation is often considered the method of choice for loading large protein quantities into hydrogels. However, only few cross-linking reactions proceed under sufficiently mild conditions to allow *in situ* encapsulation of proteins. Among these reactions, Michael-type additions and radical polymerizations have been frequently used to prepare *in situ* forming hydrogels [215, 217, 241, 320]. And recently, the Diels–Alder (DA) reaction has been employed to develop poly(ethylene glycol) (PEG)-based hydrogels for controlled antibody release [221, 254]. However, these cross-linking reactions are not tolerant toward nucleophiles, i.e., side reactions with proteins can occur [182]. For example, maleimide is a strong electrophile; it can react with nucleophilic amino acid residues such as cysteine, lysine, histidine, tryptophan or arginine [321]. This side reaction inhibits cross-linking; furthermore, protein molecules are covalently bound to the polymer network. This may result in incomplete protein release, loss of activity, and increased immunogenicity [184, 322].

For these reasons, it would be desirable to suppress side reactions between polymers and proteins during cross-linking. This would make the DA reaction, and other cross-linking reactions, more suitable for *in situ* encapsulation of proteins. For example, it has been reported that precipitation by zinc chloride or PEG can protect proteins from Michael-type additions during cross-linking [323]. However, both methods might cause protein degradation or aggregation. As a potential alternative, we investigated the use of polyanions to prevent protein conjugation and activity loss during cross-linking. Polyanions have been frequently used to formulate and stabilize therapeutic proteins [324–326]. For example, it has been shown that ionic interactions between alginate and monoclonal antibodies are present; these interactions could be exploited for sustained protein release [327]. Furthermore, sulfated β -cyclodextrin and heparan sulfate could protect acidic fibroblast growth factor (FGF) from urea-induced unfolding [328]. Martin et al. [329] have shown that non-covalent association with hydrophobically modified poly(acrylate) copolymers could prevent the thermal aggregation of immunoglobulin G. Positive effects of

polyanions on the stability have also been described for FGF-20 [330], keratinocyte growth factor-2 [331], human growth hormone [332], and parathyroid hormone [333].

In this study, a number of pharmaceutically relevant polyanions, namely alginate (ALG), dextran sulfate (DXS), heparin (HEP), hyaluronic acid (HA) and poly(acrylic acid) (PAA) (Scheme 6.1), were screened for their capability to protect proteins during hydrogel cross-linking. The DA reaction between furan and maleimide was chosen as cross-linking reaction; lysozyme was used as a model protein. To estimate the occurring protein modification, lysozyme was incubated with



Scheme 6.1: Chemical structures of alginate (ALG), dextran sulfate (DXS), heparin (HEP), hyaluronic acid (HA), and poly(acrylic acid) (PAA).

monofunctional, furyl- and maleimide-substituted methoxy poly(ethylene glycol); different pH-values and polyanion concentrations were tested. After incubation, the degree of PEGylation and the residual activity of lysozyme were analyzed. Furthermore, possible factors influencing the “shielding” effect of polyanions, such as ionic strength and molecular mass of the polyanion, were investigated. Finally, lysozyme and bevacizumab were encapsulated into hydrogels with and without

polyanions added. The *in vitro* release of the incorporated proteins was measured; furthermore, the activity and integrity of the released proteins were analyzed.

6.2 Materials and methods

6.2.1 Materials

Eight-armed poly(ethylene glycol) with molecular masses of 10,000 g mol⁻¹ (8arm-PEG10k) and 40,000 g mol⁻¹ (8armPEG40k), and methoxy poly(ethylene glycol) vinyl sulfone with a molecular mass of 5000 g mol⁻¹ (mPEG5k-vinyl sulfone) were purchased from JenKem Technology (Allen, TX, USA). Coomassie brilliant blue G-250, deuterated chloroform (CDCl₃), dextran sulfate, heparin, lysozyme (from chicken egg white), methoxy poly(ethylene glycol) with a molecular weight of 5000 g mol⁻¹ (mPEG5k), methoxy poly(ethylene glycol) thiol with a molecular mass of 6000 g mol⁻¹ (mPEG6k-thiol), micrococcus lysodeikticus, poly(acrylic acid) (100,000 g mol⁻¹ molecular mass, 35% solution), poly(acrylic acid) sodium salt (2100 g mol⁻¹ molecular mass), sodium phosphate monobasic monohydrate and D-(+)-trehalose dihydrate were received from Sigma-Aldrich (Taufkirchen, Germany). Tris(hydroxymethyl)aminomethane was purchased from GE Healthcare Europe GmbH (Freiburg, Germany). Acrylamide/bis-acrylamide (37.5:1) solution, bromphenol blue sodium salt and sodium dodecylsulfate (SDS) were received from Serva Electrophoresis GmbH (Heidelberg, Germany). Hyaluronic acid (7500 and 289,000 g mol⁻¹ molecular mass) was obtained from Lifecore Biomedical LLC (Chaska, MN, USA). Dulbecco's phosphate buffered saline (PBS) was purchased from Invitrogen GmbH (Karlsruhe, Germany). Alginate (Protanal[®] LF10/ 60FT) was purchased from FMC BioPolymer (Ratingen, Germany). Tetramethylethylenediamin (TEMED) was obtained from Carl Roth GmbH & Co KG (Karlsruhe, Germany). Boc-6-aminohexanoic acid was purchased from Bachem (Weil am Rhein, Germany). Bevacizumab (Avastin[®], 25 mg/mL, Roche Ltd, Basel, Switzerland) was kindly provided by the hospital pharmacy of the University of Regensburg (Germany). 96-Well fluorescence plates were purchased from Greiner Bio-One (Frickenhausen, Germany). All other materials were obtained from Merck KGaA (Darmstadt, Germany). Purified water was freshly prepared using a Milli-Q system (Millipore, Schwalbach, Germany).

6.2.2 Functionalization of polymers

The functionalization of 8armPEG10k with furyl (8armPEG10k-furan) and maleimide (8armPEG10k-maleimide) end-groups has been described by Kirchhof et al. [155]. The functionalization of mPEG5k with furyl (mPEG5k-furan) and maleimide (mPEG5k-maleimide) end-groups was achieved as described for 8armPEG10k-furan and 8armPEG10k-maleimide, respectively [155]. The hydrophobic modification of 8armPEG40k with 6-aminohexanoic acid, and the subsequent functionalization with furyl (8armPEG40k-C₆-furan) and maleimide (8armPEG40k-C₆-maleimide) end-groups has been described in chapter 3 [254]. The synthesis of mPEG5k-acrylamide was carried out as described by Browning et al. [334].

6.2.3 Incubation of lysozyme

The conditions during hydrogel cross-linking were mimicked by incubating lysozyme with monofunctional PEG derivatives at 37 °C in a shaking water bath for 24 h. The incubation was done in 25 mM acetic acid buffer pH 5.0, 50 mM phosphate buffer pH 7.4, and 50 mM borate buffer pH 9.0. In order to simulate cross-linking via DA reaction, 9.15 mg (1.83 μ mol) of mPEG5k-maleimide and 9.15 mg (1.83 μ mol) of mPEG5k-furan were dissolved in 400 μ L of buffer, and incubated with 0.40-0.52 mg of lysozyme. Similarly, cross-linking via Michael-type addition was simulated using 9.15 mg (1.83 μ mol) of mPEG5k-vinyl sulfone and 10.98 mg (1.83 μ mol) of mPEG6k-thiol. A radical polymerization was simulated using 9.15 mg (1.83 μ mol) of mPEG5k-acrylamide combined with a radical initiator composed of 1.83 μ L of TEMED (10% dilution) and 3.66 μ L of a 10% (m/V) ammonium persulfate solution. The incubation was performed without additives, or in the presence of different polyanions, i.e., ALG, DXS, HEP, HA, and PAA. In all cases it was checked that the pH did not change during incubation. The concentrations of ALG, DXS, HEP, and HA were 2 mg/mL; the concentration of PAA was reduced to 1 mg/mL to maintain the pH of the reaction medium.

6.2.4 Degree of lysozyme PEGylation

After incubation, samples were taken and the degree of lysozyme PEGylation was determined by SDS PAGE as previously described [182].

6.2.5 Lysozyme activity assay

To determine the activity of lysozyme, the incubation protocol was slightly modified. A lower lysozyme concentration of 0.25 mg/mL was used; moreover, lysozyme was incubated with 20 mg (4 μ mol) of mPEG5k-maleimide. In this way, the influence of polyanions on lysozyme activity could be studied more accurately. The activity of lysozyme was determined as described by Shugar [306]. In brief, lysozyme was diluted with 70 mM phosphate buffer pH 6.2 to a final concentration of 0.01 mg/mL. A 0.015% micrococcus lysodeikticus suspension was prepared using the same buffer. In a cuvette, 100 μ L of the lysozyme dilution was added to 2.5 mL of the micrococcus suspension, and the decrease of the absorbance at 450 nm was recorded for 6 min at 25 °C using a Kontron UVIKON[®] 941 spectrophotometer (Kontron Instruments S.p.A., Milan, Italy). The activity of lysozyme was calculated from the slope of the linear part of the curve.

6.2.6 Turbidity measurement

Lysozyme was diluted to a final concentration of 1.3 mg/mL; for this purpose, a 50 mM phosphate buffer pH 7.4 containing 0 mM, 37.5 mM, 75 mM, 100 mM, 150 mM or 300 mM of NaCl was used. Different amounts of PAA were added; the final concentrations were 0 mg/mL, 0.1 mg/mL, 0.2 mg/mL, 0.5 mg/mL and 1.0 mg/mL. The samples were vortexed; 200 μ L were transferred into a microtiter plate. The turbidity was measured at a wavelength of 450 nm using a FLUOstar Omega microplate reader (BMG Labtech, Durham, NC, USA).

6.2.7 Release experiments

The influence of polyanions on the *in vitro* release of lysozyme from 10% 8arm-PEG10k hydrogels was studied. For hydrogel preparation, 36.9 mg of 8armPEG10k-maleimide and 38.1 mg of 8armPEG10k-furan were separately dissolved in 300 μ L of 50 mM phosphate buffer pH 7.4. Both solutions were gently mixed; 150 μ L of a solution containing lysozyme and the polyanion, i.e., PAA, HEP or DXS, were added. Then, 250 μ L of the mixture were transferred into cylindrical glass molds with a diameter of 7 mm. The samples were allowed to cross-link overnight at 37 °C. The amount of protein loading was 2 mg per gel cylinder; the final polyanion concentrations were 0 and 0.5 mg/mL. The gel cylinders were incubated in 5.0 mL of PBS at 37 °C in a shaking water bath. At predetermined time points, samples of

300 μL were taken and replaced with fresh PBS. The amount of released lysozyme was quantified ($\lambda_{ex} = 280 \text{ nm}$, $\lambda_{em} = 335 \text{ nm}$) using a LS 55 Fluorescence spectrophotometer (Perkin Elmer, Wiesbaden, Germany). The influence of polyanions on the *in vitro* release of bevacizumab from 10% 8armPEG40k- C_6 hydrogels was carried out as described in chapter 3 [254]. The control sample (hydrogel without PAA) was cross-linked in 50 mM phosphate buffer pH 7.4; the sample containing 1 mg/mL PAA was cross-linked in 25 mM acetic acid buffer pH 5.0.

6.2.8 Size-exclusion chromatography

SEC analysis of bevacizumab was performed on a Shimadzu HPLC system (Shimadzu Corporation, Kyoto, Japan) consisting of a SIL-10AD auto injector, LC-10AT liquid chromatograph, DGU-14A degasser, CTO-10AS column oven, and SPD-10A fixed wavelength programmable UV-Vis detector. A Tosoh G3000SWXL column (Tosoh Bioscience, Griesheim, Germany) was used. Sterile filtered 50 mM phosphate buffer pH 7.4 was used as mobile phase; the flow rate was adjusted to 0.5 mL/min. Samples of 20 μL were injected and eluted for 40 min; the chromatograms were recorded at a wavelength of 280 nm.

6.2.9 Circular dichroism spectrometry

CD spectra of lysozyme were recorded on a Jasco J-815 spectropolarimeter (Jasco International, Tokyo, Japan) using a 0.2 mm quartz cuvette (Starna GmbH, Pfungstadt, Germany). For samples without polyanions, a lysozyme concentration of 1 mg/mL was used; samples containing polyanions were diluted to a lysozyme concentration of 0.2 mg/mL due to opalescence. Spectra smoothing was performed using a Savitzky-Golay polynomial.

6.2.10 Statistical analysis

All results are presented as mean \pm standard deviation, based on the data obtained from $n = 3$ samples. Statistical significance was determined by means of one-way ANOVA, followed by Tukey's *post-hoc* test using GraphPad Prism 6.0 (GraphPad Software Inc., La Jolla, CA, USA). Differences were considered statistically significant at $p < 0.05$.

6.3 Results and discussion

The hypothesis for this study was that polyanions could prevent chemical protein modification during hydrogel cross-linking. A schematic representation of this hypothesis is given in Fig. 6.1. Without the addition of polyanions, macromonomers can react with amino acids on the protein surface during hydrogel cross-linking. Consequently, protein molecules may be covalently bound to the polymer network. In contrast, in the presence of polyanions, the protein surface is thought to be covered with a “shell” that prevents reactions between macromonomers and proteins. Consequently, the amount of covalently bound protein is reduced. To verify this hypothesis, the influence of polyanions on the availability and activity of proteins after cross-linking via DA reaction was investigated. Lysozyme was used as a model protein; five different polyanions, namely alginate (ALG), dextran sulfate (DXS), heparin (HEP), hyaluronic acid (HA), and poly(acrylic acid) (PAA) were investigated. All of these polyanions are considered appropriate for pharmaceutical or biomedical applications.

6.3.1 Influence of polyanions on lysozyme PEGylation and activity

In the first experiment, the degree of protein modification during cross-linking was estimated. For this purpose, monofunctional mPEG5k-maleimide and mPEG5k-furan were used instead of branched derivatives; in this way, the conditions during cross-linking can be simulated while avoiding gel formation. Lysozyme was incubated with mPEG5k-maleimide and mPEG5k-furan either without additives (CTRL) or in the presence of polyanions. The degree of PEGylation was subsequently quantified using SDS PAGE. Lysozyme has one N-terminus and six lysine residues (Lys1, Lys13, Lys33, Lys96, Lys97, and Lys116) which are susceptible to Michael-type additions to mPEG5k-maleimide [180, 335, 336]. However, due to the better accessibility, PEGylation will mainly occur at Lys33 and Lys97. Consequently, SDS PAGE showed three major bands of unmodified lysozyme, and lysozyme modified with one or two PEG chains. PEGylation at Lys1, Lys13, Lys96 or Lys116 resulted in further bands of lysozyme modified with three or more PEG chains.

The degree of PEGylation was generally much lower at pH 5.0 than at pH 7.4 or pH 9.0 (Fig. 6.2). This effect was observed in all groups. For example, in the

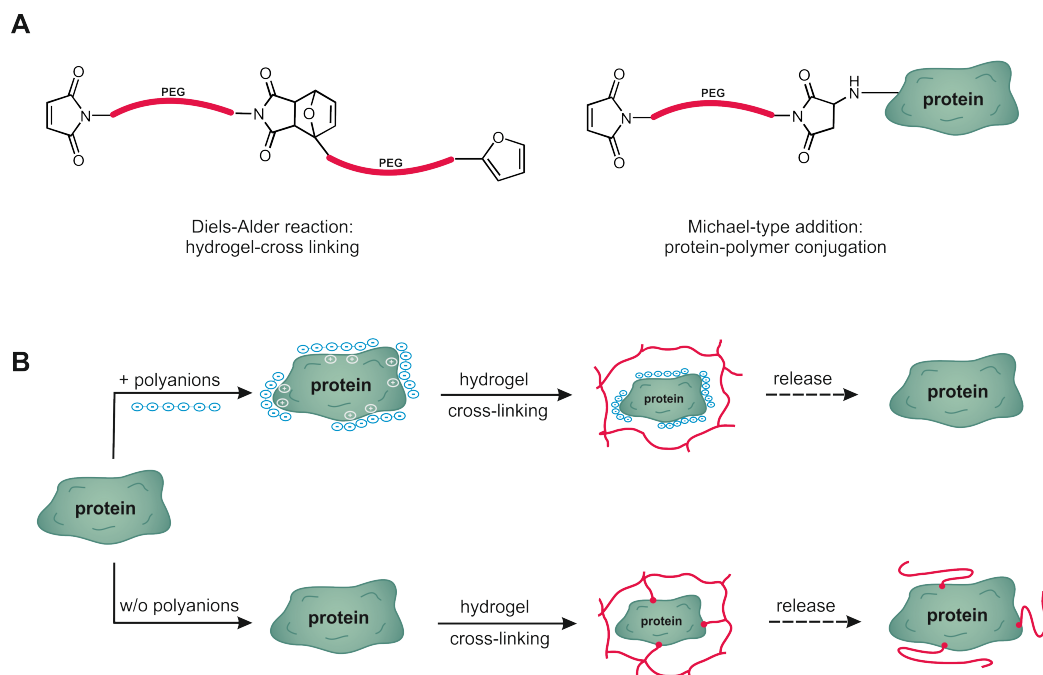


Figure 6.1: Schematic representation of the “shielding” effect of polyanions. During hydrogel cross-linking, maleimide groups can react with furyl groups (Diels–Alder reaction) or amino groups on the protein surface (Michael–type addition) (A). Polyanions interact with proteins and protect them during cross-linking (B). Without polyanions, amino acids on the protein surface can react with polymers resulting in covalent immobilization.

control group, the amounts of free lysozyme were $77.9 \pm 1.4\%$ (pH 5.0), $38.9 \pm 2.0\%$ (pH 7.4), and $38.9 \pm 0.5\%$ (pH 9.0). At acidic pH, basic amino acids are present in the ionized form. Since ammonium groups exhibit significantly lower nucleophilicity than amino groups [337], the degree of PEGylation resulting from Michael–type additions of basic amino acids to mPEG5k-maleimide is pH-dependent. Therefore, as it has already been suggested, the use of acidic reaction conditions represents an option to reduce nucleophilic side reactions during cross-linking [182]. However, as acidic pH is unphysiological and may influence protein stability, this approach might not be feasible for all proteins [338, 339].

Interestingly, as shown in Fig. 6.2, polyanions were capable of significantly reducing lysozyme PEGylation at acidic, neutral and basic pH. At pH 5.0, the degree of PEGylation was lowest, most likely due to synergistic effects of pH and polyanions. The amounts of free lysozyme were 100.0% (DXS), $99.1 \pm 0.2\%$ (PAA), $97.3 \pm 2.1\%$ (HEP), and $96.8 \pm 3.8\%$ (ALG). Lysozyme has an isoelectric point

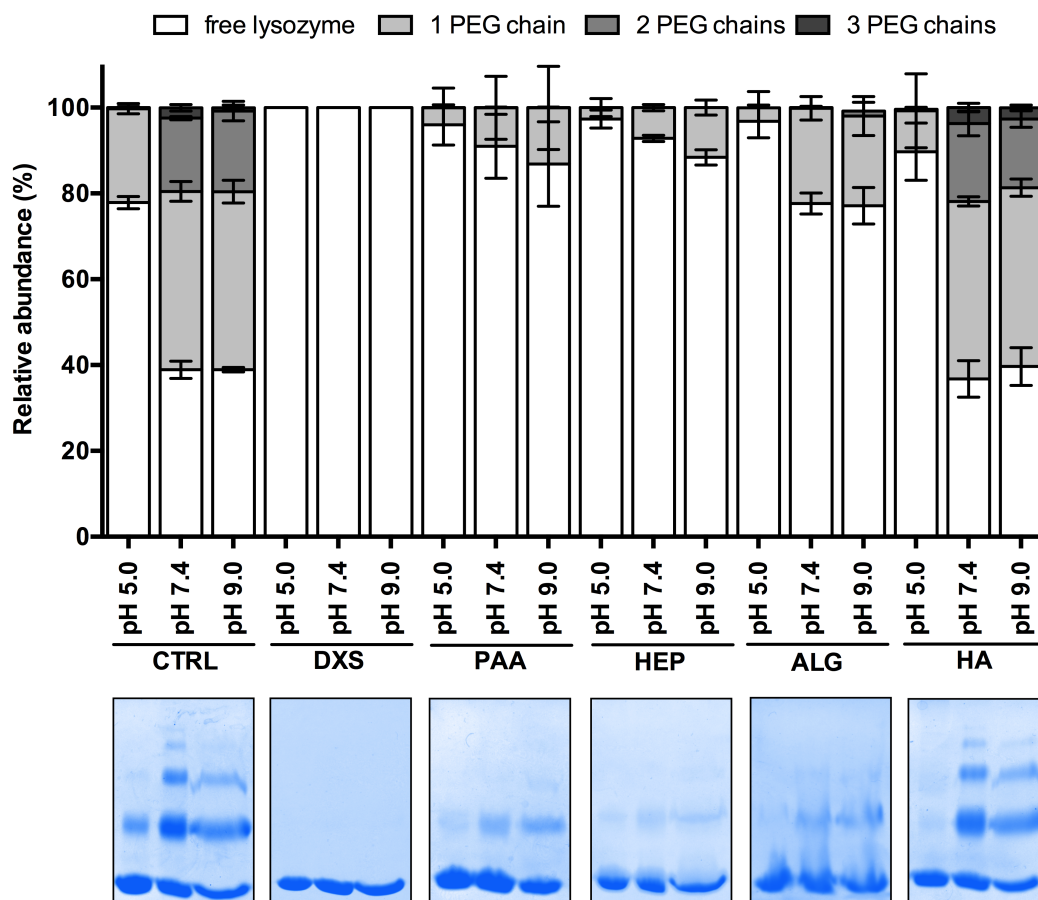


Figure 6.2: The influence of DXS, PAA, HEP, ALG and HA on the degree of PEGylation was studied and compared to a control group without polyanions (CTRL). At acidic pH, the degree of PEGylation was considerably lower than at neutral or basic pH. The addition of polyanions protected lysozyme from PEGylation with DXS, PAA and HEP being most effective.

(IEP) at about pH 11 [340]; the protein, therefore, carries a net positive charge below pH 11. As discussed above, the nucleophilicity of basic amino acids is lowest at acidic pH; furthermore, an acidic pH facilitates interactions with polyanions as protein molecules carry more positive charges. However, it should be noted that interactions with polyanions do not necessarily require a net positive charge on the protein surface. Polyanions may also bind to proteins with a net negative charge, given that there are positively charged patches present on the protein surface [341]. For example, lysozyme has eight positive charges at neutral pH [342]. At pH 7.4, the amounts of free lysozyme were 100.0% (DXS), $91.0 \pm 7.5\%$ (PAA), $92.8 \pm 0.7\%$ (HEP), and $77.7 \pm 2.5\%$ (ALG); at pH 9.0, 100.0% (DXS), $86.9 \pm 9.8\%$ (PAA),

$88.4 \pm 1.8\%$ (HEP), and $77.1 \pm 4.3\%$ (ALG) of the protein remained unmodified. In contrast to DXS, PAA, HEP and ALG, “shielding” with HA resulted in $89.8 \pm 6.7\%$ (pH 5.0), $36.8 \pm 4.2\%$ (pH 7.4), and $39.7 \pm 4.4\%$ (pH 9.0) unmodified lysozyme. The weaker effect of HA can be explained by the lower number of acid functionalities.

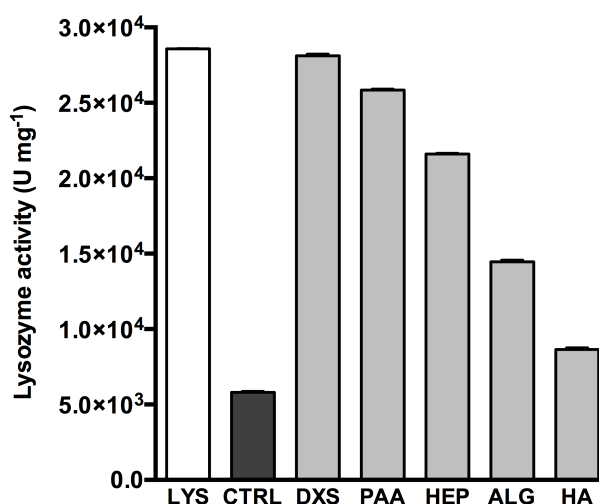


Figure 6.3: Activity of lysozyme after incubation with mPEG5k-maleimide and mPEG5k-furan at pH 7.4. The activity was determined prior to incubation (LYS), after incubation without polyanions (CTRL), and after incubation with DXS, PAA, HEP, ALG and HA. Without polyanions, the activity of lysozyme considerably decreased. Polyanions could prevent activity loss with DXS, PAA and HEP being most effective.

Since uncontrolled PEGylation can impair the biological activity of proteins, the activity of lysozyme was studied after incubation with mPEG5k-maleimide and mPEG5k-furan (Fig. 6.3). Native lysozyme (LYS) had an activity of $28,580 \pm 22 \text{ U mg}^{-1}$. After incubation with mPEG5k-maleimide and mPEG5k-furan (CTRL), the activity had decreased to $5,807 \pm 56 \text{ U mg}^{-1}$. The activity loss is explained by Michael-type additions of nucleophilic amino acids to mPEG5k-maleimide. As the most reactive lysine residue of lysozyme (i.e., Lys97) is located in a region responsible for substrate specificity [343], it is likely that PEGylation at this position causes activity loss. Changes in the secondary structure, which would also result in activity loss, were excluded by circular dichroism (CD) spectroscopy (Fig. 6.4). Since the addition of polyanions could reduce the degree of PEGylation, it can be expected that polyanions preserve the activity of lysozyme. Indeed, the addition of polyanions could reduce activity loss due to PEGylation; the residual activities

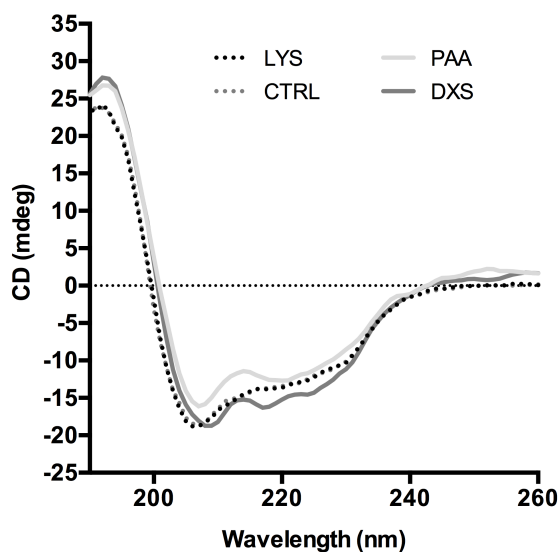


Figure 6.4: CD spectra of lysozyme after incubation with mPEG5k-maleimide and mPEG5k-furan at pH 7.4 without polyanions (CTRL), and in the presence of PAA or DXS. Lysozyme incubated in pure buffer served as a control (LYS). Neither incubation with mPEG5k-maleimide and mPEG5k-furan, nor interactions with polyanions caused changes in the secondary structure of lysozyme.

were $28,120 \pm 103 \text{ U mg}^{-1}$ (DXS), $25,850 \pm 56 \text{ U mg}^{-1}$ (PAA), $21,600 \pm 54 \text{ U mg}^{-1}$ (HEP), $14,460 \pm 113 \text{ U mg}^{-1}$ (ALG), and $8652 \pm 107 \text{ U mg}^{-1}$ (HA). Again, DXS, PAA and HEP were the most effective additives to preserve the enzymatic activity of lysozyme; HA was found to be the least effective polyanion. This is consistent with the data on PEGylation presented above. In summary, it can be stated that the addition of polyanions represents an effective way to reduce PEGylation and activity loss during hydrogel cross-linking.

6.3.2 Factors influencing the “shielding” effect of polyanions

The ability of polyanions to protect proteins from PEGylation is a remarkable finding. According to the hypothesis introduced above, this “shielding” effect is based on electrostatic interactions between proteins and polyanions. To verify this assumption, the influence of ionic strength on protein-polyanion interactions was investigated. The association of proteins and polyanions leads to the formation of colloidal particles and, thus, to an increase of turbidity. On the other hand, high ionic strength is known to reduce the attractive forces between oppositely charged molecules in solution. Therefore, the turbidity of lysozyme-PAA mixtures was

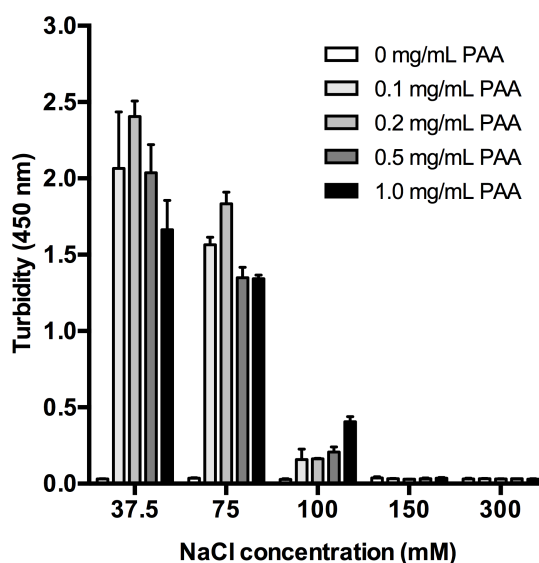


Figure 6.5: Influence of different salt concentrations on the turbidity of solutions containing lysozyme and PAA. High ionic strength decreased the extent of electrostatic interactions resulting in clear solutions above 100 mM NaCl.

measured at different salt concentrations (Fig. 6.5). At a low NaCl concentration of 37.5 mM, the analyzed samples were opalescent. This was due to interactions between lysozyme and PAA, which led to the formation of colloidal protein-polyanion complexes. However, at a NaCl concentration of 100 mM, the samples started to become clear. Finally, above a NaCl concentration of 150 mM, the samples were totally clear. These results indicate that the interactions between lysozyme and polyanions are electrostatic interactions.

If the “shielding” effect was also based on electrostatic interactions, it should be possible to reverse the protecting effect of polyanions by increasing the ionic strength. In the next experiment, lysozyme was, therefore, incubated with mPEG5k-maleimide and mPEG5k-furan at a NaCl concentration of 300 mM. As expected, none of the polyanions were able to “shield” lysozyme from PEGylation (Fig. 6.6A). For all tested polyanions, the degree of PEGylation was comparable to the control group. Similarly, at a NaCl concentration of 300 mM, the addition of polyanions could not prevent activity loss due to PEGylation (Fig. 6.6B). Therefore, it can be concluded that the “shielding” effect of polyanions is due to electrostatic interactions with proteins. At high salt concentrations, polyanions cannot bind to the protein surface; consequently, proteins are affected by PEGylation and activity loss. This should be kept in mind when concentrated buffer solutions are used. For example,

high concentrations of sodium acetate or sodium citrate reduced the “shielding” effect of polyanions (Fig. 6.7A). In contrast to that, typical cryoprotectants for freeze-drying, such as sucrose or trehalose [344, 345], did not negatively affect the protective effect of polyanions (Fig. 6.7B). To get a better understanding of the “shielding” mechanism, additional influencing factors were investigated. At first, the influence of the polyanion concentration was investigated. For this purpose, lysozyme was incubated with mPEG5k-maleimide and mPEG5k-furan at different PAA concentrations. It could be observed that the “shielding” effect was dependent on the polyanion concentration (Fig. 6.8A). When a low PAA concentration of 0.025 mg/mL was used, the residual lysozyme activity was $37.3 \pm 2.1\%$ of the initial activity. However, in comparison to the activity of the control group ($20.3 \pm 1.0\%$ of the initial activity), PAA still has a protective effect at this low concentration. With increasing PAA concentrations, the residual activity of lysozyme constantly increased until a plateau was reached at about 1.00 mg/mL. Furthermore, increasing amounts of lysozyme were incubated with mPEG5k-maleimide and mPEG5k-furan at a PAA concentration of 1.00 mg/mL. The results shown in Fig. 6.8B indicate that the “shielding” effect is almost independent from the protein concentration. Upon addition of PAA, the residual activity of lysozyme increased by 205.6% (0.05 mg/mL lysozyme) and 207.8% (0.5 mg/mL lysozyme), respectively. In addition to the polyanion concentration, the influence of the molecular mass of the polyanion was studied. For this purpose, the shielding effects of low- and high-molecular-mass polyanions were compared (Fig. 6.8C and D); two different polyanions (PAA and HA) were studied. In both cases, high-molecular-mass polyanions had a better “shielding” capacity than their low-molecular-mass counterparts; the effect was more pronounced with PAA than with HA. According to the literature, high molecular mass is one of the factors that facilitates the formation of protein-polyanion complexes [341]. However, the interactions between proteins and polyanions, and thus the “shielding” effect, may also be influenced by other factors such as charge density [346], rigidity of the polyanion backbone [347], and the existence of hydrophobic interactions [348, 349].

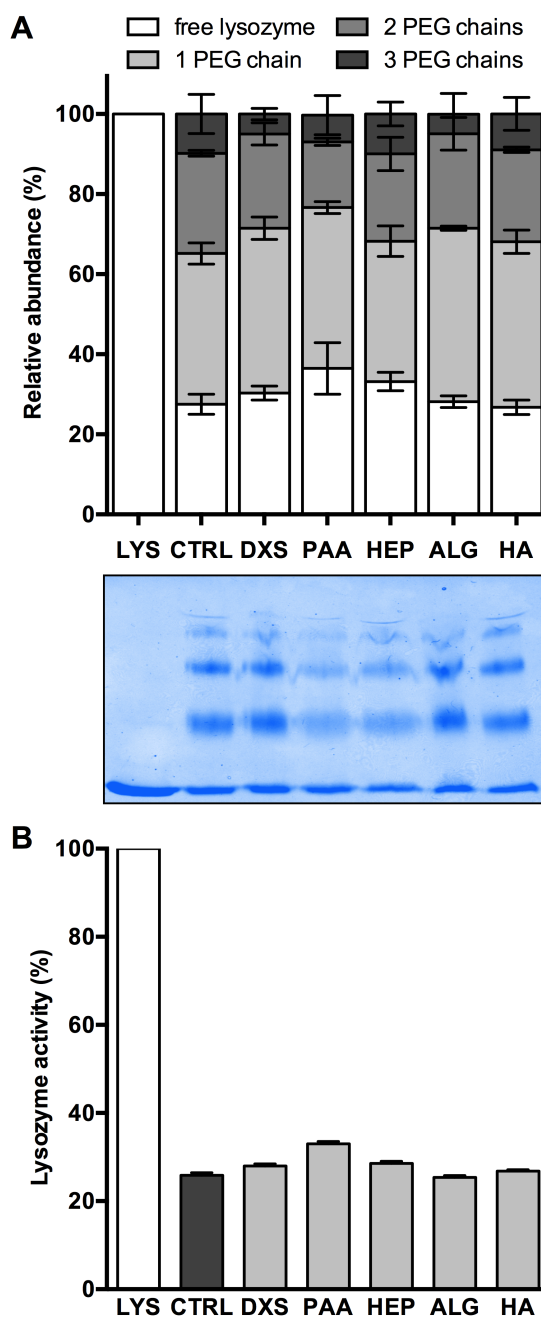


Figure 6.6: Influence of high salt concentrations (300 mM NaCl) on the “shielding” effect of polyanions at pH 7.4. The degree of PEGylation (A) and the activity of lysozyme (B) were determined after incubation with mPEG5k-maleimide and mPEG5k-furan. Fresh lysozyme (LYS), and lysozyme without polyanions (CTRL) served as controls. High salt concentrations reduced the binding of polyanions to lysozyme. Consequently, the degree of PEGylation and the enzymatic activity were similar to the control without polyanions.

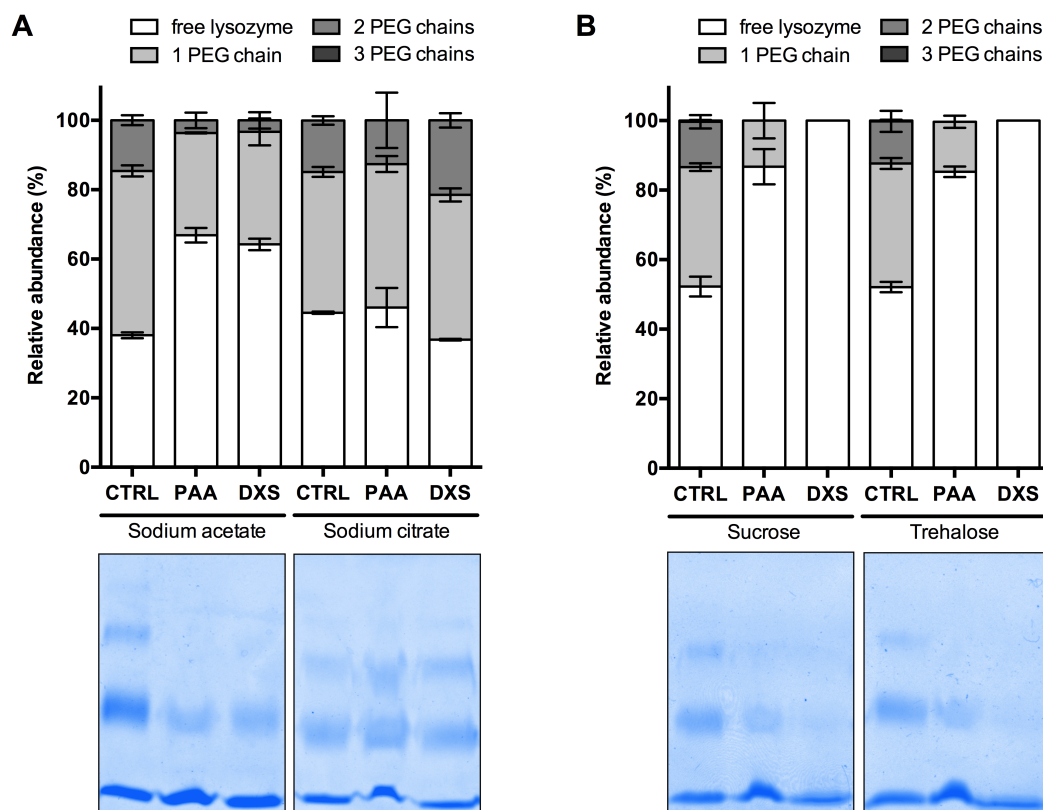


Figure 6.7: SDS PAGE of lysozyme-PEG conjugates resulting from side reactions during incubation with mPEG5k-maleimide and mPEG5k-furan at pH 7.4. The influence of sodium acetate and sodium citrate (300 mM) on the protective effect of PAA and DXS was studied (A). As already shown for NaCl, increasing the ionic strength reduced the protective effect of polyanions; the reduction was more pronounced with sodium citrate than with sodium acetate. Additionally, the influence of the cryoprotectants sucrose and trehalose (50 mg/mL) on the protective effect of PAA and DXS was studied (B). The “shielding” efficiency was not impaired by the addition of sucrose or trehalose.

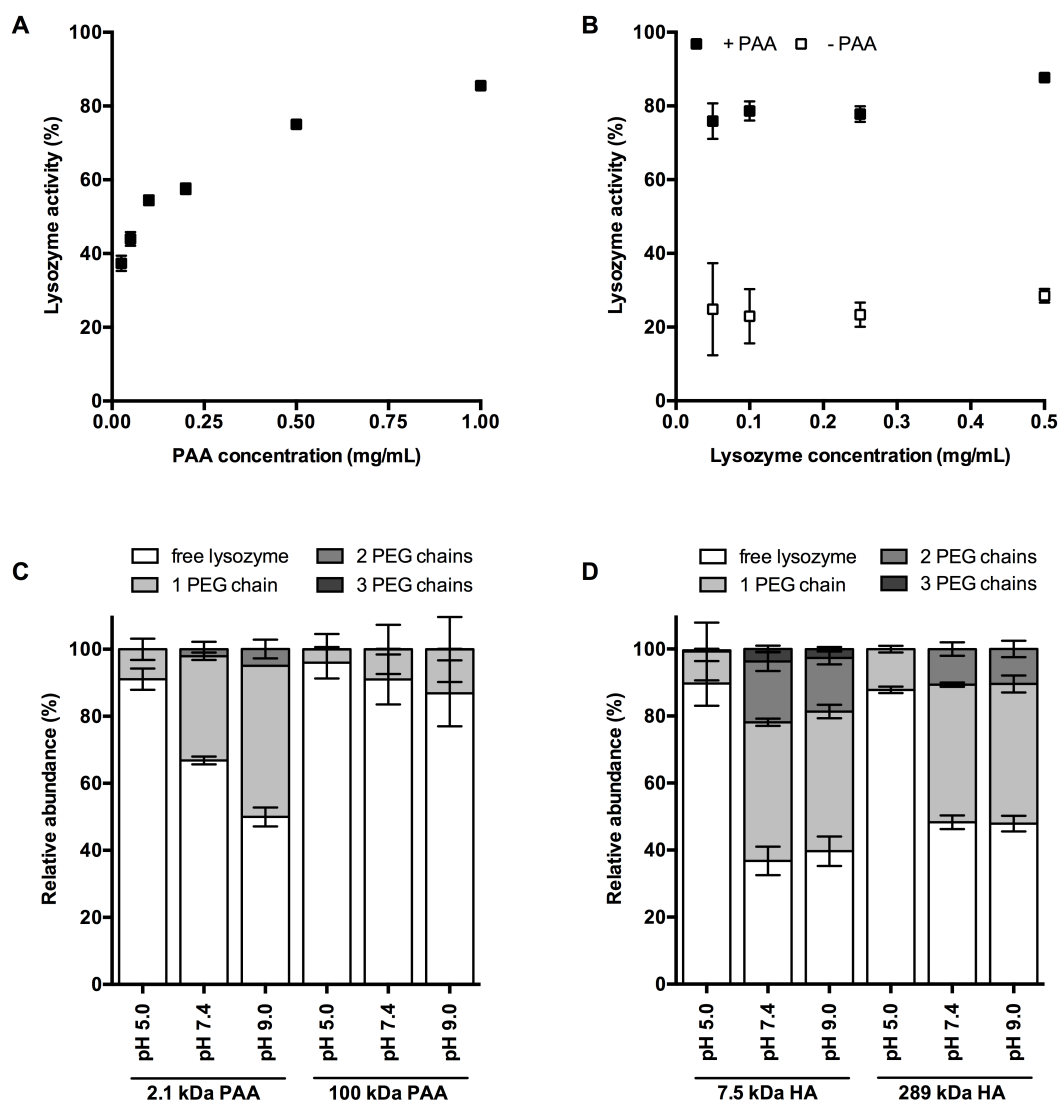


Figure 6.8: Factors influencing the “shielding” effect of polyanions. The residual lysozyme activity is dependent on the polyanion concentration (A), but almost independent from the protein concentration (B). The degree of PEGylation depends on the molecular mass of PAA (C) and HA (D). As can be seen from the lower degree of PEGylation, high molecular mass polyanions were more effective than low molecular mass polyanions.

Furthermore, it should be noted that the charge density of polyanions is related to the pK_a of the acid functionalities. Therefore, the pK_a of the polyanion is an important parameter controlling the strength of the “shielding” effect, in particular when proteins are formulated at acidic pH. For example, at low pH, the sulfate groups of DXS ($pK_a < 2$) [350] are ionized to a higher degree than the carboxylate groups of HA ($pK_a \approx 3-4$) [351]. Therefore, in order to achieve a protective effect at low pH, the use of polyanions with low pK_a might be preferred. Moreover, it should be considered that interactions with polyanions might impair the structural integrity of some proteins. This should be carefully evaluated from case to case to prevent loss of bioactivity. In summary, in order to utilize protein-polyanion complexation to reduce chemical protein modification during cross-linking, multiple variables must be taken into account and the conditions must be optimized for each specific protein-polyanion pair.

6.3.3 Investigation of alternative cross-linking mechanisms

Thus far, the ability of different polyanions to protect lysozyme during cross-linking via DA reaction was investigated. However, the “shielding” effect of polyanions might also be applicable to other cross-linking reactions. In the following experiments, the Michael-type addition of mPEG5k-vinyl sulfone and mPEG6k-thiol, and the radical polymerization of mPEG5k-acrylamide were investigated. The degree of PEGylation resulting from incubation with mPEG5k-vinyl sulfone and mPEG6k-thiol is presented in Fig. 6.9A. Lysozyme incubated at pH 7.4 (LYS) was compared to samples with (+) PAA and without (-) PAA. Without PAA, $29.3 \pm 2.0\%$ of the introduced lysozyme remained unmodified. PEGylation results from Michael-type additions of nucleophilic amino acids to mPEG5k-vinyl sulfone. This type of reaction has already been used for the PEGylation of therapeutic proteins [352, 353]. In addition, disulfide exchange reactions between cysteine residues and mPEG6k-thiol may occur. Nevertheless, the addition of PAA could significantly reduce the degree of PEGylation; with PAA, $71.1 \pm 5.4\%$ of the protein was not affected by PEGylation. In contrast to that, the radical polymerization of mPEG5k-acrylamide led to a lower degree of PEGylation, which could not be reduced by adding PAA (Fig. 6.9A). The amounts of free lysozyme were $70.2 \pm 1.7\%$ (- PAA) and $75.7 \pm 2.1\%$ (+ PAA).

As observed for PEGylation, the addition of PAA could reduce the activity loss caused by incubation with mPEG5k-vinyl sulfone and mPEG6k-thiol (Fig. 6.9B).

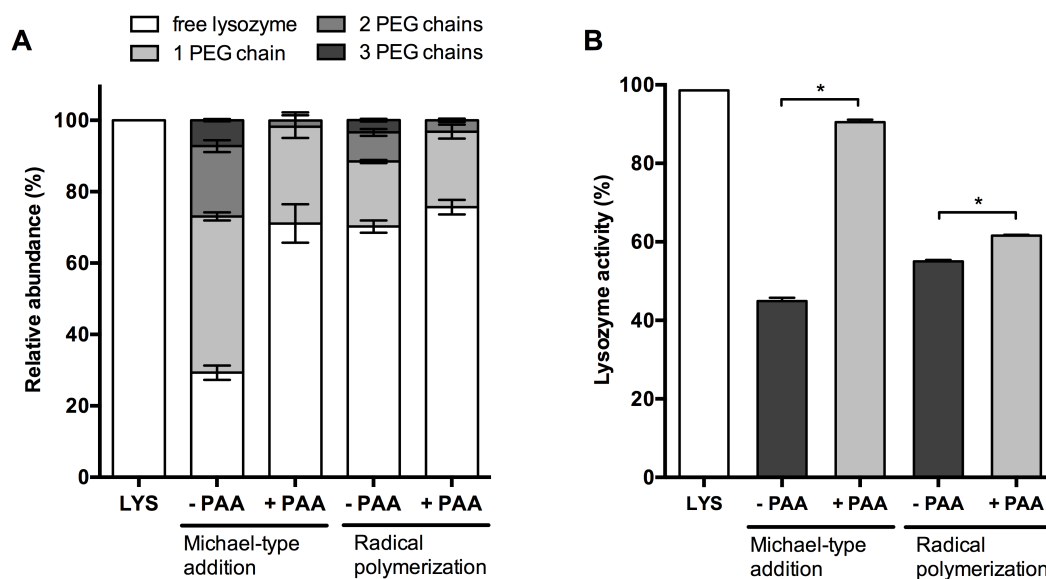


Figure 6.9: “Shielding” of lysozyme against Michael-type addition and radical polymerization at pH 7.4. The degree of PEGylation (A) and the activity of lysozyme (B) were determined without (-) PAA and with (+) PAA. PAA reduced the degree of PEGylation and loss of activity during cross-linking via Michael-type addition. During radically mediated cross-linking, the effect of PAA was considerably weaker. * indicates statistically significant differences between the specified groups.

The residual activities of lysozyme were $44.9 \pm 0.8\%$ (- PAA) and $90.5 \pm 0.6\%$ (+ PAA), respectively. In contrast to that, the activity loss caused by radical polymerization of mPEG5k-acrylamide was higher than expected from the PEGylation data (Fig. 6.9B). While only 25-30% of the protein was PEGylated, the loss of activity was 38-45%. The addition of PAA could not reduce the activity loss; the residual activities of lysozyme were $55.0 \pm 0.4\%$ (- PAA) and $61.5 \pm 0.2\%$ (+ PAA), respectively. Apparently, the activity is not only affected by PEGylation, but also by radical-mediated inactivation [354], oxidative effects [355, 356], and peroxide formation [357]. These additional effects cannot be suppressed by the addition of polyanions. It can be concluded that polyanions may also be effective in preventing chemical protein modification caused by other cross-linking methods than the DA reaction. In particular, “shielding” with polyanions proved to be effective in preventing Michael-type additions to vinyl sulfone. In contrast to that, polyanions are less effective in preventing radical-induced damage.

6.3.4 Impact of polyanions on protein release from hydrogels

In the previous experiments, lysozyme was incubated with monofunctional mPEG5k-furan and mPEG5k-maleimide to avoid gel formation. For the following experiment, eight-armed PEG (10 kDa molecular mass, 8armPEG10k) was functionalized with furyl and maleimide end-groups. The two complementary macromonomers were dissolved in buffer (10% polymer concentration), mixed with lysozyme, and cross-linked via DA reaction to yield elastic hydrogels. The average mesh size of this type of hydrogel is 5.5 nm [155]. Lysozyme, which has a hydrodynamic radius of about 1.9 nm [358, 359], should be able to freely diffuse through the gel network. Fig. 6.10A shows the cumulative release of lysozyme from 8armPEG10k hydrogels. Without

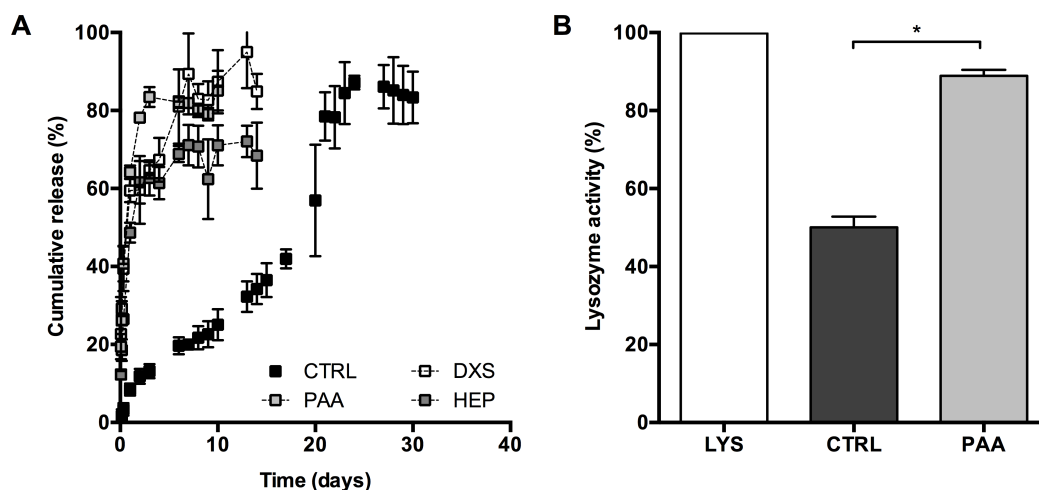


Figure 6.10: (A) Release of lysozyme from 8armPEG10k hydrogels. Cross-linking via DA reaction was performed without polyanions (CTRL), or in the presence of DXS, PAA and HEP. Without polyanions, lysozyme was immobilized within the hydrogel until the onset of degradation at day 20. In contrast to that, lysozyme was rapidly released by diffusion in the presence of polyanions. (B) Residual activity of lysozyme after release from 8armPEG10k hydrogels. The measured values were compared to the activity of fresh lysozyme (LYS). Lysozyme that was protected by PAA during cross-linking showed a considerably higher activity. * indicates statistically significant differences between the specified groups.

the addition of polyanions (CTRL), the initial release rate was unexpectedly low. Only 40% of the incorporated protein was released after 20 days. The major part of the protein was released between day 20 and 25 when the hydrogel started to degrade. This is in contrast to theoretical considerations (see above), which predict rapid protein release from 8armPEG10k hydrogels through Fickian diffusion [360]. Presumably, the majority of the protein was covalently bound to the polymer

network during cross-linking. Consequently, the release of lysozyme was controlled by degradation rather than diffusion. The experiment was repeated with DXS, PAA and HEP to “shield” the protein during cross-linking. As a result, the amount of covalently bound lysozyme was considerably reduced and the majority of the protein was released within the first 3 days. These results suggest that “shielding” with polyanions can be used to reduce chemical protein modification during cross-linking of hydrogels. The activity of the released protein should, therefore, be preserved in the presence of polyanions. To verify this assumption, the activity of the released lysozyme was determined after 30 days. The residual activity of the released lysozyme (CTRL and PAA) was compared to the activity of fresh lysozyme (LYS). Without the addition of PAA, the activity had decreased to $50.0 \pm 2.8\%$, suggesting that the released lysozyme was PEGylated (Fig. 6.10B). In contrast to that, the residual activity was $88.9 \pm 1.5\%$ when PAA was added to “shield” the protein during cross-linking. These results are in good agreement with the conclusions drawn above. The slightly reduced activity of the released lysozyme can be explained by unspecific degradation.

In the last experiment, the release of a therapeutically relevant protein was studied. For gel preparation, eight-armed PEG (40 kDa molecular mass) was reacted with 6-aminohexanoic acid (8armPEG40k-C₆) and subsequently functionalized with furyl and maleimide end-groups. Bevacizumab (Avastin[®]), a monoclonal antibody against vascular endothelial growth factor (VEGF), was incorporated into 10% 8armPEG40k-C₆ hydrogels. This antibody is currently used in the treatment of cancer and age-related macular degeneration [197, 210] and has an IEP of about 8.4 [361]. According to the literature, the hydrodynamic radius of bevacizumab is about 6.5 nm [319]; the average mesh size of 10% 8armPEG40k-C₆ hydrogels is 20.3 ± 0.6 nm [254]. When the release profiles of bevacizumab and lysozyme are compared, similar trends can be seen (Figs. 6.10A and 6.11A). At characteristic time points, i.e., after 3, 6, 10, and 14 days, the release of bevacizumab was significantly higher in the presence of PAA than in the control group without PAA (Fig. 6.11A, $p < 0.05$). The release of bevacizumab reached a plateau in both groups; the released amount was 67% (PAA) and 47% (CTRL), respectively. In addition, PAA reduced the amount of bevacizumab that was released between day 20 and 25 when the hydrogel started to degrade. These findings suggest that “shielding” with PAA can significantly decrease the fraction of covalently bound bevacizumab. Fragmentation of the antibody, possibly caused by complexation with PAA, could have been another explanation for the faster release of bevacizumab.

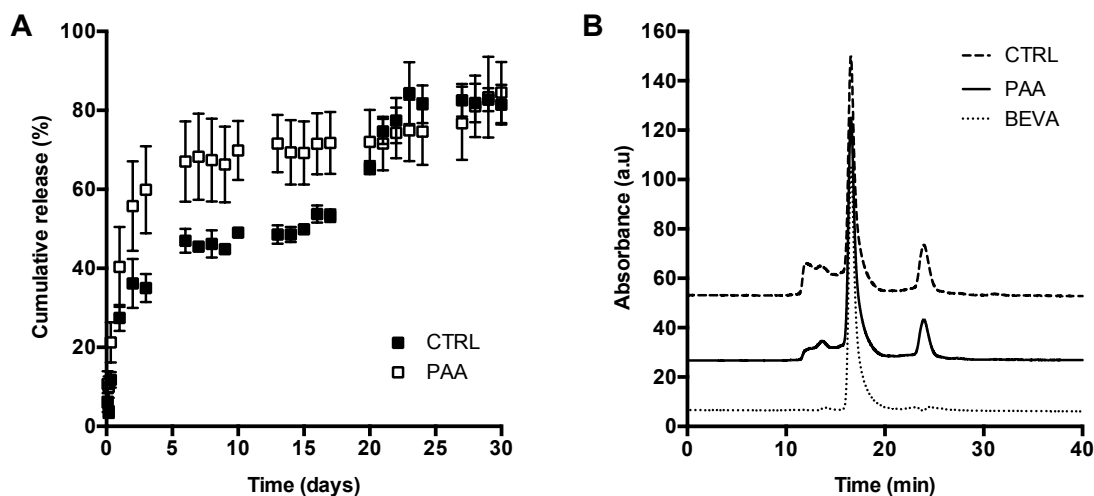


Figure 6.11: (A) Release of bevacizumab from 8armPEG40k-C₆ hydrogels. Cross-linking via DA reaction was performed without polyanion (CTRL), or in the presence of PAA. Without PAA, a higher amount of bevacizumab was covalently bound to the gel network. With PAA, the major amount of bevacizumab was rapidly released by diffusion. (B) The integrity of the released bevacizumab was confirmed by SEC. Fresh bevacizumab (BEVA) served as a control. The analysis confirmed that the released antibody was structurally intact.

Therefore, in order to exclude that the observed effect was due to fragmentation, samples were taken on day 6 of the release experiment and analyzed by SEC (Fig. 6.11B). For comparison, fresh bevacizumab was analyzed as well (BEVA). All three chromatograms showed one major peak at a retention time of 17 min, which was assigned to intact bevacizumab. The chromatograms of the PAA and the control group showed two additional peaks at retention times of 14 and 24 min. These signals were assigned to the dissolved gel components, i.e., 8armPEG40k-C₆-furan and 8armPEG40k-C₆-maleimide (Fig. 6.12). Therefore, it can be concluded from the SEC data that the released bevacizumab was structurally intact; there was no evidence for fragmentation, PEGylation, or aggregation.

In summary, the experiments demonstrate that PAA can effectively “shield” lysozyme and bevacizumab against chemical modification during cross-linking. In this way, the fraction of covalently bound protein is reduced; this results in fast, diffusion-controlled release.

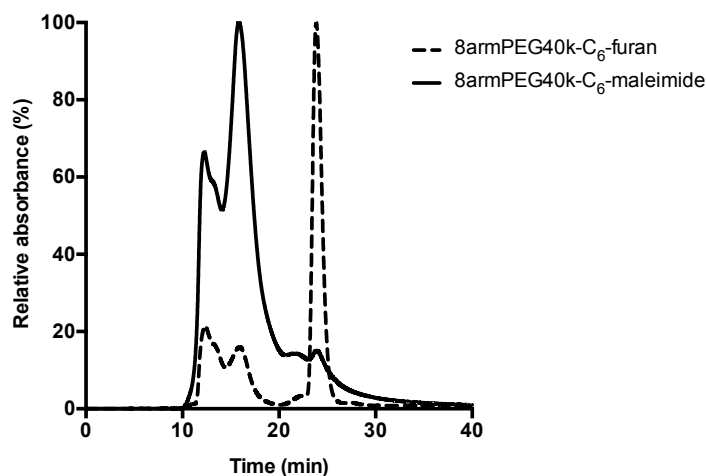


Figure 6.12: Size exclusion chromatograms of 8armPEG40k-C₆-maleimide and 8armPEG40k-C₆-furan.

6.4 Conclusion

Hydrogels can be prepared from a wide range of natural and synthetic polymers; however, only few cross-linking reactions can be carried out without adversely affecting the stability and availability of incorporated proteins. As it has been shown in the present study, the addition of polyanions represents an interesting option to reduce chemical protein modification and activity loss during cross-linking. The association of proteins with polyanions is driven by electrostatic interactions; the polyanion binds to the protein surface and reduces chemical reactions between proteins and polymers, e.g., during hydrogel formation via DA reaction or Michael-type addition. The association of proteins and polyanions is reversible; it neither causes protein aggregation or fragmentation, nor does it affect protein activity. The electrostatic interactions are effective at acidic, neutral and basic pH, which allows protein “shielding” at many different cross-linking conditions. However, it should be noted that the conditions must be optimized for each specific protein-polyanion pair. Furthermore, all polyanions included in this study can be considered biocompatible and have already been used for drug delivery and biomaterial development [362–366]. Moreover, only minimum amounts of polyanions are required to achieve protective effects. In conclusion, the possibility to “shield” proteins with polyanions facilitates the preparation of protein-loaded hydrogels. Cross-linking reactions, which usually affect the stability and availability of proteins, can be made “protein-compatible” by simply adding polyanions. In most cases, this method will not affect the material

properties, such as cross-linking density, swelling capacity, and degradability. In this way, the herein presented concept might facilitate the development of new delivery systems for therapeutic proteins.

Chapter 7

Summary and Conclusion

7.1 Summary

In 2001, the term “click chemistry” was first introduced by Sharpless and coworkers as an umbrella term for “spring-loaded” reactions that are modular, wide in scope, stereospecific, give high yields, proceed at simple conditions, and do not form toxic by-products [6]. Since that time, click reactions have had tremendous influence in many research areas including pharmaceuticals and material science.

Without a doubt, the Diels-Alder (DA) reaction is one of the click reactions with the greatest potential for the development of biomaterials and drug delivery systems. For example, besides the above-mentioned general advantages of click chemistry, the DA reaction does not require a metal catalyst. Therefore, the DA reaction has already been utilized in various biomedical areas, such as the synthesis of polymers and dendrimers, surface functionalization, bioconjugation, nanotechnology, and hydrogel design. For many of these applications the diene-dienophile pair furan and maleimide was utilized as they are readily available and the functionalization is comparably simple. For example, multi-armed poly(ethylene glycol) (PEG) functionalized with maleimide and furan have been utilized to prepare DA-hydrogels. However, the DA reaction is also associated with a number of disadvantages. For example, the reaction is reversible which may be unfavorable for the preparation of stable conjugates. However, the two most serious drawbacks of the reaction are its low reaction rate and potential side-reactions, e.g., the reaction of maleimide with nucleophilic amino acid side-chains (**Chapter 1**).

The goal of this thesis was to utilize the DA reaction for the development of hydrogels that can be applied in local antibody therapy. In order to exploit its full potential, the two main disadvantages of the DA reaction had to be circumvented while its advantages had to be utilized. To be more specific, DA hydrogels that gel more rapidly and that do not undergo side-reactions with proteins had to be developed. To this end, various approaches including chemical modification, the use of protective additives or combination with other click reactions were employed (**Chapter 2**).

For DA hydrogels, gelation is achieved through covalent cross-linking. Therefore, it was hypothesized that gel formation can be accelerated by facilitating the interaction between the reactive groups. Amphiphilic macromonomers were prepared by introducing hydrophobic 6-aminohexanoic acid (C_6) and 12-aminododecanoic acid (C_{12}) spacers between the polymer backbone and the functional end-groups. The general associative nature of the macromonomers was verified by an increase

in viscosity and the formation of associates or micelles. As a consequence of the hydrophobic association, the reactive groups were brought into close proximity and gelation occurred significantly faster, e.g., twice as fast using a C₁₂ spacer. Interestingly, gel times did not decrease when a modified and a non-modified component were combined, e.g., unmodified PEG-maleimide with modified PEG-furan. This finding further emphasizes the importance of hydrophobic association for accelerated gel formation. Moreover, hydrogels with hydrophobic modification were characterized by a lower average network mesh size and a higher elastic modulus which suggested a more efficient cross-linking process. Furthermore, through hydrophobic modification an increase of hydrogel stability could be achieved. This could be explained by the combined effects of higher cross-linking density and the increased hydrolytic resistance of maleimide moieties resulting from N-alkylation. All of these effects were influenced by spacer length: C₁₂-modification exhibited stronger effects on gelation, stability, and stiffness than C₆-modification. In addition, it was found that hydrophobic modification can be used as a tool to achieve delayed antibody release. While the *in vitro* release of bevacizumab from the unmodified DA-hydrogel was completed after only 10 days, hydrophobic modification delayed the release for about 30 days using C₆ and almost 60 days using C₁₂ spacers (**Chapter 3**).

Although gel times could be significantly decreased using hydrophobic modification instantaneous gelation still could not be achieved. In order to develop DA-hydrogels that provide immediate gelation a dual approach was employed. Instead of eight-armed PEGs, thermoresponsive four-armed poloxamines were utilized for macromonomer synthesis and functionalized with maleimide and furyl moieties. Aqueous solutions of these macromonomers exhibited an immediate gelation at body temperature. Concomitantly, the functional end-groups led to covalent cross-linking of the gels. In this way, the rapid sol-gel transition of physical gelation and the stability of chemically cross-linked gels were combined in a hybrid system. In addition, further branches were introduced to create a more versatile hydrogel platform that allowed for tailoring of the core characteristics, i.e., mechanical properties and stability. Hydrogel stability could be precisely controlled in the range of 14 to 329 days depending on the composition used. Finally, controlled release of the model antibody bevacizumab could be achieved over a period of 7, 21, and 115 days *in vitro*. The release curves were characterized by a notably low burst and a triphasic shape. Most importantly, almost all of the loaded antibody could be recovered after release and approximately 87% displayed functional binding. In

conclusion, DA-Poloxamines are rapidly gelling, mechanically stable, degradable, nontoxic, and provide controlled antibody release. As they can be tailored to match the demands of various applications they present a powerful material for controlled local antibody delivery (**Chapter 4**).

Besides slow gelation, the second major drawback of DA-hydrogels are undesired side-reactions with proteins. As potential approach to solve this issue, antibodies could be incorporated into hydrogel microparticles to safeguard them from detrimental cross-linking reactions. Moreover, such antibody-loaded microgels could find use as a delivery platform for controlled local release. However, the fabrication of antibody-loaded microgels with a narrow size distribution and without impairing protein stability is a challenging task. To achieve this goal, a fabrication method combining microfluidics and thiol-ene photoclick chemistry was employed. Microfluidics is a well-characterized approach for the generation of uniform droplets that does not expose materials to harmful stress conditions. On the other hand, the thiol-ene reaction is known to be compatible with proteins [300] and can be triggered using visible light. To fabricate the microparticles, first aqueous droplets containing antibody, macromonomers and reactants were generated using a microfluidic device. Then, green light was used to covalently cross-link the droplets and encapsulate the antibody. In order to tailor microgel properties a macromonomer library comprising both hydrolytically labile and stable eight-armed PEGs with various molecular masses was synthesized. Then, rheology was used to determine the necessary irradiation time and to study mechanical properties. These microgels had a rod-like shape and a narrow size distribution with an approximate width of 380 μm and lengths of 1400 μm or 2150 μm , depending on the process parameters. Bevacizumab was successfully incorporated into the microgels and a sustained release could be achieved over a period of 28 and 46 days. Moreover, it was confirmed that the process developed does not significantly impair the binding ability of bevacizumab. Therefore, the strategy is suitable for loading antibodies into microgels and presents a promising starting point for further development. In future experiments, the general hypothesis that the incorporation into microgels safeguards proteins needs to be verified. Moreover, for delivery purposes microgels with smaller dimensions should be generated to allow for injection or inhalation. This could be achieved by fine tuning of the flow ratio and by using tubes with smaller diameters (**Chapter 5**).

Although encapsulation into microgels might be an effective approach to overcome protein-polymer conjugation during cross-linking, it is a comparably complicated

approach. It would be ideal if Michael-type reactions of maleimide could be avoided by simply adding a protective additive. For this purpose, a number of pharmaceutically relevant polyanions were evaluated, i.e., alginate, dextran sulfate, heparin, hyaluronic acid, and poly(acrylic acid). Electrostatic interactions led to reversible binding of the polyanions to the protein surface. Thereby, the reaction of maleimide with nucleophilic moieties on the protein surface could be prevented. These results were confirmed using the model protein lysozyme and by simulating the reaction conditions with monofunctional mPEG5k-maleimide and mPEG5k-furan. For example, at pH 7.4 and without polyanions about 61% of lysozyme was PEGylated and the activity had decreased to about 20% of the initial activity. In comparison, when dextran sulfate had been added an activity of 98% remained and no PEGylation was detected. Overall, dextran sulfate, heparin, and poly(acrylic acid) were identified as the most effective additives to shield proteins during cross-linking. In addition, it could be confirmed that the “shielding” is solely based on electrostatic interactions as the effect could be reversed by adding high salt concentrations. Furthermore, it could be demonstrated that the protective effect can be utilized at acidic, neutral, and basic pH which makes it a particularly versatile tool for protein formulation and delivery. Nevertheless, in order to optimally protect proteins from undesired reactions, cross-linking should be carried out at acidic pH and with polyanions present. These conditions are optimal because on the one hand, at acidic pH the reactivity of nucleophilic groups (e.g., amines) is decreased and on the other, proteins carry a higher positive charge than at neutral pH which facilitates electrostatic interactions with polyanions (**Chapter 6**).

7.2 Conclusion

In this thesis, the DA click reaction was utilized to develop hydrogels for controlled local antibody delivery. Hydrophobic association was identified as a tool to facilitate covalent cross-linking and to obtain hydrogels that gel more rapidly, have improved mechanical properties, and a higher stability. Moreover, thermoresponsive DA-hydrogels were designed that immediately gel at body temperature and concomitantly cross-link via DA reaction. Both approaches were successful in eliminating the disadvantage of slow gelation while still utilizing the advantages of the DA reaction. As both rapid and instantaneous gelation could be useful depending on the demands of the application both materials might find use in therapy. Furthermore, the combination of microfluidics and thiol-ene photoclick chemistry

could be employed for protein incorporation into uniform microgels. It will be interesting to further assess the potential of this delivery platform for safeguarding proteins and controlled release. Finally, the “shielding” effect of polyanions against side-reactions with the protein was discovered. Adding polyanions to the precursor solutions prior to cross-linking presents a particularly elegant and simple way to overcome this serious problem. In conclusion, the materials and mechanisms described in this thesis present a great advancement for antibody delivery using click hydrogels. Regarding material properties, all major drawbacks of the DA reaction could be eliminated while its advantages were preserved. Therefore, as a next step the biocompatibility of the materials and their *in vivo* performance should be assessed. In addition, in order to broaden the spectrum of applications it should be evaluated whether these hydrogels can be applied to the delivery of other antibodies and biologics, such as fusion proteins and antibody fragments. Furthermore, a more in-depth analysis of the physicochemical properties of the antibody after release is a crucial aspect with regard to therapeutic success. In addition to presenting novel antibody delivery systems, the mechanisms that are presented in this thesis are of particular scientific significance as they can be translated to other research areas. For example, both hydrophobic association and dual gelation could be utilized in combination with other reactions to facilitate the development of novel biomaterials and delivery systems. Similarly, as “shielding” with polyanions could be utilized to safely deliver multiple other protein pharmaceuticals it might open up new avenues for protein delivery. In conclusion, the materials and mechanisms presented in this thesis have the potential to make a broad impact in the biomedical field.

References

- [1] C. D. Hein, X.-M. Liu, and D. Wang. Click chemistry, a powerful tool for pharmaceutical sciences. *Pharm. Res.*, 25(10):2216–2230, 2008.
- [2] C. M. Nimmo and M. S. Shoichet. Regenerative biomaterials that “click”: simple, aqueous-based protocols for hydrogel synthesis, surface immobilization, and 3D patterning. *Bioconjugate Chem.*, 22(11):2199–2209, 2011.
- [3] E. Lallana, A. Sousa-Herves, F. Fernandez-Trillo, R. Riguera, and E. Fernandez-Megia. Click chemistry for drug delivery nanosystems. *Pharm. Res.*, 29(1):1–34, 2011.
- [4] E. Lallana, F. Fernandez-Trillo, A. Sousa-Herves, R. Riguera, and E. Fernandez-Megia. Click chemistry with polymers, dendrimers, and hydrogels for drug delivery. *Pharm. Res.*, 29(4):902–921, 2012.
- [5] C. S. McKay and M. G. Finn. Click chemistry in complex mixtures: bioorthogonal bioconjugation. *Chem. Biol.*, 21(9):1075–1101, 2014.
- [6] H. C. Kolb, M. G. Finn, and K. B. Sharpless. Click chemistry: Diverse chemical function from a few good reactions. *Angew. Chem. Int. Ed.*, 40(11):2004–2021, 2001.
- [7] H. C. Kolb and K. B. Sharpless. The growing impact of click chemistry on drug discovery. *Drug Discov. Today*, 8(24):1128–1137, 2003.
- [8] J. E. Moses and A. D. Moorhouse. The growing applications of click chemistry. *Chem. Soc. Rev.*, 36(8):1249–1262, 2007.
- [9] W. H. Binder and R. Sachsenhofer. ‘Click’ chemistry in polymer and materials science. *Macromol. Rapid Commun.*, 28(1):15–54, 2007.
- [10] W. H. Binder and R. Sachsenhofer. ‘Click’ chemistry in polymer and material science: an update. *Macromol. Rapid Commun.*, 29:952–981, 2008.

- [11] B. S. Sumerlin and A. P. Vogt. Macromolecular engineering through click chemistry and other efficient transformations. *Macromolecules*, 43(1):1–13, 2010.
- [12] P. L. Golas and K. Matyjaszewski. Marrying click chemistry with polymerization: expanding the scope of polymeric materials. *Chem. Soc. Rev.*, 39(4):1338–1354, 2010.
- [13] C. W. Tornøe, C. Christensen, and M. Meldal. Peptidotriazoles on solid phase: [1,2,3]-triazoles by regiospecific copper(I)-catalyzed 1,3-dipolar cycloadditions of terminal alkynes to azides. *J. Org. Chem.*, 67(9):3057–3064, 2002.
- [14] V. V. Rostovtsev, L. G. Green, V. V. Fokin, and K. B. Sharpless. A stepwise Huisgen cycloaddition process: copper(I)-catalyzed regioselective “ligation” of azides and terminal alkynes. *Angew. Chem. Int. Ed.*, 41(14):2596–2599, 2002.
- [15] J. C. Jewett and C. R. Bertozzi. Cu-free click cycloaddition reactions in chemical biology. *Chem. Soc. Rev.*, 39(4):1272–1279, 2010.
- [16] N. J. Agard, J. A. Prescher, and C. R. Bertozzi. A strain-promoted [3 + 2] azide–alkyne cycloaddition for covalent modification of biomolecules in living systems. *J. Am. Chem. Soc.*, 126(46):15046–15047, 2004.
- [17] J. A. Codelli, J. M. Baskin, N. J. Agard, and C. R. Bertozzi. Second-generation difluorinated cyclooctynes for copper-free click chemistry. *J. Am. Chem. Soc.*, 130(34):11486–11493, 2008.
- [18] C. R. Becer, R. Hoogenboom, and U. S. Schubert. Click chemistry beyond metal-catalyzed cycloaddition. *Angew. Chem. Int. Ed.*, 48(27):4900–4908, 2009.
- [19] A. Sanyal. Diels–Alder cycloaddition-cycloreversion: a powerful combo in materials design. *Macromol. Chem. Phys.*, 211(13):1417–1425, 2010.
- [20] M. A. Tasdelen. Diels–Alder “click” reactions: recent applications in polymer and material science. *Polym. Chem.*, 2(10):2133–2145, 2011.
- [21] A. Gandini. The furan/maleimide Diels–Alder reaction: A versatile click–unclick tool in macromolecular synthesis. *Prog. Polym. Sci.*, 38(1):1–29, 2013.

-
- [22] P. Yates and P. Eaton. Acceleration of the Diels–Alder reaction by aluminium chloride. *J. Am. Chem. Soc.*, 82(16):4436–4437, 1960.
- [23] T. Inukai and T. Kojima. Catalytic actions of aluminum chloride on the isoprene-methyl acrylate Diels–Alder reaction. *J. Org. Chem.*, 31(4):1121–1123, 1966.
- [24] S. Otto and J. B. F. N. Engberts. Lewis-acid catalysis of a Diels–Alder reaction in water. *Tetrahedron Lett.*, 36(15):2645–2648, 1995.
- [25] S. Otto, F. Bertoncin, and J. B. F. N. Engberts. Lewis acid catalysis of a Diels–Alder reaction in water. *J. Am. Chem. Soc.*, 118(33):7702–7707, 1996.
- [26] O. Diels and K. Alder. Synthesen in der hydroaromatischen Reihe, I. Mitteilung: Anlagerungen von "Di-en"-Kohlenwasserstoffen. *Justus Liebigs Ann. Chem.*, 460(1):98–122, 1928.
- [27] O. Diels and K. Alder. Synthesen in der hydro-aromatischen Reihe, II. Mitteilung: Über Cantharidin. *Ber. dtsh. Chem. Ges. A/B*, 62(3):554–562, 1929.
- [28] K. C. Nicolaou, S. A. Snyder, T. Montagnon, and G. Vassilikogiannakis. The Diels–Alder reaction in total synthesis. *Angew. Chem. Int. Ed.*, 41(10):1668–1698, 2002.
- [29] R. B. Woodward, F. Sondheimer, D. Taub, K. Heusler, and W. M. McLamore. The total synthesis of steroids. *J. Am. Chem. Soc.*, 74(17):4223–4251, 1952.
- [30] M. Gates and G. Tschudi. The synthesis of morphine. *J. Am. Chem. Soc.*, 74(4):1109–1110, 1952.
- [31] M. Gates and G. Tschudi. The synthesis of morphine. *J. Am. Chem. Soc.*, 78(7):1380–1393, 1956.
- [32] R. B. Woodward and T. J. Katz. The mechanism of the Diels–Alder reaction. *Tetrahedron*, 5(1):70–89, 1959.
- [33] R. B. Woodward and R. Hoffmann. The Conservation of Orbital Symmetry. *Angew. Chem. Int. Ed.*, 8(11):781–853, 1969.
- [34] J. Sauer and R. Sustmann. Mechanistic aspects of Diels–Alder reactions: a critical survey. *Angew. Chem. Int. Ed.*, 19(10):779–807, 1980.

- [35] K. N. Houk, Y. T. Lin, and F. K. Brown. Evidence for the concerted mechanism of the Diels–Alder reaction of butadiene with ethylene. *J. Am. Chem. Soc.*, 108(3):554–556, 1986.
- [36] M. J. S. Dewar, S. Olivella, and J. J. P. Stewart. Mechanism of the Diels–Alder reaction: reactions of butadiene with ethylene and cyanoethylenes. *J. Am. Chem. Soc.*, 108(19):5771–5779, 1986.
- [37] K. Alder and G. Stein. Untersuchungen über den Verlauf der Diensynthese. *Angew. Chem.*, 50(28):510–519, 1937.
- [38] R. Hoffmann and R. B. Woodward. Orbital symmetries and endo-exo relationships in concerted cycloaddition reactions. *J. Am. Chem. Soc.*, 87(19):4388–4389, 1965.
- [39] N. Kuramoto, K. Hayashi, and K. Nagai. Thermoreversible reaction of Diels–Alder polymer composed of difurufuryladipate with bismaleimide-diphenylmethane. *J. Polym. Sci. A Polym. Chem.*, 32(13):2501–2504, 1994.
- [40] J. P. Kennedy and G. M. Carlson. Synthesis, characterization, and Diels–Alder extension of cyclopentadiene telechelic polyisobutylene. III. Silylcyclopentadiene-telechelic polyisobutylene. *J. Polym. Sci. Polym. Chem. Ed.*, 21(10):2973–2986, 1983.
- [41] J. P. Kennedy and G. M. Carlson. Synthesis, characterization, and Diels–Alder extension of cyclopentadiene telechelic polyisobutylene. IV. α,ω -Di(3-cyclopentadienylpropyldimethylsilyl)polyisobutylene. *J. Polym. Sci. Polym. Chem. Ed.*, 21(12):3551–3561, 1983.
- [42] L. P. Engle and K. B. Wagener. A review of thermally controlled covalent bond formation in polymer chemistry. *J. Macromol. Sci. Polymer Rev.*, 33(3):239–257, 1993.
- [43] A.-C. Knall, M. Hollauf, and C. Slugovc. Kinetic studies of inverse electron demand Diels–Alder reactions (iEDDA) of norbornenes and 3,6-dipyridin-2-yl-1,2,4,5-tetrazine. *Tetrahedron Lett.*, 55(34):4763–4766, 2014.
- [44] D. C. Rideout and R. Breslow. Hydrophobic acceleration of Diels–Alder reactions. *J. Am. Chem. Soc.*, 102(26):7816–7817, 1980.

-
- [45] R. Breslow, U. Maitra, and D. Rideout. Selective Diels–Alder reactions in aqueous solutions and suspensions. *Tetrahedron Lett.*, 24(18):1901–1904, 1983.
- [46] W. Blokzijl, M. J. Blandamer, and J. B. F. N. Engberts. Diels–Alder reactions in aqueous solutions. Enforced hydrophobic interactions between diene and dienophile. *J. Am. Chem. Soc.*, 113(11):4241–4246, 1991.
- [47] A. Meijer, S. Otto, and J. B. F. N. Engberts. Effects of the hydrophobicity of the reactants on Diels–Alder reactions in water. *J. Org. Chem.*, 63(24):8989–8994, 1998.
- [48] A. D. de Araújo, J. M. Palomo, J. Cramer, M. Köhn, H. Schröder, et al. Diels–Alder ligation and surface immobilization of proteins. *Angew. Chem. Int. Ed.*, 45(2):296–301, 2006.
- [49] B. J. Adzima, H. A. Aguirre, C. J. Kloxin, T. F. Scott, and C. N. Bowman. Rheological and chemical analysis of reverse gelation in a covalently cross-linked Diels–Alder polymer network. *Macromolecules*, 41(23):9112–9117, 2008.
- [50] G. Scheltjens, M. M. Diaz, J. Brancart, G. Van Assche, and B. Van Mele. A self-healing polymer network based on reversible covalent bonding. *React. Funct. Polym.*, 73(2):413–420, 2013.
- [51] K. C. Koehler, A. Durackova, C. J. Kloxin, and C. N. Bowman. Kinetic and thermodynamic measurements for the facile property prediction of Diels–Alder-conjugated material behavior. *AIChE J.*, 58(11):3545–3552, 2012.
- [52] R. C. Boutelle and B. H. Northrop. Substituent effects on the reversibility of furan–maleimide cycloadditions. *J. Org. Chem.*, 76(19):7994–8002, 2011.
- [53] K. Kataoka, G. S. Kwon, M. Yokoyama, T. Okano, and Y. Sakurai. Block copolymer micelles as vehicles for drug delivery. *J. Control. Release*, 24(1):119–132, 1993.
- [54] K. Kataoka, A. Harada, and Y. Nagasaki. Block copolymer micelles for drug delivery: design, characterization and biological significance. *Adv. Drug Deliv. Rev.*, 47(1):113–131, 2001.

- [55] G. Gaucher, M.-H. Dufresne, V. P. Sant, N. Kang, D. Maysinger, et al. Block copolymer micelles: preparation, characterization and application in drug delivery. *J. Control. Release*, 109:169–188, 2005.
- [56] A. Rösler, G. W. M. Vandermeulen, and H.-A. Klok. Advanced drug delivery devices via self-assembly of amphiphilic block copolymers. *Adv. Drug Deliv. Rev.*, 64:270–279, 2012.
- [57] A. V. Kabanov, P. Lemieux, S. Vinogradov, and V. Alakhov. Pluronic® block copolymers: novel functional molecules for gene therapy. *Adv. Drug Deliv. Rev.*, 54(2):223–233, 2002.
- [58] Z. Yang, G. Sahay, S. Sriadibhatla, and A. V. Kabanov. Amphiphilic block copolymers enhance cellular uptake and nuclear entry of polyplex-delivered DNA. *Bioconjugate Chem.*, 19(10):1987–1994, 2008.
- [59] I. W. Hamley. Nanostructure fabrication using block copolymers. *Nanotechnology*, 14(10):R39–R54, 2003.
- [60] K. Letchford and H. Burt. A review of the formation and classification of amphiphilic block copolymer nanoparticulate structures: micelles, nanospheres, nanocapsules and polymersomes. *Eur. J. Pharm. Biopharm.*, 65(3):259–269, 2007.
- [61] F. Gu, L. Zhang, B. A. Teply, N. Mann, A. Wang, et al. Precise engineering of targeted nanoparticles by using self-assembled biointegrated block copolymers. *Proc. Natl. Acad. Sci. USA*, 105(7):2586–2591, 2008.
- [62] J. H. Lee, J. Kopecek, and J. D. Andrade. Protein-resistant surfaces prepared by PEO-containing block copolymer surfactants. *J. Biomed. Mater. Res.*, 23(3):351–368, 1989.
- [63] J. S. Tan, D. E. Butterfield, C. L. Voycheck, K. D. Caldwell, and J. T. Li. Surface modification of nanoparticles by PEO/PPO block copolymers to minimize interactions with blood components and prolong blood circulation in rats. *Biomaterials*, 14(11):823–833, 1993.
- [64] K. Emoto, Y. Nagasaki, and K. Kataoka. Coating of surfaces with stabilized reactive micelles from poly(ethylene glycol)–poly(DL-lactic acid) block copolymer. *Langmuir*, 15(16):5212–5218, 1999.

-
- [65] S. W. Kim, B. Jeong, Y. H. Bae, and D. S. Lee. Biodegradable block copolymers as injectable drug-delivery systems. *Nature*, 388(6645):860–862, 1997.
- [66] L. Yu and J. Ding. Injectable hydrogels as unique biomedical materials. *Chem. Soc. Rev.*, 37(8):1473–1481, 2008.
- [67] C. He, S. W. Kim, and D. S. Lee. In situ gelling stimuli-sensitive block copolymer hydrogels for drug delivery. *J. Control. Release*, 127(3):189–207, 2008.
- [68] K. Inoue, M. Yamashiro, and M. Iji. Recyclable shape-memory polymer: poly(lactic acid) crosslinked by a thermoreversible Diels–Alder reaction. *J. Appl. Polym. Sci.*, 112(2):876–885, 2009.
- [69] T. Defize, R. Riva, C. Jérôme, and M. Alexandre. Multifunctional poly(ϵ -caprolactone)-forming networks by Diels–Alder cycloaddition: effect of the adduct on the shape-memory properties. *Macromol. Chem. Phys.*, 213(2):187–197, 2011.
- [70] T. Defize, R. Riva, J.-M. Raquez, P. Dubois, C. Jérôme, et al. Thermoreversibly crosslinked poly(ϵ -caprolactone) as recyclable shape-memory polymer network. *Macromol. Rapid Commun.*, 32(16):1264–1269, 2011.
- [71] C. Ninh and C. J. Bettinger. Reconfigurable biodegradable shape-memory elastomers via Diels–Alder coupling. *Biomacromolecules*, 14(7):2162–2170, 2013.
- [72] A. Lendlein and R. Langer. Biodegradable, elastic shape-memory polymers for potential biomedical applications. *Science*, 296(5573):1673–1676, 2002.
- [73] A. Lendlein, M. Behl, B. Hiebl, and C. Wischke. Shape-memory polymers as a technology platform for biomedical applications. *Expert Rev. Med. Devices*, 7(3):357–379, 2010.
- [74] S. Onbulak, S. Tempelaar, R. J. Pounder, O. Gok, R. Sanyal, et al. Synthesis and functionalization of thiol-reactive biodegradable polymers. *Macromolecules*, 45(3):1715–1722, 2012.
- [75] K. Adachi, A. K. Achimuthu, and Y. Chujo. Synthesis of organic-inorganic polymer hybrids controlled by Diels–Alder reaction. *Macromolecules*, 37(26):9793–9797, 2004.

- [76] I. Armentano, M. Dottori, E. Fortunati, S. Mattioli, and J. M. Kenny. Biodegradable polymer matrix nanocomposites for tissue engineering: A review. *Polym. Degrad. Stab.*, 95(11):2126–2146, 2010.
- [77] H. Durmaz, B. Colakoglu, U. Tunca, and G. Hizal. Preparation of block copolymers via Diels Alder reaction of maleimide- and anthracene-end functionalized polymers. *J. Polym. Sci. A Polym. Chem.*, 44(5):1667–1675, 2006.
- [78] B. Gacal, H. Durmaz, M. A. Tasdelen, G. Hizal, U. Tunca, et al. Anthracene-maleimide-based Diels–Alder “click chemistry” as a novel route to graft copolymers. *Macromolecules*, 39(16):5330–5336, 2006.
- [79] A. Dag, H. Durmaz, U. Tunca, and G. Hizal. Multiarm star block copolymers via Diels–Alder click reaction. *J. Polym. Sci. A Polym. Chem.*, 47(1):178–187, 2009.
- [80] F. Bahadori, A. Dag, H. Durmaz, N. Cakir, H. Onyuksel, et al. Synthesis and characterization of biodegradable amphiphilic star and y-shaped block copolymers as potential carriers for vinorelbine. *Polymers*, 6(1):214–242, 2014.
- [81] J. R. Jones, C. L. Liotta, D. M. Collard, and D. A. Schiraldi. Cross-linking and modification of poly(ethylene terephthalate-co-2,6-anthracenedicarboxylate) by Diels–Alder reactions with maleimides. *Macromolecules*, 32(18):5786–5792, 1999.
- [82] H. Durmaz, A. Dag, O. Altintas, T. Erdogan, G. Hizal, et al. One-pot synthesis of ABC type triblock copolymers via in situ click [3 + 2] and Diels–Alder [4 + 2] reactions. *Macromolecules*, 40(2):191–198, 2007.
- [83] A. J. Inglis, S. Sinnwell, M. H. Stenzel, and C. Barner-Kowollik. Ultrafast click conjugation of macromolecular building blocks at ambient temperature. *Angew. Chem. Int. Ed.*, 48(13):2411–2414, 2009.
- [84] A. Bousquet, C. Barner-Kowollik, and M. H. Stenzel. Synthesis of comb polymers via grafting-onto macromolecules bearing pendant diene groups via the hetero-Diels–Alder -RAFT click concept. *J. Polym. Sci. A Polym. Chem.*, 48(8):1773–1781, 2010.

- [85] B. J. L. Royles and D. M. Smith. The "inverse electron-demand" Diels–Alder reaction in polymer synthesis. Part 1. A convenient synthetic route to diethynyl aromatic compounds. *J. Chem. Soc., Perkin Trans. 1*, (4):355–358, 1994.
- [86] M. J. Bruce, G. A. McLean, B. J. L. Royles, D. M. Smith, and P. N. Standring. The "inverse electron-demand" Diels–Alder reaction in polymer synthesis. Part 2. Some bis(1,2,4-triazines) as potential bis-diene monomers. *J. Chem. Soc., Perkin Trans. 1*, (14):1789–1795, 1995.
- [87] C. F. Hansell, P. Espeel, M. M. Stamenović, I. A. Barker, A. P. Dove, et al. Additive-free clicking for polymer functionalization and coupling by tetrazine–norbornene chemistry. *J. Am. Chem. Soc.*, 133(35):13828–13831, 2011.
- [88] I. A. Barker, D. J. Hall, C. F. Hansell, F. E. Du Prez, R. K. O'Reilly, et al. Tetrazine-norbornene click reactions to functionalize degradable polymers derived from lactide. *Macromol. Rapid Commun.*, 32(17):1362–1366, 2011.
- [89] H. Gao and K. Matyjaszewski. Synthesis of star polymers by a combination of ATRP and the "click" coupling method. *Macromolecules*, 39(15):4960–4965, 2006.
- [90] W. Van Camp, V. Germonpré, L. Mespouille, P. Dubois, E. J. Goethals, et al. New poly(acrylic acid) containing segmented copolymer structures by combination of "click" chemistry and atom transfer radical polymerization. *React. Funct. Polym.*, 67(11):1168–1180, 2007.
- [91] L. M. Campos, K. L. Killops, R. Sakai, J. M. J. Paulusse, D. Damiron, et al. Development of thermal and photochemical strategies for thiol–ene click polymer functionalization. *Macromolecules*, 41(19):7063–7070, 2008.
- [92] J. W. Chan, B. Yu, C. E. Hoyle, and A. B. Lowe. Convergent synthesis of 3-arm star polymers from RAFT-prepared poly(N,N-diethylacrylamide) via a thiol–ene click reaction. *Chem. Commun.*, (40):4959–4961, 2008.
- [93] M. Liu and J. M. J. Fréchet. Designing dendrimers for drug delivery. *Pharm. Sci. Technol. Today*, 2(10):393–401, 1999.
- [94] E. R. Gillies and J. M. J. Fréchet. Dendrimers and dendritic polymers in drug delivery. *Drug Discov. Today*, 10(1):35–43, 2005.

- [95] T. Barrett, G. Ravizzini, P. Choyke, and H. Kobayashi. Dendrimers in medical nanotechnology. *IEEE Eng. Med. Biol. Mag.*, 28(1):12–22.
- [96] M. L. Szalai, D. V. McGrath, D. R. Wheeler, T. Zifer, and J. R. McElhanon. Dendrimers based on thermally reversible furan-maleimide Diels–Alder adducts. *Macromolecules*, 40(4):818–823, 2007.
- [97] J. R. McElhanon and D. R. Wheeler. Thermally responsive dendrons and dendrimers based on reversible furan-maleimide Diels–Alder adducts. *Org. Lett.*, 3(17):2681–2683, 2001.
- [98] A. Vieyres, T. Lam, R. Gillet, G. Franc, A. Castonguay, et al. Combined Cu^I -catalysed alkyne–azide cycloaddition and furan–maleimide Diels–Alder “click” chemistry approach to thermoresponsive dendrimers. *Chem. Commun.*, 46(11):1875–1877, 2010.
- [99] N. W. Polaske, D. V. McGrath, and J. R. McElhanon. Thermally reversible dendronized step-polymers based on sequential huisgen 1,3-dipolar cycloaddition and Diels–Alder “click” reactions. *Macromolecules*, 43(3):1270–1276, 2010.
- [100] A. Castonguay, E. Wilson, N. Al-Hajaj, L. Petitjean, J. Paoletti, et al. Thermosensitive dendrimer formulation for drug delivery at physiologically relevant temperatures. *Chem. Commun.*, 47(44):12146–12148, 2011.
- [101] M. M. Kose, G. Yesilbag, and A. Sanyal. Segment block dendrimers via Diels–Alder cycloaddition. *Org. Lett.*, 10(12):2353–2356, 2008.
- [102] C. Kim, H. Kim, and K. Park. Diels–Alder reaction of anthracene and N-ethylmaleimide on the carbosilane dendrimer. *J. Organomet. Chem.*, 667: 96–102, 2003.
- [103] C. Kim, H. Kim, and K. Park. Preparation and Diels–Alder reaction of carbosilane dendrimer with conjugated diene. *J. Organomet. Chem.*, 690: 4794–4800, 2005.
- [104] F. Morgenroth. Spherical polyphenylene dendrimers via Diels–Alder reactions: the first example of an A4B building block in dendrimer chemistry. *Chem. Commun.*, (10):1139–1140, 1998.

-
- [105] M. Tonga, N. Cengiz, M. M. Kose, T. Dede, and A. Sanyal. Dendronized polymers via Diels–Alder “click” reaction. *J. Polym. Sci. A Polym. Chem.*, 48(2):410–416, 2010.
- [106] O. Gok, S. Yigit, M. Merve Kose, R. Sanyal, and A. Sanyal. Dendron-polymer conjugates via the Diels–Alder “click” reaction of novel anthracene-based dendrons. *J. Polym. Sci. A Polym. Chem.*, 51(15):3191–3201, 2013.
- [107] O. Gok, H. Durmaz, E. S. Ozdes, G. Hizal, U. Tunca, et al. Maleimide-based thiol reactive multiarm star polymers via Diels–Alder /retro Diels–Alder strategy. *J. Polym. Sci. A Polym. Chem.*, 48(12):2546–2556, 2010.
- [108] H. Shin, S. Jo, and A. G. Mikos. Biomimetic materials for tissue engineering. *Biomaterials*, 24(24):4353–4364, 2003.
- [109] J. L. Drury and D. J. Mooney. Hydrogels for tissue engineering: scaffold design variables and applications. *Biomaterials*, 24(24):4337–4351, 2003.
- [110] M. D. Pierschbacher and E. Ruoslahti. Cell attachment activity of fibronectin can be duplicated by small synthetic fragments of the molecule. *Nature*, 309(5963):30–33, 1984.
- [111] U. Hersel, C. Dahmen, and H. Kessler. RGD modified polymers: biomaterials for stimulated cell adhesion and beyond. *Biomaterials*, 24(24):4385–4415, 2003.
- [112] A. D. de Araújo, J. M. Palomo, J. Cramer, O. Seitz, K. Alexandrov, et al. Diels–Alder ligation of peptides and proteins. *Chem. Eur. J.*, 12(23):6095–6109, 2006.
- [113] X.-L. Sun, L. Yang, and E. L. Chaikof. Chemoselective immobilization of biomolecules through aqueous Diels–Alder and PEG chemistry. *Tetrahedron Lett.*, 49(16):2510–2513, 2008.
- [114] X.-L. Sun, C. L. Stabler, C. S. Cazalis, and E. L. Chaikof. Carbohydrate and protein immobilization onto solid surfaces by sequential Diels–Alder and azide–alkyne cycloadditions. *Bioconjugate Chem.*, 17(1):52–57, 2006.
- [115] W.-S. Yeo, M. N. Yousaf, and M. Mrksich. Dynamic interfaces between cells and surfaces: electroactive substrates that sequentially release and attach cells. *J. Am. Chem. Soc.*, 125(49):14994–14995, 2003.

- [116] B. J. Adzima, C. J. Kloxin, C. A. DeForest, K. S. Anseth, and C. N. Bowman. 3D photofixation lithography in Diels–Alder networks. *Macromol. Rapid Commun.*, 33(24):2092–2096, 2012.
- [117] S. Arumugam, S. V. Orski, J. Locklin, and V. V. Popik. Photoreactive polymer brushes for high-density patterned surface derivatization using a Diels–Alder photoclick reaction. *J. Am. Chem. Soc.*, 134(1):179–182, 2012.
- [118] M. Proupin-Perez, R. Cosstick, L. M. Liz-Marzan, V. Salgueiriño-Maceira, and M. Brust. Studies on the attachment of DNA to silica-coated nanoparticles through a Diels–Alder reaction. *Nucleos. Nucleot. Nucl.*, 24(5-7):1075–1079, 2005.
- [119] M. Shi and M. S. Shoichet. Furan-functionalized co-polymers for targeted drug delivery: characterization, self-assembly and drug encapsulation. *J. Biomater. Sci. Polym. Ed.*, 19(9):1143–1157, 2008.
- [120] M. Shi, J. H. Wosnick, K. Ho, A. Keating, and M. S. Shoichet. Immuno-polymeric nanoparticles by Diels–Alder chemistry. *Angew. Chem.*, 119(32):6238–6243, 2007.
- [121] M. Shi, K. Ho, A. Keating, and M. S. Shoichet. Doxorubicin-conjugated immuno-nanoparticles for intracellular anticancer drug delivery. *Adv. Funct. Mater.*, 19(11):1689–1696, 2009.
- [122] D. P. Y. Chan, S. C. Owen, and M. S. Shoichet. Double click: dual functionalized polymeric micelles with antibodies and peptides. *Bioconjugate Chem.*, 24(1):105–113, 2013.
- [123] D. P. Y. Chan, G. F. Deleavey, S. C. Owen, M. J. Damha, and M. S. Shoichet. Click conjugated polymeric immuno-nanoparticles for targeted siRNA and antisense oligonucleotide delivery. *Biomaterials*, 34(33):8408–8415, 2013.
- [124] K. L. Heredia, L. Tao, G. N. Grover, and H. D. Maynard. Heterotelechelic polymers for capture and release of protein–polymer conjugates. *Polym. Chem.*, 1(2):168–170, 2010.
- [125] G. Mantovani, F. Lecolley, L. Tao, D. M. Haddleton, J. Clerx, et al. Design and synthesis of N-maleimido-functionalized hydrophilic polymers via copper-mediated living radical polymerization: a suitable alternative to PEGylation chemistry. *J. Am. Chem. Soc.*, 127(9):2966–2973, 2005.

-
- [126] J. M. Hooker, E. W. Kovacs, and M. B. Francis. Interior surface modification of bacteriophage MS2. *J. Am. Chem. Soc.*, 126(12):3718–3719, 2004.
- [127] V. Pozsgay, N. E. Vieira, and A. Yergey. A method for bioconjugation of carbohydrates using Diels–Alder cycloaddition. *Org. Lett.*, 4(19):3191–3194, 2002.
- [128] V. Marchan, S. Ortega, D. Pulido, E. Pedroso, and A. Grandas. Diels–Alder cycloadditions in water for the straightforward preparation of peptide-oligonucleotide conjugates. *Nucleic Acids Res.*, 34(3):e24, 2006.
- [129] M. L. Blackman, M. Royzen, and J. M. Fox. Tetrazine ligation: fast bioconjugation based on inverse-electron-demand Diels–Alder reactivity. *J. Am. Chem. Soc.*, 130(41):13518–13519, 2008.
- [130] M. Wiessler. The Diels–Alder -reaction with inverse-electron-demand, a very efficient versatile click-reaction concept for proper ligation of variable molecular partners. *Int. J. Med. Sci.*, 7:19–28, 2010.
- [131] D. S. Liu, A. Tangpeerachaikul, R. Selvaraj, M. T. Taylor, J. M. Fox, et al. Diels–Alder cycloaddition for fluorophore targeting to specific proteins inside living cells. *J. Am. Chem. Soc.*, 134(2):792–795, 2012.
- [132] R. Rossin, T. Lappchen, S. M. van den Bosch, R. Laforest, and M. S. Robillard. Diels–Alder reaction for tumor pretargeting: in vivo chemistry can boost tumor radiation dose compared with directly labeled antibody. *J. Nucl. Med.*, 54(11):1989–1995, 2013.
- [133] B. M. Zeglis, K. K. Sevak, T. Reiner, P. Mohindra, S. D. Carlin, et al. A pretargeted pet imaging strategy based on bioorthogonal Diels–Alder click chemistry. *J. Nucl. Med.*, 54(8):1389–1396, 2013.
- [134] R. Pipkorn, W. Waldeck, B. Diding, M. Koch, G. Mueller, et al. Inverse-electron-demand Diels–Alder reaction as a highly efficient chemoselective ligation procedure: synthesis and function of a BioShuttle for temozolomide transport into prostate cancer cells. *J. Pept. Sci.*, 15(3):235–241, 2009.
- [135] K. Braun. Treatment of glioblastoma multiforme cells with temozolomide-BioShuttle ligated by the inverse Diels–Alder ligation chemistry. *Drug Des. Dev. Ther.*, 2:289–301, 2009.

- [136] R. M. Versteegen, R. Rossin, W. ten Hoeve, H. M. Janssen, and M. S. Robillard. Click to release: instantaneous doxorubicin elimination upon tetrazine ligation. *Angew. Chem. Int. Ed.*, 52(52):14112–14116, 2013.
- [137] S. S. van Berkel, A. T. J. Dirks, M. F. Debets, F. L. van Delft, J. J. L. M. Cornelissen, et al. Metal-free triazole formation as a tool for bioconjugation. *ChemBioChem*, 8(13):1504–1508, 2007.
- [138] P. Laverman, S. A. Meeuwissen, S. S. van Berkel, W. J. G. Oyen, F. L. van Delft, et al. In-depth evaluation of the cycloaddition–retro-Diels–Alder reaction for in vivo targeting with [^{111}In]-DTPA-RGD conjugates. *Nucl. Med. Biol.*, 36(7):749–757, 2009.
- [139] J. Shi, A. R. Votruba, O. C. Farokhzad, and R. Langer. Nanotechnology in drug delivery and tissue engineering: from discovery to applications. *Nano Lett.*, 10(9):3223–3230, 2010.
- [140] A. P. Bapat, J. G. Ray, D. A. Savin, E. A. Hoff, D. L. Patton, et al. Dynamic-covalent nanostructures prepared by Diels–Alder reactions of styrene-maleic anhydride-derived copolymers obtained by one-step cascade block copolymerization. *Polym. Chem.*, 3(11):3112–3120, 2012.
- [141] P. J. Costanzo, J. D. Demaree, and F. L. Beyer. Controlling dispersion and migration of particulate additives with block copolymers and Diels–Alder chemistry. *Langmuir*, 22(24):10251–10257, 2006.
- [142] P. J. Costanzo and F. L. Beyer. Thermally driven assembly of nanoparticles in polymer matrices. *Macromolecules*, 40(11):3996–4001, 2007.
- [143] C. Subramani, N. Cengiz, K. Saha, T. N. Gevrek, X. Yu, et al. Direct fabrication of functional and biofunctional nanostructures through reactive imprinting. *Adv. Mater.*, 23(28):3165–3169, 2011.
- [144] A. B. S. Bakhtiari, D. Hsiao, G. Jin, B. D. Gates, and N. R. Branda. An efficient method based on the photothermal effect for the release of molecules from metal nanoparticle surfaces. *Angew. Chem. Int. Ed.*, 48(23):4166–4169, 2009.
- [145] S. Yamashita, H. Fukushima, Y. Niidome, T. Mori, Y. Katayama, et al. Controlled-release system mediated by a retro Diels–Alder reaction induced

- by the photothermal effect of gold nanorods. *Langmuir*, 27(23):14621–14626, 2011.
- [146] T. Vermonden, R. Censi, and W. E. Hennink. Hydrogels for protein delivery. *Chem. Rev.*, 112(5):2853–2888, 2012.
- [147] Z. Wei, J. H. Yang, X. J. Du, F. Xu, M. Zrinyi, et al. Dextran-based self-healing hydrogels formed by reversible Diels–Alder reaction under physiological conditions. *Macromol. Rapid Commun.*, 34(18):1464–1470, 2013.
- [148] H.-L. Wei, Z. Yang, Y. Chen, H.-J. Chu, J. Zhu, et al. Characterisation of N-vinyl-2-pyrrolidone-based hydrogels prepared by a Diels–Alder click reaction in water. *Eur. Polym. J.*, 46(5):1032–1039, 2010.
- [149] H.-L. Wei, Z. Yang, H.-J. Chu, J. Zhu, Z.-C. Li, et al. Facile preparation of poly(N-isopropylacrylamide)-based hydrogels via aqueous Diels–Alder click reaction. *Polymer*, 51(8):1694–1702, 2010.
- [150] H.-L. Wei, K. Yao, H.-J. Chu, Z.-C. Li, J. Zhu, et al. Click synthesis of the thermo- and pH-sensitive hydrogels containing β -cyclodextrins. *J. Mater. Sci.*, 47(1):332–340, 2011.
- [151] C. Toncelli, D. C. De Reus, F. Picchioni, and A. A. Broekhuis. Properties of reversible Diels–Alder furan/maleimide polymer networks as function of crosslink density. *Macromol. Chem. Phys.*, 213(2):157–165, 2012.
- [152] S. Rimmer, P. Tattersall, J. R. Ebdon, and N. Fullwood. New strategies for the synthesis of amphiphilic networks. *React. Funct. Polym.*, 41:177–184, 1999.
- [153] C. García-Astrain, A. Gandini, D. Coelho, I. Mondragon, A. Retegi, et al. Green chemistry for the synthesis of methacrylate-based hydrogels crosslinked through Diels–Alder reaction. *Eur. Polym. J.*, 49(12):3998–4007, 2013.
- [154] H. Tan, J. P. Rubin, and K. G. Marra. Direct synthesis of biodegradable polysaccharide derivative hydrogels through aqueous Diels–Alder chemistry. 32(12):905–911, 2011.
- [155] S. Kirchhof, F. P. Brandl, N. Hammer, and A. M. Goepferich. Investigation of the Diels–Alder reaction as a cross-linking mechanism for degradable poly(ethylene glycol) based hydrogels. *J. Mater. Chem. B*, 1(37):4855–4864, 2013.

- [156] S. Kirchhof, A. Strasser, H.-J. Wittmann, V. Messmann, N. Hammer, et al. New insights into the cross-linking and degradation mechanism of Diels–Alder hydrogels. *J. Mater. Chem. B*, 3(3):449–457, 2015.
- [157] Y.-I. Hsu, K. Masutani, Y. Kimura, and T. Yamaoka. A novel bioabsorbable gel formed from a mixed micelle solution of poly(oxyethylene)-block-poly(L-lactide) and poly(oxyethylene)-block-poly(D-lactide) by concomitant stereocomplexation and chain extension. *Macromol. Chem. Phys.*, 214(14):1559–1568, 2013.
- [158] I. Kosif, E.-J. Park, R. Sanyal, and A. Sanyal. Fabrication of maleimide containing thiol reactive hydrogels via Diels–Alder /retro-Diels–Alder strategy. *Macromolecules*, 43(9):4140–4148, 2010.
- [159] F. Brandl, F. Sommer, and A. Goepferich. Rational design of hydrogels for tissue engineering: Impact of physical factors on cell behavior. *Biomaterials*, 28(2):134–146, 2007.
- [160] C. M. Nimmo, S. C. Owen, and M. S. Shoichet. Diels–Alder click cross-linked hyaluronic acid hydrogels for tissue engineering. *Biomacromolecules*, 12(3):824–830, 2011.
- [161] S. C. Owen, S. A. Fisher, R. Y. Tam, C. M. Nimmo, and M. S. Shoichet. Hyaluronic acid click hydrogels emulate the extracellular matrix. *Langmuir*, 29(24):7393–7400, 2013.
- [162] F. Yu, X. Cao, Y. Li, L. Zeng, B. Yuan, et al. An injectable hyaluronic acid/PEG hydrogel for cartilage tissue engineering formed by integrating enzymatic crosslinking and Diels–Alder “click chemistry”. 5(3):1082–1090, 2013.
- [163] F. Yu, X. Cao, L. Zeng, Q. Zhang, and X. Chen. An interpenetrating HA/G/CS biomimic hydrogel via Diels–Alder click chemistry for cartilage tissue engineering. *Carbohydr. Polym.*, 97(1):188–195, 2013.
- [164] N. A. Silva, M. J. Cooke, R. Y. Tam, N. Sousa, A. J. Salgado, et al. The effects of peptide modified gellan gum and olfactory ensheathing glia cells on neural stem/progenitor cell fate. *Biomaterials*, 33(27):6345–6354, 2012.

-
- [165] D. L. Alge, M. A. Azagarsamy, D. F. Donohue, and K. S. Anseth. Synthetically tractable click hydrogels for three-dimensional cell culture formed using tetrazine–norbornene chemistry. *Biomacromolecules*, 14(4):949–953, 2013.
- [166] K. C. Koehler, K. S. Anseth, and C. N. Bowman. Diels–Alder mediated controlled release from a poly(ethylene glycol) based hydrogel. *Biomacromolecules*, 14(2):538–547, 2013.
- [167] K. C. Koehler, D. L. Alge, K. S. Anseth, and C. N. Bowman. A Diels–Alder modulated approach to control and sustain the release of dexamethasone and induce osteogenic differentiation of human mesenchymal stem cells. *Biomaterials*, 34(16):4150–4158, 2013.
- [168] R. A. Firestone and G. M. Smith. The roles of changes in bonding vs. packing fraction in the pressure-induced acceleration of the Diels–Alder reaction. *Chem. Ber.*, 122(6):1089–1094, 1989.
- [169] N. K. Sangwan and H.-J. Schneider. The kinetic effects of water and of cyclodextrins on Diels–Alder reactions. Host-guest chemistry. Part 18. *J. Chem. Soc., Perkin Trans. 2*, (9):1223–1227, 1989.
- [170] Z. Erno, A. M. Asadirad, V. Lemieux, and N. R. Branda. Using light and a molecular switch to ‘lock’ and ‘unlock’ the Diels–Alder reaction. *Org. Biomol. Chem.*, 10(14):2787–2792, 2012.
- [171] K. Lang, L. Davis, J. Torres-Kolbus, C. Chou, A. Deiters, et al. Genetically encoded norbornene directs site-specific cellular protein labelling via a rapid bioorthogonal reaction. *Nature Chem.*, 4(4):298–304, 2012.
- [172] K. Lang, L. Davis, S. Wallace, M. Mahesh, D. J. Cox, et al. Genetic encoding of bicyclononynes and trans-cyclooctenes for site-specific protein labeling in vitro and in live mammalian cells via rapid fluorogenic Diels–Alder reactions. *J. Am. Chem. Soc.*, 134(25):10317–10320, 2012.
- [173] E. Kaya, M. Vrabel, C. Deiml, S. Prill, V. S. Fluxa, et al. A genetically encoded norbornene amino acid for the mild and selective modification of proteins in a copper-free click reaction. *Angew. Chem. Int. Ed.*, 51(18):4466–4469, 2012.

- [174] M. J. Schmidt and D. Summerer. Red-light-controlled protein-RNA crosslinking with a genetically encoded furan. *Angew. Chem. Int. Ed.*, 52(17):4690–4693, 2013.
- [175] G. V. Kleopina, N. A. Kravchenko, and E. D. Kaverzneva. Role of the 6-amino groups of lysine in lysozyme. *Russ. Chem. Bull.*, 14(5):806–812, 1965.
- [176] R. C. Davies and A. Neuberger. Modification of lysine and arginine residues of lysozyme and the effect of enzymatic activity. *Biochim. Biophys. Acta*, 178(2):306–317, 1969.
- [177] S. A. Kidwai, A. A. Ansari, and A. Salahuddin. Effect of succinylation (3-carboxypropionylation) on the conformation and immunological activity of ovalbumin. *Biochem. J.*, 155(1):171–180, 1976.
- [178] M. Abul Qasim and A. Salahuddin. Changes in conformation and immunological activity of ovalbumin during its modification with different acid anhydrides. *Biochim. Biophys. Acta*, 536(1):50–63, 1978.
- [179] S. Murase, N. Yumoto, M. G. Petukhov, and S. Yoshikawa. Acylation of the alpha-amino group in neuropeptide Y(12-36) increases binding affinity for the Y2 receptor. *J. Biochem.*, 119(1):37–41, 1996.
- [180] T. Masuda, N. Ide, and N. Kitabatake. Effects of chemical modification of lysine residues on the sweetness of lysozyme. *Chem. Senses*, 30(3):253–264, 2005.
- [181] E. Verheyen, L. Delain-Bioton, S. van der Wal, N. el Morabit, A. Barendregt, et al. Conjugation of methacrylamide groups to a model protein via a reducible linker for immobilization and subsequent triggered release from hydrogels. *Macromol. Biosci.*, 10(12):1517–1526, 2010.
- [182] N. Hammer, F. P. Brandl, S. Kirchhof, V. Messmann, and A. M. Goepferich. Protein compatibility of selected cross-linking reactions for hydrogels. *Macromol. Biosci.*, 15(3):405–413, 2015.
- [183] T. R. Hoare and D. S. Kohane. Hydrogels in drug delivery: progress and challenges. *Polymer*, 49(8):1993–2007, 2008.
- [184] C.-C. Lin and K. S. Anseth. PEG hydrogels for the controlled release of biomolecules in regenerative medicine. *Pharm. Res.*, 26(3):631–643, 2008.

-
- [185] E. Y. Chi, S. Krishnan, T. W. Randolph, and J. F. Carpenter. Physical stability of proteins in aqueous solution: mechanism and driving forces in nonnative protein aggregation. *Pharm. Res.*, 20(9):1325–1336, 2003.
- [186] W. Wang, S. Singh, D. L. Zeng, K. King, and S. Nema. Antibody structure, instability, and formulation. *J. Pharm. Sci.*, 96(1):1–26, 2007.
- [187] S.-Y. Tang, J. Shi, and Q.-X. Guo. Accurate prediction of rate constants of Diels–Alder reactions and application to design of Diels–Alder ligation. *Org. Biomol. Chem.*, 10(13):2673–2682, 2012.
- [188] O. Leavy. Therapeutic antibodies: past, present and future. *Nat Rev Immunol.*, 10(5):297, 2010.
- [189] J. K. H. Liu. The history of monoclonal antibody development - Progress, remaining challenges and future innovations. *Ann. Med. Surg.*, 3(4):113–116, 2014.
- [190] T. T. Hansel, H. Kropshofer, T. Singer, J. A. Mitchell, and A. J. T. George. The safety and side effects of monoclonal antibodies. *Nat. Rev. Drug. Discov.*, 9:325–338, 2010.
- [191] R. G. A. Jones and A. Martino. Targeted localized use of therapeutic antibodies: a review of non-systemic, topical and oral applications. *Crit. Rev. Biotechnol.*, 36(3):506–520, 2015.
- [192] L. C. Sandin, A. Orlova, E. Gustafsson, P. Ellmark, V. Tolmachev, et al. Locally delivered CD40 agonist antibody accumulates in secondary lymphoid organs and eradicates experimental disseminated bladder cancer. *Cancer Immunol. Res.*, 2(1):80–90, 2014.
- [193] L. C. Sandin, F. Eriksson, P. Ellmark, A. S. Loskog, T. H. Tötterman, et al. Local CTLA4 blockade effectively restrains experimental pancreatic adenocarcinoma growth in vivo. *OncoImmunology*, 3(1):e27614, 2014.
- [194] M. F. Fransen, T. C. van der Sluis, F. Ossendorp, R. Arens, and C. J. M. Melief. Controlled local delivery of CTLA-4 blocking antibody induces CD8+ T-cell-dependent tumor eradication and decreases risk of toxic side effects. *Clin. Cancer Res.*, 19(19):5381–5389, 2013.

- [195] N. Butoescu, O. Jordan, and E. Doelker. Intra-articular drug delivery systems for the treatment of rheumatic diseases: A review of the factors influencing their performance. *Eur. J. Pharm. Biopharm.*, 73(2):205–218, 2009.
- [196] P. Calias, W. A. Banks, D. Begley, M. Scarpa, and P. Dickson. Intrathecal delivery of protein therapeutics to the brain: a critical reassessment. *Pharmacol. Ther.*, 144(2):114–122, 2014.
- [197] The CATT Research Group. Ranibizumab and bevacizumab for neovascular age-related macular degeneration. *N. Engl. J. Med.*, 364(20):1897–1908, 2011.
- [198] J. F. Arevalo, J. G. Sanchez, A. F. Lasave, L. Wu, M. Maia, et al. Intravitreal bevacizumab (Avastin) for diabetic retinopathy: The 2010 GLADAOF lecture. *J. Ophthalmol.*, 2011(12):1–13, 2011.
- [199] C. Volz and D. Pauly. Antibody therapies and their challenges in the treatment of age-related macular degeneration. *Eur. J. Pharm. Biopharm.*, 95:158–172, 2015.
- [200] T. U. Krohne, N. Eter, F. G. Holz, and C. H. Meyer. Intraocular pharmacokinetics of bevacizumab after a single intravitreal injection in humans. *Am. J. Ophthalmol.*, 146(4):508–512, 2008.
- [201] T. U. Krohne, Z. Liu, F. G. Holz, and C. H. Meyer. Intraocular pharmacokinetics of ranibizumab following a single intravitreal injection in humans. *Am. J. Ophthalmol.*, 154(4):682–686, 2012.
- [202] K. M. Sampat and S. J. Garg. Complications of intravitreal injections. *Curr. Opin. Ophthalmol.*, 21(3):178–183, 2010.
- [203] D. V. Goeddel, D. G. Kleid, F. Bolivar, H. L. Heyneker, D. G. Yansura, et al. Expression in *Escherichia coli* of chemically synthesized genes for human insulin. *Proc. Natl. Acad. Sci. USA*, 76(1):106–110, 1979.
- [204] C. Morrison. Fresh from the biotech pipeline - 2014. *Nat. Biotechnol.*, 33(2):125–128, 2015.
- [205] A. L. Nelson, E. Dhimolea, and J. M. Reichert. Development trends for human monoclonal antibody therapeutics. *Nat. Rev. Drug. Discov.*, 9:767–774, 2010.
- [206] P. J. Hudson and C. Souriau. Engineered antibodies. *Nat. Med.*, 9(1):129–134, 2003.

-
- [207] T. J. Vaughan, A. J. Williams, K. Pritchard, J. K. Osbourn, A. R. Pope, et al. Human antibodies with sub-nanomolar affinities isolated from a large non-immunized phage display library. *Nat. Biotechnol.*, 14(3):309–314, 1996.
- [208] M. v. Mehren, G. P. Adams, and L. M. Weiner. Monoclonal antibody therapy for cancer. *Annu. Rev. Med.*, 54(1):343–369, 2003.
- [209] R. Maini, E. W. St Clair, F. Breedveld, D. Furst, J. Kalden, et al. Infliximab (chimeric anti-tumour necrosis factor α monoclonal antibody) versus placebo in rheumatoid arthritis patients receiving concomitant methotrexate: a randomised phase III trial. *Lancet*, 354(9194):1932–1939, 1999.
- [210] P. Chames, M. Van Regenmortel, E. Weiss, and D. Baty. Therapeutic antibodies: successes, limitations and hopes for the future. *Br. J. Pharmacol.*, 157(2):220–233, 2009.
- [211] S. J. Shire, Z. Shahrokh, and J. Liu. Challenges in the development of high protein concentration formulations. *J. Pharm. Sci.*, 93(6):1390–1402, 2004.
- [212] J. Vlasak and R. Ionescu. Fragmentation of monoclonal antibodies. *mAbs*, 3(3):253–263, 2014.
- [213] R. J. Keizer, A. D. R. Huitema, J. H. M. Schellens, and J. H. Beijnen. Clinical pharmacokinetics of therapeutic monoclonal antibodies. *Clin. Pharmacokinet.*, 49(8):493–507, 2010.
- [214] W. B. Liechty, D. R. Kryscio, B. V. Slaughter, and N. A. Peppas. Polymers for drug delivery systems. *Annu. Rev. Chem. Biomol. Eng.*, 1(1):149–173, 2010.
- [215] B. Qiu, S. Stefanos, J. Ma, A. Laloo, B. A. Perry, et al. A hydrogel prepared by in situ cross-linking of a thiol-containing poly(ethylene glycol)-based copolymer: a new biomaterial for protein drug delivery. *Biomaterials*, 24(1):11–18, 2003.
- [216] L. Klouda and A. G. Mikos. Thermoresponsive hydrogels in biomedical applications. *Eur. J. Pharm. Biopharm.*, 68(1):34–45, 2008.
- [217] S. R. Van Tomme, G. Storm, and W. E. Hennink. In situ gelling hydrogels for pharmaceutical and biomedical applications. *Int. J. Pharm.*, 355:1–18, 2008.

- [218] D. Cohn, A. Sosnik, and A. Levy. Improved reverse thermo-responsive polymeric systems. *Biomaterials*, 24(21):3707–3714, 2003.
- [219] A. Sosnik and D. Cohn. Ethoxysilane-capped PEO–PPO–PEO triblocks: a new family of reverse thermo-responsive polymers. *Biomaterials*, 25(14):2851–2858, 2004.
- [220] M. Katakam, W. R. Ravis, D. L. Golden, and A. K. Banga. Controlled release of human growth hormone following subcutaneous administration in dogs. *Int. J. Pharm.*, 152(1):53–58, 1997.
- [221] S. Kirchhof, M. Gregoritz, V. Messmann, N. Hammer, A. M. Goepferich, et al. Diels–Alder hydrogels with enhanced stability: first step toward controlled release of bevacizumab. *Eur. J. Pharm. Biopharm.*, 96:217–225, 2015.
- [222] M. Gregoritz and F. P. Brandl. The Diels–Alder reaction: a powerful tool for the design of drug delivery systems and biomaterials. *Eur. J. Pharm. Biopharm.*, 97:438–453, 2015.
- [223] I. T. Dorn, K. R. Neumaier, and R. Tampé. Molecular recognition of histidine-tagged molecules by metal-chelating lipids monitored by fluorescence energy transfer and correlation spectroscopy. *J. Am. Chem. Soc.*, 120(12):2753–2763, 1998.
- [224] S. Udenfriend, S. Stein, P. Bohlen, W. Dairman, W. Leimgruber, et al. Fluorescamine: a reagent for assay of amino acids, peptides, proteins, and primary amines in the picomole range. *Science*, 178(4063):871–872, 1972.
- [225] F. Brandl, M. Henke, S. Rothschenk, R. Gschwind, M. Breunig, et al. Poly(ethylene glycol) based hydrogels for intraocular applications. *Adv. Eng. Mater.*, 9(12):1141–1149, 2007.
- [226] G. Basu Ray, I. Chakraborty, and S. P. Moulik. Pyrene absorption can be a convenient method for probing critical micellar concentration (cmc) and indexing micellar polarity. *J. Colloid Interface Sci.*, 294(1):248–254, 2006.
- [227] R. Hennig, A. Vesper, S. Kirchhof, and A. Goepferich. Branched polymer–drug conjugates for multivalent blockade of angiotensin II receptors. *Mol. Pharm.*, 12:3292–3302, 2015.

-
- [228] K. Kalyanasundaram and J. K. Thomas. Environmental effects on vibronic band intensities in pyrene monomer fluorescence and their application in studies of micellar systems. *J. Am. Chem. Soc.*, 99(7):2039–2044, 1977.
- [229] E. Kumacheva, Y. Rharbi, M. A. Winnik, L. Guo, K. C. Tam, et al. Fluorescence studies of an alkaline swellable associative polymer in aqueous solution. *Langmuir*, 13(2):182–186, 1997.
- [230] Q. Gao, Q. Liang, F. Yu, J. Xu, Q. Zhao, et al. Synthesis and characterization of novel amphiphilic copolymer stearic acid-coupled F127 nanoparticles for nano-technology based drug delivery system. *Colloids Surf., B*, 88(2):741–748, 2011.
- [231] Y. Wang and M. A. Winnik. Onset of aggregation for water-soluble polymeric associative thickeners: a fluorescence study. *Langmuir*, 6(9):1437–1439, 1990.
- [232] A. Yekta, B. Xu, J. Duhamel, H. Adiwidjaja, and M. A. Winnik. Fluorescence studies of associating polymers in water: determination of the chain end aggregation number and a model for the association process. *Macromolecules*, 28(4):956–966, 1995.
- [233] E. Alami, M. Almgren, W. Brown, and J. François. Aggregation of hydrophobically end-capped poly(ethylene oxide) in aqueous solutions. fluorescence and light-scattering studies. *Macromolecules*, 29(6):2229–2243, 1996.
- [234] A. Halperin. Polymeric micelles: a star model. *Macromolecules*, 20(11):2943–2946, 1987.
- [235] R. D. Hester and D. R. Squire. Rheology of waterborne coatings. *J. Coatings Tech.*, 69(1):109–114, 1997.
- [236] T. Annable. The rheology of solutions of associating polymers: comparison of experimental behavior with transient network theory. *J. Rheol.*, 37(4):695–726, 1993.
- [237] F. Tanaka and S. F. Edwards. Viscoelastic properties of physically crosslinked networks. 1. Transient network theory. *Macromolecules*, 25(5):1516–1523, 1992.
- [238] M. A. Winnik and A. Yekta. Associative polymers in aqueous solution. *Curr. Opin. Colloid Interface Sci.*, 2(4):424–436, 1997.

- [239] P. J. Flory. *Principles of polymer chemistry*. Cornell University Pr., Ithaca, N.Y., 10th edition, 1953.
- [240] J. C. Bray and E. W. Merrill. Poly(vinyl alcohol) hydrogels. Formation by electron beam irradiation of aqueous solutions and subsequent crystallization. *J. Appl. Polym. Sci.*, 17(12):3779–3794, 1973.
- [241] D. L. Elbert, A. B. Pratt, M. P. Lutolf, S. Halstenberg, and J. A. Hubbell. Protein delivery from materials formed by self-selective conjugate addition reactions. *J. Control. Release*, 76:11–25, 2001.
- [242] B. Kronberg and P. Stenius. The effect of surface polarity on the absorption of nonionic surfactants. *J. Colloid Interface Sci.*, 102(2):410–417, 2010.
- [243] T. Canal and N. A. Peppas. Correlation between mesh size and equilibrium degree of swelling of polymeric networks. *J. Biomed. Mater. Res.*, 23(10):1183–1193, 1989.
- [244] K. S. Anseth, C. N. Bowman, and L. Brannon-Peppas. Mechanical properties of hydrogels and their experimental determination. *Biomaterials*, 17:1647–1657, 2003.
- [245] T. Inoue, G. Chen, K. Nakamae, and A. S. Hoffman. A hydrophobically-modified bioadhesive polyelectrolyte hydrogel for drug delivery. *J. Control. Release*, 49:167–176, 1997.
- [246] Y. Zhang, C.-Y. Won, and C.-C. Chu. Synthesis and characterization of biodegradable network hydrogels having both hydrophobic and hydrophilic components with controlled swelling behavior. *J. Polym. Sci. A Polym. Chem.*, 37(24):4554–4569, 1999.
- [247] Y. Yin, Y. Yang, and H. Xu. Swelling behavior of hydrogels for colon-site drug delivery. *J. Appl. Polym. Sci.*, 83(13):2835–2842, 2002.
- [248] S. Matsui and H. Aida. Hydrolysis of some N-alkylmaleimides. *J. Chem. Soc., Perkin Trans. 2*, (12):1277–1280, 1978.
- [249] C. P. Ryan, M. E. B. Smith, F. F. Schumacher, D. Grohmann, D. Papaioannou, et al. Tunable reagents for multi-functional bioconjugation: reversible or permanent chemical modification of proteins and peptides by control of maleimide hydrolysis. *Chem. Commun.*, 47(19):5452–5454, 2011.

-
- [250] R. I. Nathani, V. Chudasama, C. P. Ryan, P. R. Moody, R. E. Morgan, et al. Reversible protein affinity-labelling using bromomaleimide-based reagents. *Org. Biomol. Chem.*, 11(15):2408–2411, 2013.
- [251] R. P. Lyon, J. R. Setter, T. D. Bovee, S. O. Doronina, J. H. Hunter, et al. Self-hydrolyzing maleimides improve the stability and pharmacological properties of antibody-drug conjugates. *Nat. Biotechnol.*, 32(10):1059–1062, 2014.
- [252] N.-J. Cho, M. Elazar, A. Xiong, W. Lee, E. Chiao, et al. Viral infection of human progenitor and liver-derived cells encapsulated in three-dimensional PEG-based hydrogel. *Biomed. Mater.*, 4(1):011001, 2009.
- [253] W. Lee, N. J. Cho, A. Xiong, J. S. Glenn, and C. W. Frank. Hydrophobic nanoparticles improve permeability of cell-encapsulating poly(ethylene glycol) hydrogels while maintaining patternability. *Proc. Natl. Acad. Sci. USA*, 107(48):20709–20714, 2010.
- [254] M. Gregoritz, V. Messmann, A. M. Goepferich, and F. P. Brandl. Design of hydrogels for delayed antibody release utilizing hydrophobic association and Diels–Alder chemistry in tandem. *J. Mater. Chem. B*, 4(19):3398–3408, 2016.
- [255] A. S. Hoffman. Stimuli-responsive polymers: Biomedical applications and challenges for clinical translation. *Adv. Drug Deliv. Rev.*, 65(1):10–16, 2013.
- [256] M. C. Koetting, J. T. Peters, S. D. Steichen, and N. A. Peppas. Stimulus-responsive hydrogels: theory, modern advances, and applications. *Mater. Sci. Eng., R*, 93:1–49, 2015.
- [257] Y. Qiu and K. Park. Environment-sensitive hydrogels for drug delivery. *Adv. Drug Deliv. Rev.*, 53(3):321–339, 2001.
- [258] E. Ruel-Gariépy and J.-C. Leroux. In situ-forming hydrogels - review of temperature-sensitive systems. *Eur. J. Pharm. Biopharm.*, 58(2):409–426, 2004.
- [259] K. W. M. Boere, J. van den Dikkenberg, Y. Gao, J. Visser, W. E. Hennink, et al. Thermogelling and chemoselectively cross-linked hydrogels with controlled mechanical properties and degradation behavior. *Biomacromolecules*, 16(9):2840–2851, 2015.

- [260] F. Cellesi, N. Tirelli, and J. A. Hubbell. Materials for cell encapsulation via a new tandem approach combining reverse thermal gelation and covalent crosslinking. *Macromol. Chem. Phys.*, 203:1466–1472, 2002.
- [261] F. Cellesi, N. Tirelli, and J. A. Hubbell. Towards a fully-synthetic substitute of alginate: development of a new process using thermal gelation and chemical cross-linking. *Biomaterials*, 25(21):5115–5124, 2004.
- [262] F. Cellesi and N. Tirelli. A new process for cell microencapsulation and other biomaterial applications: Thermal gelation and chemical cross-linking in ‘tandem’. *J. Mater. Sci.*, 16:559–565, 2005.
- [263] E. Cho, J. S. Lee, and K. Webb. Formulation and characterization of poloxamine-based hydrogels as tissue sealants. *Acta Biomater.*, 8(6):2223–2232, 2012.
- [264] R. Censi, P. J. Fieten, P. di Martino, W. E. Hennink, and T. Vermonden. In situ forming hydrogels by tandem thermal gelling and Michael addition reaction between thermosensitive triblock copolymers and thiolated hyaluronan. *Macromolecules*, 43(13):5771–5778, 2010.
- [265] D. P. Nair, M. Podgórski, S. Chatani, T. Gong, W. Xi, et al. The thiol-Michael addition click reaction: a powerful and widely used tool in materials chemistry. *Chem. Mater.*, 26(1):724–744, 2014.
- [266] C. D. Pritchard, T. M. O’Shea, D. J. Siegwart, E. Calo, D. G. Anderson, et al. An injectable thiol-acrylate poly(ethylene glycol) hydrogel for sustained release of methylprednisolone sodium succinate. *Biomaterials*, 32(2):587–597, 2011.
- [267] A. Sosnik. Reversal of multidrug resistance by the inhibition of ATP-binding cassette pumps employing “Generally Recognized As Safe” (GRAS) nanopharmaceuticals: A review. *Adv. Drug Deliv. Rev.*, 65(13-14):1828–1851, 2013.
- [268] G. Dumortier, J. L. Grossiord, F. Agnely, and J. C. Chaumeil. A review of poloxamer 407 pharmaceutical and pharmacological characteristics. *Pharm. Res.*, 23(12):2709–2728, 2006.
- [269] L. Bromberg. Temperature-responsive gels and thermogelling polymer matrices for protein and peptide delivery. *Adv. Drug Deliv. Rev.*, 31(3):197–221, 1998.

-
- [270] D. Schweizer, T. Serno, and A. Goepferich. Controlled release of therapeutic antibody formats . *Eur. J. Pharm. Biopharm.*, 88(2):291–309, 2014.
- [271] S. E. Quaggin. Turning a blind eye to anti-VEGF toxicities. *J. Clin. Invest.*, 122(11):3849–3851, 2012.
- [272] K. M. Ford, M. Saint-Geniez, T. E. Walshe, and P. A. D’Amore. Expression and role of VEGF-A in the ciliary body. *Invest. Ophthalmol. Vis. Sci.*, 53(12):7520–7527, 2012.
- [273] K. J. McHugh, R. Guarecuco, R. Langer, and A. Jaklenec. Single-injection vaccines: Progress, challenges, and opportunities. *J. Control. Release*, 219: 596–609, 2015.
- [274] J. Cleland. Single-administration vaccines: controlled-release technology to mimic repeated immunizations. *Trends Biotechnol.*, 17(1):25–29, 1999.
- [275] S. Y. Tzeng, R. Guarecuco, K. J. McHugh, S. Rose, E. M. Rosenberg, et al. Thermostabilization of inactivated polio vaccine in PLGA-based microspheres for pulsatile release. *J. Control. Release*, 233:101–113, 2016.
- [276] M. C. Manning, D. K. Chou, B. M. Murphy, R. W. Payne, and D. S. Katayama. Stability of protein pharmaceuticals: an update. *Pharm. Res.*, 27(4):544–575, 2010.
- [277] H.-C. Mahler, W. Friess, U. Grauschopf, and S. Kiese. Protein aggregation: pathways, induction factors and analysis. *J. Pharm. Sci.*, 98(9):2909–2934, 2009.
- [278] M. Rabe, D. Verdes, and S. Seeger. Understanding protein adsorption phenomena at solid surfaces. *Adv. Colloid Interface Sci.*, 162(1-2):87–106, 2011.
- [279] J. K. Oh, R. Drumright, D. J. Siegwart, and K. Matyjaszewski. The development of microgels/nanogels for drug delivery applications. *Prog. Polym. Sci.*, 33(4):448–477, 2008.
- [280] J. K. Oh, D. I. Lee, and J. M. Park. Biopolymer-based microgels/nanogels for drug delivery applications. *Prog. Polym. Sci.*, 34(12):1261–1282, 2009.

- [281] N. M. B. Smeets and T. Hoare. Designing responsive microgels for drug delivery applications. *J. Polym. Sci. A Polym. Chem.*, 51(14):3027–3043, 2013.
- [282] M. Gregoritz, A. M. Goepferich, and F. P. Brandl. Polyanions effectively prevent protein conjugation and activity loss during hydrogel cross-linking. *J. Control. Release*, 238:92–102, 2016.
- [283] Y. Jiang, J. Chen, C. Deng, E. J. Suuronen, and Z. Zhong. Click hydrogels, microgels and nanogels: Emerging platforms for drug delivery and tissue engineering. *Biomaterials*, 35(18):4969–4985, 2014.
- [284] C. X. Wang, S. Utech, J. D. Gopez, M. F. J. Mabesoone, C. J. Hawker, et al. Non-covalent microgel particles containing functional payloads: coacervation of PEG-based triblocks via microfluidics. *ACS Appl. Mater. Interfaces*, 8(26):16914–16921, 2016.
- [285] P. Jonkheijm, D. Weinrich, M. Köhn, H. Engelkamp, P. C. M. Christianen, et al. Photochemical surface patterning by the thiol-ene reaction. *Angew. Chem.*, 120(23):4493–4496, 2008.
- [286] D. Weinrich, P.-C. Lin, P. Jonkheijm, U. T. T. Nguyen, H. Schröder, et al. Oriented immobilization of farnesylated proteins by the thiol-ene reaction. *Angew. Chem. Int. Ed.*, 49(7):1252–1257, 2010.
- [287] B. D. Fairbanks, M. P. Schwartz, A. E. Halevi, C. R. Nuttelman, C. N. Bowman, et al. A versatile synthetic extracellular matrix mimic via thiol-norbornene photopolymerization. *Adv. Mater.*, 21(48):5005–5010, 2009.
- [288] S. B. Anderson, C.-C. Lin, D. V. Kuntzler, and K. S. Anseth. The performance of human mesenchymal stem cells encapsulated in cell-degradable polymer-peptide hydrogels. *Biomaterials*, 32(14):3564–3574, 2011.
- [289] J. J. Roberts and S. J. Bryant. Comparison of photopolymerizable thiol-ene PEG and acrylate-based PEG hydrogels for cartilage development. *Biomaterials*, 34(38):9969–9979, 2013.
- [290] C. S. Ki, T.-Y. Lin, M. Korc, and C.-C. Lin. Thiol-ene hydrogels as desmoplasia-mimetic matrices for modeling pancreatic cancer cell growth, invasion, and drug resistance. *Biomaterials*, 35(36):9668–9677, 2014.

-
- [291] C.-C. Lin, C. S. Ki, and H. Shih. Thiol–norbornene photoclick hydrogels for tissue engineering applications. *J. Appl. Polym. Sci.*, 132(8):41563, 2015.
- [292] D. Liu, B. Yu, X. Jiang, and J. Yin. Responsive hybrid microcapsules by the one-step interfacial thiol–ene photopolymerization. *Langmuir*, 29(17):5307–5314, 2013.
- [293] O. Z. Durham, S. Krishnan, and D. A. Shipp. Polymer microspheres prepared by water-borne thiol–ene suspension photopolymerization. *ACS Macro Lett.*, 1(9):1134–1137, 2012.
- [294] N. A. Impellitteri, M. W. Toepke, S. K. L. Levengood, and W. L. Murphy. Specific VEGF sequestering and release using peptide-functionalized hydrogel microspheres. *Biomaterials*, 33(12):3475–3484, 2012.
- [295] A. K. Fraser, C. S. Ki, and C.-C. Lin. PEG-based microgels formed by visible-light-mediated thiol-ene photo-click reactions. *Macromol. Chem. Phys.*, 215(6):507–515, 2014.
- [296] H. Shih and C.-C. Lin. Cross-linking and degradation of step-growth hydrogels formed by thiol–ene photoclick chemistry. *Biomacromolecules*, 13(7):2003–2012, 2012.
- [297] H. Shih, A. K. Fraser, and C.-C. Lin. Interfacial thiol-ene photoclick reactions for forming multilayer hydrogels. *ACS Appl. Mater. Interfaces*, 5(5):1673–1680, 2013.
- [298] P. M. Kharkar, M. S. Rehmann, K. M. Skeens, E. Maverakis, and A. M. Kloxin. Thiol–ene click hydrogels for therapeutic delivery. *ACS Biomater. Sci. Eng.*, 2(2):165–179, 2016.
- [299] C. E. Hoyle and C. N. Bowman. Thiol-ene click chemistry. *Angew. Chem.*, 49(9):1540–1573, 2010.
- [300] J. D. McCall and K. S. Anseth. Thiol–ene photopolymerizations provide a facile method to encapsulate proteins and maintain their bioactivity. *Biomacromolecules*, 13(8):2410–2417, 2012.
- [301] A. A. Aimetti, A. J. Machen, and K. S. Anseth. Poly(ethylene glycol) hydrogels formed by thiol-ene photopolymerization for enzyme-responsive protein delivery. *Biomaterials*, 30(30):6048–6054, 2009.

- [302] J. A. Benton, B. D. Fairbanks, and K. S. Anseth. Characterization of valvular interstitial cell function in three dimensional matrix metalloproteinase degradable PEG hydrogels. *Biomaterials*, 30(34):6593–6603, 2009.
- [303] C.-C. Lin, A. Raza, and H. Shih. PEG hydrogels formed by thiol-ene photo-click chemistry and their effect on the formation and recovery of insulin-secreting cell spheroids. *Biomaterials*, 32(36):9685–9695, 2011.
- [304] A. S. Sawhney, C. P. Pathak, and J. A. Hubbell. Interfacial photopolymerization of poly(ethylene glycol)-based hydrogels upon alginate-poly(l-lysine) microcapsules for enhanced biocompatibility. *Biomaterials*, 14(13):1008–1016, 1993.
- [305] G. M. Cruise, O. D. Hegre, D. S. Scharp, and J. A. Hubbell. A sensitivity study of the key parameters in the interfacial photopolymerization of poly(ethylene glycol) diacrylate upon porcine islets. *Biotechnol. Bioeng.*, 57(6):655–665, 1998.
- [306] D. Shugar. The measurement of lysozyme activity and the ultra-violet inactivation of lysozyme. *Biochim. Biophys. Acta*, 8:302–309, 1952.
- [307] H.-U. Bergmeyer and E. Bernt. *Methods of enzymatic analysis*, volume 2. Academic Press, New York, N.Y., 1974.
- [308] W. E. Hennink and C. F. van Nostrum. Novel crosslinking methods to design hydrogels. *Adv. Drug Deliv. Rev.*, 54:13–36, 2002.
- [309] E. R. Stadtman and R. L. Levine. Free radical-mediated oxidation of free amino acids and amino acid residues in proteins. *Amino Acids*, 25:207–218, 2003.
- [310] M. S. Kharasch, A. T. Read, and F. R. Mayo. The peroxide effect in the addition of reagents to unsaturated compounds. XVI. The addition of thioglycolic acid to styrene and isobutylene. *Chem. Ind.*, 57:752–754, 1938.
- [311] N. B. Cramer, S. K. Reddy, A. K. O’Brien, and C. N. Bowman. Thiol-ene photopolymerization mechanism and rate limiting step changes for various vinyl functional group chemistries. *Macromolecules*, 36(21):7964–7969, 2003.
- [312] T. Thorsen, R. W. Roberts, F. H. Arnold, and S. R. Quake. Dynamic pattern formation in a vesicle-generating microfluidic device. *Phys. Rev. Lett.*, 86(18):4163–4166, 2001.

-
- [313] P. Zhu and L. Wang. Passive and active droplet generation with microfluidics: a review. *Lab Chip*, 17:34–75, 2016.
- [314] C. N. Baroud, F. Gallaire, and R. Dangla. Dynamics of microfluidic droplets. *Lab Chip*, 10(16):2032–2045, 2010.
- [315] P. Garstecki, M. J. Fuerstman, H. A. Stone, and G. M. Whitesides. Formation of droplets and bubbles in a microfluidic T-junction - scaling and mechanism of break-up. *Lab Chip*, 6(3):437–446, 2006.
- [316] X.-B. Li, F.-C. Li, J.-C. Yang, H. Kinoshita, M. Oishi, et al. Study on the mechanism of droplet formation in T-junction microchannel. *Chem. Eng. Sci.*, 69(1):340–351, 2012.
- [317] C. R. Thomas and D. Geer. Effects of shear on proteins in solution. *Biotechnol. Lett.*, 33(3):443–456, 2010.
- [318] L. S. Jones, A. Kaufmann, and C. R. Middaugh. Silicone oil induced aggregation of proteins. *J. Pharm. Sci.*, 94(4):918–927, 2005.
- [319] S. K. Li, M. R. Liddell, and H. Wen. Effective electrophoretic mobilities and charges of anti-VEGF proteins determined by capillary zone electrophoresis. *J. Pharm. Biomed. Anal.*, 55(3):603–607, 2011.
- [320] W. Zhu and J. Ding. Synthesis and characterization of a redox-initiated, injectable, biodegradable hydrogel. *J. Appl. Polym. Sci.*, 99(5):2375–2383, 2005.
- [321] G. T. Hermanson. *Bioconjugate techniques*. Academic Press Inc, Amsterdam, NL, 2013.
- [322] C. Hiemstra, Z. Zhong, M. J. van Steenberg, W. E. Hennink, and J. Feijen. Release of model proteins and basic fibroblast growth factor from in situ forming degradable dextran hydrogels. *J. Control. Release*, 122(1):71–78, 2007.
- [323] P. van de Wetering, A. T. Metters, R. G. Schoenmakers, and J. A. Hubbell. Poly(ethylene glycol) hydrogels formed by conjugate addition with controllable swelling, degradation, and release of pharmaceutically active proteins. *J. Control. Release*, 102:619–627, 2005.

- [324] W. Gombotz. Protein release from alginate matrices. *Adv. Drug Deliv. Rev.*, 31(3):267–285, 1998.
- [325] W. Wang. Instability, stabilization, and formulation of liquid protein pharmaceuticals. *Int. J. Pharm.*, 185(2):129–188, 1999.
- [326] T. J. Kamerzell, R. Esfandiary, S. B. Joshi, C. R. Middaugh, and D. B. Volkin. Protein-excipient interactions: Mechanisms and biophysical characterization applied to protein formulation development. *Adv. Drug Deliv. Rev.*, 63(13):1118–1159, 2011.
- [327] D. Schweizer, K. Schönhammer, M. Jahn, and A. Göpferich. Protein–polyanion interactions for the controlled release of monoclonal antibodies. *Biomacromolecules*, 14(1):75–83, 2013.
- [328] C. J. Burke, D. B. Volkin, H. Mach, and C. R. Middaugh. Effect of polyanions on the unfolding of acidic fibroblast growth factor. *Biochemistry*, 32(25):6419–6426, 1993.
- [329] N. Martin, D. Ma, A. Herbet, D. Boquet, F. M. Winnik, et al. Prevention of Thermally Induced Aggregation of IgG Antibodies by Noncovalent Interaction with Poly(acrylate) Derivatives. *Biomacromolecules*, 15(8):2952–2962, 2014.
- [330] H. Fan, S. N. Vitharana, T. Chen, D. O’Keefe, and C. R. Middaugh. Effects of pH and polyanions on the thermal stability of fibroblast growth factor 20. *Mol. Pharm.*, 4(2):232–240, 2007.
- [331] T. Derrick, A. O. Grillo, S. N. Vitharana, L. Jones, J. Rexroad, et al. Effect of polyanions on the structure and stability of repiferminTM (keratinocyte growth factor-2). *J. Pharm. Sci.*, 96(4):761–776, 2007.
- [332] S. B. Joshi, T. J. Kamerzell, C. McNown, and C. R. Middaugh. The interaction of heparin/polyanions with bovine, porcine, and human growth hormone. *J. Pharm. Sci.*, 97(4):1368–1385, 2008.
- [333] T. J. Kamerzell, S. B. Joshi, D. McClean, L. Peplinskie, K. Toney, et al. Parathyroid hormone is a heparin/polyanion binding protein: Binding energetics and structure modification. *Protein Sci.*, 16(6):1193–1203, 2007.
- [334] M. B. Browning and E. Cosgriff-Hernandez. Development of a biostable replacement for PEGDA hydrogels. *Biomacromolecules*, 13(3):779–786, 2012.

-
- [335] C. C. F. Blake, D. F. Koenig, G. A. Mair, A. C. T. North, D. C. Phillips, et al. Structure of hen egg-white lysozyme: a three-dimensional fourier synthesis at 2 Å resolution. *Nature*, 206(4986):757–761, 1965.
- [336] D. Suckau, M. Mak, and M. Przybylski. Protein surface topology-probing by selective chemical modification and mass spectrometric peptide mapping. *Proc. Natl. Acad. Sci. USA*, 89(12):5630–5634, 1992.
- [337] M. Friedman, J. F. Cavins, and J. S. Wall. Relative nucleophilic reactivities of amino groups and mercaptide ions in addition reactions with α,β -unsaturated compounds. *J. Am. Chem. Soc.*, 87(16):3672–3682, 1965.
- [338] A.-S. Yang and B. Honig. On the pH dependence of protein stability. *J. Mol. Biol.*, 231(2):459–474, 1993.
- [339] A.-S. Yang and B. Honig. Structural origins of pH and ionic strength effects on protein stability. *J. Mol. Biol.*, 237(5):602–614, 1994.
- [340] L. R. Wetter and H. F. Deutsch. Immunological studies on egg white proteins. *J. Biol. Chem.*, 192(1):237–242, 1951.
- [341] J. M. Park, B. B. Muhoberac, P. L. Dubin, and J. Xia. Effects of protein charge heterogeneity in protein-polyelectrolyte complexation. *Macromolecules*, 25(1):290–295, 1992.
- [342] A. C. Hamill, S.-C. Wang, and C. T. Lee. Probing lysozyme conformation with light reveals a new folding intermediate. *Biochemistry*, 44(46):15139–15149, 2005.
- [343] A. Jung, A. E. Sippel, M. Grez, and G. Schütz. Exons encode functional and structural units of chicken lysozyme. *Proc. Natl. Acad. Sci. USA*, 77(10):5759–5763, 1980.
- [344] T. Arakawa, S. J. Prestrelski, W. C. Kenney, and J. F. Carpenter. Factors affecting short-term and long-term stabilities of proteins. *Adv. Drug Deliv. Rev.*, 46(1-3):307–326, 2001.
- [345] Y. H. Liao, M. B. Brown, A. Quader, and G. P. Martin. Protective mechanism of stabilizing excipients against dehydration in the freeze-drying of proteins. *Pharm. Res.*, 19(12):1854–1861, 2002.

- [346] K. W. Mattison, P. L. Dubin, and I. J. Brittain. Complex formation between bovine serum albumin and strong polyelectrolytes: effect of polymer charge density. *J. Phys. Chem. B*, 102(19):3830–3836, 1998.
- [347] C. L. Cooper, A. Goulding, A. B. Kayitmazer, S. Ulrich, S. Stoll, et al. Effects of polyelectrolyte chain stiffness, charge mobility, and charge sequences on binding to proteins and micelles. *Biomacromolecules*, 7(4):1025–1035, 2006.
- [348] I. Porcar, H. Cottet, P. Gareil, and C. Tribet. Association between protein particles and long amphiphilic polymers: effect of the polymer hydrophobicity on binding isotherms. *Macromolecules*, 32(12):3922–3929, 1999.
- [349] J. Y. Gao and P. L. Dubin. Binding of proteins to copolymers of varying hydrophobicity. *Biopolymers*, 49(2):185–193, 1999.
- [350] D. Sacco and E. Dellacherie. Interaction of a macromolecular polyanion, dextran sulfate, with human hemoglobin. *FEBS Letters*, 199(2):254–258, 2001.
- [351] G. Tripodo, A. Trapani, M. L. Torre, G. Giammona, G. Trapani, et al. Hyaluronic acid and its derivatives in drug delivery and imaging: Recent advances and challenges. *Eur. J. Pharm. Biopharm.*, 97:400–416, 2015.
- [352] M. Morpurgo, F. M. Veronese, D. Kachensky, and J. M. Harris. Preparation and characterization of poly(ethylene glycol) vinyl sulfone. *Bioconjugate Chem.*, 7(3):363–368, 1996.
- [353] M. J. Roberts, M. D. Bentley, and J. M. Harris. Chemistry for peptide and protein PEGylation. *Adv. Drug Deliv. Rev.*, 54(4):459–476, 2002.
- [354] C.-C. Lin, S. M. Sawicki, and A. T. Metters. Free-radical-mediated protein inactivation and recovery during protein photoencapsulation. *Biomacromolecules*, 9(1):75–83, 2008.
- [355] R. T. Dean, S. Fu, R. Stocker, and M. J. Davies. Biochemistry and pathology of radical-mediated protein oxidation. *Biochem. J.*, 324(Pt 1):1–18, 1997.
- [356] R. J. Elias, D. J. McClements, and E. A. Decker. Antioxidant activity of cysteine, tryptophan, and methionine residues in continuous phase β -lactoglobulin in oil-in-water emulsions. *J. Agric. Food Chem.*, 53(26):10248–10253, 2005.

-
- [357] S. Gebicki and J. M. Gebicki. Formation of peroxides in amino acids and proteins exposed to oxygen free radicals. *Biochem. J.*, 289(3):743–749, 1993.
- [358] D. F. Nicoli and G. B. Benedek. Study of thermal denaturation of lysozyme and other globular proteins by light-scattering spectroscopy. *Biopolymers*, 15(12):2421–2437, 1976.
- [359] J. J. Grigsby, H. W. Blanch, and J. M. Prausnitz. Diffusivities of lysozyme in aqueous MgCl_2 solutions from dynamic light-scattering data: effect of protein and salt concentrations. *J. Phys. Chem. B*, 104(15):3645–3650, 2000.
- [360] S. Kirchhof, M. Abrami, V. Messmann, N. Hammer, A. M. Goepferich, et al. Diels–Alder Hydrogels for Controlled Antibody Release: Correlation between Mesh Size and Release Rate. *Mol. Pharm.*, 12(9):3358–3368, 2015.
- [361] M. Vlčková, F. Kalman, and M. A. Schwarz. Pharmaceutical applications of isoelectric focusing on microchip with imaged UV detection. *J. Chromatogr. A*, 1181(1-2):145–152, 2008.
- [362] H. H. Tønnesen and J. Karlsen. Alginate in drug delivery systems. *Drug. Dev. Ind. Pharm.*, 28(6):621–630, 2002.
- [363] F. P. Seib, M. Herklotz, K. A. Burke, M. F. Maitz, C. Werner, et al. Multifunctional silk–heparin biomaterials for vascular tissue engineering applications. *Biomaterials*, 35(1):83–91, 2014.
- [364] F. Dosio, S. Arpicco, B. Stella, and E. Fattal. Hyaluronic acid for anticancer drug and nucleic acid delivery. *Adv. Drug Deliv. Rev.*, 97:204–236, 2016.
- [365] B. Deutel, F. Laffleur, T. Palmberger, A. Saxer, M. Thaler, et al. In vitro characterization of insulin containing thiomeric microparticles as nasal drug delivery system. *Eur. J. Pharm. Sci.*, 81:157–161, 2016.
- [366] W.-C. Lin, D.-G. Yu, and M.-C. Yang. Blood compatibility of thermoplastic polyurethane membrane immobilized with water-soluble chitosan/dextran sulfate. *Colloids Surf., B*, 44(2-3):82–92, 2005.

List of Figures

| | | |
|-----|---|----|
| 1.1 | Synthesis of biodegradable shape-memory elastomers | 13 |
| 1.2 | Lipoic acid-conjugation of thermosensitive dendrimers via DA reaction | 16 |
| 1.3 | Generation of complex 3D structures by photolithography | 18 |
| 1.4 | Functionalization of nanoparticles with antibodies | 21 |
| 1.5 | Fluorescent labeling of silica-gold core-shell nanoparticles using a thermoreversible DA linker | 24 |
| 1.6 | Preparation of degradable DA hydrogels | 27 |
| 1.7 | rDA mediated release of RGDS peptides from PEG hydrogels . . . | 29 |
| 1.8 | Michael-type addition reaction of maleimide groups and use of nucleophile-tolerant dienophiles | 33 |
| 1.9 | Possible applications of the DA reaction in pharmaceuticals and biomedical engineering. | 34 |
| 3.1 | Emission spectra of pyrene in solutions of cetareth-20, 8armPEG40k- C ₁₂ -NH-Boc, and water | 49 |
| 3.2 | Association of hydrophobically modified macromonomers in aqueous solution | 52 |
| 3.3 | Viscosity of 8armPEG40k-OH, 8armPEG40k-C ₆ -NH-Boc and 8armPEG40k-C ₁₂ -NH-Boc solutions | 53 |
| 3.4 | Gel times of 8armPEG40k, 8armPEG40k-C ₆ and 8armPEG40k-C ₁₂ hydrogels | 54 |
| 3.5 | Swelling and degradation of 8armPEG40k, 8armPEG40k-C ₆ and 8armPEG40k-C ₁₂ hydrogels | 58 |
| 3.6 | Ring-opening hydrolysis of 8armPEG40k-maleimide, 8armPEG40k- C ₆ -maleimide and 8armPEG40k-C ₁₂ -maleimide | 60 |
| 3.7 | Release of bevacizumab from 8armPEG40k, 8armPEG40k-C ₆ and 8armPEG40k-C ₁₂ hydrogels | 61 |
| 4.1 | Rheological behavior of poloxamine and DA-Poloxamine solutions in the course of a three-step temperature program | 72 |

| | | |
|-----|--|-----|
| 4.2 | Thermal gelation and increase of stiffness for different DA-Poloxamine compositions | 74 |
| 4.3 | Swelling and degradation of DA-Poloxamine hydrogels with different compositions | 75 |
| 4.4 | Ring-opening hydrolysis of 4armPoloxamine-maleimide and 8armPoloxamine-maleimide | 78 |
| 4.5 | Cellular toxicity of DA-Poloxamine hydrogels | 79 |
| 4.6 | Release of bevacizumab from of DA-Poloxamine hydrogels | 80 |
| 5.1 | Experimental setup to study gelation via thiol-ene reaction in response to irradiation with green light in real-time | 92 |
| 5.2 | Swelling and degradation of 8armPEG40k-e-NB and 8armPEG40k-a-NB hydrogels | 96 |
| 5.3 | Gel formation of 8armPEG-NB solutions upon irradiation with green light | 97 |
| 5.4 | Experimental setup for the fabrication of antibody-loaded microgels | 100 |
| 5.5 | Cell viability after direct contact with microgels or exposure to extracts | 102 |
| 5.6 | Release of bevacizumab from thiol-ene microgels | 105 |
| 6.1 | Schematic representation of the protective effect of polyanions . . . | 116 |
| 6.2 | SDS PAGE of lysozyme-PEG conjugates resulting from Michael-type addition reactions | 117 |
| 6.3 | Activity of lysozyme after incubation with mPEG5k-maleimide and mPEG5k-furan | 118 |
| 6.4 | CD spectra of lysozyme after incubation with mPEG5k-maleimide and mPEG5k-furan | 119 |
| 6.5 | Influence of ionic strength on the turbidity of solutions containing lysozyme and poly(acrylic acid) | 120 |
| 6.6 | Influence of high ionic strength on the protective effect of polyanions | 122 |
| 6.7 | Influence of buffer and cryoprotectants on the protective effect of polyanions | 123 |
| 6.8 | Influence of polyanion concentration, molecular mass, and protein concentration on the protective effect of polyanions | 124 |
| 6.9 | Protective effect of polyanions against Michael-type addition reactions and radical polymerizations | 126 |

| | | |
|------|---|-----|
| 6.10 | Release of lysozyme from 8armPEG10k hydrogels with and without polyanions | 127 |
| 6.11 | Release of bevacizumab from 8armPEG40k-C ₆ hydrogels with and without polyanions | 129 |
| 6.12 | Size exclusion chromatograms of 8armPEG40k-C ₆ -maleimide and 8armPEG40k-C ₆ -furan | 130 |

List of Schemes

| | | |
|-----|--|-----|
| 1.1 | Subtypes of the Diels–Alder reaction | 7 |
| 3.1 | Chemical structures of 8armPEG40k-maleimide and 8armPEG40k-furan | 44 |
| 3.2 | Chemical structures of hydrophobically modified macromonomers . | 45 |
| 4.1 | Chemical structures of four- and eight-armed poloxamines functionalized with maleimide and furyl groups | 68 |
| 4.2 | Cross-linking and degradation of DA-Poloxamine hydrogels | 76 |
| 5.1 | Chemical structures of 8armPEG-norbornenes with hydrolytically cleaveable or stable end-groups | 90 |
| 5.2 | Thiol-ene reaction of PEG-norbornene with DTT and ester hydrolysis which is fundamental for hydrogel degradation | 95 |
| 6.1 | Chemical structures of alginate, dextran sulfate, heparin, hyaluronic acid and poly(acrylic acid) | 110 |

List of Tables

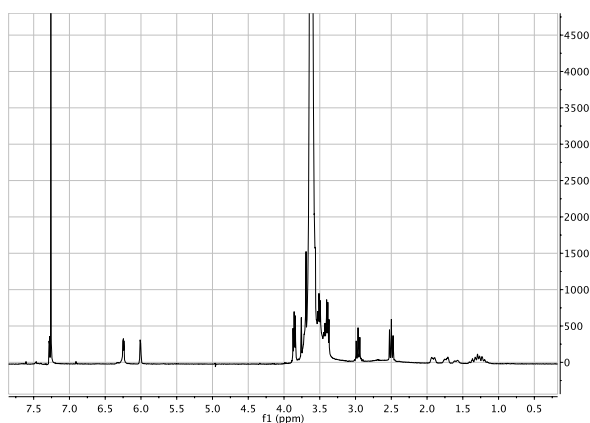
| | | |
|-----|--|-----|
| 3.1 | Network mesh size and E modulus of 8armPEG40k, 8armPEG40k-C ₆ and 8armPEG40k-C ₁₂ hydrogels | 56 |
| 3.2 | Calculated rate constants and half-lives of 8armPEG40k-maleimide, 8armPEG40k-C ₆ -maleimide and 8armPEG40k-C ₁₂ -maleimide | 60 |
| 4.1 | $ G^* $ values for different DA-Poloxamine hydrogels directly after increasing the temperature and after 90 min of incubation | 74 |
| 4.2 | Calculated rate constants and half-lives of 4armPoloxamine-maleimide and 8armPoloxamine-maleimide | 77 |
| 4.3 | Binding ability of bevacizumab released from DA-Poloxamine hydrogels | 82 |
| 5.1 | $ G^* $ plateau values for different thiol-ene hydrogels | 99 |
| 5.2 | Residual activity of model proteins after exposure to stress factors arising during microgel fabrication. | 101 |
| 5.3 | Average network mesh size of different thiol-ene hydrogels | 104 |

Appendix

Supplementary Spectroscopic Information

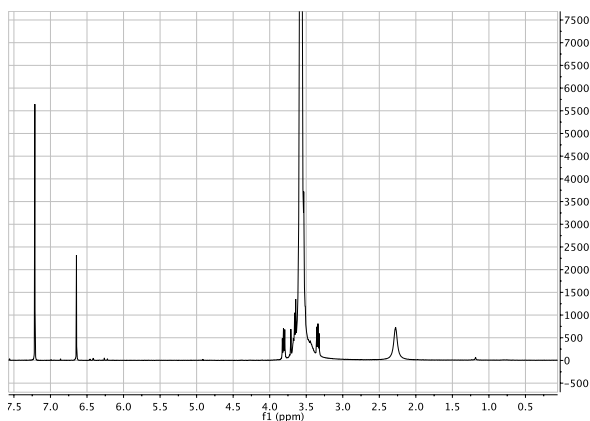
A) ^1H -NMR spectra for the polymers described in chapter 3

8armPEG40k-furan



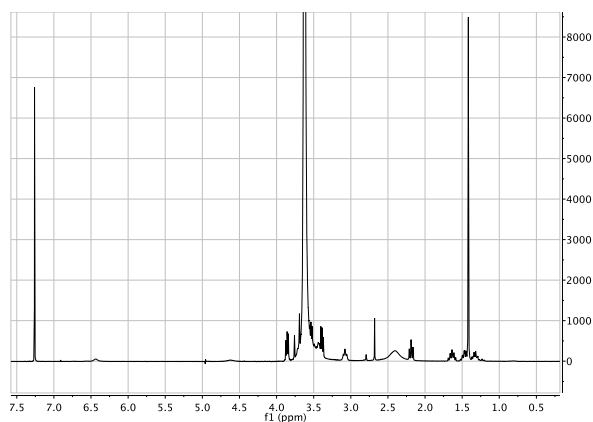
^1H -NMR (CDCl_3 , 300 MHz): δ (ppm) = 2.47 (t, 16H, $-\text{C}(\text{O})\text{CH}_2\text{CH}_2\text{Ar}$), 2.97 (t, 16H, $-\text{C}(\text{O})\text{CH}_2\text{CH}_2\text{Ar}$), 3.62 (s, $-\text{OCH}_2\text{CH}_2-$), 6.01 (s, 8H, Ar), 6.24 (s, 8H, Ar), 7.28 (s, 8H, Ar).

8armPEG40k-maleimide



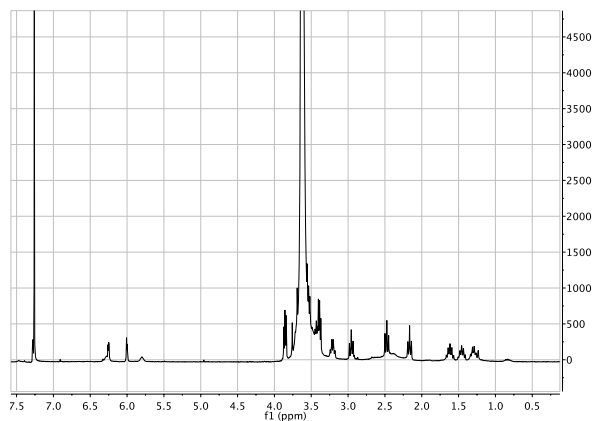
^1H -NMR (CDCl_3 , 300 MHz): δ (ppm) = 3.62 (s, $-\text{OCH}_2\text{CH}_2-$), 6.64 (s, 16H, $-\text{C}(\text{O})\text{CH}=\text{CHC}(\text{O})-$).

8armPEG40k-C₆-NH-Boc

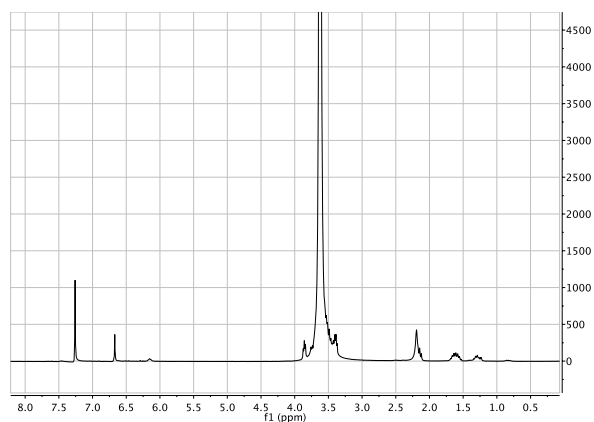


¹H-NMR (CDCl₃, 300 MHz): δ (ppm) = 1.32 (m, 16H, -C(O)CH₂CH₂CH₂CH₂CH₂NH-), 1.42 (s, 72H, -NHC(O)OC(CH₃)₃), 1.47 (m, 16H, -C(O)CH₂CH₂CH₂CH₂CH₂NH), 1.63 (m, 16H, -C(O)CH₂CH₂CH₂CH₂CH₂NH-), 2.17 (m, 16H, -C(O)CH₂CH₂CH₂CH₂CH₂NH-), 3.08 (m, 16H, -C(O)CH₂CH₂CH₂CH₂CH₂NH-), 3.62 (s, -OCH₂CH₂-).

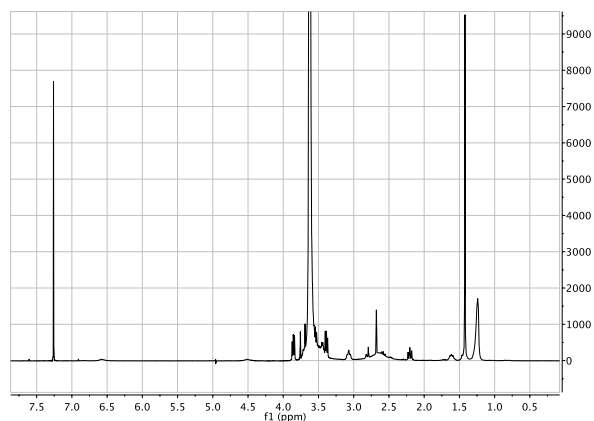
8armPEG40k-C₆-furan



¹H-NMR (CDCl₃, 300 MHz): δ (ppm) = 1.29 (m, 16H, -C(O)CH₂CH₂CH₂CH₂CH₂NH-), 1.46 (m, 16H, -C(O)CH₂CH₂CH₂CH₂CH₂NH-), 1.62 (m, 16H, -C(O)CH₂CH₂CH₂CH₂CH₂NH-), 2.17 (m, 16H, -C(O)CH₂CH₂CH₂CH₂CH₂NH-), 2.47 (t, 16H, -C(O)CH₂CH₂Ar), 2.96 (t, 16H, -C(O)CH₂CH₂Ar), 3.20 (m, 16H, -C(O)CH₂CH₂CH₂CH₂CH₂NH-), 3.62 (s, -OCH₂CH₂-), 6.00 (s, 8H, Ar), 6.25 (s, 8H, Ar), 7.27 (s, 8H, Ar).

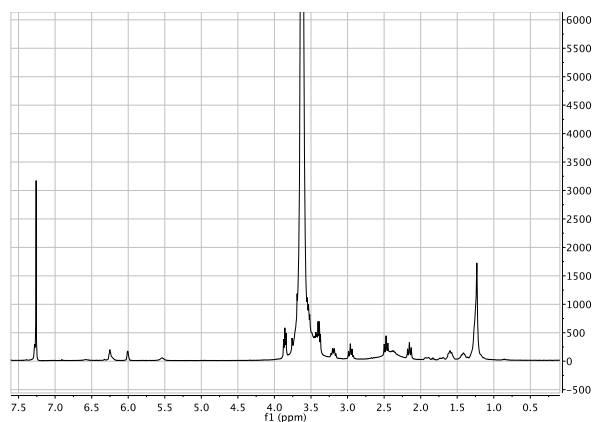
8armPEG40k-C₆-maleimide

¹H-NMR (CDCl₃, 300 MHz): δ (ppm) = 1.29 (m, 16H, -C(O)CH₂CH₂CH₂CH₂CH₂N-), 1.61 (m, 32H, -C(O)CH₂CH₂CH₂CH₂CH₂N-), 2.15 (m, 16H, -C(O)CH₂CH₂CH₂CH₂CH₂N-), 3.62 (s, -OCH₂CH₂-), 6.67 (s, 16H, -C(O)CH=CHC(O)-).

8armPEG40k-C₁₂-NH-Boc

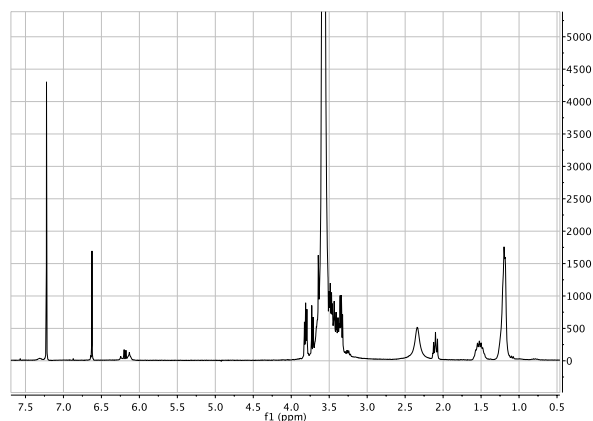
¹H-NMR (CDCl₃, 300 MHz): δ (ppm) = 1.24 (m, 112H, -C(O)CH₂(CH₂)₇CH₂CH₂CH₂NH-), 1.42 (s, 72H, -NHC(O)OC(CH₃)₃), 1.43 (m, 16H, -C(O)CH₂(CH₂)₇CH₂CH₂CH₂NH-), 1.60 (m, 16H, -C(O)CH₂(CH₂)₇CH₂CH₂CH₂NH-), 2.20 (m, 16H, -C(O)CH₂(CH₂)₇CH₂CH₂CH₂NH-), 3.08 (m, 16H, -C(O)CH₂(CH₂)₇CH₂CH₂CH₂NH-), 3.62 (s, -OCH₂CH₂-).

8armPEG40k-C₁₂-furan



¹H-NMR (CDCl₃, 300 MHz): δ (ppm) = 1.23 (m, 112H, -C(O)CH₂(CH₂)₇CH₂CH₂CH₂NH-), 1.42 (m, 16H, -C(O)CH₂(CH₂)₇CH₂CH₂CH₂NH-), 1.60 (m, 16H, -C(O)CH₂(CH₂)₇CH₂CH₂CH₂NH-), 2.15 (m, 16H, -C(O)CH₂(CH₂)₇CH₂CH₂CH₂NH-), 2.47 (t, 16H, -C(O)CH₂CH₂Ar), 2.96 (t, 16H, -C(O)CH₂CH₂Ar), 3.20 (m, 16H, -C(O)CH₂(CH₂)₇CH₂CH₂CH₂NH-), 3.62 (s, -OCH₂CH₂-), 6.00 (s, 8H, Ar), 6.26 (s, 8H, Ar), 7.26 (s, 8H, Ar).

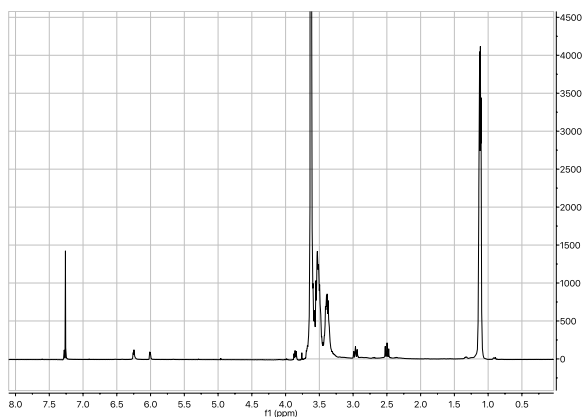
8armPEG40k-C₁₂-maleimide



¹H-NMR (CDCl₃, 300 MHz): δ (ppm) = 1.23 (m, 112H, -C(O)CH₂(CH₂)₇CH₂CH₂CH₂N-), 1.56 (m, 32H, -C(O)CH₂(CH₂)₇CH₂CH₂CH₂N-), 2.14 (m, 16H, -C(O)CH₂(CH₂)₇CH₂CH₂CH₂N-), 3.62 (s, -OCH₂CH₂-), 6.66 (s, 16H, -C(O)CH=CHC(O)-).

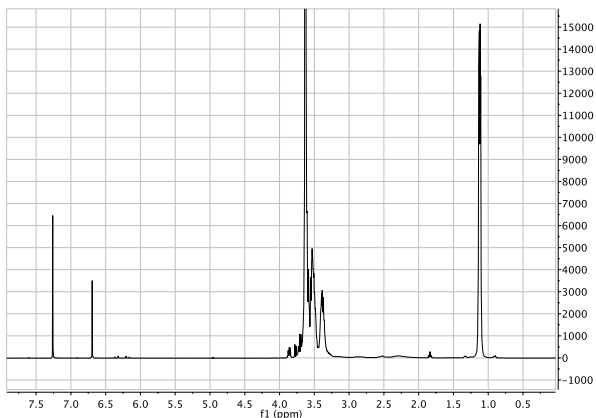
B) ^1H -NMR spectra for the polymers described in chapter 4

4armPoloxamine-furan



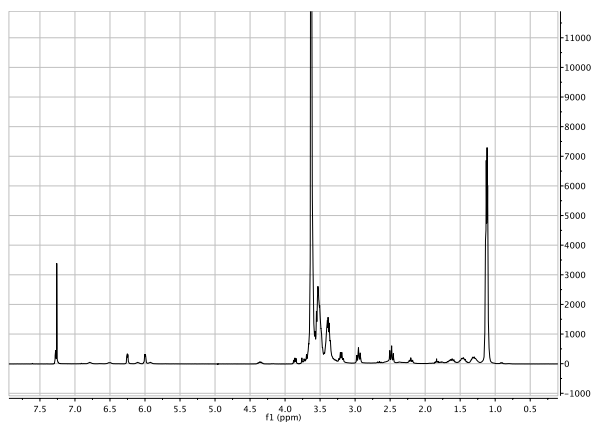
^1H -NMR (CDCl_3 , 300 MHz): δ (ppm) = 1.12 (- $\text{OCH}_2\text{CH}(\text{CH}_3)$ -), 2.50 (t, 8H, - $\text{C}(\text{O})\text{CH}_2\text{CH}_2\text{Ar}$), 2.97 (t, 8H, - $\text{C}(\text{O})\text{CH}_2\text{CH}_2\text{Ar}$), 3.40 (m, - $\text{OCH}_2\text{CH}(\text{CH}_3)$ -), 3.54 (m, - $\text{OCH}_2\text{CH}(\text{CH}_3)$ -), 3.63 (s, - OCH_2CH_2 -), 6.02 (s, 4H, Ar), 6.24 (s, 4H, Ar), 7.28 (s, 4H, Ar).

4armPoloxamine-maleimide



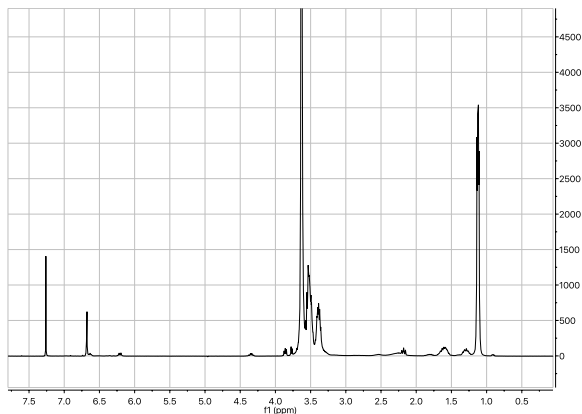
^1H -NMR (CDCl_3 , 300 MHz): δ (ppm) = 1.12 (m, - $\text{OCH}_2\text{CH}(\text{CH}_3)$ -), 3.40 (m, - $\text{OCH}_2\text{CH}(\text{CH}_3)$ -), 3.54 (m, - $\text{OCH}_2\text{CH}(\text{CH}_3)$ -), 3.63 (s, - OCH_2CH_2 -), 6.69 (s, 8H, - $\text{C}(\text{O})\text{CH}=\text{CHC}(\text{O})$ -).

8armPoloxamine-furan



^1H -NMR (CDCl_3 , 300 MHz): δ (ppm) = 1.12 ($-\text{OCH}_2\text{CH}(\text{CH}_3)-$), 1.30-1.82 (48 H, $-\text{CH}_2\text{CH}_2\text{CH}_2\text{CH}_2\text{NH}-$), 2.20 (t, 8H, $-\text{C}(\text{O})\text{CH}_2\text{CH}_2\text{CH}_2\text{CH}_2\text{CH}_2\text{NH}-$), 2.48 (t, 16H, $-\text{C}(\text{O})\text{CH}_2\text{CH}_2\text{Ar}$), 2.95 (t, 16H, $-\text{C}(\text{O})\text{CH}_2\text{CH}_2\text{Ar}$), 3.21 (t, 16H, $-\text{CH}_2\text{CH}_2\text{CH}_2\text{CH}_2\text{NH}-$), 3.40 (m, $-\text{OCH}_2\text{CH}(\text{CH}_3)-$), 3.54 (m, $-\text{OCH}_2\text{CH}(\text{CH}_3)-$), 3.63 (s, $-\text{OCH}_2\text{CH}_2-$), 4.35 (m, 4H, $-\text{C}(\text{O})\text{C}(\text{NHR})\text{HCH}_2\text{CH}_2\text{CH}_2\text{CH}_2\text{NH}-$), 6.00 (s, 8H, Ar), 6.26 (s, 8H, Ar), 7.28 (s, 8H, Ar).

8armPoloxamine-maleimide



^1H -NMR (CDCl_3 , 300 MHz): δ (ppm) = 1.12 ($-\text{OCH}_2\text{CH}(\text{CH}_3)-$), 1.28-1.82 (48 H, $-\text{CH}_2\text{CH}_2\text{CH}_2\text{CH}_2\text{N}-$), 2.18 (t, 8H, $-\text{C}(\text{O})\text{CH}_2\text{CH}_2\text{CH}_2\text{CH}_2\text{CH}_2\text{N}-$), 3.39 (m, $-\text{OCH}_2\text{CH}(\text{CH}_3)-$), 3.54 (m, $-\text{OCH}_2\text{CH}(\text{CH}_3)-$), 3.63 (s, $-\text{OCH}_2\text{CH}_2-$), 4.35 (m, 4H, $-\text{C}(\text{O})\text{C}(\text{NHR})\text{HCH}_2\text{CH}_2\text{CH}_2\text{CH}_2\text{N}-$), 6.68 (s, 16H, $-\text{C}(\text{O})\text{CH}=\text{CHC}(\text{O})-$).

Acronyms

| | |
|---------------------------|--|
| 2D | two-dimensional |
| 3D | three-dimensional |
| Ala | alanine |
| ALG | alginate |
| AMD | age-related macular degeneration |
| ANOVA | analysis of variance |
| Arg | arginine |
| Asp | aspartic acid |
| ATRP | atom transfer free radical polymerization |
| Boc | <i>tert</i> -butyloxycarbonyl |
| C ₆ | 6-aminohexanoic acid spacer |
| C ₁₂ | 12-aminododecanoic acid spacer |
| CD | circular dichroism |
| CMC | critical micelle concentration |
| CPP | cell penetrating peptide |
| CTRL | control |
| CuAAC | copper(I)-catalyzed azide–alkyne Huisgen cycloaddition |
| DA | Diels–Alder |
| DCC | <i>N,N'</i> -dicyclohexylcarbodiimide |
| DIPEA | <i>N,N</i> -diisopropylethylamine |
| DMAP | 4-dimethylaminopyridine |
| DNA | deoxyribonucleic acid |
| DTT | dithiothreitol |
| DXS | dextran sulfate |
| ECM | extracellular matrix |
| ELISA | enzyme-linked immunosorbent assay |
| EMEM | Eagle's minimum essential medium |
| EO | ethylene oxide chain |
| FGF | fibroblast growth factor |

| | |
|--------|--|
| Fmoc | fluorenylmethyloxycarbonyl |
| Gly | glycine |
| GRGDS | Gly–Arg–Gly–Asp–Ser |
| HA | hyaluronic acid |
| HC | hydrocarbon chain |
| HEP | heparin |
| HER2 | human epidermal growth factor receptor 2 |
| HLB | hydrophilic lipophilic balance |
| HMEC | human mammary epithelial cell |
| hMSC | human mesenchymal stem cell |
| IEDDA | inverse electron-demand Diels–Alder |
| IEP | isoelectric point |
| IKVAV | isoleucine–lysine–valine–alanine–valine |
| Ile | isoleucine |
| ISO | International Organization for Standardization |
| LCST | lower critical solution temperature |
| LDH | L-lactate dehydrogenase |
| LED | light-emitting diode |
| LYS | native lysozyme |
| Lys | lysine |
| MaLA | Lipoic acid |
| MES | 2-(<i>N</i> -morpholino)ethanesulfonic acid |
| mPEG5k | methoxy poly(ethylene glycol), 5 kDa |
| MTT | 3-(4,5-dimethylthiazol-2-yl)-2,5-diphenyltetrazolium bromide |
| NB | norbornene |
| NHS | <i>N</i> -hydroxysuccinimide |
| NIR | near-infrared |
| NLS | nuclear localization sequence |
| NMR | nuclear magnetic resonance |
| NSPC | neural stem/progenitor cell |
| PAA | poly(acrylic acid) |
| PAGE | polyacrylamide gel electrophoresis |
| PBS | phosphate buffered saline |
| PDR | proliferative diabetic retinopathy |
| PEEK | poly(etheretherketone) |
| PEG | poly(ethylene glycol) |

| | |
|----------------------|--|
| 8armPEG10k | eight-armed poly(ethylene glycol), 10 kDa |
| 8armPEG20k | eight-armed poly(ethylene glycol), 20 kDa |
| 8armPEG40k | eight-armed poly(ethylene glycol), 40 kDa |
| PET | positron emission tomography |
| PLA | poly(lactic acid) |
| PMMA | poly(methyl methacrylate) |
| 4armPoloxamine . . . | four-armed poloxamine |
| 8armPoloxamine . . . | eight-armed poloxamine |
| PPG | poly(propylene glycol) |
| PS | polystyrene |
| PTFE | poly(tetrafluoroethylene) |
| RAFT | reversible addition fragmentation chain transfer |
| rDA | retro-Diels–Alder |
| RGD | arginine–glycine–aspartic acid |
| RGDS | arginine–glycine–aspartic acid–serine |
| RNA | ribonucleic acid |
| ROMP | ring-opening metathesis polymerization |
| SDS | sodium dodecyl sulfate |
| SEC | size-exclusion chromatography |
| Ser | serine |
| SPAAC | strain-promoted azide–alkyne cycloaddition |
| SPR | surface plasmon resonance |
| TEMED | tetramethylethylenediamine |
| TMZ | temozolomide |
| Tyr | tyrosine |
| UV | ultraviolet |
| Val | valine |
| VEGF | vascular endothelial growth factor |
| YIGSR | tyrosine–isoleucine–glycine–serine–arginine |

Symbols

| | |
|--------------------------|---|
| C_n | Flory characteristic ratio |
| χ_{12} | Flory–Huggins polymer-solvent interaction parameter |
| E | Young’s modulus of compression |
| f | branching factor of the macromonomers |
| $ G^* $ | absolute value of the complex shear modulus |
| G' | storage modulus |
| G'' | loss modulus |
| k_{obs} | pseudo-first-order rate constant |
| l | average bond length |
| m_p | total mass of the polymer in the hydrogel |
| M_r | relative molecular mass |
| $t_{1/2}$ | half-life time |
| V_1 | molar volume of the swelling agent |
| v_{2c} | polymer fraction of the gel after cross-linking |
| v_{2s} | polymer fraction of the gel in the swollen state |
| V_{gc} | volume of the gel cylinder after cross-linking |
| V_{gs} | volume of the gel cylinder after swelling |
| V_p | volume of the dry polymer |
| δ | chemical shift |
| δ | phase angle |
| η | dynamic viscosity |
| λ_{em} | emission wavelength |
| λ_{ex} | excitation wavelength |
| ν_e | number of moles of elastically active chains |
| ξ | average network mesh size |

Curriculum Vitae

Personal Information

Name: Manuel Manfred Gregoritz
Date of birth: 14th of July 1988
Place of birth: Erding
Nationality: German

Professional Training

| | |
|-------------------|--|
| 11/2013 – 09/2017 | Graduate Student Department of Pharmaceutical Technology, University of Regensburg |
| 01/2014 – 04/2017 | Specialist Pharmacist in Pharmaceutical Technology Department of Pharmaceutical Technology, University of Regensburg |
| 12/2013 | Licensure as Pharmacist |
| 05/2013 – 10/2013 | Practical Training Rathaus Apotheke, Neufinsing |
| 10/2012 – 04/2013 | Practical Training Department of Biomedical Engineering, Cornell University, Ithaca, NY, USA |
| 10/2007 – 10/2012 | Studies of Pharmacy Ludwig-Maximilian University of Munich Joint degree with Pharmaceutical Sciences (B.Sc./M.Sc.) |
| 10/2010 – 04/2012 | Studies of Pharmaceutical Sciences (M.Sc.) Ludwig-Maximilian University of Munich Master's thesis: <i>"Method development for the preparation of standardized protein-like particles"</i> supervised by Prof. Dr. Wolfgang Frieß. |
| 10/2007 – 08/2010 | Studies of Pharmaceutical Sciences (B.Sc.) Ludwig-Maximilian University of Munich Bachelor's thesis: <i>"Evaluation of candidates derived from whole genome analysis potentially involved in prostate cancer chemoresistance"</i> supervised by Prof. Dr. Ernst Wagner. |

Scientific Work Experience

| | |
|--------------------------|--|
| 04/2016 – Present | Assistant Editor European Journal of Pharmaceutics and Biopharmaceutics |
| 09/2011 – 06/2012 | Research Intern and Master's Thesis Coriolis Pharma, Martinsried |
| 08/2010 – 05/2011 | Student Research Assistant Walther-Straub-Institute of Pharmacology and Toxicology, Munich |

Education

| | |
|--------------------------|---|
| 06/2007 | Abitur |
| 09/1998 – 06/2007 | Grammar School Franz-Marc-Gymnasium, Markt Schwaben |

Publications

Publications in Scientific Journals

1. **Manuel Gregoritza**, Kathrin Abstiens, Moritz Graf, and Achim M. Goepferich. Fabrication of antibody-loaded microgels using microfluidics and thiol-ene photoclick chemistry. *Submitted for publication*, 2017. (**Chapter 5**)
2. **Manuel Gregoritza**, Viktoria Messmann, Kathrin Abstiens, Ferdinand P. Brandl, and Achim M. Goepferich. Controlled antibody release from degradable thermoresponsive hydrogels cross-linked by Diels–Alder chemistry. *Biomacromolecules*, 18(8):2410–2418, 2017. (**Chapter 4**)
3. Ursula Storch, Anna-Lena Forst, Franziska Pardatscher, Serap Erdogmus, Maximilian Philipp, **Manuel Gregoritza**, Michael Mederos y Schnitzler, and Thomas Gudermann. Dynamic NHERF interaction with TRPC4/5 proteins is required for channel gating with diacylglycerol. *Proceedings of the National Academy of Sciences of the United States of America*, 114 (1):E37–E46, 2017.
4. **Manuel Gregoritza**, Achim M. Goepferich, and Ferdinand P. Brandl. Polyanions effectively prevent protein conjugation and activity loss during hydrogel cross-linking. *Journal of Controlled Release*, 238:92–102, 2016. (**Chapter 6**)
5. **Manuel Gregoritza**, Viktoria Messmann, Achim M. Goepferich, and Ferdinand P. Brandl. Design of hydrogels for delayed antibody release utilizing hydrophobic association and Diels–Alder chemistry in tandem. *Journal of Materials Chemistry B*, 4:3398–3408, 2016. (**Chapter 3**)
6. **Manuel Gregoritza** and Ferdinand P. Brandl. The Diels–Alder reaction: A powerful tool for the design of drug delivery systems and biomaterials. *European Journal of Pharmaceutics and Biopharmaceutics*, 97, part B:438–453, 2015. (**Chapter 1**)
7. Susanne Kirchhof, **Manuel Gregoritza**, Viktoria Messmann, Nadine Hammer, Achim M. Goepferich, and Ferdinand P. Brandl. Diels–Alder hydrogels with enhanced stability: First step toward controlled release of bevacizumab. *European Journal of Pharmaceutics and Biopharmaceutics*, 96:217–225, 2015.
8. Sarah Zöls, **Manuel Gregoritza**, Ruedeeporn Tantipolphan, Michael Wiggenhorn, Gerhard Winter, Wolfgang Friess, and Andrea Hawe. How subvisible particles become invisible - Relevance of the refractive index for protein particle analysis. *Journal of Pharmaceutical Sciences*, 102 (5):1434–1446, 2013.

Patent

1. **Manuel Gregoritza**, Achim M. Goepferich, and Ferdinand P. Brandl. Hydrogels and hydrogel-forming compositions with dual gelation mechanism. European Patent Application, April 2017.

Poster Presentations

1. **Manuel Gregoritz**a, Viktoria Messmann, Ferdinand P. Brandl, and Achim M. Goepferich. Controlled antibody release from degradable thermoresponsive hydrogels cross-linked by Diels-Alder chemistry. 254th ACS National Meeting, Washington D.C., USA, 2017.
2. **Manuel Gregoritz**a, Viktoria Messmann, Achim M. Goepferich, and Ferdinand P. Brandl. Development of microgel particles for antibody delivery using microfluidics and thiol-ene photoclick chemistry. 2nd European conference on pharmaceuticals, Krakow, Poland, 2017.
3. **Manuel Gregoritz**a, Viktoria Messmann, Achim M. Goepferich, and Ferdinand P. Brandl. Polyanions effectively prevent protein activity loss during hydrogel cross-linking. 10th World Meeting on Pharmaceuticals, Biopharmaceuticals and Pharmaceutical Technology, Glasgow, United Kingdom, 2016.

Scientific Talks

1. **Manuel Gregoritz**a, Viktoria Messmann, Achim M. Goepferich, and Ferdinand P. Brandl. Dual gelation enables delayed antibody release from Diels-Alder hydrogels. 10th World Biomaterials Congress, Montréal, Canada, 2016.
2. Ferdinand P. Brandl and **Manuel Gregoritz**a. Hydrogels for controlled release of protein therapeutics. DPhG Jahrestagung, Munich, Germany, 2016.

Journal Covers

1. Biomacromolecules, Volume 18, Issue 8, August 2017.
2. Journal of Controlled Release, Volume 238, September 2016.

Acknowledgements

First and foremost, I would like to express my sincerest gratitude to my advisor Prof. Dr. Achim Göpferich for accepting me into his research group and for committing this highly interesting project to me. I am very grateful for his dedicated guidance, his enthusiasm for my project, and the many inspiring discussions we had. I would like to thank him for his trust in my abilities and for encouraging me to follow my scientific ideas. I am deeply thankful for all his support, for providing an outstanding working environment, and for the opportunity to present my project at several international conferences.

Second, I would like to thank Dr. Ferdinand Brandl for all his advice and support throughout my doctoral studies. I am very grateful for his scientific input, our many fruitful discussions, and his critical revisions of my manuscripts. I thank him for his continuous interest in the progress of my research and for always having an open mind towards new ideas.

I express my gratitude to Prof. Dr. Rainer Müller for his help with FT-IR measurements. Moreover, I would like to thank Klaus-Jürgen Tiefenbach and Prof. Dr. Reinhard Sterner for the opportunity to conduct circular dichroism measurements.

I am deeply grateful to all my former and present colleagues for providing a friendly and motivating working atmosphere. In particular, I would like to thank the following colleagues:

Alexandra Haunberger for the many great training sessions in the gym, inspiring conversations, and her friendship.

My lab mates Sara Maslanka Figueroa and Michaela Guter for the enjoyable time and the friendly atmosphere.

Dr. Robert Hennig for intriguing scientific discussions, great workouts, and his friendship.

Acknowledgements

Dr. Susanne Kirchhof and Dr. Nadine Hammer for the constructive collaboration and for sharing their expertise with me.

Further thanks goes to Eva Wrobel for her excellent support and organization.

I express my gratitude to all technical assistants of the Department of Pharmaceutical Technology. In particular, I would like to thank Viktoria Messmann for her positive attitude and the excellent support with numerous experiments and syntheses. It was always a pleasure working with you! Moreover I would like to thank Renate Liebl for her assistance with cell culture experiments and Stefan Kolb for constructing several devices.

I thank Abby Brooks for doing a great job during her research internship and for proofreading several chapters of this thesis.

The German Research Foundation (DFG) is acknowledged for providing financial support for my project.

I am deeply grateful to Kathrin for always being there for me. Thank you for all your support, your patience, and your love.

Finally, I would like to thank my parents for everything they have done for me. I am deeply appreciative of your unconditional support and thank you for always encouraging me to follow my interests and dreams.

The whole is greater than
the sum of its parts.

(Aristotle)

Statement in Lieu of an Oath

I hereby confirm that I have written this thesis on my own and that I have not used any other media or materials than the ones referred to in this thesis.

Regensburg, 15th of September 2017

(Manuel Gregoritz)